Building a cascading multi-product biorefinery process for *Ascophyllum nodosum*: a green chemistry approach

A thesis submitted to University College London for the degree of

Doctor of Philosophy (PhD) in Biochemical Engineering

By

Alex Olivares-Molina

The Advanced Centre for Biochemical Engineering

Department of Biochemical Engineering

University College London

Torrington Place, London, WC1E 7JE, UK

March 2021

I, Alex Olivares-Molina, confirm that the work presented in this thesis is my own. Where information has been derived from other sources, I confirm that this has been indicated in the thesis.

_____

Abstract

Brown macroalgae are an attractive third-generation feedstock for biofuel, as well as a source of natural products. A cascading biorefinery approach extracts potentially bioactive compounds, i.e., polyphenols, fucoidan, and commodity products i.e., alginate, proteins in the same process. In order to design a green chemistry-compliant process and reduce the use of organic solvents in bioactive product extraction, aqueous two-phase systems (ATPS) and low-concentration biodegradable acid extractions were applied. The present work aimed to develop a multi-product biorefinery concept using *Ascophyllum nodosum* as a model feedstock using life cycle assessment (LCA), techno-economic analysis (TEA), and technical feasibility trials (TFT) as early-design tools for its development. After a biochemical characterisation of three potential model species, *A. nodosum* was selected as model feedstock based on the high accumulation of high-value products with potential breakthrough in the market. *A.nodosum* exhibited higher contents of polyphenols, lipids, protein, and minerals than the other species analysed, with 4.63% DW, 8.13% DW, 11.33% DW, and 29.54% DW, respectively. Once the biochemical characterisation was completed, three biorefining scenarios using different technology pathways (solvent, physicochemical, and green techniques) were modelled to process 1,000 metric tonnes (MT) biomass/year, in order to evaluate their economic and environmental metrics. From all evaluated scenarios, a green chemistry-compliant cascading sequence showed the lowest capital expenditure (CAPEX) (£30 million), operational expenditure (OPEX) (£11 million), cost of goods per kg of feedstock processed (CoG/kg) (£0.08) and production costs (£0.03/kg), along with the highest internal rate of return (IRR) (75.0%). Additionally, this scenario exhibited the lowest environmental impacts in all categories assessed, around 2 – 10 times lower than the other scenarios. In addition, the cascading sequence performance was evaluated to obtain first-hand data and re-iterate the models. The cascading sequence approach has

been proposed to maximise resource efficiency and, in this work, a cascading sequence aimed at the sequential extraction of fucoidan, alginate, polyphenols, and proteins. Bioprocessing hotspots were identified for polyphenol and fucoidan extraction steps and further optimised using automated high-throughput screenings (HTS) and Design of Experiments (DoE), recovering 89% of total polyphenols, and showing a 33% increase in fucoidan recovery. Finally, after completing the bioprocessing hotspots, economic and environmental models were re-iterated to confirm the robustness of the biorefinery concept developed. The re-iterated version of the green chemistry-compliant cascading sequence exhibited better recovery performance in the optimised extraction stages, and thus showed better sales revenues (£91 million) than its previous version, a higher IRR (82.1%), and lower CoG/kg (£0.05) and production costs (£0.01/kg). The re-iterated version of the cascading sequence also exhibited the lowest environmental impacts in every category assessed, of all scenarios analysed in this project.

These findings confirm that a holistic approach to early bioprocesses design is a valuable addition for decision-making tool options in the development of green-compliant multi-product third generation biorefineries.

Impact statement

The process uncertainties of novel extraction bioprocesses at early-stages of technical development are high, hindering the identification of environmental and/or economic hotspots at the beginning of the process development stage. Choices made at early development stages have a larger potential to impact the final technology since they are passed onto subsequent stages. The work in this thesis is centred on the use of techno-economic analysis (TEA) and life cycle assessment (LCA) as early-design tools for sustainable bioprocess development, as well as the use of green chemistry principles to build more sustainable extraction processes in a multi-product cascading sequence biorefinery context, i.e., aqueous two-phase systems and biodegradable mild acid extractions.

Specifically, the work presented in this thesis looks at the potential of using a holistic methodology for biorefinery process development, with a modelling approach involving the use of TEA and LCA to select the best biorefinery process in the early stages of development, and later technical feasibility trials of the modelled process to identify processing hotspots and optimise them with the use of high-throughput screening (HTS) techniques and Design of Experiments (DoE), to finally re-iterate the models with first-hand data, to get a more accurate description of the biorefinery concept. The motivation for using TEA, LCA, DoE and high-throughput experimentation is that greater amounts of information can be gathered from limited experimental resources. This is particularly important at early stages of development for sustainable processes where several scenarios need to be evaluated at the same time. Such an approach provides greater process insights to researchers so that robust multi-product biorefinery processes can be developed more efficiently.

The methods presented in this thesis will help scientists to develop commercially relevant cascading biorefinery processes compliant to green chemistry principles. This

approach will benefit decision makers in the field of third generation biorefineries first, due to the holistic approach of the use of early-design tools like LCA and TEA along with preliminary technical feasibility trials to aid the decision process in early stages of sustainable bioprocesses; and secondly, the end-user as the cost of the high-value products extracted from macroalgae could be cheaper for two reasons: 1) The combined approach using experiments and modelling allows for research and development efforts to be conducted more efficiently and 2) The use of green chemistry strategies to extract and recover high-value products could save money as the inherent process may be cheaper than using conventional separation techniques. A direct application from the outcomes of this thesis was the formulation of the Algae UK/IBioIC funded project titled "*Green Chemistry for Blue Pigments: An LCA-based toolkit to support decision making for algal bioprocesses*", an industrial collaboration project with Scottish company ScotBio to develop a greener approach to extracting C-phycocyanin from *Arthrospira platensis*. Prior to designing their good manufacturing practices (GMP) facilities, LCA was applied to evaluate bioprocess options in order to identify environmental hotspots. The automated high-throughput screening method for aqueous two-phase systems developed in this project was applied to understand if this could be a feasible downstream option.

Acknowledgments

Firstly, I would like to thank my supervisor Dr Brenda Parker, for her continued support throughout these years, for the opportunity to work in a field that I feel very passionate about, for challenging me with new ideas, and for sharing her expertise every time I needed. This has been a motivating and stimulating ride. I also want to thank my secondary supervisor, Prof Nigel Titchener-Hooker for his great knowledge of the field and for always offer key insights during my research.

I would like to thank to all the members of the Industrial Biotechnology Lab, for kindly sharing their knowledge every time I asked, helping me when troubleshooting was needed, and of course for the occasional and very necessary laughs when stressful times happened.

To all the great friends I made during my time at the Department of Biochemical Engineering, Vincent, Becci, Rosalía, Neha, Jaime, Víctor, Max, Gerry, and Marco Rotondi, for all the amazing scientific and non-scientific conversations we had, for the great moments we spent in the vineyard, for their support throughout this experience, the occasional drinks after work, and for backing me up in every crazy idea I had.

The most important thanks must go to my parents, Alex and Alicia, and sister Carolina for their unconditional love and encouragement through these four years, your caring felt strong even 14,000 km away. To Ana, for her love, kindness and support throughout this time, thank you for listening every time I felt terrible, and for being my rock through this process.

Finally, I would like to thank to the National Agency of Research and Development (ANID) for funding this research with a Becas Chile scholarship that allowed me to embark in this exciting project.

Contents

Table of figures

List of tables

Abbreviations and nomenclature

ACE	Angiotensin-I-Converting Enzyme
ALCA	Attributional Life Cycle Assessment
ANOVA	Analysis of Variance
ATPS	Aqueous Two-Phase System
Br_2	Bromine
BSA	Bovine Serum Albumin
CAPEX	Capital Expenditure
CFC	Chlorofluorocarbons
CFC-11-eq.	Freon-11 Equivalent
CF_3COOH	Trifluoracetic Acid
$CHCl_3$	Chloroform
Chl a	Chlorophyll *a*
Chl (x+c)	Chlorophyll *c* and Total Carotenoids
CH_3OH	Methanol
CLCA	Consequential Life Cycle Assessment
CO_2	Carbon Dioxide
CO_2-eq.	Carbon Dioxide Equivalent
CoG	Cost of Goods
CoG/kg	Cost of Goods per Kilogram of Feedstock Processed
Comp-LCA	Comparative Life Cycle Assessment
COVID-19	Coronavirus Disease 2019
$CuSO_4 \cdot 5H_2O$	Copper Sulphate Pentahydrate
$C_2HCl_3O_2$	Trichloroacetic Acid
C_2H_5OH	Ethanol

C_2H_6OS	Dimethyl Sulphoxide
$C_{2n}H_{4n+2}O_{n+1}$	Polyethylene Glycol
C_3H_6O	Acetone
C_3H_7NO	Dimethyl Formamide
C5	Pentose
C6	Hexose
$C_6H_2(OH)_3COOH$	Gallic Acid
C_6H_6O	Phenol
$C_6H_6O_3$	Phloroglucinol
$C_6H_{12}O_6$	Glucose
$C_{14}H_{14}N_3NaO_3S$	Methyl Orange
DMF	Dimethyl Formamide
DMSO	Dimethyl Sulphoxide
DNA	Deoxyribonucleic Acid
DoE	Design of Experiments
DW	Dry Weight
EAE	Enzyme-Assisted Extraction
FAO	Food & Agriculture Organisation
FCI	Fixed Capital Investment
G	α-L-Guluronate
GAE	Gallic Acid Equivalent
GCB	Green Chemistry Biorefinery
GE	Glucose Equivalent
GHG	Greenhouse Gases
GMP	Good Manufacturing Practices

Green Chem	Green Chemistry Scenario
HCl	Hydrochloric Acid
HPAEC-PAD	High Performance Anion-Exchange Chromatography with Pulsed Amperometric Detection
HTS	High-Throughput Screening
H_2O	Water or Oxidane
H_2SO_4	Sulphuric Acid
H_3PO_4	Phosphoric Acid
IC_{50}	Half-Maximal Inhibitory Concentration
IRR	Internal Rate of Return
ISO	International Organisation for Standardisation
KH_2PO_4	Potassium Phosphate Monobasic
$KNaC_4H_4O_6 \cdot 4H_2O$	Potassium Sodium Tartrate
KOH	Potassium Hydroxide
K_p	Partition Coefficient
K_2HPO_4	Potassium Phosphate Dibasic
K_2CO_3	Potassium Carbonate
K_3PO_4	Tripotassium Phosphate
LCA	Life Cycle Assessment
LCC	Life Cycle Costing
LCI	Life Cycle Inventory
LCIA	Life Cycle Impact Assessment
LCSA	Life Cycle Sustainability Assessment
LHS	Liquid Handling Station
LiHa	Liquid Handling Arm
Li_2SO_4	Lithium Sulphate

LLE	Liquid-Liquid Extraction
M	β-D-Mannuronate
MAE	Microwave-Assisted Extraction
MT	Metric Tonne
MW	Molecular Weight
m^3-eq.	Cubic Metres Equivalent
N-eq.	Nitrogen Equivalent
$NaC_{12}H_{25}SO_4$	Sodium Dodecyl Sulphate
NaOH	Sodium Hydroxide
Na_2CO_3	Sodium Carbonate
Na_2WO_4	Sodium Tungstate
Novel Tech	Novel Technologies Scenario
NPV	Net Present Value
NTB	Novel Technologies Biorefinery
Oil-eq.	Oil Equivalent
OPEX	Operational Expenditure
p_c	Critical Pressure
PEG	Polyethylene Glycol
P-eq.	Phosphorus Equivalent
PGE	Phloroglucinol Equivalent
pI	Isoelectric Point
PUFAs	Polyunsaturated Fatty Acids
QC/QA	Quality Control/Quality Assurance
R-PC	R-Phycocyanin
R-PE	R-Phycoerythrin
RSD	Relative Standard Deviation

R^2	Coefficient of Determination
SARS-CoV-2	Severe Acute Respiratory Syndrome Coronavirus 2
SBB	Solvent-Based Biorefinery
SCO	Single Cell Oils
SD	Standard Deviation
SDS	Sodium Dodecyl Sulphate
SEM	Standard Error of the Mean
SFAs	Saturated Fatty Acids
SFE	Supercritical Fluid Extraction
S-LCA	Social Life Cycle Assessment
Solvent-based	Solvent-Based Scenario
SO_2-eq.	Sulphur Dioxide Equivalent
T_c	Critical Temperature
TCA	Trichloroacetic Acid
TCC	Total Carbohydrate Content
TEA	Techno-Economic Analysis
TFA	Trifluoroacetic Acid
TFT	Technical Feasibility Trial
TLL	Tie Line Length
TPoC	Total Polyphenol Content
TPrC	Total Protein Content
TRL	Technology Readiness Level
UAE	Ultrasound-Assisted Extraction
UATR-FTIR	Universal Attenuated Total Reflectance Fourier Transform Infrared
UK	United Kingdom
UPLC	Ultra-Performance Liquid Chromatography

WAR	Waste Reduction Algorithm
WEPO	Water Extraction and Particle Formation On-Line
μW	Microwave

Chapter 1: Introduction

1. Literature review

To curb carbon emissions and reduce our global environmental footprint, there is an increasing demand for renewable chemicals, and therefore a need to develop the technology pathways to produce them from biomass feedstocks (Centi et al., 2019). Following this approach, the concept of Bioeconomy or bio-based economy has been coined, which refers to an economy where the basic building blocks for materials, chemicals, and energy are derived from renewable biological resources (McCormick and Kautto, 2013). This type of economy can meet many of the requirements for sustainability from environmental, social and economic perspectives if it is planned intelligently. For Bioeconomy policy makers, the complexity of implementing bio-based economy strategies can start on regional levels e.g., biorefinery deployments (Philp, 2018). A biorefinery can be defined as “the sustainable processing of biomass into a spectrum of bio-based products and bioenergy” and is considered as an integral unit that can accept various biological feedstocks and convert them into a range of useful products, such as food, animal feed, nutraceuticals, pharmaceuticals and chemicals (Clark et al., 2012). In order to maximise sustainable production from biomass, biorefinery technology has expanded in the last 30 years to include non-food crops and residues for bioenergy and towards lignocellulosic biomass (Ghatak, 2011). These are known as second generation biorefineries, based in the use of lignocellulosic feedstocks or by-products from the wood industry (Morais and Bogel-Lukasik, 2013), for the production of bioenergy, platform chemicals, and/or bioactive compounds, as a way of completely valorising feedstock and facilitating the economics of this approach (Backa et al., 2012). Nevertheless, due to immature market structure and conversion technologies, commercially viable production of second-generation biofuels is still challenging (Nguyen et al., 2019), combined with the ethical debate about the use of land whether to produce

food or energy new land-free growth type of feedstocks have been researched. The concept of Blue Economy has gained interest in the past years as an ocean-based counterpart to the Green Economy development plans, where macroalgae can play a fundamental role in the growth of the sector (Cisneros-Montemayor et al., 2019). Macroalgae, or seaweed, is the collective name for photosynthetic multicellular marine species formed of simple tissues. Described as third generation biorefineries, these systems use marine algae as their main feedstock for the production of bulk chemical compounds, high-value products, and/or energy (Jung et al., 2013). Given the rich diversity of unique biomolecules synthesised by macroalgae, there is a growing research interest for the development of pharmaceuticals against different diseases, like the metabolic syndrome (Wang et al., 2018), anti-inflammatory, antioxidant (Smit, 2004), antimicrobial activities (Lordan et al., 2011), also there has been an interest in the development of functional foods (Lordan et al., 2011) and nutraceutical (Suleria et al., 2015) or cosmeceutical applications (Thomas and Kim, 2013). Therefore, there is a case for extraction of multiple metabolites from a single feedstock. Improvements in the macroalgae biorefinery approach to obtain bioactive products are possible with the development of cheaper, simpler, and environmentally friendly novel extraction techniques. Consecutive extractive processes to obtain different metabolites and added-value products from seaweeds are used in the hydrocolloid industry (Baghel et al., 2015; Jung et al., 2013; Yuan and Macquarrie, 2015a). These approaches aim to enhance the use of this biomass, extracting other valuable natural products often discarded to add valorisation to the feedstock.

In the last decade, Blue Economy discourses from Western societies have tended more towards ‘business-as-usual’ planning, focusing on technological and financial aspects of economic growth rather than the original and more holistic triple bottom line perspective of sustainability. As a result of this, development has been often shaped by objectives from the private sector or funding agencies with a focus on economic growth (Brent et al., 2018), while large non-governmental organisations push the inclusion of guidelines

for the reduction of environmental impacts and conservation of the environment (Hoegh-Guldberg et al., 2015). It is therefore important to evaluate new third generation biorefinery development from an economic and environmental perspective for an appropriate holistic approach for sustainable processes.

Lastly, to analyse the biorefinery extraction process as a complete functional bioprocess, it is necessary to evaluate its economic and environmental performance. It is for that reason techno-economic analysis (TEA) and life cycle assessment (LCA) are used in the decision-making process on the setup of a biorefinery concept. These are tools designed to validate and to give robustness to the system looking at it on a holistic approach, in an attempt to fulfil the triple bottom line framework, defined as the "creation of products through economically-sound processes that minimise negative environmental impacts while conserving energy and natural resources" (Akbar and Irohara, 2018), to assure sustainable industrial growth.

1.1. Macroalgae-based biorefinery concepts with potential use in industry

Macroalgae can be classified in three major groups, depending on their pigments associated with photosynthesis, Chlorophyta or green algae, mainly using chlorophyll as their main photosynthetic pigment, Rhodophyta or red algae, primarily utilising carotenoids to capture sunlight, and Phaeophyceae or brown algae which use xanthophylls to aid their photosynthetic process (Stengel et al., 2011). Macroalgae have been used traditionally as food e.g., wakame, and Pyropia (Nori) sheets in Japan, or bull kelp (Cochayuyo) in Chilean cuisine. The most commercially developed areas for seaweed exploitation are mainly to produce food and hydrocolloids such as agar, carrageenan and alginate (Hafting et al., 2015), that are used in several industries, such as thickening agents in several foods, like ice cream, canned soups, or meat conservation; in cosmetics, as part of nail polishers, among several uses. Worldwide, around 291 different species from 43 countries are used, with around 32 million tonnes of seaweeds produced (FAO, 2020). The development of large-scale seaweed

cultivation techniques has been focused on the production of commoditised biomass and not necessarily optimised to produce valuable bioactive compounds. For the future expansion of biorefinery operations based on macroalgal feedstock, it is desirable to obtain seaweed from aquatic farms, due to the fact wild seaweed population are an essential component in marine ecosystems (Andersen, 2017). According to the food and agriculture organisation (FAO), aquaculture was the major source of aquatic plant production (dominated by macroalgae) in 2018 (95.8%) (FAO, 2020). Global production of cultivated aquatic plants has had more than a 2-fold increase from 1995 (13.5 million tonnes) to 2018 (32.4 million tonnes), with China and Indonesia being the major producers, 18.5 and 9.32 million tonnes respectively (FAO, 2020). Species like *Undaria pinnatifida, Pyropia* spp., *Porphyra* spp. are produced almost exclusively for direct human consumption. On the other hand, most macroalgae are cultured for the phycocolloid industry (agar, alginate, and carrageenan), with *Laminaria japonica*, *Eucheuma/Kappaphycus* spp., and *Gracilaria* spp. the most exploited with 11.4, 9.2, and 3.5 million tonnes respectively at year 2018. This is an important opportunity for a green chemistry multi-product biorefinery in order to maximise value from the remaining macroalgal residue, through selective extraction of high value bioproducts (Baghel et al., 2016).

Industrial extraction of alginate from macroalgal biomass has existed since the 1920's (Pangestuti and Kim, 2015), with remarkable uses as food products, fertilisers, and cosmetics (Cikoš et al., 2019), these markets use seaweed via extracting single biological compounds i.e., alginate, or using the whole biomass as commoditised product rather than extract multiple products from the same biomass in a cascading sequence approach. There is still a considerable gap between macroalgal biorefining and the more established industrial lignocellulosic biorefineries whereby multiple high value products and chemical precursors are extracted from wood, in the case of macroalgal biorefineries they're still in their first stages of development, whereas lignocellulosic biorefineries are well established industrial processes, therefore the aim is to reach the same technology

development in seaweed biorefinery than the development lignocellulosic biorefinery already possess. In **Fig 1-1** it is shown a “thought experiment” showing the processing of 1,000 kg of lignocellulosic feedstock in the industrially-established cascading process at Borregaard biorefinery against a conceptual cascading process using brown seaweed. From this thought experiment it is observed that using the same initial biomass, several high value products can be obtained from the macroalgal process, even producing less residue than the Borregaard biorefinery. As stated before, this was a conceptual experiment and more information is needed to made a more robust claim, but this simple theoretical comparison highlights the potential macroalgal biorefineries can offer.

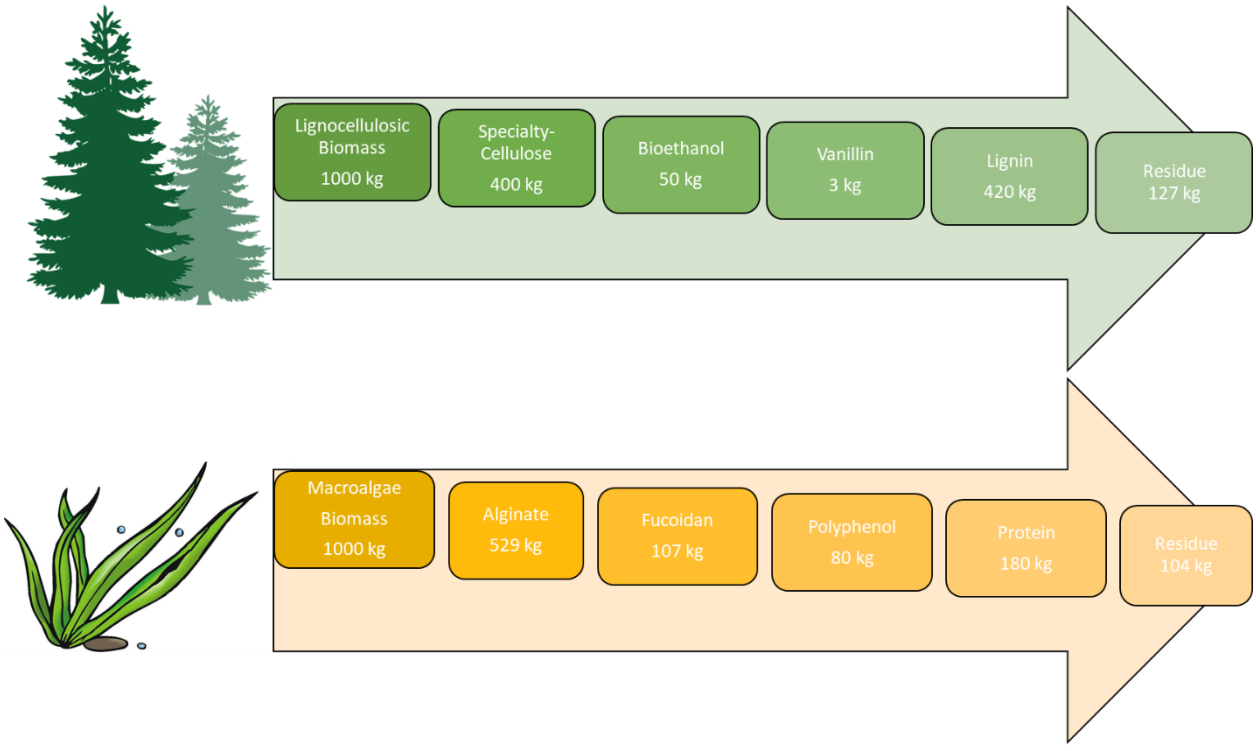

Fig 1-1. Schematic representation of the processing of 1,000 kg of lignocellulosic biomass in the industrially-established cascading process at Borregaard biorefinery plant, contrasting with a theoretical exercise showing the processing of an industrial macroalgal multi-product extraction process. Top portion of the diagram adapted from Backa et al. (2012).

As a proportion of the commercially harvested seaweed biomass processed into products, a large percentage is treated as waste. For instance, in the extraction of agar from agarophytic seaweeds approximately 17% of the biomass is used while the remaining 83% is considered waste or low-value products (Baghel et al., 2015). However, macroalgae have the capacity to produce a vast array of high-value bioactive compounds for pharmaceuticals, health foods, and natural pigments alongside commodity chemicals such as agar or alginate. Reports on the utilisation of macroalgae in a biorefinery context are shown in **Table 1-1**. In addition, the economic feasibility of macroalgal biofuels such as bioethanol could be significantly enhanced by a high-value co-product strategy, or vice versa, developing a biorefining approach in the extraction of high-value products and give valorisation to the residue by producing biofuels from it. Several reports have shown the potential of seaweeds as feedstocks in biorefinery approaches for the production of biofuels (Brockmann et al., 2015; Golberg et al., 2014) including reports of scaled up processes (Camus et al., 2016). For example, Brockmann et al. (2015) presented an LCA of a bioethanol facility using *Ulva* sp. located in Brittany, France, with a theoretical yield of 0.136 kg ethanol/kg dry weight (DW) macroalgae and attesting that a biorefinery using macroalgae is an environmentally efficient biofuel comparing it to fossil fuel and bioethanol from sugarcane, with the residue being used as cattle feed (**Table 1-1**). Along the same lines Golberg et al. (2014) showed a combined approach using thermodynamic, metabolic, and sustainability analyses to produce bioethanol from *Ulva* sp., demonstrating that this process can be used to implement macroalgae-based biorefineries in developing countries. Lastly, Camus et al. (2016) scaled-up bioethanol production of *Macrocystis pyrifera* up to 75 L fermentation using a genetically modified strain of *E. coli* producing 0.213 kg ethanol/kg dry algae, reaching 64% of the maximum theoretical yield, with the production of depolymerised seaweed as protein, and mannitol.

On the other hand, biorefining processes focused on the extraction of high-value products are still in the laboratory scale (Baghel et al., 2016; Kostas et al., 2017).

Conventional solvent extraction technologies are one of the most used techniques to obtain natural products from macroalgae. One of the limitations of these systems is the possible toxicity problems due to trace amounts of solvent in purified samples of biological compounds (Britton et al., 2009). Usually, solvent extractions had been used in analytical extractions, combining several extraction stages using different solvents or different concentrations, in order to recover the total of a given natural compound, i.e., total soluble polyphenols extracted using aqueous acetone 70:30 v/v, followed by methanol, water, pure acetone, and diethyl ether (Koivikko et al., 2005), making the application of this extraction process in an industrial processing environment more difficult.

Table 1-1. Examples of different macroalgae-based biorefinery concepts applying cascading extraction processes.

Algal group	Species	Final product	Co- or by-products	Techniques used	Process scale	Reference
Brown algae	*Laminaria digitata, Fucus vesiculosus,* and *Saccharina latissima*	Fucoidan	Laminarin, feed supplement	Water extraction + concentration + acid extraction	Model with 1 kg initial feedstock	Zhang and Thomsen (2021)
	Ecklonia radiata, M. pyrifera, Durvillaea potatorum, and *Seirococcus axillaris*	Fucoidan	Alginate, acetone fractions	Acid extraction + basic extraction + acetone precipitation	~ 250 mL cascading steps	Lorbeer et al. (2017)•
	Sargassum spp.	Biodiesel	Carbohydrates	Hot water extraction + solvent extraction + transesterification	1 L cascading steps	Ruangrit et al. (2021)
	L. digitata	Bioethanol	Fucoidan, alginate, methanolic extract	Acid extraction + enzymatic saccharification + Fermentation	~20 mL cascading steps	Kostas et al. (2017)
Green algae	*Ulva ohnoi*	Cellulose	Seaweed salt and protein	Aqueous pre-treatment + acid extraction + basic extraction	1 L cascading steps	Glasson et al. (2017)
	U. ohnoi	Cellulose	Salt, starch, lipid, ulvan, protein	Water extraction + solvent extraction + salt extraction + basic extraction+ water extraction	0.5 L – 2.8 L cascading steps	Prabhu et al. (2020)
	Ulva lactuca	Methane	Sap, ulvan, protein	Aqueous treatment + thermal treatment + chemical extraction + anaerobic fermentation	~1 L – 2 L cascading steps	Mhatre et al. (2019)
	Ulva spp. and *Cladophora* spp.	Biodiesel	Carbohydrates	Hot water extraction + solvent extraction + transesterification	1 L cascading steps	Ruangrit et al. (2021)
Red algae	*Solieria filiformis*	Carrageenan	Water-soluble extract, fatty acids	Enzymatic extraction + organic extraction + Microwave extraction	50 – 200 mL cascading steps	Peñuela et al. (2018)
	Kappaphycus alvarezii	Bioethanol	Sap, carrageenan, Biogas	Alkali treatment + fermentation & distillation + anaerobic digestion	Not specified	Ingle et al. (2018)

1.2. Potential use of cascading extraction sequences in macroalgae biorefinery

The principle of cascading extraction processes within the biorefinery context has been proposed to maximise resource efficiency, exploiting feedstock for high added-value products, before using residual material as an energy source (Keegan et al., 2013). Multi-product biorefineries based on annual crops or lignocellulosic feedstocks are now operating on an industrial scale (Modahl et al., 2015). Nowadays, several different cascading extraction processes in biorefining exist, the vast majority of which have the aim to produce ethanol from lignocellulosic biomass. The Borregaard advanced biorefinery plant in Sarpsborg, Norway is a commercially successful example of a cascading process applied in a biorefinery running for more than 8 decades (Backa et al., 2012). Founded in 1889, with its bioethanol production started in 1938, and its vanillin plant finished in 1968, Borregaard is the only supplier of wood-based vanillin in the world. The extraction of cellulose fibre, vanillin, lignin, and bioethanol is efficient (**Fig 1-1**), leaving only a small part of the wood to be converted into bioenergy. The process starts with the input of wood chips and small timber into the digester, the feedstock is delignified next with sulphite cooking liquor according to target specifications producing a fibrous pulp, lignosulphonates and soluble sugars. The resulting fibrous pulp is treated with a hot alkali step and bleached; this process removes impurities and adjusts the cellulose chain length. The pulp is labelled as specialty cellulose, materials for production of cellulose ethers, cellulose acetate and nitrocellulose. Hemicelluloses and short celluloses in the cooking liquor are mainly hexose (C6) sugars (80%). The sulphite liquor is fermented to produce ethanol. After fermentation and distillation, the remaining liquor is used to produce lignin-based chemicals. The final portion of the cascading process is vanillin extraction, where the lignosulphonate fraction of the final portion of the liquor is oxidised under alkaline conditions to produce the vanillin, and further purification.

In the cascading process of this biorefinery from 1,000 kg dry spruce wood they can produce 400 kg of specialty cellulose 400 kg lignosulfonate, 70 kg solid biofuel, 50 kg

bioethanol, 50 kg carbon dioxide and 3 kg vanillin, with under 5% of the total input of wood ends up in the waste treatment plant (Backa et al., 2012). To make a comparison between pine trees and macroalgae productivity, we can say that around 222 tonnes of dry weight sawlogs of *Pinus radiata* per hectare are produced in a time span of 35 years, around 6.34 ton/ha/yr. On the other hand, in a brown alga culture an average of 26 tonnes DW/ha/yr. are produced, a 4-fold production per year compared to pine production (Andersen, 2017).

Despite this promise, at present there is not an industrially scaled-up cascading extractive process using macroalgae as feedstock in a biorefinery concept (Rajak et al., 2020). Most industrial processes involving macroalgae are focused on phycocolloids or cosmetics production, on the other hand extraction of high-value products have not been scaled-up due to economic challenges, reason enough to impulse a cascading sequence approach to obtain these products; in **Fig 1-2** a schematic representation of a macroalgae-based biorefinery is proposed. Most efforts in this area are still in the laboratory scale and can be seen in **Table 1-1**. It is interesting to note that the research efforts in this matter have been focused in all macroalgae groups, instead of intense effort in just one of them, this might be due to the diverse and different natural compounds that are of economic interest, namely proteins, pigments, fermentable carbohydrates, and even lipids, found in each of them.

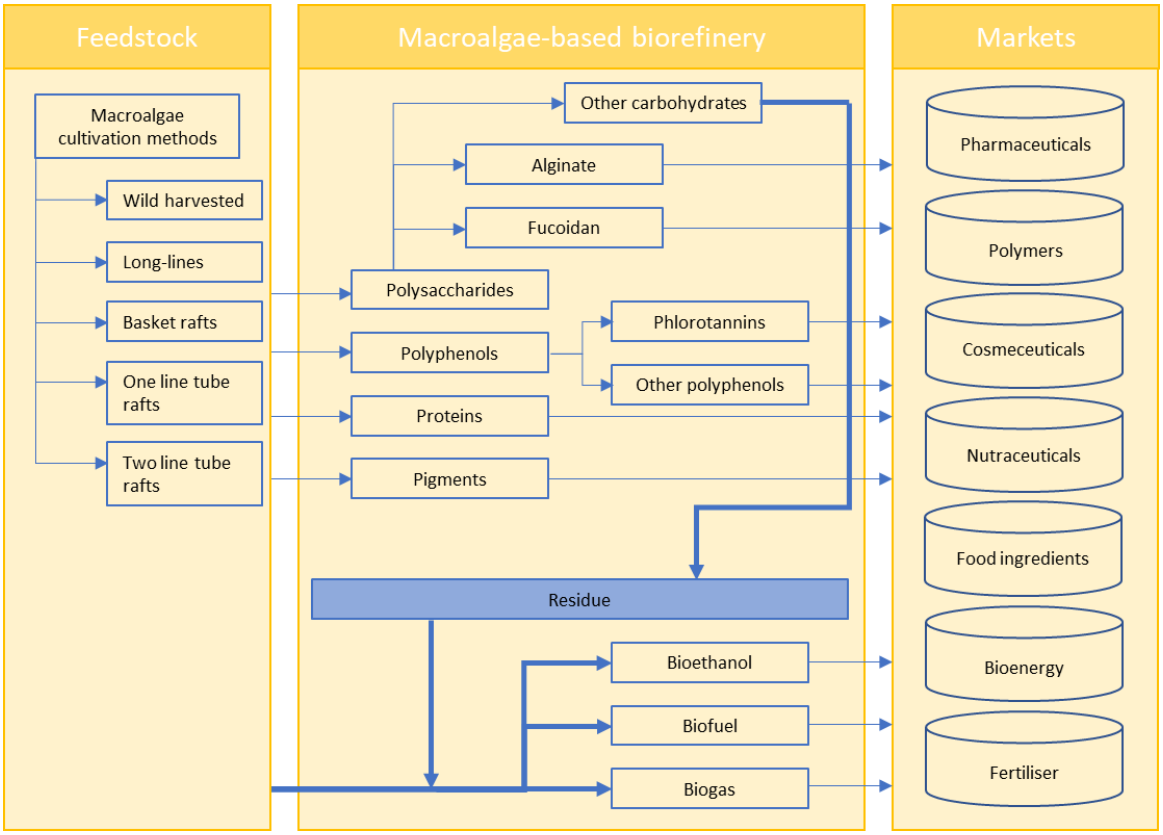

Fig 1-2. Schematic representation of a theoretical brown macroalgae-based biorefinery generalised on potential outputs from various species.

1.3. Chemical compounds with potential in macroalgae biorefinery

The intensification in the research effort to extract biological products from macroalgae had identified several key compounds in each algae type, e.g., in brown seaweeds polyphenols (Olivares-Molina and Fernández, 2016), fucoidan (Zhao et al., 2018), and fucoxanthin (Viera et al., 2018); in red seaweeds carrageenan (Masarin et al., 2016), R-phycocyanin (R-PC) and R-phycoerythrin (R-PE) (Sampath-Wiley and Neefus, 2007); and in green seaweeds ulvan (Kidgell et al., 2019), cellulose (Prabhu et al., 2020), and chlorophyll (Fabrowska et al., 2016) are some of the examples of key biological compounds with potential applications in the market that can be obtained via biorefinery approach. The extractions of high-value or bulk natural products in biorefineries have been explored in order to give more valorisation to the feedstock. Natural products are one of the biggest contributors in the development of new treatments against a wide spectrum of different diseases, with more than 80% of substances in the traditional drug discovery processes having been made from natural products or inspired by a natural compound (Harvey, 2008; Mishra and Tiwari, 2011). In recent years, the widespread use of high-throughput screening and the post-genomic era has provided valuable new ways to search for bioactive compounds, and macroalgae have gained considerable interest among the scientific community due to their ability to synthesise secondary metabolites not found in land plants (Jeon et al., 2012). Given the fact that nearly 70% of the planet's surface is covered with water, and as such it is habitat to half of the global biodiversity becoming in the largest supplier of bioactive compounds (Kadam et al., 2013), offering opportunities to research these bioactives and developing new potential ventures in the expansion of Blue Economy.

Macroalgae are a rich source of natural products, due to the heterogeneous species that form part of the group, their different metabolic pathways and life strategies and, for their diverse defence mechanisms against grazers and other environmental aspects, e.g., spatial and seasonal differences, sun light availability, salinity, temperature, among others (Macaya et al., 2005; Stengel et al., 2011). Assessment of the bioactivities of

compounds from macroalgae, i.e., polyphenols, sulphated carbohydrates, or peptides have occurred the last decades for the development of bioproducts, such as pharmaceuticals, nutraceuticals, cosmeceuticals, bioplastics, among others (Smit, 2004). Applications such as anti-obesity, antipathogen, antimicrobial activities, their use in cosmeceuticals and prebiotics have been established and reviewed (De Jesus Raposo et al., 2016; Güven et al., 2010; Pérez et al., 2016; Thomas and Kim, 2013; Vera et al., 2011; Wan-Loy and Siew-Moi, 2016). In the following sections key classes of compounds of interest for extraction as part of a biorefinery concept will be highlighted.

1.3.1. Polysaccharides and sulphated polysaccharides

Macroalgae contain highly variable percentages of polysaccharides by dry weight of biomass (Vavilala and D'Souza, 2015) depending on the season and species, for instance, macroalgae contain total polysaccharide concentrations ranging from 4 to 76% DW, separating between storage and sulphated polysaccharides (**Table 1-2**). Carbohydrates exhibits a considerable diversity of compounds within species, although are composed from a relatively small number of monosaccharides, mostly C6 molecules except for alginate containing a mix of C6 and pentose (C5) monosaccharides, with molecular size ranges varying from 7.3 kDa to 1626 kDa (Gómez-Ordóñez et al., 2012). These building-blocks can be arranged in different combinations by a wide range of possible linkages, forming polysaccharides with considerable complexity (Stengel et al., 2011). The cell wall polysaccharides are mainly composed by units of cellulose and hemicellulose, neutral polymers, and are found to physically support the thallus in water (Vavilala and D'Souza, 2015). Cell wall and storage polysaccharides are species specific, and their concentration may change due to seasonal variations.

Some of the macroalgal polysaccharides of commercial importance are phycocolloids, such as alginate, carrageenan, and agar; another important carbohydrate due to its potential bioactivities is fucoidan. Alginic acid or alginate is a co-polymer of α-L-guluronate (G) and its C5 epimer β-D-mannuronate (M), and organised as

homopolymeric G or M blocks, alternating GM blocks, and/or random heteropolymeric G/M blocks; different species can provide alginate polysaccharides with varying combinations of these building blocks. Carrageenans are formed by linear galactans with disaccharide repeat units of α (1→3)-D-galactose and β (1→4)-galactose, ester-sulphated to a varying degree depending on species and extraction method. On the other hand, agars are formed also by galactans, but with units of α(1→3)-L-galactose and β(1→4)-galactose instead, that may be partially methylated (Stengel et al., 2011). They are used in several commercial applications such as thickeners, stabilisers, gelifiers, or emulsifiers (Menon, 2012). These polysaccharides can be classified as cell wall structural polysaccharides, mucopolysaccharides and storage polysaccharides (Laurienzo, 2010). Finally, fucoidan also known as fucose-containing sulphated polysaccharides, hereon Fucoidan, are sulphated polysaccharides found in the extracellular matrix in brown algae, are formed by a backbone of (1→3)-α-L-fucopyranosyl, or alternating (1→3)- and (1→4)-α-L-fucopyranosyl, and also contains sulphated galactofucans built of (1→6)-β-D-galactopyranosyl and/or (1→2)-β-D-mannopyranosyl units with fucose or fuco-oligosaccharide branching, and glucuronic acid, xylose or glucose substitutions (Garcia-Vaquero et al., 2017).

Sulphated polysaccharides (**Fig 1-3**) have received considerable attention for their potential bioactivity. These compounds are known for provide cell adhesion and the ones present in the intracellular spaces offer a protective barrier against pathogens, in macroalgae (Mestechkina and Shcherbukhin, 2010). Sulphated polysaccharides are present within all the three marine macroalgae groups, however they have species specific variants; in brown algae the most common forms are fucans (specially fucoidans); sulphated galactans (carrageenan and agaran) from red algae are widely used in the food industry because of their rheological properties such as gelling and thickening; and ulvans, heteroglycuronan and sulphated galactans from green seaweeds (Jiao et al., 2011; Pomin, 2011).

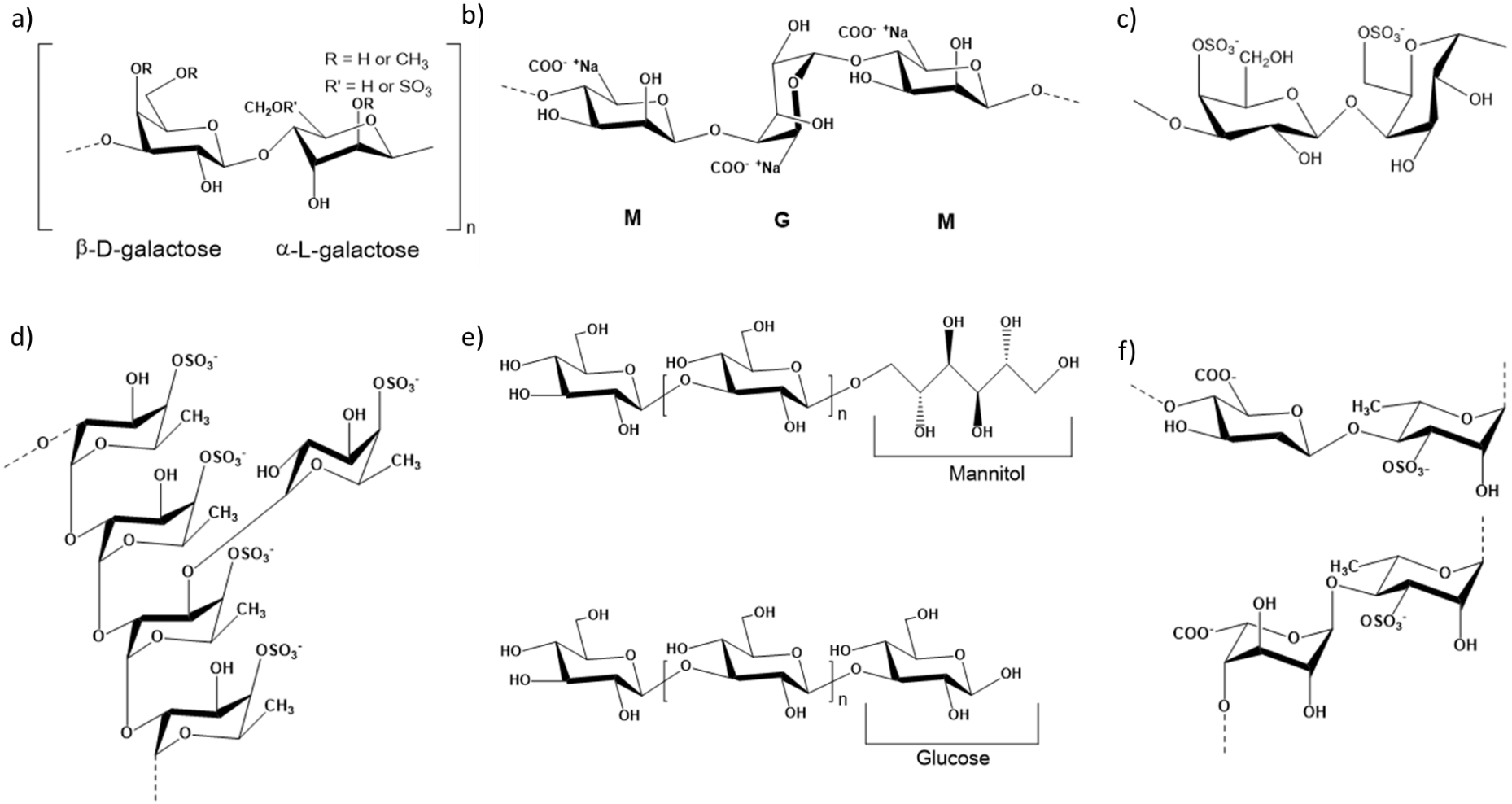

Fig 1-3. Some characteristic storage and sulphated polysaccharides present in the three groups of seaweeds: a) agar, R corresponds to the different radical group that can bind in that place; b) alginate, M and G corresponds to the building blocks used to synthesise these polysaccharides; c) μ-carrageenan; d) fucoidan; e) laminaran, showing the linkage of mannitol or glucose; f) ulvan.

Table 1-2. Total polysaccharides (% dry weight) in seaweed species across the globe.

Algal group	Storage carbohydrate	Sulphated polysaccharide	Genus	Total polysaccharides (%)	Reference
Brown algae	Laminaran	Fucoidan	Ascophyllum	69.6±0.2	Rioux et al. (2007)
			Fucus	65.7±0.4	Rioux et al. (2007)
			Laminaria & Saccharina	57.8±2.8	Rioux et al. (2007)
			Fucus	53.7	Tibbetts et al. (2016)
				42 – 70	Rioux et al. (2017)
			Undaria	35 – 45	Rioux et al. (2017)
			Macrocystis	47.05±1.63	Vásquez et al. (2019)
			Durvillaea	56.4±0.4 – 71.4±0.5	Ortiz et al. (2006)
Green Algae	Laminaran starch	Ulvan	Ulva	60.5±0.6	Ortiz et al. (2006)
				15 – 65	Rioux et al. (2017)
			Enteromorpha	61.5	Bocanegra et al. (2009)
Red algae	Floridean glycogen	Carrageenan	Porphyra	40.5	Bocanegra et al. (2009)
			Gracilaria & Agarophyton	58.4	Bocanegra et al. (2009)
			Chondrus	50.2 – 57.6	Tibbetts et al. (2016)
			Palmaria	31.7 – 59.0	Tibbetts et al. (2016)

1.3.2. Phenolic compounds, polyphenols and phlorotannins

Phenolic compounds (**Fig 1-4**) contain one or more phenol rings (polyphenols) in their structure which may be halogenated conferring biological activities. Phenolics are usually secondary metabolites, synthesised as stress compounds and commonly used by the seaweeds as a chemical defence mechanism against grazers, bacterial threats or other fouling organisms (Stengel et al., 2011), due to their capacity to confer the algae an astringent flavour, making them less palatable for these organisms (Macaya et al., 2005; Pérez et al., 2016). Phenolics are present in the three major seaweed groups, bromophenols for example are synthesised in the three groups.

Mycosporine-like amino acids, are low molecular weight (MW) (<400 Da), water soluble molecules composed of a cyclohexenone or cyclohexenimine chromophore with the nitrogen substituent. They belong to a family of secondary metabolites which their biosynthesis takes place through the first branch of the shikimate pathway (Chrapusta et al., 2017). They are most commonly produced and best characterised in Rhodophyta, some reports have declared the presence of these molecules in Chlorophyta and Phaeophyceae (Sinha et al., 2007).

One significant exception to polyphenols as secondary metabolites are phlorotannins in brown seaweeds, which exhibit primary functions e.g., in growth and development of the cell wall in Fucales (Schoenwaelder and Wiencke, 1999). Phlorotannins are only present in brown algae, and they are oligomeric or polymeric derivatives of the phloroglucinol monomer unit and biosynthesised through the malonate – acetate pathway, also known as the polyketide pathway (Li et al., 2011). Phlorotannins are highly hydrophilic compounds and with a wide range of MWs ranging between 126 Da (corresponding to the phloroglucinol unit) to 650 kDa (Li et al., 2011). Depending on the mean of linkage phlorotannins can be classified into four subclasses such as fuhalols and phlorethols (ether linkage), fucols (phenyl linkage), fucophlorethols (ether and phenyl linkage) and eckols (dibenzodioxin linkage) (Li et al., 2011). Phlorotannins have been extensively studied in the last decade, due to their described biological activities, such as

antioxidant, anti-proliferative, antimicrobial, anti-inflammatory, enzyme-inhibitory activities, among others (Nguyen et al., 2012). For example, phlorotannin extracts from *Eisenia bicyclis* exhibited α-glucosidase- and α-amylase-inhibitory activities, enzymes involved in diabetes, with the best half-maximal inhibitory concentration (IC_{50}) values of 93.33 nmol/L against α-glucosidase, and 42.91 μmol/L against α-amylase (Eom et al., 2012). Another enzyme-inhibiting activity from *Lessonia nigrescens* polyphenolic extracts, this time against angiotensin-I-converting enzyme (ACE), showed an ACE inhibition of 95.61±0.33% and an IC_{50} of 10.10±1.55 μg PGE/mg seaweed (Olivares-Molina and Fernández, 2016).

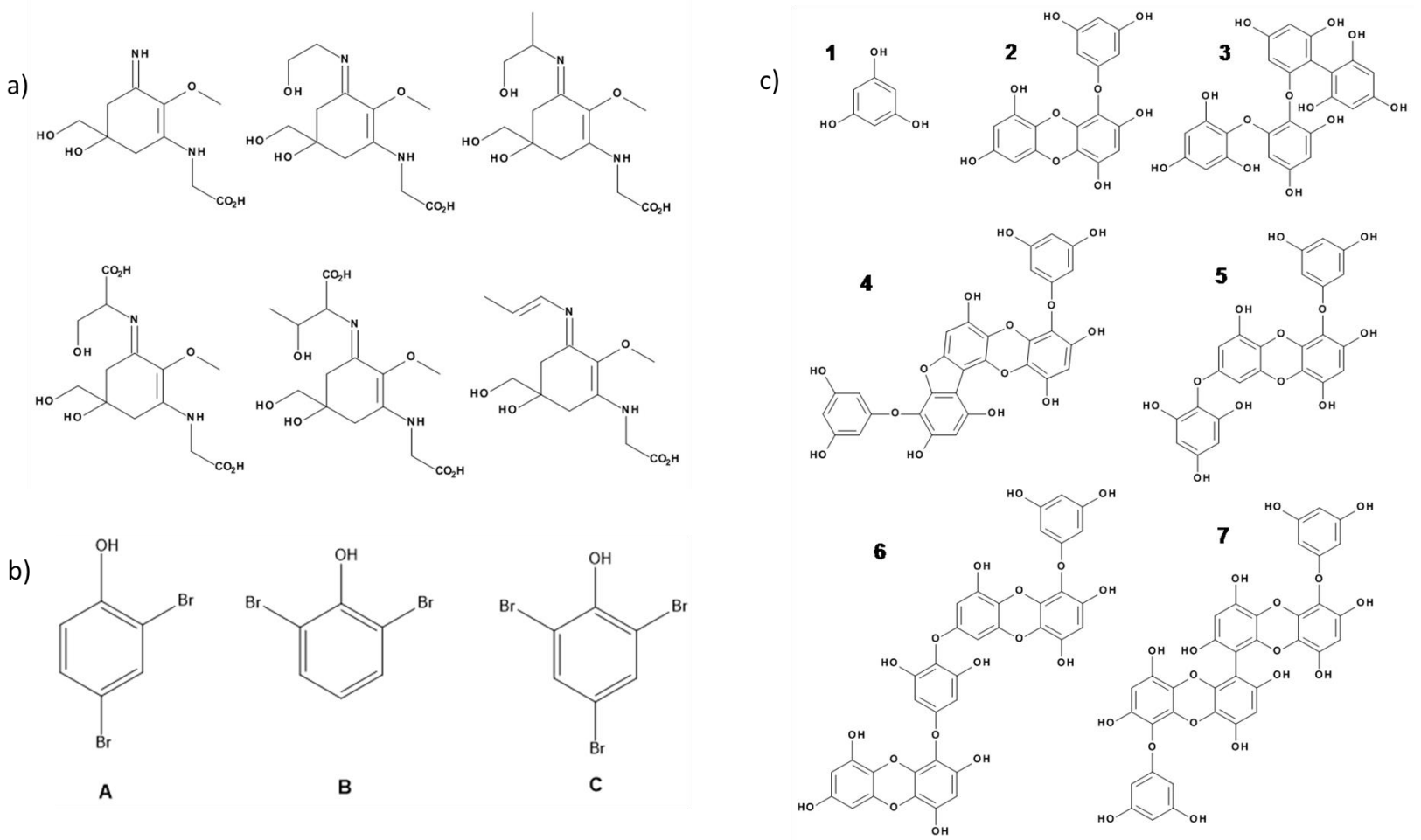

Fig 1-4. Examples of phenolic compounds found in seaweeds: a) mycosporine-like amino acids; b) bromophenols, A) 2,4-bromophenol; B) 2,6-bronophenol; C) 2,4,6-bromophenol. c) Phlorotannins 1. Phloroglucinol; 2. Eckol; 3. Fucodiphloroethol G 4. Phlorofucofuroeckol A; 5. 7-phloroeckol; 6. Dieckol; 7. 6,6'-bieckol.

1.3.3. Proteins and peptides

Protein contents differ within the three different macroalgal groups, with red seaweeds reaching the highest amount, between 25-45% DW, following green macroalgae with values around 9-26% DW, and lastly brown algae with values of 15% DW or lower (Harnedy and FitzGerald, 2011; Loveday, 2019), however protein content is dependent on season and geographical location and is linked to variables including nutrient supply. Macroalgal proteins represent a diverse and relatively less intense investigated group with regards to composition, structure, and bioactive potential than other algal constituents (Harnedy and FitzGerald, 2011). Apart from existing as free proteins or peptides they may be bound to carbohydrates, for instance glycoproteins and proteoglycans or pigments (e.g., phycobiliproteins), further increasing the spectrum of proteinaceous algal compounds.

Proteins have shown various bioactivities, like antioxidant, antibiotic, immuno-stimulating, enzyme-inhibiting activities (Holdt and Kraan, 2011), thus, it can be an attractive source to obtain these metabolites in a cascading sequence approach. These bioactivities have been described along the three groups, for example different protein extracts from the brown macroalga *U. pinnatifida* showed ACE inhibitory activity showing an IC_{50} ranging from 2.7 µM-43.7 µM using hot water extraction, 1.5 µM-42.3 µM from extracts obtained with protease S “Amano”, and 64.2 µM-213 µM of extracts obtained using Pepsin (Bleakley and Hayes, 2017).

Algal proteins are of importance as a source of dietary protein, essential amino acids, as well for the bioactive potentials of specific lectins, enzymes, and protein derivatives such as peptides (Stengel et al., 2011). Nutritionally speaking, most macroalgae are rich in aspartic and glutamic acid, some green algae like *Ulva pertusa* contains histidine at similar levels than legumes and egg proteins (Harnedy and FitzGerald, 2011), and in brown seaweeds the presence of taurine has been reported (Dawczynski et al., 2007).

1.3.4. Lipids

Mostly all the information that exists about algal lipids is from microalgae, research in lipids from macroalgae is still in its infancy, probably due to the fact they are relatively less abundant and have not drawn attention for biofuel production or nutritional formulations. Algal fatty acids are either saturated (SFAs), mono-unsaturated, or polyunsaturated acids (PUFAs); the last ones refer to chains longer than 18 carbon atoms which are important to human and animal nutrition, and which must be consumed from food sources. PUFAs include n−6 (ω-6) and n−3 (ω-3) fatty acids, for example arachidonic and eicosapentaenoic acid, respectively (Sánchez-Machado et al., 2004).

Lipid content in macroalgae has been described under 8% DW (Stengel et al., 2011). One of the most comprehensive studies in macroalgae was performed by Kumari et al. (2010), where they studied the lipid content of 27 macroalgae with values ranging from 0.57% to 3.5% DW, showing differences in their lipids profile. Chlorophyta and Phaeophyceae presented higher C18 PUFAs contents than Rhodophyta, while the latter and brown algae showed higher C20 PUFAs content than green algae (Kumari et al., 2010). Lipids content vary broadly between and within taxa, although total lipid content rather than profile is the main factor for some applications, i.e. biofuel production (Griffiths and Harrison, 2009). In contrast, lipid profiles can be of specific importance for applications in human health for example (Shannon and Abu-Ghannam, 2019). Lipids and fatty acids from macroalgae have recently received consideration due to their potential for uses in cosmeceuticals and beauty products, as antioxidant, anti-wrinkling, emollient, and regenerating agents, with some companies utilising micronised macroalgae to create cosmetic and even medical product (Kim, 2014). A company called Thalgo Cosmetic specialises in the production of cosmetics based on algae. The company produces a wide range of cosmetics, for example, antiaging serum and face creams, anti-acne face creams, moisturizing body lotions, facemasks, and sun protection products using *L. digitata*, *F. vesiculosus*, *Lithothamnium calcareum*, and other micronised algae (Fabrowska et al., 2015). There are also several companies on the

Polish market that produce cosmetics with micronised algae. Bielenda for example, offers body masks with micronised Fucus, and Laminaria, and a line of face algae masks for various types of skin containing mostly brown algae. Another cosmetics producer is Ziaja with the Sopot Spa series (face creams, body butter, peeling, micellar fluid) containing *P. umbilicalis*, *Enteromorpha compressa*, and *L. digitata* or Dermika with anticellulite body mask including micronised *F .vesiculosus* and *A. nodosum* (Fabrowska et al., 2015).

In general, lipid levels and composition, fatty acid levels included, vary according to season, growth conditions, location, and species (Terasaki et al., 2009). The composition also varies between geographic regions, for instance within the Chlorophyta phylum warm water species presents less PUFAs in their composition and more SFAs and oleic acid than organisms living in colder waters (Kumari et al., 2010).

1.3.5. Pigments

Photoautotrophic organisms fix carbon with the help of pigments associated with the photosynthetic process and some accessory pigments. Chlorophyll *a* being used by all of them, along with and several types of accessory pigments which are specific to particular algal groups (Stengel et al., 2011), with all groups exhibiting the presence of phycobilins and carotenoids (**Table 1-3**). Additional to Chlorophyll *a*, chlorophyll *b* is present in green seaweeds, and different classes of chlorophyll *c* are found in brown macroalgae.

Depending on their chemical structure seaweed pigments can be classified into the following different categories: closed tetrapyrroles such as chlorophyll *a* and *b* (chlorins), porphyrins (chlorophyll *c*), open tetrapyrroles (phycobilipigments), and finally carotenoids (polyisoprenoids with terminal cyclohexane rings; carotenes and xanthophylls).

Possibly the most commercially valuable group of pigments are carotenoids and phycobilins, but extraction of these compounds is developed mainly in microalgae, specifically green microalgae, and cyanobacteria (Prasanna et al., 2007). Carotenoids are divided in carotenes and xanthophylls; the most commonly occurring carotene is β-

carotene, and in macroalgae is produced mainly by Rhodophyta. Typical algal xanthophylls include astaxanthin, fucoxanthin, and zeaxanthin which all are reported commercial worth (Prasanna et al., 2007). While astaxanthin has established applications in aquaculture, extraction of these compounds for human nutraceutical supplements and bioactives is a growing market due to evidence of antioxidant, anticancer or antiviral properties, amongst others (Viera et al., 2018).

Phycobiliproteins (phycoerythrin, different phycocyanins, and allophycocyanins) from red algae have a long tradition of use as dyes in food, cosmetics, and as fluorescent markers in biomedical research (Stengel et al., 2011).

Table 1-3. Distribution of chlorophylls and main accessory pigments within the main algal groups, and minor pigments and those pigments so far reported only for some taxa within groups.

Group	Chlorophyll	Main accessory pigments	Examples of minor pigments or pigments with limited distribution within groups	Reference
Phaeophyceae	a c_1 c_2	β-carotene fucoxanthin zeaxanthin violaxanthin	Anteraxanthin-like cryptoxanthin-like cryptoxanthin-5,6-epoxide-like latoxanthin-like mactraxanthin-like carotenoids neoxanthin	Fernandes et al. (2016) Haugan and Liaaen-Jensen (1994)
Chlorophyta	a b	α-carotenes β-carotenes γ-carotenes lutein siphonoxanthin siphonein	Anteraxanthin astaxanthin canthaxanthin echinone neoxanthin violaxanthin zeaxanthin	Stengel et al. (2011) Wright et al. (1991)
Rhodophyta	a d	r-Phycocyanin b-phycoerythrin c-phycoerythrin r-phycoerythrin allophycocyanin α-carotene β-carotene	Antheraxanthin cryptoxanthin lutein violaxanthin zeaxanthin	Schubert et al. (2006) Takaichi et al. (2016)

1.4. Green technologies with potential in cascading extraction process

Biorefinery processes are not inherently sustainable, often relying on organic solvents such as strong acid or alkaline solutions, non-biodegradable chemicals, like sulphite-based solutions (Backa et al., 2012), acetonitrile (Schiener et al., 2016), among others. The change into a more sustainable view in biorefineries is one of the decisive steps for the future of the sector. Nevertheless, lack of information of environmental burdens regarding solvent use in biorefinery process make this exercise more complex to assess. Information comparing different process routes to produce bioethanol from lignocellulosic feedstock has been reported by Jeswani et al. (2015), where they compare thermochemical and biochemical conversions of biomass to ethanol. It has been reported that creating a product, namely bioethanol or platform chemicals, could require more energy than its fossil-based equivalent (Julio et al., 2017). It is for this reason that the need for green extraction processes to ensure sustainability has to be one of the developmental strategies for a Blue Economy approach for sustainability. There is a requirement for pre-treatment and extraction processes to be compatible with the concept of a cascading biorefinery to enable multi-product valorisation of biomass.

Green technologies have been proposed for pre-treatment of biomass to facilitate product extraction. These can take the form of biological treatments like enzyme-assisted (EAE) extractions (Wijesinghe and Jeon, 2012), or physical treatments such as microwave-assisted (MAE) (Alara et al., 2018); ultrasound-assisted (UAE) (Papoutsis et al., 2018). As an alternative to current practices that involve organic solvent for extraction or utilise strong acid or basic solutions, green technologies, such as extractions using aqueous two-phase systems (ATPS), supercritical fluid extraction (SFE), ionic liquids and deep eutectic solvents (Klein-Marcuschamer et al., 2011; Saravana et al., 2018; Sharma et al., 2015), that can be combined with ATPS as well; hydrothermal liquefaction (López Barreiro et al., 2015), or steam explosion (Ruiz et al., 2013) have been proposed to replace the use of organic solvents. Techniques such as liquid-liquid extraction (LLE) (Eriz et al., 2011), have been successfully applied to microalgal feedstock. For instance,

ATPS on microalgae metabolites has been reported, i.e., fucoxanthin from *Isochrysis galbana* and *Phaeodactylum tricornutum* (Gómez-Loredo et al., 2014), reporting recovery yields of 89% and 95%, respectively, with purity values of 79% and 66%, separately.

1.4.1. Pre-treatment techniques

a. Enzyme-assisted extraction (EAE)

EAE has been used extensively in second generation bioethanol biorefineries for pre-treatment of biomass, and to produce fermentable sugar from more complex polysaccharides. As the utilization of commercial enzyme in saccharification process is considered as expensive, production of enzymes from cheap substrate, immobilization of enzymes, and recycle and reuse of the enzymes are alternative solutions to make the enzymatic saccharification process commercially more viable for the bioethanol industry has made them feasible for pre-treatment, with cellulases and hemicellulases being the most commonly used to hydrolyse the cell wall of lignocellulosic feedstocks (Dey et al., 2020). For instance, immobilised enzymes and/or microorganisms producing key enzymes have been used in the production of bioethanol from lignocellulosic species in batch and continuous processes (Karagoz et al., 2019). On-site production of enzymes has been proposed as a potential step to reduce the operation cost (Guo et al., 2018). EAE has gained interest due to its potential to aid the production of bioethanol from macroalgae (Adetunji et al., 2017), but the lack of specific commercially available enzymes for macroalgae polysaccharides limits this approach. Enzymes used for lignocellulosics, and other commercial multi-enzyme mixes are used for seaweed bioethanol production (Torres et al., 2019); in addition, seaweed-specific enzymes had been reported in the production of bioethanol from macroalgae, i.e., degradation of brown seaweed polysaccharides with alginate lyases and laminarases (Lee and Lee, 2016).

Focusing on the degree of hydrolysis, first the appropriate enzyme to hydrolyse specific polymers present in the intact macroalgae has to be chosen (Wijesinghe and Jeon, 2012). This may require a screening approach of the hydrolysis conditions. A suggested strategy to identify the optimum condition for an EAE process is the high-throughput screening to identify areas, in a defined search space, where the enzymatic hydrolysis exhibits a better performance. Key parameters influencing enzymatic hydrolysis in a biorefinery context include pH, temperature, proportion of substrate to enzyme or enzyme concentration, substrate and product inhibition agitation, size of the interested molecules and mass transfer (Jeon et al., 2012).

To execute EAE at high performance, temperature and pH should be adjusted to their optimal conditions, to ensure the start of the enzymatic cascade reaction. Demonstration of the cascade reaction for the production of bioethanol from green seaweeds has been described by Reisky et al. (2019), where they reported a bacterial enzymatic cascade involving 12 carbohydrate-active enzymes, including two polysaccharide lyases, three sulphatases, and seven glycoside hydrolases to sequentially break down ulvan into fermentable monosaccharides. **Table 1-4** shows some examples of how EAE has been applied to macroalgal feedstocks.

EAE removes the barriers of water solubility and insolubility for bioactive compounds by degrading the cell wall for the release of polyphenols, carbohydrates (Olivares-Molina and Fernández, 2016), proteins (Vásquez et al., 2019), among others (Kadam et al., 2013). In the context of macroalgae carbohydrates extraction, EAE offers the benefits of high catalytic efficiency and preserves original efficacy of the compounds to a high degree when compared to organic solvents, for instance comparison of solvent-extracted polyphenol and carbohydrates from brown seaweeds were compared against enzymatic extracts obtained using α-amylase, enzymatic extracts exhibited the highest ACE inhibition of all extracts with a 95.61±0.33% inhibition, while solvent extracts only inhibited 91.66±2.19% (Olivares-Molina and Fernández, 2016).

Economically viable scale up of EAE is reliant upon the cost of enzymes and the loading required to process large volumes of raw materials that handled (Adetunji et al., 2017). The reproducibility of EAE processes needs to be established with large volumes. Enzymatic reactions need to be robust to deal with heterogeneity in biomass feedstock and the heat and mass transfer challenges of working in large scale vessels (Puri et al., 2012).

Table 1-4. Examples of EAE performed on macroalgae feedstocks.

Marine algae	Bioactive compound	Hydrolysis conditions	Process scale	Reference
Porphyra yezoensis	Proteins	Enzymes from the gut of abalones 2% w/v, room temperature, pH 6.0, 40 min.	100 mL	Amano and Noda (1990)
Ulva pertusa	Proteins	Cellulase and macerozyme mix 2% w/v, room temperature, pH 6.0, 40 min.	100 mL	Amano and Noda (1992)
Ecklonia cava	Polyphenols	Food industrial carbohydrases 5% w/v, 40-60°C, pH 4.5-8.0, 12 h.	100 mL	Heo et al. (2005)
Osmundea pinnatifida	Multiproduct extracts	Viscozyme L 100 mg, 50°C, pH 4.5, 24 h	50 mL	Rodrigues et al. (2019)
Sargassum muticum	Multiproduct extracts	Alcalase 100 mg, 50°C, pH 8.0, 24 h.	50 mL	Rodrigues et al. (2019)
Nizamuddinia zanardinii	Sulphated polysaccharides	Alcalase 5% v/v, 50°C, pH 8.0, 24 h.	200 mL	Alboofetileh et al. (2019)

b. Microwave-assisted extraction (MAE)

A microwave (μW) is an electromagnetic wave consisting of two oscillating perpendicular fields; electric and magnetic fields. μWs can pass through various materials and interact with the polar constituents to produce heat. The heating produced for the μWs interact directly with the molecules by ionic conduction and dipole rotation, and thus, only selective and targeted materials can be heated based on their dielectric constant. The effectiveness of the μW heating depends on the dissipation factor of the material, which

measures the ability of the sample to absorb μW energy and dissipate heat to the surrounding molecules (Mandal et al., 2008). For example, MAE has been used for the production of bio-oil from sewage sludge in pilot scale (Yunpu et al., 2016).

The operation conditions for MAE processes vary depending the macroalga utilised or the target compound to extract i.e. parameters that may affect MAE performance include composition of the extractant used, for instance employing solvents diluted with water (H_2O) allowing more green processes or moving entirely to extractions with water; solid-liquid ratio, extraction time and temperature, μW power, stirring, area of the contact surface, and the macroalgal tissue specific features, including its H_2O content.

For example, MAE has been used for extraction of sulphated polysaccharides (fucoidan) from *F. vesiculosus* (Rodriguez-Jasso et al., 2011). Different conditions of pressure (200-800 kPa), extraction time (1-31 min), and solid-liquid ratio (1:25 to 5:25 g/mL) were evaluated during this process. Total sugar yield (%), sulphate content (%), and algal residue after extraction (%) were also determined for every experimental condition. During the study, the extraction yield was significantly affected by all variables investigated. MAE at 800 kPa, for 1 min of treatment time, using 1 g of alga per 25 mL of water was the optimum condition for fucoidan recovery. MAE also has been applied for the extraction of polyphenols from *Saccharina japonica* (He et al., 2013). Different solid-liquid ratio was explored (1:8 – 1:12 g/mL), irradiation power, between 400 – 600 W, and extraction time (5 – 25 min). Best extraction yield was obtained using a solid-liquid ratio of 1:8 g/mL, extraction time of 25 min and irradiation power of 400 W.

Two advantages of MAE are the reduced extraction time and lower solvent requirements relative to conventional solvent extraction (Magnusson et al., 2017). There is a homogenous temperature gradient due to the non-conventional heating principle in a MAE process, the equipment size can be reduced, yet current equipment sizes for biorefinery processes are still in development (Ciriminna et al., 2016), and another advantage is the reduction of extraction time that indirectly protects the final product from degradation. Nevertheless, MAE presents some disadvantages as well, as it is an

energy intensive process due to the radiation power used; also, an additional separation process after completed the radiation is necessary to remove solids and debris from the extract liquor (Esquivel-Hernández et al., 2017).

c. Ultrasound-assisted extraction (UAE)

Sound waves with frequencies from 20 kHz (above the audible range of the human ears: 1-16 kHz) are referred to as ultrasound/sonication. These waves differ from electromagnetic waves in that a medium (solid, liquid or gas) is required for their propagation, involving a series of expansion (which pulls molecules apart) and compression cycles (which push them together). For a liquid medium, the expansion cycle can create bubbles/cavities which grow and subsequently experience collapse as the negative pressure exerted exceed the local tensile strength of the liquid. This process by which bubbles form, grow and collapse is known as “cavitation”, and is the basis for UAE. The cavitation process lasts about 400 µs during which high temperatures and pressures, about 5000°C and 1000 atm., respectively can be witnessed at the surface of the material treated.

Extraction yields are influenced by rigidity of the tissue structure. Variables such as alga tissue turgidity and the mobility of particles in the cell cytoplasm, can be expected to influence ultrasound energy spreading and extraction efficacy (Vilkhu et al., 2008). The differences may result as various degrees of compound susceptibility to ultrasound shockwaves and possibility that cavitation bubbles will interact with the alga surface producing microjetting, this process results in the peeling, destruction and breakdown of the surface of the macroalga, supporting the transfer of biological products to the extraction matrix (Venkatesan et al., 2017).

Yields will be influenced by the moisture content of the macroalga and particle size, this moisture content will vary depending on the drying method used, i.e., sun-dried samples will have higher moisture content than freeze-dried samples.

Correct choice of the solvent is the key to successful UAE. Solvent selection is decided by the solubility of the products to extract, it can be organic or non-organic depending on the target molecule, the interactions between solvent and macroalgae, and the power of ultrasound cavitation phenomena in the solvent (Chemat et al., 2017). Moreover, temperature, pressure, frequency, and sonication times are variable parameters for ultrasound extractions (Shirsath et al., 2012), and consequently influence yield and composition. According to Chemat et al. (2017), a higher temperature for UAE means a higher productivity in the extraction process through the increase of the number of cavitation bubbles and a larger solid-solvent contact area.

Nevertheless, this effect is diminished when the temperature is close to the solvent's boiling point. It is also imperative to avoid the degradation of thermolabile compounds (Chemat et al., 2009). For example, polyphenols conventionally extracted with methanol at 4°C and increasing the extraction temperature will automatically decrease the quantity and quality of the extract, therefore it is advised to work for short periods of time with this type of pre-treatment (Palma and Barroso, 2002).

In general, the maximum effectiveness of UAE, regarding to yield and composition of the extracts, can be accomplished by increasing the ultrasound power, reducing the moisture of macroalgae samples to improve solid-solvent interaction, and optimising the temperature to allow shorter extraction times (Chemat et al., 2009).

Intrinsic benefits of this pre-treatment method have been outlined by Adetunji et al. (2017) and include: more effective mixing and micro-mixing, faster mass and energy transfer, reduced thermal and concentration gradients and extraction temperatures, selective extraction, reduction in the size of equipment, quicker response to process extraction control, faster start-up, and increased production compared to conventional solvent extractions.

The reduction in solvent requirement is highly dependent on the attenuation of ultrasound waves in the dispersed phase. Depending on the conditions of extraction of a given system, this may mean that UAE does not greatly reduce solvent requirement after

all (Wang and Weller, 2006). Potential shortcoming on the effectiveness of ultrasound performance is the biomass-specific extraction kinetics of the alga during the recovery of the target biomolecules. Further, regarding to instrumentation, the decline in ultrasound intensity away from the proximity of the emitter means that uniformity might not be reached for all the materials dispersed in the solvents (Adetunji et al., 2017), when an ultrasound process is scaled-up to pilot-scale trials or higher the decline in ultrasound intensity in larger volumes has shown to become a challenge, thus, the need to increase the residence time of the feedstock around the sonication probe to reach the same yields of lab-scale trials had to be tested (Preece et al., 2017).

1.4.2. Extraction techniques

a. Aqueous two-phase systems (ATPS)

An ATPS is a liquid-liquid system formed from the incompatibility between two aqueous solutions of structurally different components creating two immiscible aqueous phases when assembled at critical concentrations (Rosa et al., 2010). ATPS can be formed of two polymers (commonly polyethylene glycol (PEG) and dextran) or a polymer and a salt (e.g., sulphate, phosphate, or citrate). These systems can be used to selectively partition biomolecules from other cellular components based on molecular properties such as the isoelectric point (pI). This type of integrated process, combining separation and purification with removal of debris into a separate phase (Rosa et al., 2010) is known as aqueous two-phase extraction.

The mechanism of separation in ATPS is complex and not easy to predict. In general, the partition of bioactives is a result of Van der Waals and ionic interactions of the biomolecules with the surrounding phase (Goja et al., 2013). Some of the key mechanisms have been identified: electrostatic, hydrophobic, and steric hindrance interactions between the phases and the compound of interest.

The most important factors that influence ATPS are those inherent to the phases, for example in ATPS based in PEG polymer characteristics like weight, size, and

concentration are important factors to consider. For instance, a higher molecular weight of PEG produces a smaller coefficient factor, between top and bottom phases, and then lower polymer concentration is needed for higher separation (Raja et al., 2012), on the other hand low molecular weight PEG has a hydrophilic end group with shorter polymer chains that reduces the hydrophobicity, while better partitioning can be achieved due to the low interfacial tension of low molecular weight (Goja et al., 2013). Regarding to the concentration of PEG, it has been demonstrated that highest concentrations of PEG lowered the partition coefficient (K_p) (Hemavathi and Raghavarao, 2011; Mehrnoush et al., 2011).

In PEG/salt based ATPS, increases in salt concentration result in an increase in K_p of bioproducts in upper phase or interface because of salting out. In general, biomolecules charged negatively tends to separate to the upper phase in these systems while those with positive charge commonly go to the bottom phase (Bora et al., 2005). The selection of salts for the setup of an ATPS depends on their capacity to promote hydrophobic interactions between biomolecules. Phosphate is the most commonly used salt (Raja et al., 2012), but nowadays other salts are being used as well, mainly because pollution related issues due to the phosphate effluent streams released to the environment. Some alternative salts used are sulphates and citrates (Murugesan and Perumalsamy, 2005). Anions are most effective in the separation (sulphate > phosphate > acetate) than cations (ammonium > potassium > sodium > magnesium > calcium) (Roe, 2001).

Another important factor involved in the performance of ATPS despite the composition of the phases is pH. Partitioning of metabolites into the phases in an ATPS is determined by their pI. The pH of the system, however, affects the charge of the wanted compound and ion composition as well as introduces differential partitioning into the two phases. Consequently, the initial pH of the system must be above the pI of target bioactives (Benavides and Rito-Palomares, 2008). In general, the effectiveness of the pH can be either by changing the charge of the solute or by altering the ratio of the charged species present. In a macroalgae context, when ATPS is used to extract proteins, peptides, or

polyphenols, these compounds tend to partition to the top phase due to their polar nature; different concentration and molecular weights of PEG might affect this partition as well. On the other hand, carbohydrates from macroalgae are anionic compounds and tend to partition to the bottom salt-rich phases because of their charge; correct selection of the phase-forming salt might increase the partition yield of these compounds. The tie line length (TLL) is often used to express the effect of system composition on partitioned material and has the same units as the component concentrations (i.e., % w/w) (Kaul, 2000). The ATPS becomes more hydrophobic with increasing TLL due to reduction of water availability (Mehrnoush et al., 2012).

Due to the complexity of interactions, separation of compounds in ATPS is mostly an empirical process. Optimum operation conditions are specific to the system phases and the target compound to extract. Prediction of the behaviour of target compounds in the system may be challenging due to the several forces involved in the partitioning of the compounds, i.e., hydrophobic, and electrochemical forces, size-dependent and conformation-dependent partitioning, bio-specific affinity, such as pI. To screen parameters more effectively, and reduce lead times of development, Design of Experiments (DoE) can be used to find the optimal purification process conditions. This enables assessment of the impact of the different experimental factors involved and to better evaluate the interactions between them (Rosa et al., 2010). Reports on the high-throughput screening (HTS) approach of selection of ATPS has been shown in proteins, enzymes, and deoxyribonucleic acid (DNA) (Asenjo and Andrews, 2012; Bensch et al., 2011; Wiendahl et al., 2012; Zimmermann et al., 2017). ATPS development can be hindered through analytical challenges as monitoring the characteristics of bioactives is the basic requirement for assessment of bioprocesses, which are affected frequently by the presence of high concentrations of polymers or salt (Goja et al., 2013). One of the first applications of ATPS in seaweed was performed by Jordan and Vilter (1991) (**Table 1-5**). The authors recovered bromoperoxidases from *L. digitata* and *L. saccharina* using a two-phase system composed of PEG 1550 and potassium carbonate (K_2CO_3). This

ATPS extracted around 720-765 U/g of bromoperoxidases, resulting in 93% of the total content. In **Table 1-5** are summarised some examples of ATPS conditions of these products (biopharmaceuticals, enzymes, and pigments).

Table 1-5. Examples of ATPS applied on extraction of macroalgal compounds extracted.

ATPS	Source	Target molecule	Process scale	Reference
PEG 1500-K_2CO_3	*S. polyschides*	Haloperoxidases	~100 g	Almeida et al. (1998)
PEG 1550-K_2CO_3	*L. digitata*	Bromoperoxidases	~1.0 kg	Jordan and Vilter (1991)
PEG 1550-K_2CO_3	*Laminaria saccharina*	Bromoperoxidases	~1.0 kg	Jordan and Vilter (1991)
PEG 3350-phosphate	*G. pusillum*	R-PE	N. D.	Mittal et al. (2019)
PEG 1450-phosphate	*G. pusillum*	R-PE	N. D.	Mittal et al. (2019)
PEG 1000-$(NH_4)_2SO_4$	*Enteromorpha* spp.	Sulphated polysaccharides	8.0 g	Du et al. (2018)

*N.D.: Not described

This technique has several potential advantages due to the low energy inputs and ambient operating conditions. Scale up is facilitated by the compatibility with standard mixer-settler equipment, making capital expenditure low (Glyk et al., 2015). In comparison with techniques such as solvent extraction using acid or basic solutions (Garcia-Vaquero et al., 2017), ATPS enables a comparatively quick separation with little denaturation as volatile organic components are not used. Considering that ~70% of the 2-phase system used for partitioning is water, along with the chance of recycling the phase-forming components, the use of hazardous chemicals in the process is diminished (Hatti-Kaul, 2000). Some drawbacks for the implementation of ATPS on an industrial setup are the cost of the polymer phases and the phase separation at higher volumes. Gravimetric phase separation in systems above 1 m^3 with a separation coefficient of 1 can take up to 15 h for highly viscous PEG-salt systems (Soares et al., 2015). Systems

with a high concentration of salts may also suffer from the ability of the phases to corrode metal pumps or other equipment (Rosa et al., 2009). Recycling of the phase-forming components may involve an additional step to separate the interest compound contained in the extraction phase. The recycled phase-forming components must fulfil the purity and performance requirements of a new ATPS re-using them (Rosa et al., 2010).

b. Supercritical fluid extraction (SFE)

SFE is a variation of a solid-liquid extraction, where a supercritical fluid replaces the solvent. SFE is a technique in which the solvent is in pressure and temperature conditions higher than its critical parameters. This critical environment reflects conditions in which liquid evaporation or gas condensation is not possible. The supercritical fluid conserves the dissolution capacity of liquids and transport properties of gases. Near the critical point there is a sudden growth of liquid density when pressure elevates. In this region solubility of many compounds is several folds higher than normal conditions and it would result from conventional thermodynamics of perfect gases. These properties make it suitable for extracting compounds in a short time with high yields and quality (Kadam et al., 2013).

SFE has been successfully applied at scale for extraction of fatty acids, pigments, phenolics, and flavonoids in macroalgae (Messyasz et al., 2017). In SFE the most used solvent is carbon dioxide (CO_2), due to its low critical parameters (T_c = 304.1 K, p_c = 73.8 bar) and its “green” characteristics, these are non-toxic, non-corrosive solvent that can be simply removed from the extract. Furthermore, CO_2 is inexpensive, accessible, and innocuous to the products, non-flammable, and exhibit great affinity to volatile compounds. In gaseous form, CO_2 can be easily and entirely separated from extract, leaving no hazardous residues, when compared to other conventional extraction methods (Michalak and Chojnacka, 2014). One of the main limitations of extraction with supercritical CO_2 is the low affinity of this solvent to extract polar compounds. Application

of modifying agents as an addition to CO_2 that would alter its polarity can be a solution to this problem. Examples of modifiers are ethanol, methanol, acetone, propanol, and water (Rój et al., 2015). Extraction of fatty acids performed with supercritical CO_2 and ethanol of *Ulva clathrate*, *Cladophora glomerata*, and *Polysiphonia fucoides*, showing a range of saturated and unsaturated fatty acids between C9:0 to C22:0 (Messyasz et al., 2017).

Chemical composition and particle size of biomass, different types of tissues, and other factors, like pre-treatment and conditions of storage of the biomass could also affect the yield and composition of the extract in SFE (Ahluwalia et al., 2013). Pressure, temperature, solvent type, solvent flow rate, and extraction time are critical process variables to be optimised for maximising extraction yields (Azmir et al., 2013). SFE with CO_2 has been demonstrated with macroalgal feedstocks for the extraction of fucoxanthin from *Sargassum muticum* with operating conditions of 400 bar and 55°C and fucoidan from *U. pinnatifida*, *Fucus evanescens*, *S. japonica*, and *Sargassum oligocystum*, with pressure conditions around 400 – 550 bar, and temperatures varying between 40 – 60°C (Esquivel-Hernández et al., 2017). As shown in **Table 1-6**, SFE offers flexibility and can be used to extract a range of polar and non-polar natural products from algal feedstocks.

The principal advantages of SFE are high solubility of polar compounds in CO_2, higher rate of mass exchange, no traces of solvent in the extract and in extraction residue (Rój et al., 2015), but the energy use in kWh is intensive due to the use of high pressure in the bioprocess; therefore, making the process energy-intensive and in some cases economically non-viable (Attard et al., 2015). Specialised high pressure equipment is required, thus making the initial capital expenditure a considerable commitment, and making it challenging to scale-up (Rodríguez-Meizoso et al., 2012).

Table 1-6. Operation conditions of SFE of bioactives from different micro- and macroalgae.

Marine algae	Compound	Conditions	Reference
Hypnea charoides	PUFAs	SFE system, CO_2, 40 to 50°C, 24.1 to 37.9 MPa, 2 h.	Cheung (1999)
Sargassum muticum	Polyphenols	SFE system, CO_2 modified with 12% ethanol, 60°C, 15.2 MPa, 90 min.	Anaëlle et al. (2013)
Hypnea musciformis	Polyphenols	SFE system, CO_2 modified with 8% ethanol, 40-60°C, 30 MPa, 7.5 h	Rozo et al. (2019)
F. vesiculosus	Antifungal extract	SFE system, CO_2, 50°C, 300 bar.	Tyskiewicz et al. (2019)
Sargassum muticum	Lipids	SFE system, CO_2, 45°C, 290 bar, 10 kg/h.	Terme et al. (2018)

To summarise, in **Table 1-7** can be seen all the techniques explained in this section comparing all the topics discussed here.

Table 1-7. Summary of the extraction techniques analysed.

Features	EAE	MAE	UAE	ATPS	SFE
Concept/methodology	Enzymatic hydrolysis of polymers	Electromagnetic wave absorption	Sound wave (>20 Hz) absorption	Incompatibility of two-aqueous solutions	Creation of liquid-like density and gas-like viscosity fluid
Principles for aiding Extraction	Increase porosity and release compound from attached polymer matrix	Disruption of hydrogen bonds thus causing cell wall to be porous	Causes tissue disruption, cell wall peeling, surface erosion, and breakdown of particles	The isoelectric point of the sample determines partitioning.	Increased penetration power and good solubilisation power into solid matrix
Specificity of action on biopolymer degradation	Specific	Not specific	Not specific	Not specific	Not specific
Scale-up	Possible but require more research	Possible	Not possible yet	Possible	Possible
Operation safety	Safe	Safe	Safe	Safe	Not safe
Pressure	Low (Environmental P)	Medium (~1 – 8 bar)	Low (Environmental P)	Low (Environmental P)	High P (~180 – 550 bar)
Temperature	Low (~25-40°C)	High (Microscopic boils)	High (Microscopic boils)	Low (Room T)	Medium (~40 - 70°C)
Cost	Enzymes are expensive while future trend might lead to cost reduction	Relatively low	Relatively low	Relatively low	Expensive to set up, while running cost is inexpensive
Side reactions/effect	No side reaction apart from intended action	Overheating of some region	Possibility of forming free radicals	No side reaction, nontoxic and non-flammable	No side reaction, nontoxic, and non-flammable
Suitability to heat-labile compounds	No effect on heat-labile compounds	Can cause damage to heat-labile compounds	No effect on heat-labile compounds	No effect on heat-labile compounds	No effect on heat-labile compounds

1.5. Techno-economic analyses (TEA) as a tool in macroalgae biorefinery

The intrinsic complexities of an economy based in the use of renewable feedstocks show a series of risks, uncertainties, and ever-changing circumstances, that make the investing in biorefineries more difficult, is in this scenario where TEA appeared to give robustness in the decision-making process for new biorefinery scenarios (Abbati de Assis et al., 2017). TEA has been used extensively to assess potential biorefinery concepts in recent years, mainly from first- and second-generation feedstocks focused on produce mainly bioethanol. The retail price of commercial bioethanol, or ethanol E85 in the USA, is around $3.85 per diesel gallon equivalent (Clean Cities, 2021). A summary of various TEA studies for biomass can be found on **Table 1-8**. Specifically to macroalgae, Konda et al. (2015) analysed the use of the brown seaweed *S. latissima* to produce bioethanol from its fermentable carbohydrates, using a value of $100/metric tonne (MT) feedstock value. They found in this report that the minimum ethanol selling price was in the range of $3.6-8.5/gal with a reduction of $2.9-7.5/gal using as $50/MT feedstock value. These results showed the economic challenges of this biorefinery concept. The challenges of this process were the main driver to analyse the co-production of alginate as well to highlight the importance of multiple sources of revenue. On another report, Charoensiddhi et al. (2018) modelled the economic feasibility of the industrial scale production of high-value bioactive compounds for the production of functional foods from the kelp *E. radiata*. They compared 4 different scenarios combining enzymatic- and/or solvent-assisted extraction with MW fractionation. The most profitable scenario was using enzymatic-assisted extraction followed by fractionation to produce 2 fractions (low and high MW polysaccharide and polyphenol fractions) with a net present value (NPV) of 81.88 $M and a payback time of 1.59 years. The least economically sound scenario was using solvent- and enzymatic-assisted extraction followed by MW fractionation, with a negative NPV of -8.26 $M and a payback time of 6.26 years. Even though most of these reports are theoretical exercises, there are examples with real collected data and modelling experimental processes. One current trend that has been

gaining notoriety is single cell oils (SCO), which are intracellular storage lipids comprising of fatty acids. SCO are produced by oleaginous organisms, i.e. microalgae, which are able to accumulate between 20% - 80% DW (Ochsenreither et al., 2016). Parsons et al. (2019). assessed the production process for SCO using the algae *S. latissima* on two different scenarios, results showed that SCO lipids and fats can be comparable to a terrestrial oil mix, with a break-even selling price between €5300 - €31000/ton refined SCO depending on seaweed price, although sensitivity analyses showed that potential technological improvements could enhance economic performance, and despite the current limitations of the process, macroalgae offers a viable option to produce exotic oils like cocoa or shea butter in price. This study used a different approach to use macroalgal biomass thus, instead of utilising the biomass for the extraction of high-value chemicals, the authors utilised the macroalgal biomass as a heterotrophic feedstock to produce SCO. Despite this different approach this study was one of the first reports using first-hand data from macroalgae species used in TEA. Finally, as an example of a TEA for high-value extraction process DeRose et al., (2019) modelled the economic feasibility of a process converting low lipid algae grown in algal turfs systems to fuels from renewable feedstocks; this TEA compared two processes, a biochemical pathway, and a hydrothermal liquefaction pathway. The results of this TEA indicated that the minimum selling fuel price in the biochemical and hydrothermal pathways was $12.85/gal and $10.41/gal, respectively, and when this results are compared against the prices reported by Clean Cities (2021), it is noticeable that the process is not economically viable at the moment. Most of TEA studies focused on macroalgal biorefineries are energy-focused rather than product-focused, concentrated in the production of bioethanol or other sources of bioenergy (Filote et al., 2021). A paradigm shift is needed to extract natural products with potential breakthrough in different markets before ethanol production, that can help in the overall profitability of the process. This change of focus can be reached with the use of green chemistry techniques to support the decarbonisation efforts to make more sustainable biorefineries

(Kerton et al., 2013). TEA may be combined with other evaluation tools, such as LCA, in a robust framework for the decision process for the development of new biorefinery processes.

Table 1-8. Examples of techno-economic analyses performed in different biorefinery feedstocks.

Generation	Feedstock	Product	Co- or by-product	Methodology	Reference
1st	Willow, switchgrass and miscanthus	Biofuel	Bioenergy, fibre pellets	TEA + LCA	Liu et al. (2017)
1st	Sugarcane	Biojet fuel	Lignin	TEA + GHG	Santos et al. (2018)
2nd	Olive stone	Xylitol	Ethanol, Furfural, PHB, Bioenergy	TEA + WAR	Hernández et al. (2014)
2nd	Corn stover	Ethanol or isobutanol	-	TEA	Brown (2018)
2nd	Banagrass	Ethyl acetate	Ethanol	TEA + LCA	Rajendran and Murthy (2017)
2nd	Spruce	Ethanol	-	TEA	Rodrigues Gurgel da Silva et al. (2018)
3rd	*C. vulgaris* and *B. braunii*	Lipids	-	TEA + LCA	Nezammahalleh et al. (2018)
3rd	*E. radiata*	Functional food product	-	TEA	Charoensiddhi et al. (2018)
3rd	*S. latissima*	Ethanol	Alginate	TEA	Konda et al. (2015)
3rd	Green alga	Biofuel	-	TEA + LCA	DeRose et al. (2019)

GHG: greenhouse gases; LCA: life cycle assessment; WAR: waste reduction algorithm

1.6. Life cycle assessment as a tool in macroalgae biorefinery

In order to quantify environmental impacts of a biorefinery process, LCA can be used as a tool to identify environmental hotspots. An LCA is a standardised framework that follows the guidelines of the International Organisation of Standardisation (ISO) 14040, 14041, and ISO 14044 (International Organization for Standardization, 2006), and gives a systematic and holistic tool to environmental impact assessments (Sadhukhan et al., 2019). As the name indicates, the perspective of LCA is the entire life of the product or process under investigation. An LCA quantifies the resource consumption (materials and energy), emissions, and the resulting environmental impacts throughout the supply chain, including raw material extraction and conversion, manufacturing, transportation, distribution, use, and final fate. The defined structure of LCA studies consists of the following stages: (i) goal and scope definition: where the cornerstones of the study are established; (ii) life cycle inventory (LCI): where all the mass and energy flows are calculated, and the focus is placed in collect data and structure the life cycle in separate unit processes; (iii) life cycle impact assessment (LCIA): where all mass and energy flows from LCI are converted in different impacts categories to analyse the environmental performance of the product or process; and (iv) life cycle interpretation: where the identification of significant issues, evaluation of the LCA and/or conclusions are drawn. Within the main impact categories assessed in the LCIA stages are climate change, which refers to the average increase of the temperature of the atmosphere, which could be caused by both natural and human-induced processes (Rajendran and Murthy, 2017). Climate change potential is measured in terms of kg of carbon dioxide equivalent (CO_2-eq.) in ReCiPe v1.13; ozone depletion, referring to the exhaustion of the ozone layer which safeguards from radiation. If the ozone layer is damaged it could lead to skin cancers and cataracts and in addition, it also affects crop cultivation, plants, and marine life. Substances which deplete ozone layer were chlorofluorocarbons (CFC) which were used in refrigerants, solvents, and foaming agents. Hence, ozone depletion was measured in kg of freon-11 equivalent (CFC-11-eq.) Terrestrial acidification relates

to the increasing concentration of hydrogen ions which leads to the addition of acids into the environment and was measured in terms of kg of sulphur dioxide equivalent (SO_2-eq.) Freshwater and marine eutrophication relates to the augmentation of an aquatic ecosystem with nutrients which increases the growth of algae and other weeds and was measured in terms of kg of phosphorus equivalent (P-eq.) for freshwater and kg of nitrogen equivalent (N-eq.) for marine eutrophication. Water depletion refers to the amount of water not being returned to its original source and measured in cubic metres equivalent (m^3-eq.) Finally, fossil depletion corresponds to the reduction of fossil fuels and was quantified with respect to fossil fuels as kg of oil-equivalent (oil-eq.) LCA can be performed using two modelling approaches, consequential LCA (CLCA) and attributional LCA (ALCA). CLCA can be defined as “system modelling approach in which activities in a product system are linked so that activities are included in the product system to the extent that they are expected to change as a consequence of a change in demand for the functional unit”, and ALCA can be described as “system modelling approach in which inputs and outputs are attributed to the functional unit of a product system by linking and/or partitioning the unit processes of the system according to a normative rule” (UNEP/SETAC Life Cycle Initiative, 2011). A supply chain scheme can be observed in **Fig 1-5** describing the operations involved in a theoretical biorefining process focused on the extraction of high-value products from brown macroalgae.

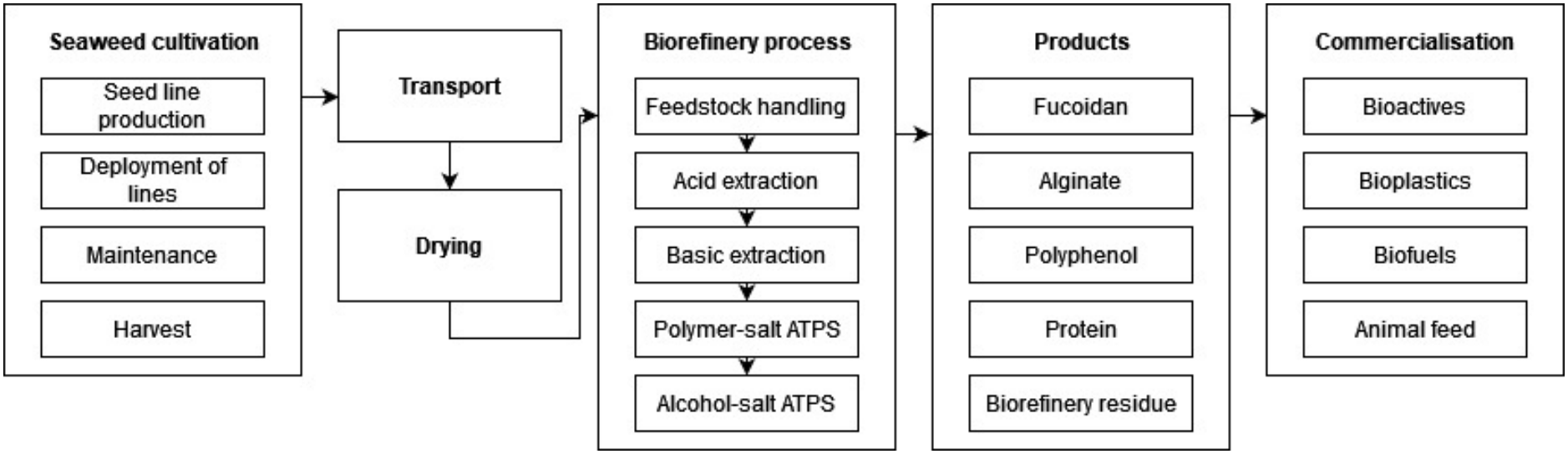

Fig 1-5. Scheme of the supply chain of a theoretical biorefinery process specialised in the extraction of high-value products from brown macroalgae. Seaweed cultivation is composed of seed line production, deployment of lines, maintenance during the growth phase and harvest; Transport involving water transport from cultivation site to harbour and road transport from harbour to biorefinery facility; Drying of biomass prior processing; Biorefinery process consisting of 5 main stages, i.e. feedstock handling, acid extraction to recover fucoidan, basic extraction to recover alginate, polymer-salt ATPS to recover polyphenol, and alcohol-salt ATPS to recover protein; Products formulation; and Commercialisation as bioactive components, bioplastics, biofuels, and/or animal feed.

LCA usually is an iterative process and its utilisation to measure the 'greenness' of products and processes has been championed as a strategic need in the development and use of sustainable technologies (Jiménez-González and Overcash, 2014). LCA can be combined with TEA to assess the sustainability of a biorefinery process in a more holistic way. As a way to illustrate the benefits of combine economic and environmental studies for early-stage technology assessment the combined LCA and TEA developed by DeRose et al. (2019) to produce biofuel from green algae grown on algal turfs systems can be analysed, even though it used microalgae instead of macroalgae. The global warming potential of the biochemical and hydrothermal pathways are 111.2 g CO_2-eq./MJ and -2 g CO_2-eq./MJ, respectively; hydrothermal pathway showed lower emissions than soybean and diesel emissions. LCA can be also combined with first-hand experimental results, for instance, the use of ATPS with ionic liquids has been reported for the extraction of R-PE from *Gracilaria* sp. in thermo-responsive systems, also analysing the greenhouse gases emissions of the processes using the EcoInvent database (Vicente et al., 2019). Reports of LCA on macroalgae biorefinery operations have focussed on the impacts of offshore cultivation (Filote et al., 2021). An assessment of *L. digitata* and *S. latissima* cultivation followed by 2 different biorefining processes, either an energy or protein production pathway, were assessed under different scenarios (Seghetta et al., 2017). All scenarios exhibited mitigation in climate change, and sensitivity analyses showed that all scenarios can further reduce their impact around 84 – 128% by technical improvements in the seeded line design, with the production of biogas from dried *L. digitata* via anaerobic digestion the most favourable one, with -18.7×10^2 kg CO_2-eq./ha and an energy demand of 1.7×10^4 MJ/ha, the lowest of all scenarios. On the other hand, biogas production via anaerobic digestion from dried *S. latissima* is the least favourable, but still reducing emissions compared to the control process, with -2.6×10^2 CO_2-eq./ha, and the protein pathway via hydrolysation using dried *S. latissima* had the higher energy demand, 5.9×10^4 MJ/ha. Reports of LCA on potential multi-product macroalgae biorefinery have been reported by Seghetta et al. (2016),

describing a cascading process to produce ethanol, proteins, fertilizers, on a cradle to grave approach. Results showed a mitigation of climate change factors of -0.1×10^2 g CO_2-eq./ha with an energy demand of 3.9×10^4 MJ/ha. Due to assimilation of nitrogen, there was a reduction in marine eutrophication (-16.3 kg N-eq./ha). It's important to highlight that in both studies changes in the cultivation technology generated changes in the human toxicity impact category, for example changing iron-made ballasts for stones to weight the seeded longlines had a lower impact due to the avoided emissions of chromium VI released from the iron bars to the ocean.

Green biorefining processes of bioactive compounds have also been analysed under this framework, a water extraction and particle formation on-line (WEPO) process was developed to extract antioxidants from rosemary leaves (Rodríguez-Meizoso et al., 2012), results showed a global warming potential of 1.8 kg CO_2-eq./g of antioxidant, 0.361 kg CO_2-eq./g, and 2.2 kg CO_2-eq./g if the process is deployed in Spain, Sweden, or Germany, respectively. Differences between the countries are due to the primary energy sources used for electricity generation, thus, the high dependence on fossil fuel burning of Spain and Germany resulted in higher impact factors. Other examples of the use of LCA in other biorefinery concepts can be seen in **Table 1-9**.

Table 1-9. Examples of life cycle assessments performed in different third generation biorefinery concepts.

Feedstock	Product	Co- or by-product	Functional unit	Methodology	Reference
L. digitata	Biomethane	-	1 MJ of compressed biomethane	ALCA	Czyrnek-Delêtre et al. (2017)
L. digitata and *S. latissima*	a) Biogas b) Macroalga hydrolysate	a) Fertiliser b) Proteins	1 ha of cultivated macroalga	Comp-LCA	Seghetta et al. (2017)
L. digitata and *S. latissima*	Ethanol	Fertilizer and fish feed	1 ton of macroalga	LCA	Seghetta et al. (2016)
L. digitata, *F. vesiculosus* and *S. latissima*	Fucoidan, laminarin	Feed supplement	1 kg of dry feedstock processed	Comp-LCA	Zhang and Thomsen (2021)
L. digitata	a) Biogas b) Bioethanol	a) - b) Biogas	1 ton of dry macroalga	Comp-LCA	Alvarado-Morales et al. (2013)
Sargassum, sea lettuce, and Eucheuma	Protein	Platform chemicals, minerals and nutrients	1 kg dry macroalga	Comp-LCA	Sadhukhan et al. (2019)
Gracilaria chilensis and *M. pyrifera*	a) Biogas b) Bioethanol c) Bioethanol	a) - b) - c) Biogas	1 MJ of energy produced	Comp-LCA	Aitken et al. (2014)
S. latissima	Single cell oils	-	1 ton of refined SCO	Comp-LCA	Parsons et al. (2019)

ALCA: Attributional LCA; CLCA: Consequential LCA; Comp-LCA: Comparative LCA

1.7. Final remarks

Macroalgae are untapped resources that offer a valuable sustainable feedstock for the design of third generation biorefineries. The natural products from macroalgae can be used in different industry sectors, such as the food industry with gelifying agents like alginate or agar, as well as fertilisers with the vitamin and mineral content of them. Potential applications of macroalgal bioactives had been reported with polyphenols, sulphated polysaccharides, proteins, and peptides having prospective breakthrough development in markets like biopharmaceuticals, cosmeceuticals, and nutraceuticals. Cascading extraction processes are a mechanism to maximise the product outputs from a macroalgal feedstock for the integral valorisation of the biomass, while helping the Blue Economy directives. As the development of third generation biorefineries progresses, the use of green chemistry extraction processes in a biorefinery context needs to be pushed forward in order to guarantee the sustainability of the bioprocess. This needs to be supported via modelling of economic and environmental metrics to give a robust and holistic decision process in the setup of new biorefinery concepts.

2. Overview of the thesis

2.1. Motivation and objectives

The previous sections of this chapter have underlined the need to switch to an economy more focused in renewable resources, emphasising the potential of the ocean-derived products for this endeavour. This switch can be reached with the use of marine macroalgae and their naturally-occurring compounds as potential products for the development of the Blue Economy, by means of the discovery and production of biopharmaceuticals, nutraceuticals, and cosmeceuticals using the chemical properties and bioactivities these compounds have exhibited. This chapter has also described the use of biorefineries to accomplish these goals, the challenges to implement seaweed-based biorefineries and the needs to valorise the biomass in a multi-product cascading sequence approach. The potential use of green chemistry principles to develop more

sustainable biorefining facilities has been highlighted as well. Lastly, this chapter described the use of early-design tools to provide key insights to the decision-making process, acknowledging the recent reports available with information regarding to third generation biorefinery concepts.

With this background and considering the natural variability in the chemical composition of seaweeds this project started asking: *"What is the most suitable macroalgal species from the coasts of the United Kingdom (UK) for the further exploration and development of a biorefinery concept?* (**Chapter 3**)".

Articles describing the use of early-design tools in biorefining scenarios using macroalgae have focused on the upstream processing portion of the operation, instead of the recovery and purification of high-value and bulk compounds. For that reason, the next question answered in this project was: *"What is the economic, environmental, and technical performance of a cascading biorefinery, specialised in the extraction of high-value compounds from macroalgae?* (**Chapter 4**)".

There are currently no published studies on the use of aqueous two-phase systems to recover polyphenols from marine macroalgae, as well as the lack of rapid screening techniques for polar compounds from plant matrices. This knowledge gap leads to the next question addressed in this project: "*What effect do the use of high-throughput screening will have in the development of an extraction process for polyphenols from brown seaweed using aqueous two-phase systems?*" (**Chapter 5**).

In the same lines, studies reporting the recovery and improvement of the extraction conditions of fucoidan are based in the use of strong acids like hydrochloric acid (HCl). Reports using mild acids are scarce, and there is no further optimisation in the extraction conditions, consequently the next questions explored in this project were: "*How do the use of a mild acid affects the recovery performance of fucoidan from brown seaweeds? And what are the optimal extraction conditions for the process?*" (**Chapter 6**).

Furthermore, there are a few studies using experimental data to evaluate the economic and environmental impacts of the use of macroalgae in a biorefinery approach. As

previously explained these studies are focused on the upstream processing portion of the operation, hence the final question addressed in this project was: "*What impact will have the use of first-hand data in early-design tools, to help in the decision-making process of new technology pathways based in green chemistry principles?*" (**Chapter 7**).

The aim of this research is to develop a multi-product biorefinery concept using macroalgae as a feedstock and using environmental and economic metrics to confirm and validate the robustness of the process. In this work a cascading sequence of extraction was established to recover fucoidan, alginate, polyphenols, and proteins from the brown macroalga *Ascophyllum nodosum* using green chemistry techniques.

2.2. Outline of thesis

The rationale followed for the development of this thesis can be seen in **Fig 1-6**. This thesis consists of seven additional chapters. In **Chapter 2** the general methods used to extract and/or quantify the macroalgal bioproducts of interest used to generate the results seen in **Chapter 3** to **Chapter 7** are described.

Chapter 3 explore different potential seaweed species to use in this project as feedstock in a biorefinery process, compounds of the algae candidates were characterised and compared between them and with literature results to make the selection of the most suitable feedstock.

Chapter 4 starts with the establishment of several biorefining scenarios using different technology pathways, in order to build the first approach of a cascading sequence for multi-product seaweed biorefineries, modelled to evaluate the economic and environmental performance of them, following the assessment of the technical feasibility of the chosen cascading sequence in the lab, in order to establish a preliminary decisional tool based in TEA and LCA for potential processes in third-generation biorefineries.

In **Chapter 5** and following the conclusions and suggestions of **Chapter 4** a high-throughput optimisation approach was used to improve the recovery of polyphenols

using aqueous two-phase systems. An automated method was developed for the construction of the systems and quantification of the recovery using phloroglucinol as a model polyphenol. In addition, a quantification method for polyphenols in presence of non-ionic detergents was established, and thus an optimised protocol was developed to recover polyphenols from *A. nodosum* using aqueous two-phase systems.

In **Chapter 6**, and as well as **Chapter 5**, following the conclusions given in **Chapter 4** an improvement in the recovery step of fucoidan was explored using different acid extraction processes, and following DoE methodology the best extraction conditions for this process were defined, and as a result a recovery strategy using citric acid in low concentrations was established.

In **Chapter 7**, the improved processes for the extraction of polyphenols and fucoidan developed in **Chapter 5** and **6** are inserted in the cascading sequence built in **Chapter 4**. The feasibility of this final assembly is tested in the lab, showing a new cascading sequence developed to extract fucoidan, alginate, polyphenol, and proteins from *A. nodosum* using green chemistry principles. The sequence is evaluated to confirm that an economic and environmentally sound process was established, and as a result utilise this approach as a holistic framework to evaluate the decision to implement a new biorefinery process.

Chapter 8 consolidates the work of the thesis and discusses opportunities and possible lines of investigation for future work.

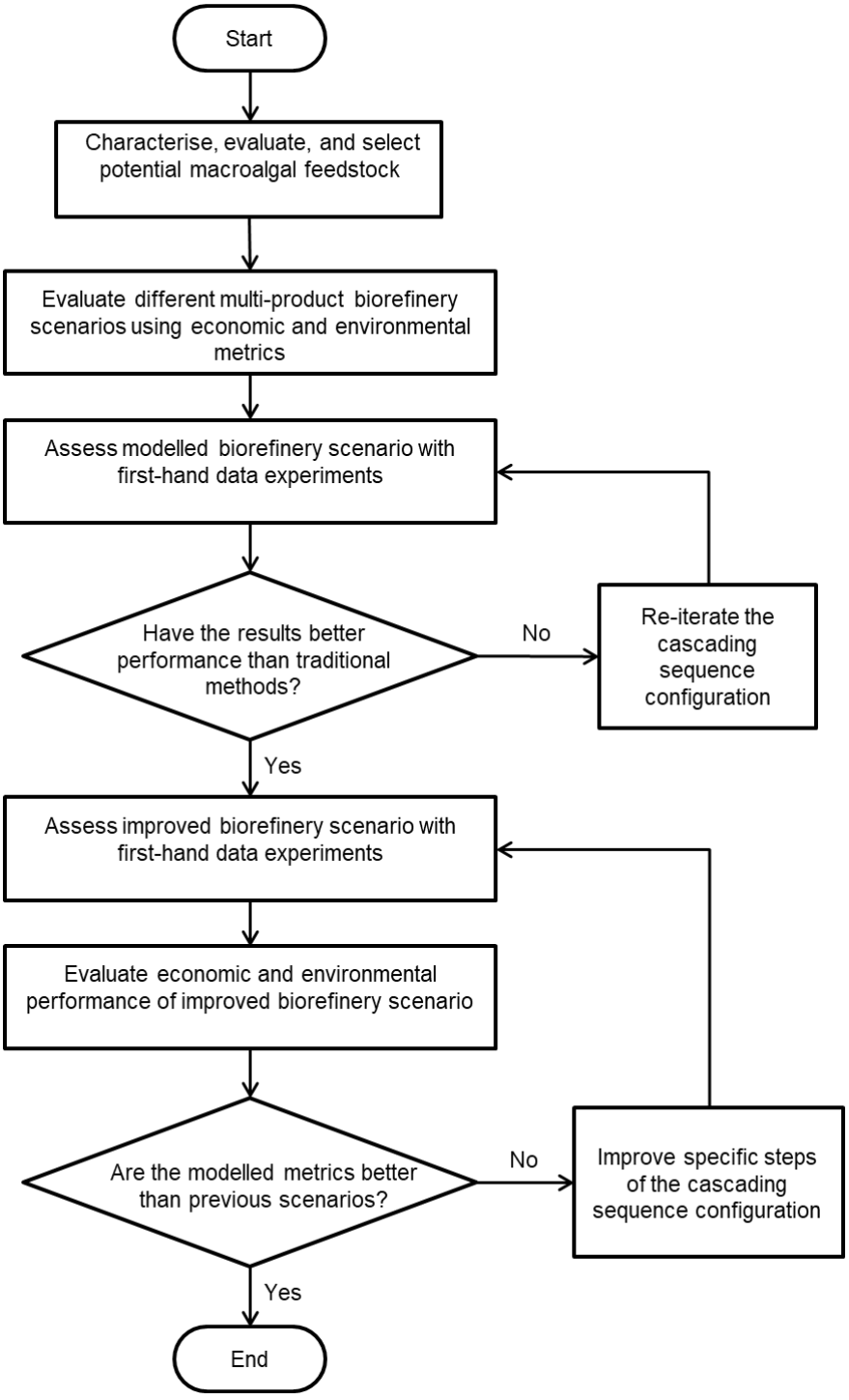

Fig 1-6. Proposed flow diagram for the development of a cascading third generation biorefinery.

Chapter 2: Materials and Methods

1. Materials

1.1. Macroalgal material

Three macroalgae species were examined for their potential as feedstock models for the development of this project; *Chondrus crispus* (red alga), *Himanthalia elongata* (brown alga) and *A. nodosum* (brown alga). *C. crispus* was purchased from Wild Irish Seaweeds Ltd (County Clare, Ireland) and *H. elongata* was purchased from Atlantic Seaweeds Ltd (London, UK), both species were wild harvested and transported whole to the laboratory where they were oven-dried overnight at 90°C. The biomass was then pulverised into macroalgae powder using a ball mill to a particle size of 300 µm. *A. nodosum* material was purchased from Hebridean Seaweeds Company Ltd (Isle of Lewis, UK), where it was wild harvested, dried, and milled on-site to a particle size of 300 µm and then dispatched to the laboratory. All macroalgae material was kept dry and stored in plastic containers at room temperature to proceed with the subsequent experiments.

1.2. Reagents and solutions

Analytical grade phenol (C_6H_6O), trifluoroacetic acid (TFA, CF_3COOH), glucose ($C_6H_{12}O_6$), potassium sodium tartrate tetrahydrate ($KNaC_4H_4O_6{\cdot}4H_2O$), copper sulphate pentahydrate ($CuSO_4{\cdot}5H_2O$) Folin-Ciocalteu reagent (mixture composed of lithium sulphate (Li_2SO_4), sodium tungstate (Na_2WO_4), phosphoric acid (H_3PO_4), HCl, and bromine (Br_2)), bovine serum albumin (BSA, CAS: 9048-46-8), potassium hydroxide (KOH), sodium hydroxide (NaOH), sodium carbonate (Na_2CO_3), gallic acid ($C_6H_2(OH)_3COOH$), dimethyl sulphoxide (DMSO, C_2H_6OS), potassium phosphate monobasic (KH_2PO_4) and dibasic (K_2HPO_4), tripotassium phosphate (K_3PO_4), phloroglucinol ($C_6H_6O_3$), PEG ($C_{2n}H_{4n+2}O_{n+1}$) 1000, 2000, 3000 and 6000 were purchased from Sigma-Aldrich (Saint Louis, Missouri, USA). Sulphuric acid (H_2SO_4), trichloroacetic

acid (TCA, $C_2HCl_3O_2$), and sodium dodecyl sulphate (SDS, $NaC_{12}H_{25}SO_4$) were from Merck (Darmstadt, Germany). Analytical grade acetone (C_3H_6O), copper sulphate pentahydrate ($CuSO_4 \cdot 5H_2O$), methanol (CH_3OH), ethanol (C_2H_5OH) and methyl orange ($C_{14}H_{14}N_3NaO_3S$) dye were from VWR International (Radnor, Pennsylvania, USA). Dimethyl formamide (DMF, C_3H_7NO) was purchased from Honeywell (Charlotte, North Carolina, USA). HCl and chloroform ($CHCl_3$) were from Fisher Scientific (Hampton, New Hampshire, USA). A Millipore milli-Q (Burlington, Massachusetts, USA) water purification system was used to purify the water used in all experiments.

2. Analytical extraction protocols in macroalgae

2.1. Analytical extraction of total carbohydrates

Total extraction of carbohydrates was performed according to DuBois et al. (1956) with minor modifications. Briefly, 25 mg of macroalgae was placed in a screw top test tube with an aliquot of 10 mL of 1M H_2SO_4, the mix was then heated at 90°C for 1 hour in a water bath. Samples were cooled down at room temperature and centrifuged for 10 min at 5500 rpm to remove biomass from supernatant. The sample supernatant was later quantified using the phenol-HCl method and at 480 nm according to **Section 4.2** from **Chapter 2**.

2.2. Analytical soluble polyphenol extraction

Polyphenol extraction was completed according to Olivares-Molina and Fernández (2016) with minor modifications. Firstly, 200 mg of dried and milled macroalgae was weighed and placed into screw cap glass test tube. An aliquot of 10 mL of acetone:milli-Q water 70:30 (v/v) was added, and samples were incubated for 1 h with continuous shaking at 250 rpm in an ISF-1-V Climo-Shaker Incubator and Platform Shaker (Kuhner, Switzerland) at room temperature. This step was repeated four times, and between extractions samples were centrifuged at 3200×*g* for 6 minutes in an Avanti J-E centrifuge (Beckman Coulter, UK). Supernatants of each individual sample were collected in a

single container, to produce one individual sample of each replicate. After extraction acetone was removed by evaporation in a Genevac EZ-2 centrifugal evaporator (SP Scientific, USA). The aqueous extracts were centrifuged for 15 minutes at 3,200×*g* to remove residual biomass, and the supernatant then was vacuum filtered through 0.7 µm pore GF/F filters (Whatman, UK), and frozen for subsequent analyses.

2.3. Analytical extraction of total proteins

The extraction was performed according to the method outlined in Slocombe et al. (2013). 5.0 mg of dried macroalgae biomass was weighed and placed into micro-centrifuge tubes. Then, 200 µL of 24% w/v TCA was added to every sample, and the mixture was heated for 15 minutes at 95°C in a Thermomixer C heater block (Eppendorf, Germany). After this, the samples were allowed to cool down at room temperature, and TCA was diluted to 6% w/v by adding 600 µL of milli-Q water, making a total volume of 800 µL. Next, samples were centrifuged for 24 min at 14,000×*g*, and the supernatant was discarded. The resulting pellet was re-suspended in 500 µL of Lowry D reagent (see **Section 4.5** from **Chapter 2**) and it was incubated at 55°C for 120 minutes. Later, samples were cooled down at room temperature and centrifuged again for 24 minutes at 14,000×*g* and the supernatants were recovered. Finally, with the extraction finished the protein content was quantified as described in **Section 3.4** from **Chapter 2**.

3. Cascading extraction step protocols in macroalgae

3.1. Extraction of fucoidan

Extraction of fucoidan was performed according to Lorbeer et al. (2015) with the following modifications. Briefly, 7.5 g of biomass were placed in 150 mL of aqueous HCl solution pH 5.5 (prior to the addition of the alga) and extracted with continuous shaking at 250 rpm and 33°C in an ISF-1-V Climo-Shaker Incubator and Platform Shaker (Kuhner, Switzerland) for 80 min. After extraction, the solution was neutralised by the drop-wise addition of 2M NaOH. Biomass was later removed by centrifugation in an

Avanti J-E standalone centrifuge (Beckman Coulter, USA) at 10,000×*g* at 4°C for 20 min collected and stored at -20°C for further experiments. The extract liquor collected was mixed with two volumes of anhydrous ethanol and left overnight at 4°C to precipitate the sulphated polysaccharides. The precipitate was later recovered with an Avanti J-E standalone centrifuge (Beckman Coulter, USA) at 10,000×*g* at 4°C for 20 min and freeze-dried using a Lyostar 3 (SP Scientific, USA). Dried material and precipitation supernatant were stored at -20°C for further experiments.

3.2. Extraction of alginate

Alginate extraction was adapted of Gomaa et al. (2018). Macroalgal powder or residual biomass (~6.6 g) from the fucoidan extraction step was placed in 200 mL of Na_2CO_3 2% w/v and extracted with continuous shaking at 250 rpm and 45°C in an ISF-1-V Climo-Shaker Incubator and Platform Shaker (Kuhner, Switzerland) for 2 h. Next, the mixture was centrifuged at 10,000×*g* at 4°C for 20 min in an Avanti J-E standalone centrifuge (Beckman Coulter, USA) to separate residual biomass from the alginate liquor. Residue was recovered for further experiments and the alginate liquor was mixed with two volumes of anhydrous ethanol and stored overnight at 4°C to allow the precipitation of sodium alginate strands. The precipitated alginate was recovered by centrifugation at 10,000×*g* at 4°C for 20 min and freeze-dried using a Lyostar 3 (SP Scientific, USA). Dried sodium alginate and supernatant from the precipitation step were stored at -20°C for further experiments.

3.3. Extraction of polyphenol

The extraction of polyphenols was performed according to Xavier et al. (2017) using ATPS. To prepare the system, an aqueous solution of PEG 2000 was combined with aqueous K_2HPO_4 in a relation 22.0:10.5% w/w. Macroalgal powder or residual biomass was added to the system to complete a total weight of the system of 50 g in accordance with a 0.5:10 solid-liquid ratio. The ATPS was mixed thoroughly for 30 s and allowed to

split the phases in a separatory funnel for 1 h at room temperature. After the extraction top and bottom phases were collected and the residual biomass in the bottom phase was separated using a Centrifuge 5810 R (Eppendorf, Germany) for 20 min at 10,000×*g*. Both phases were stored at -20°C for further experiments and residual biomass was recovered and stored at -20°C for further experiments.

3.4. Extraction of proteins

The protein extraction was performed using ATPS as explained by Phong et al. (2017). The system was formed by 20% w/w methanol combined with 30% w/w aqueous K_3PO_4 and completed with milli-Q water. Macroalgal biomass or biorefinery residue was added to the ATPS to complete a total mass of the whole system of 50 g following the solid-liquid ratio of 0.02:10. The ATPS was mixed thoroughly, and the system was allowed to divide the phases in a separatory funnel for 1 h at room temperature. After the extraction both phases were collected, and the final residue was separated via centrifugation in a 5810 R Centrifuge (Eppendorf, Germany). All phases were stored at -20°C for subsequent experiments.

4. Quantification of biological products from macroalgae

4.1. Moisture and ash content

The moisture and ash contents of macroalgae were determined according to AOAC (2000) protocols. Briefly, 100 mg of fresh biomass was weighed and placed in a porcelain crucible. The crucibles with the samples were oven-dried for 2.5 hours at 90°C. Samples were then cooled down for 10 minutes at room temperature, and were weighed again to determine the moisture content using the following equation:

$$\% \, Moisture = 100 - \frac{(M_{90} \times 100)}{M_i} \quad \textbf{(Eq. 2-1)}$$

Where, **% Moisture**: moisture content of the sample, **M_i**: mass of the sample at room temperature, and **M_{90}**: mass of the sample after 2.5 h at 90 °C.

For ash content, 100 mg of dried biomass obtained from the moisture determination at 90°C was weighed and placed in a porcelain crucible. The crucibles were placed in a muffle furnace, from the Energy and The Environment Group from the Mechanical Engineering Department at University College London, to progressively heat the samples until calcination of the biomass at 600°C for 2 hours. Next, samples were cooled down overnight and weighed again to determine the ashes content with the following equation:

$$\% \, Ashes = 100 - \frac{(M_{600} \times 100)}{M_i} \quad \textbf{(Eq. 2-2)}$$

Where, **% Ashes**: ashes content of the sample, **M_i**: mass of the sample at room temperature, and **M_{600}**: mass of the sample after 2 h at 600 °C.

4.2. Total soluble carbohydrate content

The carbohydrate content was assayed by colorimetric determination according to DuBois et al. (1956). First, 100 mg of biomass was weighed and re-suspended in 2 mL of 2 M TFA solution, and then this mix was heated until 121°C for 120 minutes in a Priorclave PS/MID/C40 autoclave (Priorclave Ltd, London, UK) used as a hydrolysis reactor. Next, an aliquot was taken and diluted 1:10, from the diluted solution 1 mL is taken and mixed with 0.6 mL of phenol 5% w/v aqueous solution, samples were vortexed for 3 seconds and then 3.6 mL of concentrated H_2SO_4 was rapidly added to the samples, which were vortexed again for 3 seconds. Samples were left 30 minutes at room temperature to cool. Finally, intensity of orange coloration in samples was measured at 480 nm in a Biomate 3S spectrophotometer (Thermo Scientific, USA). Blank samples were prepared using milli-Q water instead of total carbohydrate extract. A standard curve

of glucose was prepared using a concentration range of 0 – 100 µg/mL. The total carbohydrate contents were expressed as microgram of glucose equivalent per milligram of dried alga (µg GE/mg alga).

4.3. Total protein quantification

Protein content was quantified using the protocol developed by Lowry et al. (1951), as modified by Price (1965). Different "Lowry" reagents were made prior the quantification. Lowry A (2% w/v Na_2CO_3 anhydrous in 0.1 N NaOH), Lowry B (1% w/v potassium sodium tartrate tetrahydrate in milli-Q water), Lowry C (0.5% w/v $CuSO_4 \cdot 5H_2O$ in milli-Q water), and Lowry D (made on the day of the analysis from Lowry A, B, and C in the following proportions: 48:1:1). Folin-Ciocalteu 2 N reagent is used in this assay in a dilution of 1:1 v/v with milli-Q water. Once all reagents were prepared, 50 µL of protein extract was placed in a micro-centrifuge tube followed by 950 µL of Lowry D reagent; samples were mixed by inversion, and incubated at room temperature for 10 min. Next, 100 µL of Folin-Ciocalteu reagent was added to every sample and immediately mixed by inversion. Samples were allowed to stand for 30 min at room temperature, after which 200 µL of each sample was placed in a 96-well plate and the absorbance was measured at 600 nm using an Infinite M200 PRO microplate reader (Tecan, Switzerland). Blank samples were prepared using milli-Q water instead of protein extract. BSA was used as a standard, and a calibration curve was made using a range of concentrations from 0 – 5.0 µg/µL. The total protein content was expressed as micrograms of BSA equivalent per mg of dried alga (µg BSA Eq/mg alga).

4.4. Total lipid analysis

The method used for the total lipid determination was developed by Bligh and Dyer (1959) with the following modifications. Briefly, 500 mg of dried biomass was weighed and packed in a filter paper container and placed in a screw-cap glass test tube. Next, knowing the moisture fraction of the samples, milli-Q water was added to achieve a total

volume of 4 mL. Following this, 10 mL of methanol and 5 mL of chloroform were added to make a chloroform:methanol:water ratio of 1:2:0.8. The samples were homogenised by vortex for 5 minutes. Another aliquot of 5 mL of chloroform was then added and vortexed for 2 minutes, followed by an aliquot of 5 mL of milli-Q water and subsequent homogenisation in vortex for 2 more minutes, resulting in a final ratio of 2:2:1.8. After this step, the phases were allowed to separate, and the bottom phase (chloroform phase) was collected with a glass syringe and deposited in a glass watch dish to evaporate under fume hood, the glass watch dish with the lipid extract was weighed later.

To obtain the total lipid content of the sample was used the following equation:

$$\%\ Lipids = \frac{d \times b}{w \times \left(c - \frac{d}{0.92}\right)} \times 100 \qquad \textbf{(Eq. 2-3)}$$

Where, **% Lipids**: Lipid content of the sample, **b**: added volume of chloroform; **c**: aliquot volume of chloroform; **d**: lipids weight in the glass watch dish; **w**: initial weight of the sample; **0.92**: lipid's specific gravity; dimensionless term.

4.5. Total polyphenol content analysis

The total polyphenol content was quantified according to the method developed by Jerez et al. (2007) with the following modifications made by Olivares-Molina and Fernández (2016). Briefly, 100 µL of polyphenol extract was mixed with 500 µL of Folin-Ciocalteu reagent (diluted 1:10 v/v), this mix was homogenised using a vortex, and allowed to stand 3 minutes at room temperature. After this, 400 µL of 7.5% w/v Na_2CO_3 was added to the mixture, homogenised, and incubated for 15 minutes at 45°C. After this incubation 200 µL of each sample was placed in a 96-well plate and the absorbance was measured at 765 nm in an Infinite M200 PRO microplate reader (Tecan, Switzerland). Blank samples were prepared using milli-Q water instead of polyphenol extract. Phloroglucinol was used as a standard, and a calibration curve was made in the linear segment of the curve, using a range of concentrations of 10 – 60 µg/mL. The polyphenol content was

expressed as micrograms of phloroglucinol equivalent per mg of dried alga (µg PGE/mg alga).

4.6. Quantification of total polyphenols in presence of PEG.

The total polyphenol content cannot be quantified in presence of non-ionic detergents due to the precipitation of the Folin-Ciocalteu reagent. To be able to quantify the total polyphenolic content a surfactant was added, and the original method developed by Jerez et al. (2007) was modified accordingly. 100 µL of polyphenol extract was mixed with 500 µL of Folin-Ciocalteu reagent (diluted 1:10 v/v) and 20 µL of SDS, this mix was homogenised using a vortex, and allowed to stand 3 minutes at room temperature. After this, samples were centrifuged at 14000×*g* for 10 min and supernatant was transferred to a new micro-centrifuge tube. Next, 400 µL of 7.5% w/v Na_2CO_3 was added to the mixture, homogenised, and incubated for 15 minutes at 45°C in a Thermomixer R 2.0 mL block (Eppendorf, Germany). Following the incubation 200 µL of every sample were placed in a 96-well plate and the absorbance was measured at 765 nm in an Infinite M200 PRO microplate reader (Tecan, Switzerland). Blank samples were prepared using milli-Q water instead of polyphenol extract. Phloroglucinol was used as a standard, and a calibration curve was made in the linear segment of the curve, using a range of concentrations of 10 – 60 µg/mL. The polyphenolic content is expressed as micrograms of phloroglucinol equivalent per mg of dried alga (µg PGE/mg alga).

4.7. Pigment analysis

4.7.1. Chlorophyll *a* and total carotenoids

The content of Chlorophyll *a* and total carotenoids including chlorophyll *c* was performed according to Wellburn (1994). To extract the pigments, two different solvents were used, DMF and DMSO. Using DMF, 2.0 mg of biomass were weighed and placed in a micro-centrifuge tube, and then 1.0 mL of this solvent was added to the sample and shook in a Thermomixer C heater-shaker block (Eppendorf, Germany) at room temperature for 15

minutes. After this, the samples were centrifuged for 10 minutes at 10,000×g in a Mikro 120 centrifuge (Hettich, Germany). The pellet formed was usually white/clear and the supernatant greenish, however, if the pellet was still coloured, the sample was shaken and centrifuged again. Next, absorbance at 480, 647, and 664.5 nm were measured, and Chlorophyll *a* and total carotenoids were determined using **Eq. 2-4** and **2-5**. All experiments were performed in an environment that allowed sample protection from the light. A blank sample was made using pure DMF.

$$Chl\ a = 12.70A_{664.5} - 2.79A_{647} \quad \textbf{(Eq. 2-4)}$$

$$Chl\ (x+c) = \frac{1000A_{480} - 2.14Chl\ a - 70.16 \times (20.70A_{647} - 4.62A_{664.5})}{245} \quad \textbf{(Eq. 2-5)}$$

Where, **Chl *a***:Chlorohpyll *a*, **Chl *(x+c)***: Chlorophyll *c* and total carotenoids, $\mathbf{A_{480}}$: absorbance of the sample at 480 nm, $\mathbf{A_{647}}$: absorbance of the sample at 647 nm, $\mathbf{A_{664.5}}$: absorbance of the sample at 664.5 nm

In the case of DMSO, 2.0 mg of biomass were weighed and placed in a micro-centrifuge tube, then 1.0 mL of DMSO at 60°C was poured in the sample and heated at 60°C, following this the sample was shaken in a heater-shaker block for 15 minutes. Next, samples were centrifuged for 10 minutes at 10,000×g. Finally, absorbance was read at 480, 649, and 665 nm, and Chlorophyll *a* and total carotenoids were determined using **Eq. 2-6** and **2-7**. A blank was prepared using pure DMSO.

$$Chl\ a = 12.19A_{665} - 3.45A_{649} \quad \textbf{(Eq. 2-6)}$$

$$Chl\ (x+c) = \frac{1000A_{480} - 2.14Chl\ a - 70.16 \times (21.99A_{649} - 5.32A_{665})}{220} \quad \textbf{(Eq. 2-7)}$$

Where, **Chl *a***:Chlorohpyll *a*, **Chl *(x+c)***: Chlorophyll *c* and total carotenoids, $\mathbf{A_{480}}$: absorbance of the sample at 480 nm $\mathbf{A_{649}}$: absorbance of the sample at 649 nm $\mathbf{A_{665}}$: absorbance of the sample at 665 nm

With both procedures, the results obtained were expressed in microgram of pigment per milligram of dried alga (e.g., µg Chl *a*/mg alga).

4.7.2. R-phycocyanin and R-phycoerythrin

R-phycocyanin (R-PC) and R-phycoerythrin (R-PE) were measured in *C. crispus* using the method developed by Sampath-Wiley and Neefus (2007). Briefly, 100 mg of macroalgae biomass was weighed and placed in a micro-centrifuge tube; 1.0 mL of 0.1 M phosphate buffer (pH 6.8) was added and incubated overnight at 4°C. Next, samples were mixed thoroughly and centrifuged at 6,300×*g* for 15 minutes. The supernatant was collected, and the pellet was treated again with 0.6 mL of phosphate buffer, mixed thoroughly, and centrifuged at 6,300×*g* for 15 minutes, then the two supernatants were combined. The absorbance of the samples was measured at 564, 618, and 730 nm, and the content of R-PC and R-PE was determined using **Eq. 2-8** and **2-9**.

$$R - PC = 0.154(A_{618} - A_{730}) \quad \textbf{(Eq. 2-8)}$$

$$R - PE = 0.1247\big((A_{564} - A_{730}) - 0.4583(A_{618} - A_{730})\big) \quad \textbf{(Eq. 2-9)}$$

Where, **R-PC**: R-phycocyanin, **R-PE**: R-phycoerythrin, $\mathbf{A_{564}}$: absorbance of the sample at 564 nm $\mathbf{A_{618}}$: absorbance of the sample at 618 nm $\mathbf{A_{730}}$: absorbance of the sample at 730 nm.

The results were presented in mg of pigment per kilogram of dried alga (e.g., mg R-PE/kg alga).

4.8. Universal attenuated total reflectance-Fourie transform infrared (UATR-FTIR) spectra of fucoidan and alginate

The Fourier transform infrared (FT-IR) spectroscopy imaging measurements were performed using a PerkinElmer Spectrum Two spectrometer with a universal attenuated total reflectance (UATR) diamond/$LiTaO_3$ accessory arm (PerkinElmer, USA). For the sample imaging, around 10 mg of freeze-dried sample were placed in the diamond surface and pressed with the pressure arm till a force gauge of 90–110 units were achieved. UATR-FTIR spectra were collected over the 4000–400 cm^{-1} range by accumulation of 32 scans at 4 cm^{-1} resolutions. The spectra were recorded using the Spectrum 10™ software suite (version 10.5.0 PerkinElmer, USA). Prior to sample imaging a background spectrum was recorded and subtracted from the sample spectra. All experiments were performed in triplicate Gómez-Ordóñez and Rupérez (2011).

4.9. HPAEC-PAD quantification of monosaccharides profiles

The monosaccharide profile and concentration were quantified according to Bruhn et al. (2017) using a Dionex ICS-5000+ Reagent-Free Ion Chromatography, electrochemical detection using ED 40 and computer controller; an AminoPac™ PA10 column (2×250 mm) along with a guard column (2×50 mm) was employed, with a mobile phase of 5.0 mM of KOH at an isocratic flow rate of 0.25 mL/min. The injection volume was 10 µL and the column temperature was kept at 30°C. Monosaccharide standards of mannitol, fucose, arabinose, rhamnose, galactose, glucose, and xylose were used to generate the standard curves ranging 0.125–2.0 g/L. All samples obtained from the hydrolysation steps (see **Section 2.1** from **Chapter 2**) were loaded and quantified in triplicates.

4.10. Sulphate content

The sulphate group content of the freeze-dried fucoidan samples was quantified with a sulphate assay kit (Merck, USA) following supplier's procedures. Proprietary reagents were mixed with a re-suspended sample of fucoidan to produce a turbidity dependant reaction which was read at 460 nm using a Biomate 3S spectrophotometer (Thermo Scientific, USA). Blank samples were prepared using milli-Q water. A standard curve of sodium sulphate was prepared using a concentration range of 0.50 – 50.0 mg SO_4^-/L.

5. High-throughput screening methods

5.1. Apparatus

HTS experiments were performed using a Freedom Evo™ 200 (Tecan, Crailsheim, Germany) automated liquid handling station (LHS). This LHS was used to prepare all ATPS, binodal determination, and phloroglucinol partitioning. Freedom Evo™ 200 was equipped with an 8-channel air liquid handling (LiHa) arm with conductive polypropylene disposable tips connected to 0.5 mL dilutors. This station was controlled by Evoware Standard 2.6™ software.

5.2. Optimisation strategy for the extraction of polyphenols

The strategy used to optimise ATPS partitioning followed a scale-down approach combined with high-throughput screening. The determination of the binodal curves was performed using 10 µL methyl orange dye, a hydrophobic compound that will always partition to the top phase. 2% w/w screening variation of the phase-forming components was used to build the said curves.

The manual preparation of phase systems was conducted in 1.5 mL micro-centrifuge tubes. Appropriate amounts of PEG solutions were added, followed by potassium phosphate buffer, water, and methyl orange dye. The systems were mixed using a vortex for 15 s, followed by a settling time of 1.5 h. All systems were built to a working volume

of 800 µL. Pipettes were used for sampling the bottom phase. All experiments were conducted at 23±2°C.

Completed the manual determination, and prior to the automated determination of the curves pipetting was calibrated by adjusting the relevant parameters such as aspiration and dispensing speed and height, air gap sizes and waiting times for each solution to be pipetted and a 2% w/w screening variation of the phase-forming components was used. Phase systems were prepared by subsequent addition of PEG 1000, 2000, 3000, and 6000, phosphate buffer and water in 1.2 mL 96-deep-well plates. For the determination of binodal curves a 10 µL of methyl orange was added into each sample well. All systems reached a total volume of 800 µL and were mixed through repeated aspiration and dispensing cycles and allowed to separate for 1.5 h. After the settling time is completed, 50 µL were aspirated from the bottom of the deep-well plate and transferred into a microplate. For the systems investigated in this study, methyl orange always partitions to the top phase. In one-phase systems, methyl orange is distributed homogenously over the entire system. In two-phase systems on the other hand, the dye partitioned completely to the top phase leading to an almost transparent bottom phase. Finally, separation of phases was observed and phase-forming systems where it occurred were selected together with the one-phase systems preceding them (without phase separation) to build the binodal curves estimating the parameters of the exponential fit (**Eq. 5-1**) developed by Merchuk et al. (1998) using the curve fitting toolbox on MATLAB.

After the estimation of the binodal curves screening, the partition of polyphenols was assessed using HTS with the LHS and using phloroglucinol as a model molecule. All the systems assessed were built on the same manner as explained in the automated determination of the curves, but a fixed amount of phloroglucinol was added to each ATPS (10 µL) instead of methyl orange, and samples were mixed after seven aspiration/dispensing cycles (Bensch et al., 2011). All the systems were allowed to partition for 1.5 hour, and after completed this step 50 µL were aspirated from the top

phase of the deep-well plate and transferred to a microplate for absorbance quantification at 267 nm.

The best candidate ATPS mixtures to partition polyphenols were identified and further scale-up of these systems was evaluated. Systems were scaled up 40 times completing a total volume of 50 mL and the recovery yield between the scaled-down and scaled-up systems was quantified according to the **Section 4.6** from this **Chapter**.

6. Improvement strategy for the extraction of fucoidan

Two extraction methods using three different acids, citric acid, HCl and H_2SO_4, were tested to determine the best protocol to obtain fucoidan from macroalgae. The first method was performed according to **Section 3.1** from **Chapter 2** instructions, but the conditions were expanded to include analytical grade citric acid and H_2SO_4 solutions pH 5.5. The second method was performed according to Gomaa et al. (2018). 2.25 g of biomass were placed in 150 mL of 0.2 M acid solution and extracted with continuous shaking at 250 rpm and 30°C in an ISF-1-V Climo-Shaker Incubator and Platform Shaker (Kuhner, Switzerland) for 120 min. After extraction, the solution was neutralised by the drop-wise addition of 2M NaOH. Biomass was later removed by centrifugation in an Avanti J-E standalone centrifuge (Beckman Coulter, USA) at 10,000×*g* at 4°C for 20 min and collected for further experiments. The extract liquor collected was mixed with two volumes of anhydrous ethanol and left overnight at 4°C to precipitate the sulphated polysaccharides. The precipitate was later recovered using an Avanti J-E standalone centrifuge (Beckman Coulter, USA) at 10,000×*g* at 4°C for 20 min and freeze-dried using a Lyostar 3 (SP Scientific, USA). Dried material and precipitation supernatant were stored at -20°C for further experiments. After selected the best acid to extract fucoidan, the best conditions for the extraction were selected using DoE.

A simple 2^2 factorial design with three replicates at the centre point was used to evaluate the combined effect of two variables (temperature and initial biomass loading) in the fucoidan extraction step, each at three levels, on one response, which was fucoidan

recovery. The experimental domain was defined around the conditions of the different acid trials stated above, using solids loading conditions between 2.25 and 7.50 g, and temperature between 30 to 50°C. To confirm results obtained an expanded domain was used extending no further than twice the distance from the centre-point of the domain. The expanded domain used an increased initial biomass of 10 g. All data was analysed with Design-Expert 11™ (Stat-Ease Inc, USA) and JMP Pro 15™ (SAS Institute, UK) suites.

7. Statistical analysis

Data were expressed as the means ± standard deviations (SD). For group comparisons the Student t-test for independent samples was performed where applicable ($p < 0.05$). When analysis of variance (ANOVA) was needed the distribution of grouped variables was calculated first, to determine the homoscedasticity of data. In addition, to check if data was parametric, Levene's and Cochran's C tests were applied ($p > 0.05$). After confirmed the homogeneity of data, a one-way ANOVA was performed to verify if significant differences ($p < 0.05$) occurred between the samples. Parametric data was analysed using the *post-hoc* Tukey HSD test ($p < 0.05$). Non-parametric data was analysed by Kruskal-Wallis ANOVA ($p < 0.05$) test, followed by a multiple comparison of means ($p < 0.05$). All statistical analyses were performed in STATISTICA 7.0 suite.

Chapter 3: Characterisation and selection of potential macroalgal feedstock for a multi-product biorefinery.

1. Introduction

Selecting the right feedstock for a biorefinery process determines the compounds available for extraction, and therefore informs process design. In the context of Blue Economy development strategies, the use of macroalgae in a biorefinery facility would impact developing areas, i.e., creating jobs for coastal or island communities and environmental benefits concerning the sequestration of CO_2 and nitrogen (Wood et al., 2017). The commercialisation of red and brown macroalgae has been proved feasible with a compound annual growth rate of 9.1% per year (Grand View Research, 2020), and the extraction of their components has gained interest due to several components with real applications in industry (White and Wilson, 2015), in the form of gelling agents, and several compounds with potential breakthrough applications in the market (Samaraweera et al., 2012), as components for cosmeceutical, biopharmaceutical, and nutraceutical applications, as well as compostable substitutes for plastic packaging.

Macroalgae industrial activities in the UK has been based in the harvest of wild communities along the shore, and used mainly for food, feed, and fertilisers (Wood et al., 2017). Despite the lack of information about harvesting quotas in the UK, data compiled from Ireland showed that the most commercially harvested species were brown and red seaweeds, with *A. nodosum*, *H. elongata*, and *C. crispus* as examples (Edwards and Watson, 2011). *C. crispus* or Irish moss is a cartilaginous, dark purplish/red macroalga inhabiting the coasts of the British Isles as well as parts of Northern Europe and the Atlantic coasts of Canada. This seaweed has been harvested through the years for its hydrocolloids and the uses of them in several industries (Craigie et al., 2019). *H. elongata*, also known as sea spaghetti, is a brown seaweed found in the Northeast Atlantic Ocean traditionally consumed as sea vegetable (Rioux et al., 2017) and with

reported biological activities (Martelli et al., 2020). *A. nodosum* or knotted wrack is a brown macroalga commonly found in the Northern Atlantic Ocean harvested for the extraction of alginates, or the production of animal feed (Schiener et al., 2017). These three macroalgae are currently used in different sectors, but only to use the biomass as a commodity or to only extract a single commodity chemical, moreover their use in a possible cascading extraction sequence approach had not been reported at the time of execution of this chapter. Therefore, these three organisms were considered for evaluation of their chemical composition.

In this chapter, three seaweed candidates were characterised and then compared their potential as biorefinery feedstock based in the content of certain important metabolites with economic interest in the market. For this reason, this chapter uses the analytical extractive methods and quantification protocols described in **Chapter 2** (**Section 2** and **4**, respectively) to select the most suitable candidate for the following experiments, and thus establish the biochemical composition of macroalgal material sourced from the UK to aid to utilise it as a benchmark for the subsequent decision-making processes in the project.

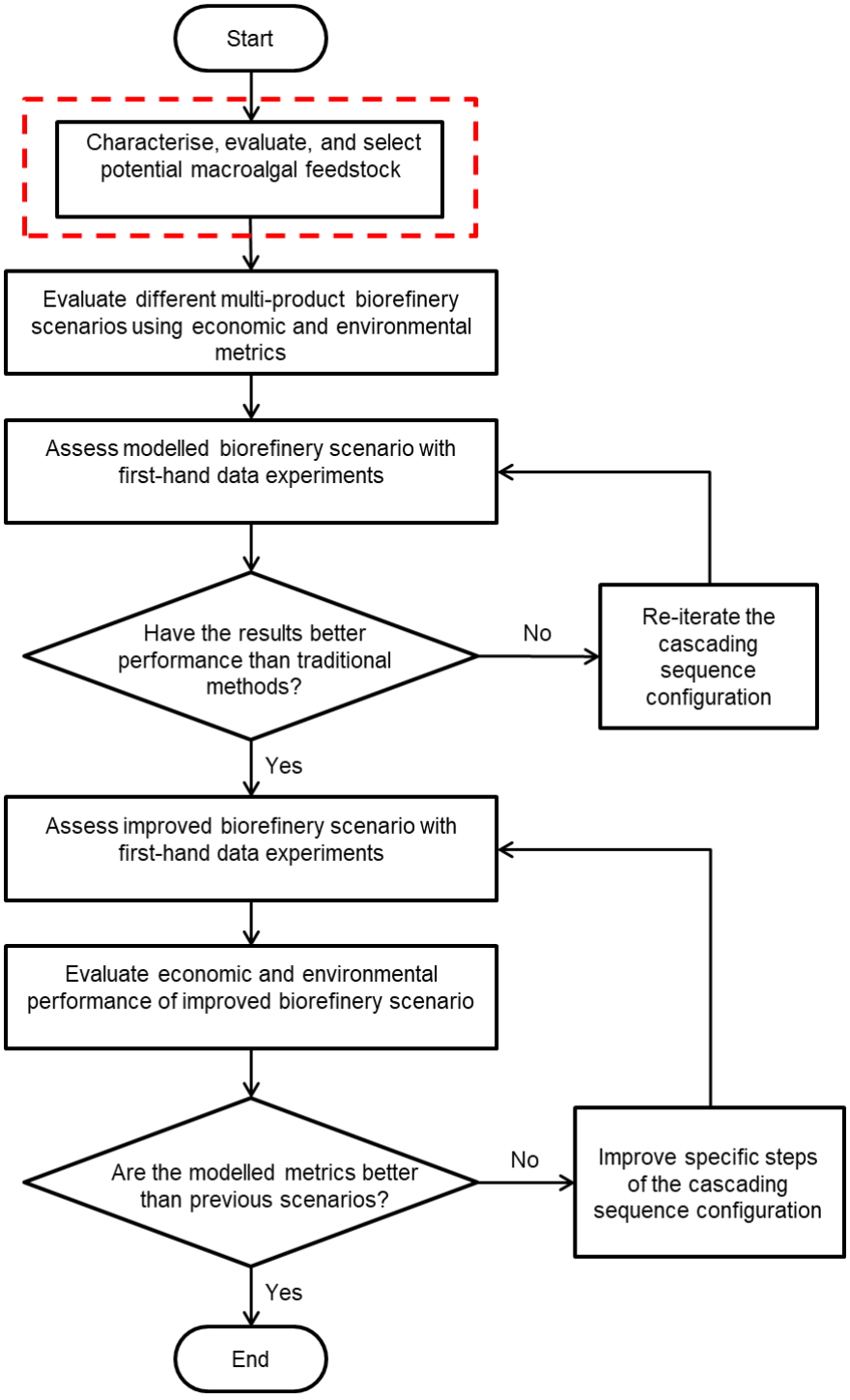

Fig 3-1. Proposed overall methodology for the development of a multi-product macroalgal biorefinery. In the red dashed box is highlighted the step covered in this chapter.

2. Results and discussion

The portion covered in this chapter compared with the overall project scheme can be observed in **Fig 3-1**. Carbohydrate, as a proportion of dried biomass differed between these species, with values in *C. crispus* of 69.36±15.81% DW, the higher percentage obtained for all the constituents in these macroalgae, *H. elongata* showed a content of 53.73±1.88% DW, and *A. nodosum* with 34.22±4.14% DW. The protein and moisture content of all macroalgae were around the second highest components found in all candidates with percentages of ~8.0% DW or ~8.0 g/100 g algae in *H. elongata*; 4.34±2.50% DW and 5.38±0.27 g/100 g algae respectively for *C. crispus*, and approximately 11.33±0.21% DW and 12.01±0.08 g/100 g algae respectively in *A. nodosum*. The lipid content was higher than reported in literature (Bocanegra et al., 2009; Sánchez-Machado et al., 2004) for *H. elongata* and *A. nodosum*, although it was lower in the case of *C. crispus*. Polyphenol content was higher in *A. nodosum* with around 5% DW, following *H. elongata* (1.62±0.03% DW) and *C. crispus* (0.24±0.02% DW). The polyphenol and protein content varied widely across the three algae. The summary of the chemical composition of the macroalgae candidate feedstocks can be seen in **Table 3-1**. The other components that formed the remaining dry weight content are likely to include structural carbohydrates, and crude fibres.

Table 3-1. Proximate chemical composition of potential feedstocks on a dry weight basis.

Species	Proximate chemical composition % dry weight (% DW)					
	Moisture*	Ash	Carbohydrate	Protein	Lipid	Polyphenol
C. crispus	5.38±0.27	18.66±4.17	69.36±15.81	4.34±2.50	2.02±0.78	0.24±0.02
H. elongata	7.72±0.25	27.49±1.94	53.73±1.88	7.80±0.49	1.64±0.44	1.62±0.03
A. nodosum	12.01±0.08	29.21±0.60	34.22±4.14	11.33±0.21	8.04±0.98	4.63±0.48

*: Moisture was expressed in g/100 g algae

The biochemical characterisation of these algae exhibited similar results when compared with previous studies from different parts of the world (Cofrades et al., 2010; Sánchez-Machado et al., 2004; Tibbetts et al., 2016). Although, all the quantified constituents were similar to prior reports, variations in the measures were observed; this difference potentially resulted from the use of different locations and different collection periods, the age of the algae population, and algae species, as had been reported by other authors: polyphenols (Troncoso et al., 2015), lipids (Kendel et al., 2013), carbohydrates (Westermeier and Gómez, 1996), among others.

Pigment content was also determined (**Table 3-2**). Chlorophyll *a* in *H. elongata* exhibited the higher concentration of all pigments measured with 556.70±74.60 mg Chl *a*/g alga, followed by chlorophyll *a* and fucoxanthin in *A. nodosum*, 486.87±82.99 mg Chl *a*/g alga and 182.92±18.7 mg Fcx/g alga, highest pigment concentration in *C. crispus* was R-PE with 116.27±3.26 mg R-PE/g alga.

Table 3-2. Concentration of photosynthetic pigments in the feedstocks candidates.

Species	Pigment composition (mg pigment/kg DW alga)				
	Chl *a*	Chl (x+c)	R-PC	R-PE	Fcx
C. crispus	18.80±9.43	2.75±2.28	73.29±6.38	116.27±3.26	-
H. elongata	556.70±74.60	60.15±17.92	-	-	-
A. nodosum	486.87±82.33	98.01±16.77	-	-	182.92±18.7

Chl *a*: Chlorophyll a; Chl (x+c): Chlorophyll c; R-PC: Phycocyanin; R-PE: Phycoerythrin; Fcx: Fucoxanthin.

The breakdown and analysis of the all the macroalgal components in the potential candidates is described and discussed in the following sections.

2.1. Total soluble carbohydrate content

The concentration of soluble carbohydrate can be observed in **Fig 3-2**. The carbohydrate content in *C. crispus* was around 2 times higher than *A. nodosum* content, with values of 693.55±158.08 g GE/kg DW alga in the red macroalgae, and 338.42±41.44 g GE/kg DW alga for *A. nodosum*; *H. elongata* exhibited a content of 537.31±18.10 g GE/kg DW alga.

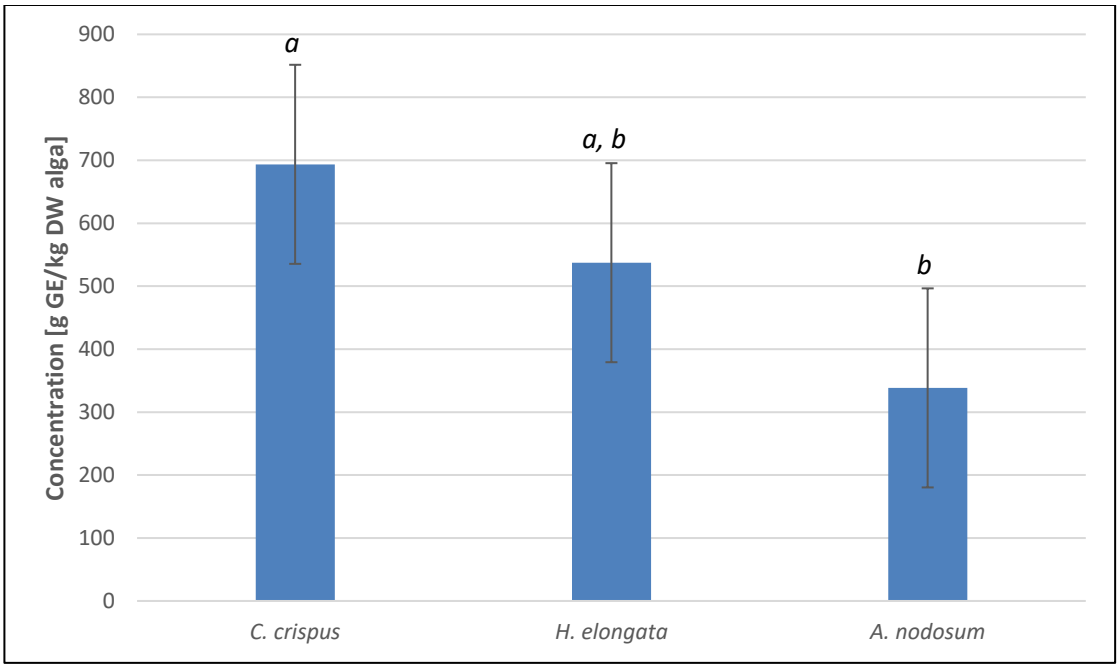

Fig 3-2. Total soluble carbohydrate concentration in three species of algae. Values are expressed as grams of glucose equivalent per kilogram of dried alga. All values are mean ± standard deviation (n=3). Values from the same studied macroalga with different letters (a, and b) are significantly different ($p < 0.05$).

Tibbetts et al. (2016) presented percentages of dry weight of 57.6% DW and 50.2% DW in two different cultures of *C. crispus*, contrasting with the 69.36±15.81% DW obtained here, and 56.1% DW in *A. nodosum*, opposing the 33.84±4.14% DW found in this work. On the other hand, *H. elongata* presented a higher content than other reports, 22.0% DW (Jiménez-Escrig et al., 2011) against 53.73±1.88% DW displayed here. These changes in the composition when compared with published results may be due to seasonal variations, geographical differences, and even age of the organism at the time

of the harvest (Westermeier and Gómez, 1996), and another factor affecting might be the drying methods and storage conditions which have shown effects in the concentration of biological compounds (Kadam et al., 2015a).

2.2. Protein extraction optimisation

A small-scale protein extraction process developed for microalgae (Slocombe et al., 2013), was adapted for macroalgae. In order to obtain the most accurate measure for the protein content, assays were performed changing the time of extraction, to determine if this variable affected the yield of extraction in the two types assessed here, *C. crispus* for red macroalgae, and *H. elongata* for brown macroalgae; *A. nodosum* was not used due to logistic issues with the acquisition of the biomass at the time of the experimental setup. For that reason, extraction times at 30, 60, and 120 minutes were tested in both species, the results can be observed in **Fig 3-3**. Values from *C. crispus* showed high variability across all the three different treatments. The protein concentration increased with time in both macroalgae. The higher concentration was obtained in *H. elongata* at 120 minutes with 74.98±3.92 g BSA Eq/kg DW alga, followed by *C. crispus* incubated for 120 minutes (62.78±39.19 g BSA Eq/kg DW alga).

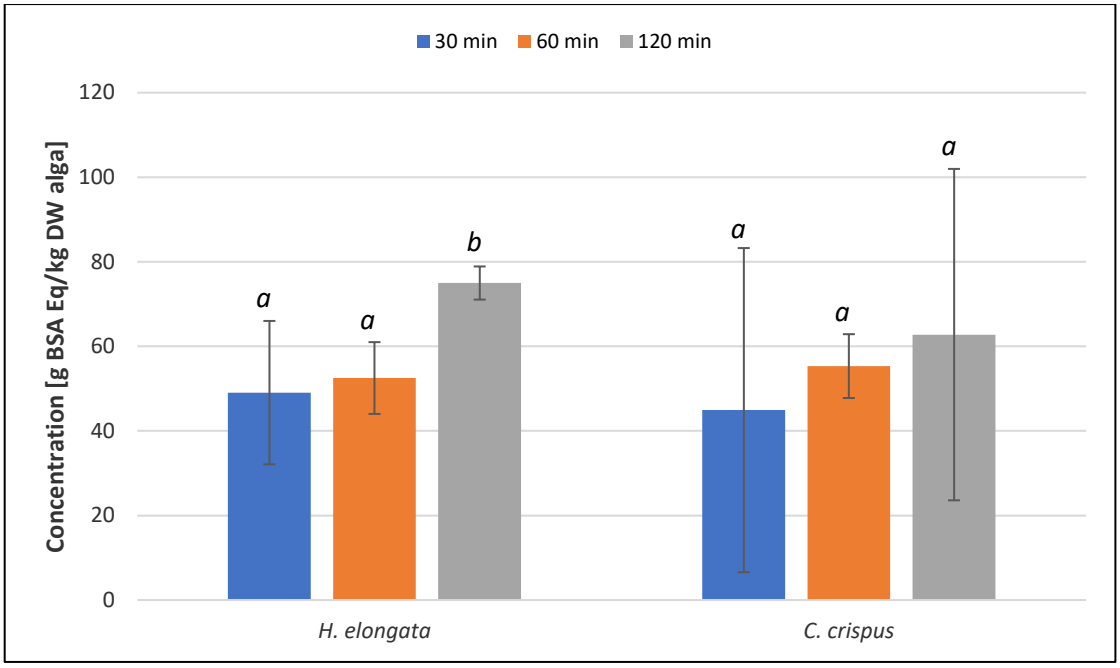

Fig 3-3. Total protein concentration from two macroalgae using different extraction times. All values are expressed as grams of BSA equivalent per kilogram of dried alga. Values are mean ± standard deviation (n=3). Values from the same studied macroalga with different letters (a, and b) are significantly different.

The lowest value was 44.91±38.34 g BSA Eq/kg DW alga in *C. crispus* incubated for 30 minutes, and 49.05±16.96 g BSA Eq/kg DW alga. Finally, both incubations of 60 minutes showed similar values, 52.51±8.49 g BSA Eq/kg DW alga for *H. elongata*, and 55.33±7.55 g BSA Eq/kg DW alga for *C. crispus*. The statistical analysis exhibited non-significant differences between the three treatments in *C. crispus* ($p > 0.05$), on the other hand incubation for 120 min in *H. elongata* presented statistically significant differences with the other two treatments ($p < 0.05$) (**Fig 3-3**). Given this results an extraction time of 120 minutes was selected for further analytical extractions on *A. nodosum*.

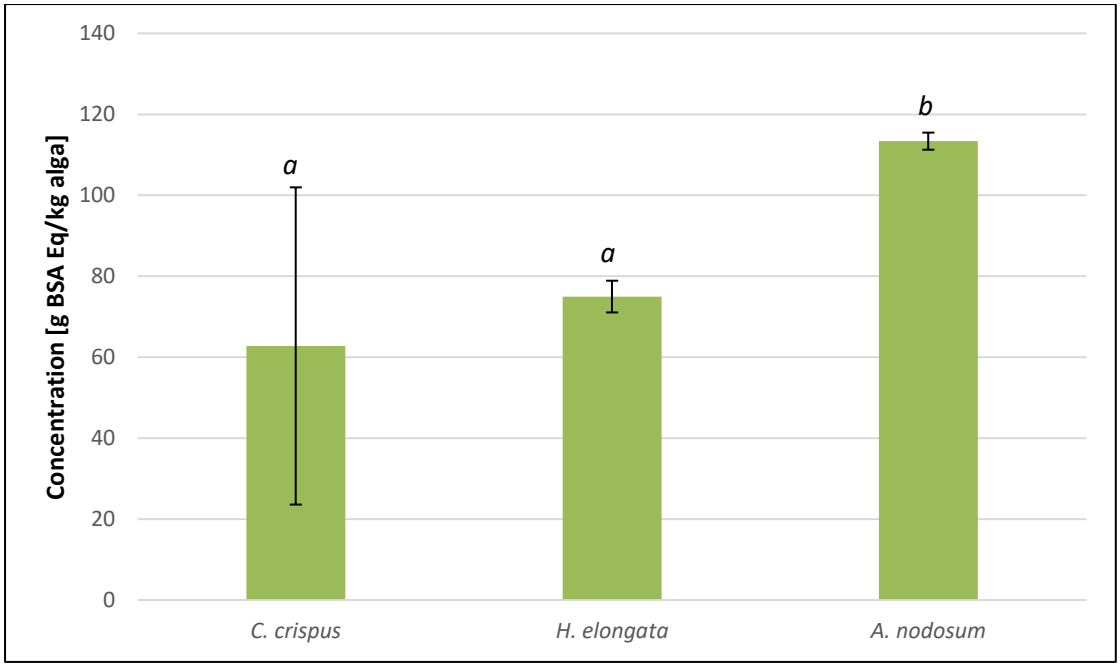

Fig 3-4. Comparison of protein content of the three seaweed potential feedstock candidates. All values are expressed as grams of BSA equivalent per kilogram of dried alga. Values are mean ± standard deviation (n=3). Values are mean ± standard deviation (n=3). Values from the same studied macroalga with different letters (a, and b) are significantly different ($p < 0.05$).

A. nodosum showed the highest concentration of the three species with 113.38±2.11 g BSA Eq/kg DW alga (**Fig 3-4**), followed by *H. elongata* with 74.98±3.92 g BSA Eq/kg DW alga, and *C. crispus* with 62.78±39.19 g BSA Eq/kg DW alga. *A. nodosum* presented statistically significant differences with the other two species ($p > 0.05$). Higher protein concentration was obtained in this work than reported previously; Lorenzo et al. (2017) reported protein concentration of 8.70±.0.07% DW in *A. nodosum*, contrasting the 11.33±0.21% DW obtained here. These differences of protein content within the same specie might be due to geographical and environmental differences, *A. nodosum* from Lorenzo et al. (2017) was harvested in Spain in summertime of 2015, while *A. nodosum* used in this work was collected in the Isle of Lewis, UK during wintertime of 2017. Another factor that might have increased the differences between these two studies was the milling process, because Lorenzo et al. (2017) grinded their feedstock up to 0.8 mm

contrasting with the 0.3 mm utilised in this study which allowed a higher surface-to-volume ratio in this study (Kadam et al., 2015b).

2.3. Total lipid content

The lipid content can be seen in **Fig 3-5**. *C. crispus* and *H. elongata* exhibited similar content ($p > 0.05$) above 15 g lipid/kg DW alga, on the other hand *A. nodosum* showed 80.37±9.79 g lipid/kg DW alga. *C. crispus* showed a lipid content of 20.19±7.77 g lipid/kg DW alga, and *H. elongata* showed 16.39±4.38 g lipid/kg DW alga. Lipid content displayed in this report was higher than other studies performed in both macroalgal groups, for instance, 0.93±0.05% DW, and 0.97±0.07% DW (Sánchez-Machado et al., 2004), and 1.5% DW (Cofrades et al., 2010), against 1.64±0.44% DW here exhibited in *H. elongata*, in the case of *C. crispus* the lipid content (2.02±0.78% DW) was lower than the one reported by Tibbetts et al. (2016) in two different cultures (4.2% DW and 2.7% DW). *A. nodosum* reported higher value than most reports in brown seaweeds, but it is not the highest value reported, *Stypopodium schimperi* (Phaeophyceae) has reported lipid content up to 11.5% DW (Bocanegra et al., 2009).

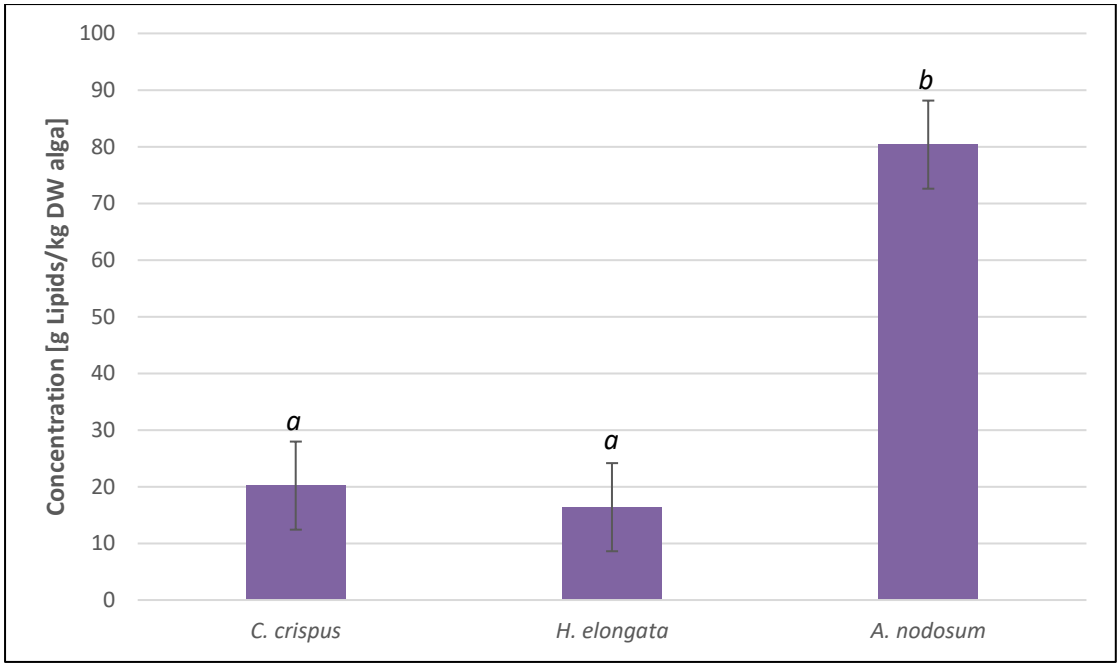

Fig 3-5. Total lipid content of feedstock candidates. Values are expressed as grams of lipid per kilogram of dried alga. Values are mean ± standard deviation (n=3). Values from the same studied macroalga with different letters (a, and b) are significantly different ($p < 0.05$).

2.4. Total polyphenol content analysis

The polyphenol content can be observed in **Fig 3-6**. As previously reported, the content of polyphenol is higher in brown seaweeds than in red seaweeds (Koivikko et al., 2005; Stengel et al., 2011). *A. nodosum* showed the highest polyphenol content of all species with 45.80±4.58 g PGE/kg DW alga, *H. elongata* presented a polyphenolic content of 16.18±0.28 g PGE/kg DW alga, almost a 7-fold more polyphenols than *C. crispus*, which showed a concentration of 2.43±0.16 g PGE/kg DW alga. *C. crispus* presented less polyphenol content than results published by Tibbetts et al. (2016) (4.0 and 4.2 g PGE/kg DW alga). On the other hand, *H. elongata* exhibited higher polyphenol concentration than previous reports, Belda et al. (2016) published polyphenol values around 1.10% DW, and in this report a percentage of 1.62±0.03% DW was obtained. All results showed statistically significant differences between them ($p > 0.05$).

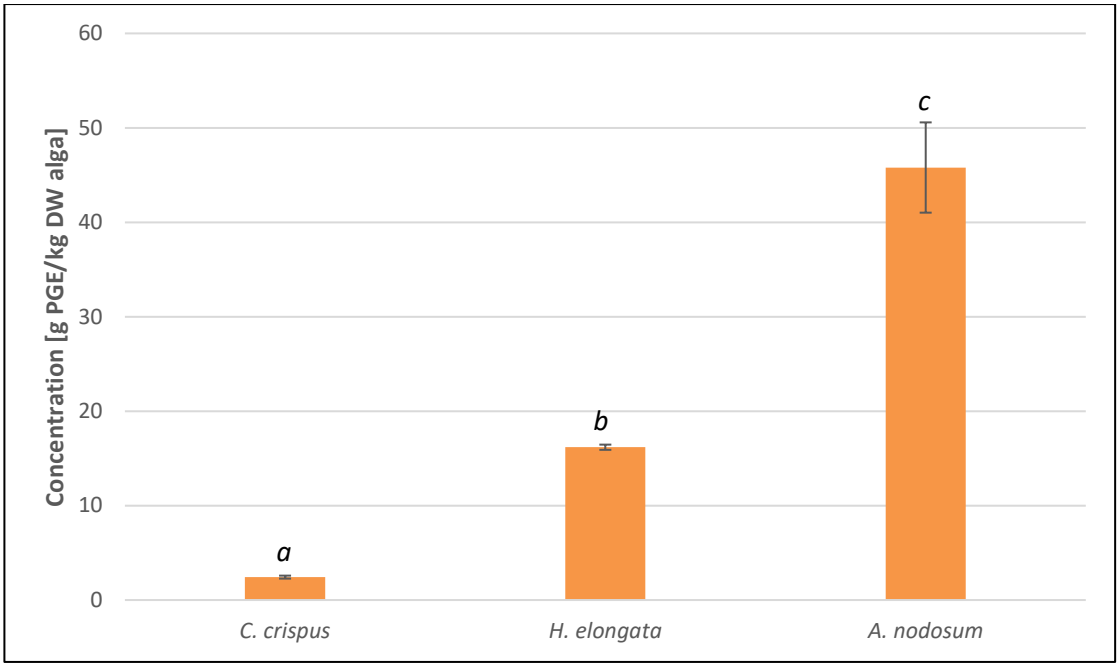

Fig 3-6. Total polyphenol content in three different macroalgae species. All values are expressed as grams of phloroglucinol equivalent per kilogram of dried alga. Values are mean ± standard deviation (n=3).

2.5. Pigment analysis

2.5.1. Chlorophyll *a* quantification

Chlorophyll *a* was measured using two different methods, DMSO and DMF, to check if there were differences in the application of both procedures compared to data reported in other studies (Schmid and Stengel, 2015). These two solvents were selected because the type of plant tissue often suits one type of solvent better than the other, and DMF and DMSO are solvents commonly used with terrestrial plants, therefore were tested on macroalgae. The highest concentrations were obtained in *H. elongata* using both methods (**Fig 3-7**), with values rounding ~560 mg Chl *a*/g DW alga, being the extraction condition using DMSO the one with the highest content (596.27±78.95 mg Chl *a*/g DW alga), followed by the experiment using DMF with a concentration of 531.72±69.46 mg Chl *a*/g DW alga. None of the different treatments applied exhibited statistically significant differences ($p > 0.05$). *A. nodosum* did not present significant differences between treatments ($p > 0.05$), with lower concentrations than *H. elongata* with values of

486.86±82.33 mg Chl *a*/g DW alga and 453.26±77.45 mg Chl *a*/g DW alga, for DMSO and DMF respectively. In *C. crispus* instead, the highest value was obtained with the DMF treatment (29.81±4.98 mg Chl *a*/g DW alga), and showed statistically significant differences with the DMSO condition, which exhibited a value of 14.19±4.41 mg Chl *a*/g DW alga. All macroalgae groups possess Chlorophyll *a* in spite of the presence of auxiliary pigments; this might be the reason of the low values obtained in *C. crispus* (Torres et al., 2019).

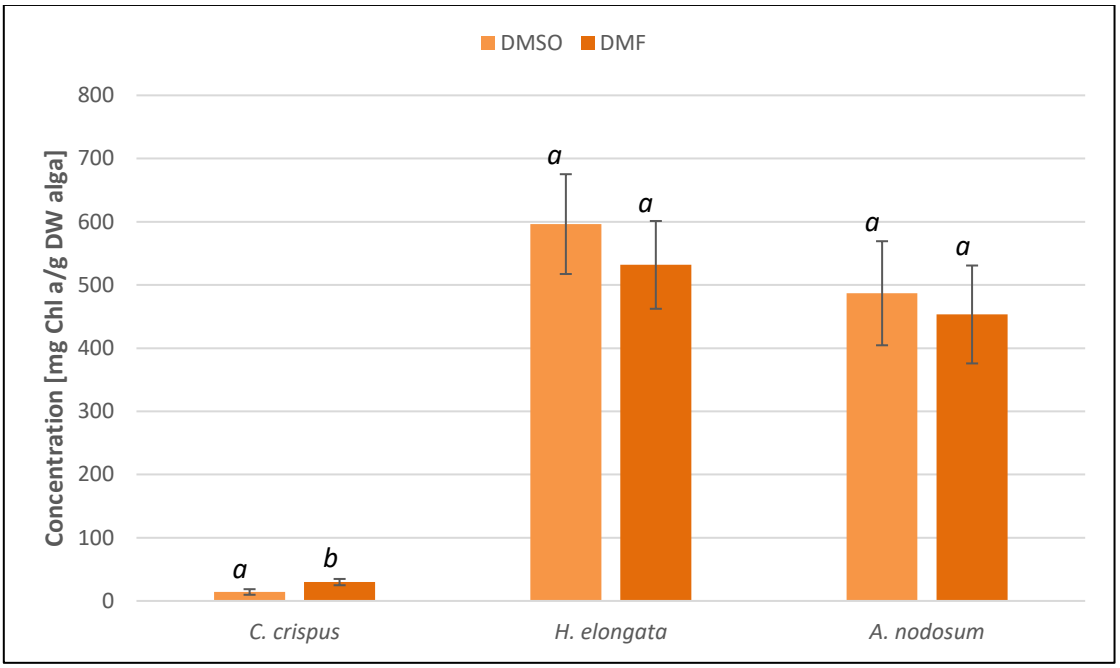

Fig 3-7. Chlorophyll a value from three algae using different solvents extraction. Values are expressed as milligram of chlorophyll a per kilogram of dried alga. All values are means ± standard deviation (n=3). Values from the same studied alga with different letters are significantly different.

2.5.2. Chlorophyll *c* and carotenoids quantification

Chlorophyll *c* and carotenoids (**Fig 3-8**) as well as chlorophyll *a* were quantified using the same experimental design, two different conditions using DMSO and DMF. The highest concentrations were obtained in *A. nodosum* with the DMSO treatment as the highest, exhibiting a pigment content of 98.01±16.77 mg Chl (*x*+*c*)/g DW alga and the DMF

treatment with 73.98±7.88 mg Chl (*x*+*c*)/g DW alga. Pigment content in *H. elongata* showed a concentration of 76.75±9.72 mg Chl (*x*+*c*)/g DW alga with the DMSO condition extraction; the test with DMF was the lowest in this candidate with a concentration of 40.45±5.28 mg Chl (*x*+*c*)/g DW alga. The different treatments applied in both brown seaweeds showed statistically significant differences between them ($p < 0.05$).

In the case of *C. crispus*, the different treatments did not exhibit statistically significant differences ($p > 0.05$), and the DMF trial present the highest concentration of all of them with 4.30±0.95 mg Chl (*x*+*c*)/g DW alga, followed by the test with DMSO (3.22±2.69 mg Chl (*x*+*c*)/g DW alga).

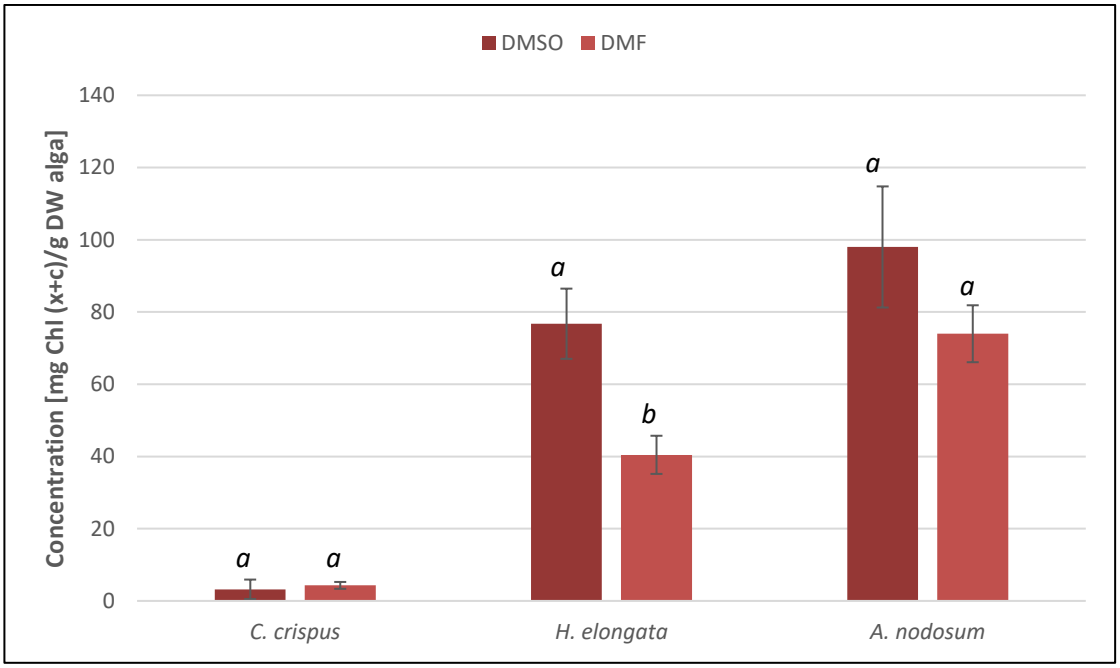

Fig 3-8. Chlorophyll c and carotenoids values from three algae conditions on two different extraction methods. Values are expressed as milligram of carotenoid per kilogram of dried alga. All values are means ± standard deviation (n=3). Values from the same studied alga with different letters are significantly different.

2.5.3. R-phycocyanin (R-PC) and R-phycoerythrin (R-PE)

R-PC and R-PE were quantified only in *C. crispus*, due to their complete absence in brown macroalgae (Stengel et al., 2011). To evaluate the viability of this method two

different trials were performed changing the solid-liquid ratio in them. In the first test using 0.1 g of biomass, and the second 0.05 g of the red alga. Differences were not observed between the two treatments (p > 0.05) in both auxiliary pigments. R-PE showed the highest concentrations and almost the same values in both trials (**Fig 3-9**), 116.38±4.77 mg R-PE/g DW alga in the 0.05 g condition, and 116.17±1.94 mg R-PE/g DW alga in the 0.10 g condition. On the other hand, R-PC show lower values than R-PE, 76.83±4.72 mg R-PC/g DW alga, and 69.76±6.47 mg R-PC/g DW alga, for 0.05 g and 0.10 g, respectively.

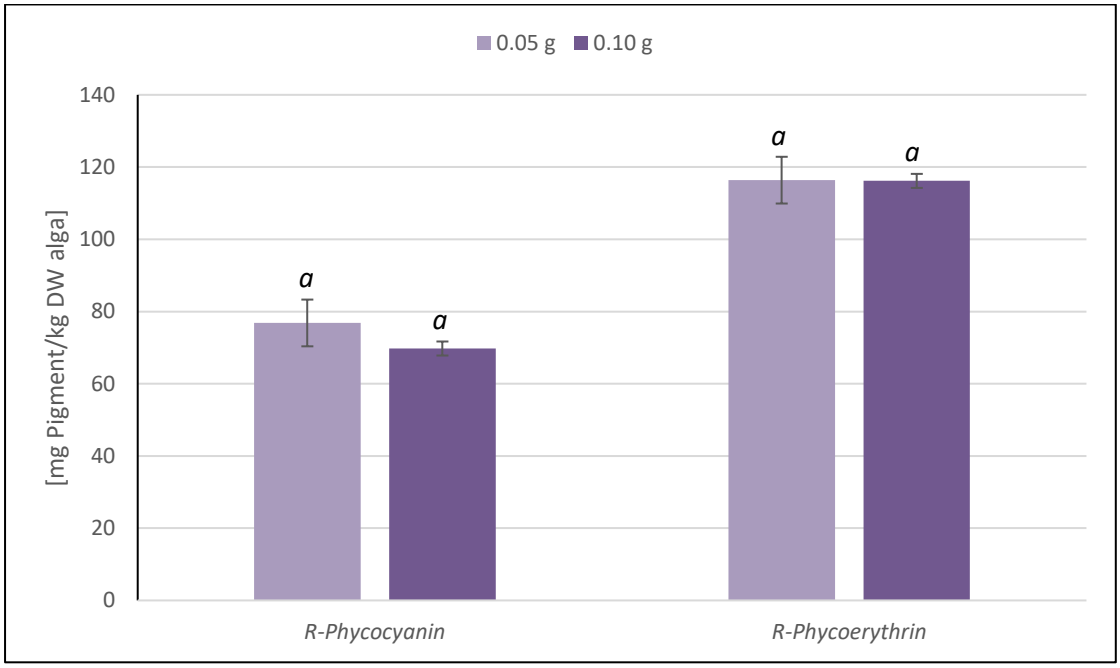

Fig 3-9. R-phycocyanin and R-phycoerythrin values using different solid-liquid ratios. All values are expressed as milligram of pigment per kilogram of dried alga. Values are means ± standard deviation (n=3). Values from the same studied compound with the same letter are not significantly different.

2.5.4. Fucoxanthin content in *A. nodosum*

Fucoxanthin content was quantified in *A. nodosum*, but not in *H. elongata* due to logistical reasons, also was not measured in *C. crispus* due their absence in this species (Pádua et al., 2015), and using DMSO as solvent treatment. Differences were not

observed between the different extraction trials ($p < 0.05$) with an average content of 182.92±18.7 µg Fcx/g DW alga. Results from literature reported slightly higher values of this xanthophyll, Shannon and Abu-Ghannam (2017) informed ~0.25 µg Fcx/g DW alga in wild-harvested specimens of *A. nodosum*, Stengel and Dring (1998) reported values in *A. nodosum* of 0.202±0.008 µg Fcx/g DW alga. These differences in the concentration might be due to geographic and/or seasonal variations in the collection of the specimens (Schmid et al., 2017).

Finally, a summary of the proximate biochemical characterisation of three algal candidates can be seen in **Table 3-1**. It was observed that *C. crispus* presented the highest content of carbohydrates of all three feedstock candidates (69.36±15.81% DW), followed by *H. elongata* (53.73±1.88% DW) and finally *A. nodosum* (34.22±4.14% DW). *C. crispus* carbohydrates are usually bulk chemicals used in industry, mainly carrageenan (Holdt and Kraan, 2011), as well as brown seaweeds, with alginate (Menon, 2012), both polysaccharides with wide applications as hydrocolloids in different industrial sectors. Brown seaweeds also present sulphated polysaccharides (embedded in this chapter under total carbohydrates) with fucoidan being the most studied in recent years (Fernando et al., 2019; Foley et al., 2011) due to its potential bioactivities with potential in the development of biopharmaceuticals, as supplements for nutraceuticals, and as potential active ingredient in cosmeceuticals, therefore the extraction of this high-value compound along with a bulk chemical like alginate is interesting in a biorefinery context, because the rather simple extraction and commercialisation of a bulk chemical can help to ameliorate the potential more expensive extraction process of a high-value compound such as fucoidan (Keegan et al., 2013). A combined percentage of around 6% DW of lipids, proteins, and polyphenols made *C. crispus* a less interesting candidate to use, due to the low concentration and therefore the lack of potential high-value compounds in this alga, with only a bulk chemical with interest in the industry, in the form of mainly carrageenan.

Higher contents of polyphenols than reports in literature from both brown macroalgae candidates was highly desirable due to the reported bioactivities of this compounds and the potential uses of them (Afonso et al., 2019; Hu et al., 2011; Lopes et al., 2017).

Protein content in *A. nodosum* was higher than *H. elongata*, this was taken into consideration for the selection of this species rather than the other. Potential applications of proteins from macroalgae include antioxidant activities, also as a viable option of plant-based protein sources (Torres et al., 2019)

The high lipid content present in *A. nodosum* (8.04±0.98% DW) was also taken into consideration for the selection of this candidate, for the potential uses in nutraceutical formulations using n-6 and n-3 fatty acids (Ward and Singh, 2005) or anti-inflammatory activities (Torres et al., 2019).

Values of total carbohydrates (34.22±4.14% DW), polyphenols (4.63±0.48% DW), lipids (8.04±0.98% DW), and proteins (11.33±0.21% DW) obtained in *A. nodosum* were taken into consideration for the selection of this brown macroalgae as the feedstock for further experiments in this project.

3. Conclusions

This chapter aimed to select a suitable feedstock for a multi-product third generation biorefinery process from three potential candidates available in the shores of the UK, to help in the development of Blue Economy strategies for sustainable development of the industry. The selection criterion for the appropriate seaweed candidate was based on the high accumulation of biological compounds with potential economic revenues after extracted, i.e., polyphenols, proteins, and lipids.

The results highlighted *A. nodosum* as the more suitable candidate to use, over *H. elongata*, and *C. crispus*. This seaweed was selected to use in all further chapters of this project as the model biorefinery feedstock, due to the accumulation of high-value compounds with potential application in several industries, as well as bulk chemicals with well-defined market applications. *A. nodosum* showed higher content of polyphenols, minerals, proteins, and lipids than the other candidates. Although *A. nodosum* showed the lowest concentration of carbohydrates, the presence of sulphated polysaccharides and their value in the market still potentiate *A. nodosum* as the more suitable candidate for subsequent experiments.

Chapter 4: Preliminary assessment of the economic, environmental, and technical feasibility of cascading biorefinery sequences scenarios for *A. nodosum*

1. Introduction

In the early stages of assessing new manufacturing processes, including bioprocess development, techno-economic analyses (TEA) and life cycle assessments (LCA) are often recognised as a potential tool to evaluate economic and environmental impacts of emerging technologies from “cradle to grave” and to facilitate decision making processes (Carbajales-Dale et al., 2020). Early-stage decisions within technology development can have significant impacts on the future economic and environmental performance of the technology as they are passed along subsequently. The “Collingridge dilemma” becomes apparent: at an early stage of technological development there is wide scope for change but knowledge of performance of scale up is sparse. However, the possibilities narrow as more information becomes available and design parameters become locked (Arvidsson et al., 2018). Moreover, technology appraisal at early development stages can assist bioprocesses development scientists to understand the implications of design choices on future consequences. This approach can prevent regrettable investments, reduce costs, avoid environmental consequences, and provide support to make important decisions without major disruptions. Use of combined TEA–LCA has great potential to drive the development of emerging technologies with improved environmental performance and economic viability by identifying financial and environmental hotspots and comparing with existing alternatives when used at early design stages, contrasting against other technology concepts at similar technology readiness level (TRL). TRL is a methodical qualitative scaling method to assess the maturity of technology ranging from TRL1: scientific breakthrough to TRL9: technology commercialisation and to compare maturity between different technologies as well (Gavankar et al., 2015). The term industrial

sustainability has been coined based on the technical feasibility, economic viability and environmental sustainability of a product or process (Wenda et al., 2011). The International Energy Agency Bioenergy Task 42 “Biorefining in a Circular Economy” defined a biorefinery as “the sustainable processing of biomass into a spectrum of bio-based products (food, feed, chemicals, and materials) and bioenergy (biofuels, power and/or heat)”. In addition, Task 42 considers the existence of two types of biorefineries depending on the final use of the products. The energy-driven biorefineries involve those cases, where the final purpose is energy production; thus, the main products in these platforms are biofuels, power and/or heat. On the other hand, product-driven biorefineries consider as a main purpose to obtain molecules/molecular building blocks that have defined applications outside bioenergy e.g., bioactive compounds, polymers, biomaterials, food and animal feed, and fertilisers (Cardona-Alzate et al., 2020). Biorefinery processes have substantial economic, environmental, and social effects and could provide promising opportunities for the macroalgae industry. In seaweed-based biorefineries the product-based biorefining platform approach have been suggested as a more successful strategy to utilise the biomass more efficiently to reach the goals of a Blue Economy approach, due to the biggest challenges faced in the development of bioenergy-based processes using this feedstock (Seghetta et al., 2017). The sustainable manufacture of products is an essential component of the transition from a linear economy into a more resource-efficient and waste-free circular economy (Sheldon, 2018). In order to facilitate this endeavour is necessary to have reliable tools to assess the sustainability of different technologies, thus the application of TEA and LCA for the evaluation of prospective technologies to validate process greenness and economic profitability. Techno-economic assessment is a methodology that builds on the information derived from mass and energy balances for process development and technical optimisation, which can estimate the economic viability of conceptual bioprocesses (see **Section 1.5** from **Chapter 1**). TEA provides insights into the technological impacts and costs of various sections in the overall production process by

assigning monetary values to all of the materials, energy, and other consumables needed to run a production facility (Ögmundarson et al., 2020). On the other hand, life cycle assessment is a standardised framework that follows the guidelines of the ISO 14040, 14041, and 14044 (International Organization for Standardization, 2006), and gives a systematic and holistic tool to environmental impact assessments (Sadhukhan et al., 2019). LCA studies can be costly and time consuming. However, the efficiency of conducting LCA can be increased by using TEA as a tool to generate the required process data on LCI inputs and outputs along the product life cycle. It is essential to perform an integrated techno-economic and environmental analysis to understand the overall impact of producing various products from seaweeds. Rajendran and Murthy (2017) have considered twelve biorefinery scenarios producing ethanol, ethyl acetate, dodecane, hexane, ethylene and electricity from different lignocellulosic feedstocks and analysed these scenarios using TEA and LCA, concluding that producing ethyl acetate from Banagrass was the most economic and sustainable scenario. DeRose et al. (2019) and Nezammahalleh et al. (2018) have performed integrated TEA and LCA in microalgae processes to produce biofuels, highlighting the combined use of both tools in process development. Although the integrated use of TEA and LCA has been demonstrated in renewable feedstock, the reports in macroalgae biorefinery dedicated to the extraction of high-value compounds are scarce (Sadhukhan et al., 2019). The overall goal of this chapter was to create three scenarios of a third generation multi-product biorefinery concept specialised in the extraction of high-value compounds and commodity chemicals using different technology pathways, and analyse their quantitative economic and environmental performance with the use of TEA and LCA as early-design tools, and evaluate their nexus in the decision-making process of prospective biorefinery cascading sequences with the attempt to create a decisional tool to inform experimental work. Finally, technical feasibility trials (TFT) were performed on the cascading sequence to evaluate the actual process performance, to confirm the biorefinery process viability and to identify process hotspots for further exploration in a new iteration of the models.

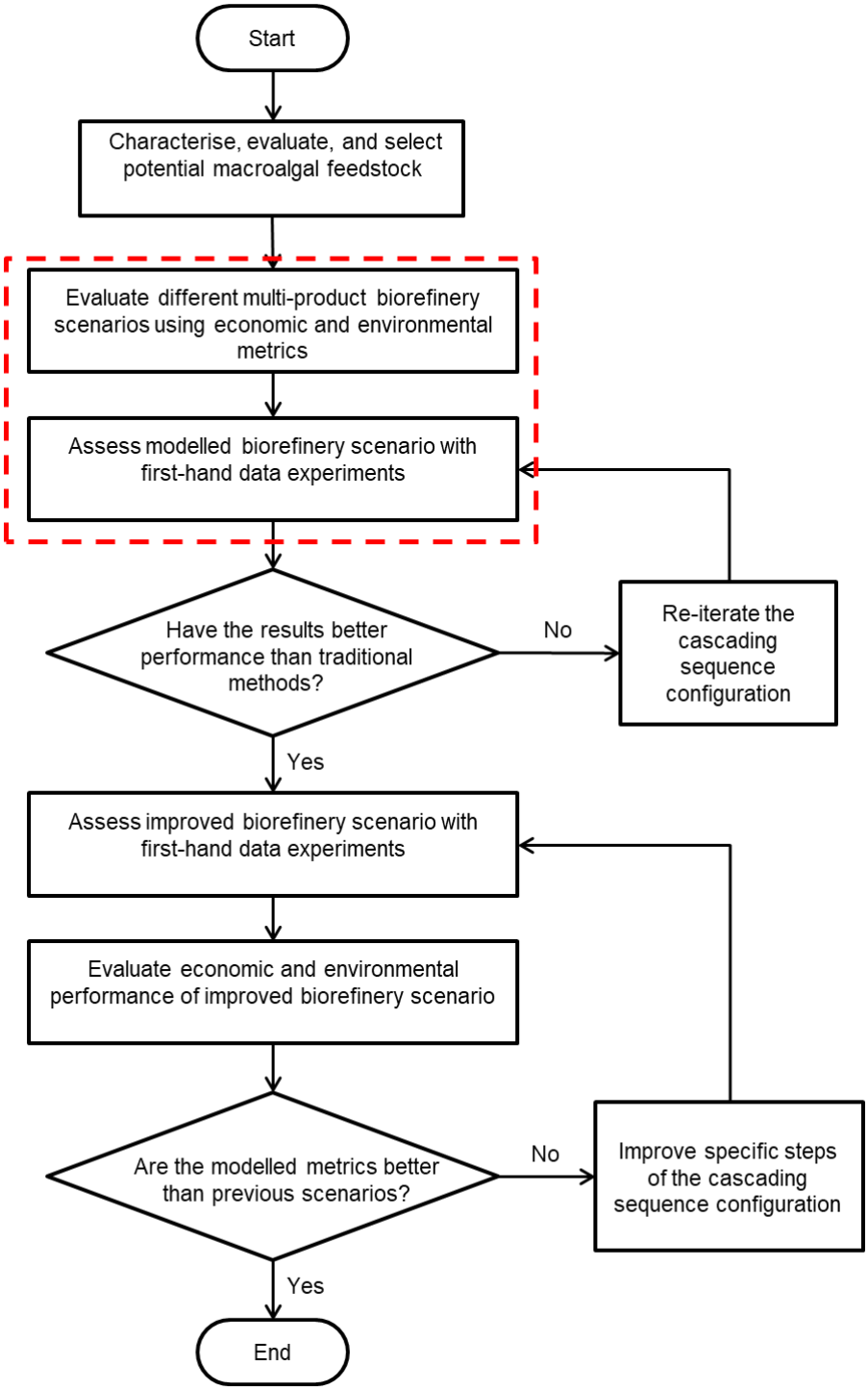

Fig 4-1. Proposed overall methodology for the development of a multi-product macroalgal biorefinery. In the red dashed box is highlighted the step covered in this chapter.

2. Modelling methods

2.1. Biomass harvesting and composition

The portion covered in this chapter can be observed in **Fig 4-1**. Based on the findings from **Chapter 3,** *A. nodosum* was considered as the biomass source. As the upstream cultivation aspects are out of scope of this evaluation, data on average yearly tonnage of sustainable harvest data was obtained from Morrissey et al. (2001) conducted on the Irish coasts due to similarity with the climate conditions found in the UK. The biorefinery capacity considered in this study was set on a processing volume of 1,000 dry MT biomass/year (see **Section 2.2** from **Chapter 4**).

The composition of *A. nodosum* was quantified in the previous chapter and compared against feedstock composition provided by the supplier (**Table 4-1**).

Table 4-1. Chemical composition of *A. nodosum* obtained from experimental analysis and information given by commercial supplier.

Composition (per 100 g DW)	This study	Commercial supplier
Total protein	11.33 g	5.40 g
Total carbohydrate	34.22 g	57.90 g
Total lipids	8.13 g	3.20 g
Total polyphenols	4.63 g	-
Moisture	12.15 g	11.60 g
Ash	29.54 g	21.93 g

2.2. General assumptions and justifications

The site for the proposed plant was on the Great Britain Island, UK where the primary source of electricity is from the United K National Grid. The choice of plant size was 1,000 dry MT biomass/year based on conservative estimates used in economic modelling of new lignocellulosic-based biorefinery concepts from the National Renewable Energy Laboratory, USA (Dutta et al., 2011; Kazi et al., 2010). While the plant size is small considering other biorefinery concepts, this was the most feasible

capacity for the TRL considered in the different scenarios. The facilities were modelled to operate 300 days per year. These operating conditions were used in the subsequent life cycle inventory and impact assessments.

A list of economic indicators used in this chapter is presented in **Table 4-2**. Most of the economic indicators were based on BioSolve Process 7 (Biopharm Services, UK) database and suppliers, while the cost of fucoxanthin, fucoidan, polyphenol, alginate, lipids, and protein were obtained from (Andersen, 2017). A straight-line depreciation method was used, and 10 years was assumed to the depreciation period for equipment. The plant was considered to have a lifetime of 10 years, while 36 months was considered as the construction period. The start-up time was assumed to be 6 months, and the salvage value of the equipment's after its lifetime was 5% of its installed cost (Rajendran and Murthy, 2017). The income tax was fixed at 2% of the total fixed capital investment (FCI) (Towler and Sinnott, 2008). The cost of utilities was derived from UK Government statistics.

2.3. Model development

The list of key assumptions used to build these scenarios can be seen in **Appendix A**. The first iteration process simulation for the different scenarios was performed using multiple pathways regarding to the production of biochemical, with these processes already reported on literature. The three scenarios were coded based on their technology pathways used.

Scenario 1: based on the use of traditional solvent and conventional extraction processes in macroalgae was called "*Solvent-based*" scenario.

Scenario 2: based on the use of novel extraction techniques utilising physicochemical principles to disrupt the biomass and release the interest products was coded "*Novel Tech*" scenario.

Scenario 3: constructed using green chemistry strategies and extraction techniques compliant to them, was defined as "*Green Chem*" scenario.

The overall process schematic for the three scenarios is shown in **Fig 4-2**, **4-3**, and **4-4**. All process scenario models were constructed using Microsoft Excel suite, where the mass and energy balances, equipment and reagents costing, parameters of pieces of equipment used in the process, and efficiency yields of each extraction step were included. The inputs and outputs in the process were identified. The selected products for recovery in the first iteration of all scenarios were: fucoxanthin, lipids, polyphenols, fucoidan, and alginate; these compounds were selected due to the interest in their bioactivities and potential development of biopharmaceuticals, nutraceuticals and/or cosmeceuticals (lipids, fucoidan, polyphenols, and fucoxanthin, and protein instead of lipids in *Green Chem* scenario), and the well-established extracting interest of alginate as a bulk chemical used in several industries (White and Wilson, 2015). Before processing of the biomass in the different scenarios, *A. nodosum* was transported to the site where the modelled facility would operate, where the field-dried biomass is conveyed to a silo before further processing.

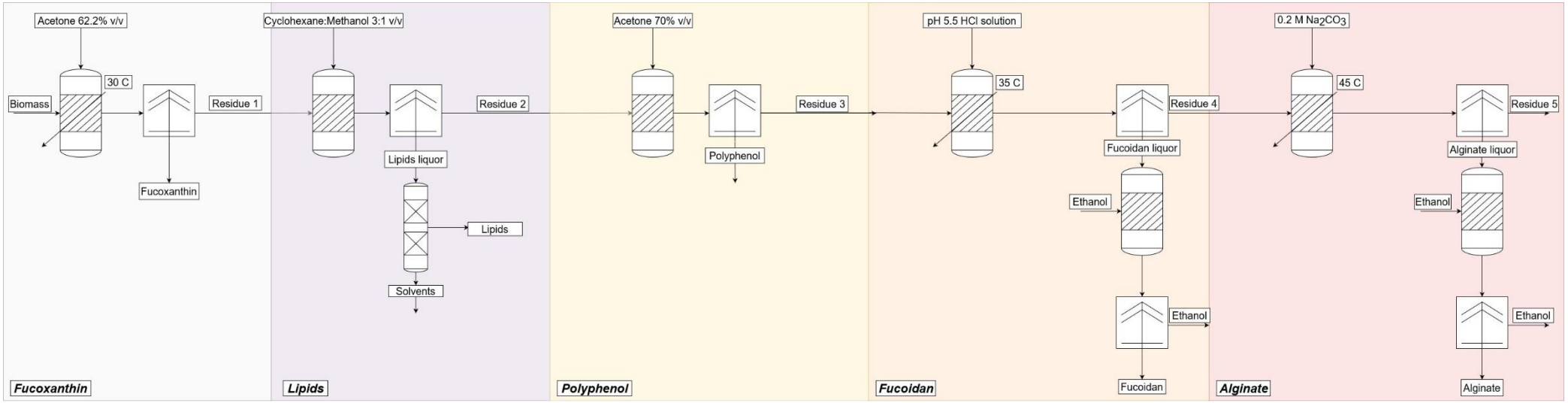

Fig 4-2. General flow diagram for the proposed sequential extraction process for the Solvent-based scenario.

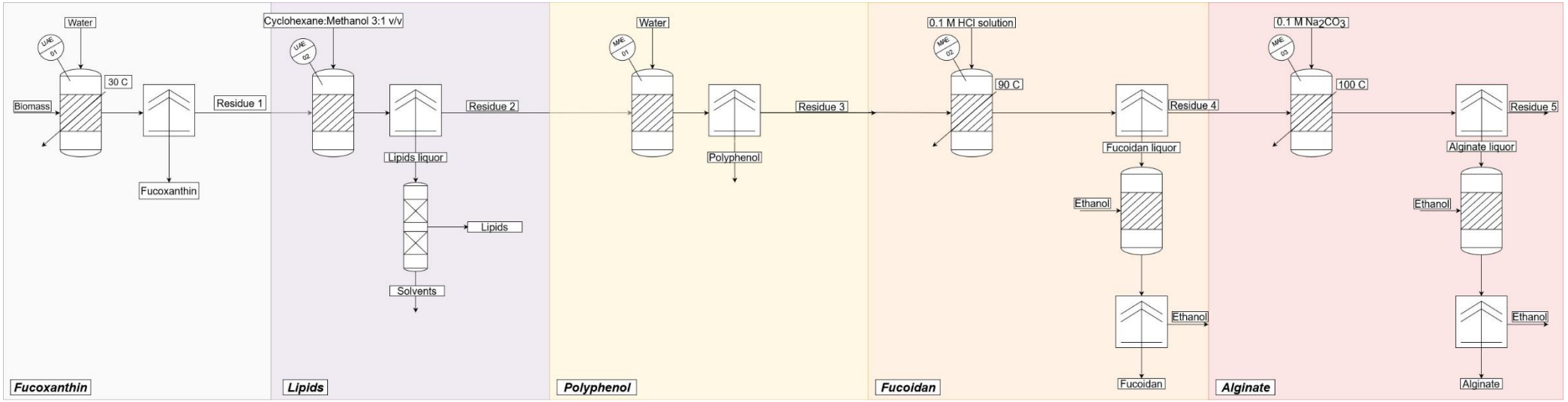

Fig 4-3. General flow diagram for the proposed sequential extraction process for the Novel Technologies scenario.

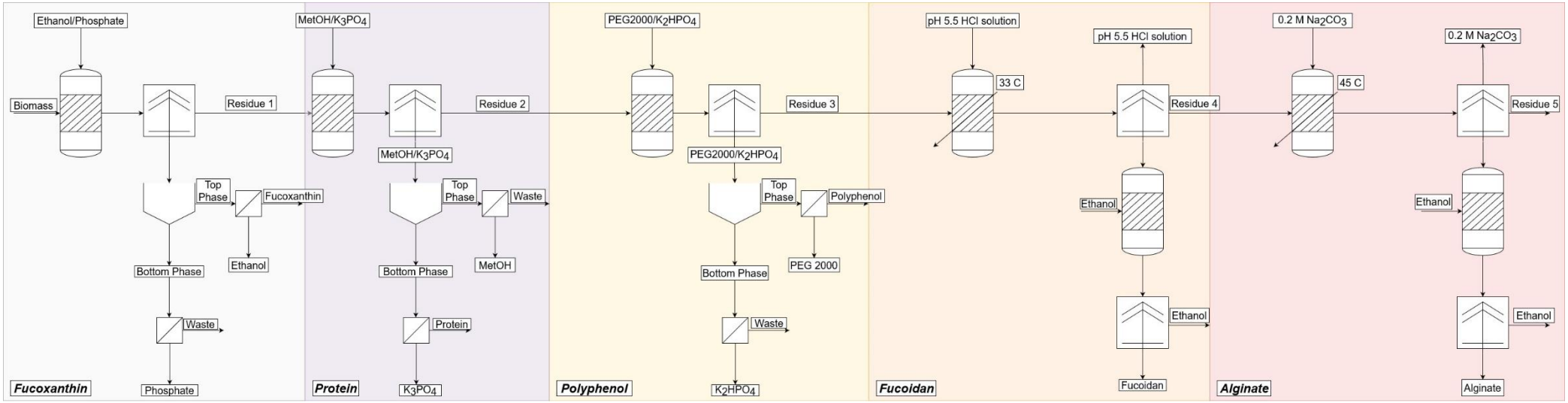

Fig 4-4. General flow diagram for the proposed sequential extraction process for the Green Chemistry scenario.

2.3.1. Solvent-based biorefinery scenario

"*Solvent-based*" was the first cascading process scenario proposed for this biorefinery concept, using solvents and conventional unit operations already used and tried in other concepts (Humbird et al., 2011). A feedstock of 1,000 MT of dried and milled *A. nodosum* was used for the development of the model. As seen in **Fig 4-2**, the first extraction step was decided to be fucoxanthin, as described by Shannon and Abu-Ghannam (2017) using a mix of acetone:water 62.2%, pH 5.7 at 30°C (**Appendix B**). The mix was separated into solids and liquids fractions using a disc-stack centrifuge and the solids fraction, defined as biorefinery residue was pumped to the next extraction stage. After this step, lipid recovery was performed using liquid-liquid extraction with cyclohexane:methanol 3:1 as extractant matrix (Ashokkumar et al., 2017). After the extraction step was completed, the mix was disc-stack centrifuged, and the solid biorefinery residue fraction was derived to the next cascading stage. The liquor containing the lipids was distilled to evaporate methanol and cyclohexane to recover the lipid fraction. After this step has been completed, the polyphenol content present in the solid biorefinery residue was extracted using acetone:water 70:30 v/v mix according to Koivikko et al. (2005), it was considered that polyphenols were not extracted in the fucoxanthin step, which uses the same solvent, due to the higher Hildebrand solubility parameter showed by the solution in this stage, and the greater affinity of polyphenols to this solution (Koivikko et al., 2005). The liquor was centrifuged, and the solid fraction was derived to the next extraction stage. Fucoidan was recovered next using a HCl solution at pH 5.5 as an extraction solvent at 35°C (Lorbeer et al., 2015). The output slurry was centrifuged to separate solids from the liquid fraction. The liquid fraction was treated with ethanol to precipitate the fucoidan in it. Following this, alginate was extracted from the remaining biorefinery residue of the previous step, using 0.2 M Na_2CO_3 solution at 45°C (Lorbeer et al., 2015). The extraction blend was centrifuged and the liquid fraction containing dissolved alginate was separated from the final biorefinery residue. The liquid fraction whereas alginate was in a dissolved state was treated with anhydrous ethanol to

make them precipitate. Final biorefinery residue was considered for disposal to a municipal waste.

2.3.2. Physicochemical technologies-based biorefinery

The biorefinery based in the use of physicochemical technologies, defined here as "*Novel Tech*" and based in the use of microwave- (MAE) and ultrasound-assisted extraction (UAE), applying UAE in the first two cascading steps and completing the last three processes with MAE. A baseline input of 1,000 MT dried and milled *A. nodosum* per year was used for the development of the model scenario. As seen in **Fig 4-3**, the first extraction step was the fucoxanthin fraction, this bioproduct was obtained with the use of UAE at 20 min using water as extraction solvent (Phong et al., 2017), followed by a centrifugation step to separate solids from the liquid fraction containing the pigment. Following this cascading step, lipids were extracted using UAE as well, with a mixture of cyclohexane:methanol 3:1 as extraction medium (Ashokkumar et al., 2017). Solvents were distilled to recover the lipid fraction. After this, the polyphenol content was extracted from the biomass using MAE with water as a solvent according to Magnusson et al. (2017). The liquor was separated from the solids using a disc-stack centrifuge considering a concentration factor of 0.7 (**Appendix B**), and the resulting solid fraction was moved to the next step. Fucoidan content was recovered using MAE as well irradiating at 90°C for 15 min using 0.1M HCl solution as extractant (Yuan and Macquarrie, 2015a). The mix was centrifuged to separate into solid and liquid fractions. The liquid fraction was treated with ethanol to precipitate the fucoidan in it. Subsequently, alginate was extracted using MAE as well at 100°C for 10 min in 0.1 M Na_2CO_3 solution (Yuan and Macquarrie, 2015b). The extraction blend was centrifuged and the liquid fraction, whereas alginate was in a dissolved state, was treated with anhydrous ethanol to make it precipitate. Final biorefinery residue was disposed into a municipal waste outside the system boundaries.

2.3.3. Green chemistry-based biorefinery

This biorefinery concept considered processes compliant to green chemistry principles, thus ATPS, liquid-liquid extraction and low acid and base extractions were used; also, a base of 1,000 MT dry *A. nodosum* per year was used (**Fig 4-4**). The first fucoxanthin extraction step was performed according to Gómez-Loredo et al. (2014) using an ethanol-salt based ATPS at room temperature for 2 h. After the settling time top phase was separated from bottom phase, and the remaining mixture was centrifuged to separate the biorefinery residue from the bottom phase. Publications reporting the use of green chemistry techniques to recover lipids from macroalgae could not been found at the time of execution of these experiments, thus protein extraction was selected instead of lipids. Following the pigment extraction, proteins were extracted using another ATPS extraction composed of methanol-K_3PO_4 for 2 h at room temperature (Phong et al., 2018). After the settling time top phase was separated from bottom phase, and the mix was separated using a disc-stack centrifuge as explained in **Section 2.3.2** from this **Chapter**. The solids fraction was fed to the next step. Once this step has been completed, polyphenol content was extracted with a polymer-salt based ATPS process (Xavier et al., 2017) using PEG 2000 and potassium phosphate salt. After a settling time of 1.5 h, the top phase was separated from the bottom one, while the bottom phase was centrifuged to separate the biorefinery residue into the next step. Fucoidan was obtained with a low acid concentration extraction process using a pH 5.5 HCl solution for 80 min at 33°C (Lorbeer et al., 2015). The output slurry was centrifuged to separate solids from the liquid fraction. The liquid fraction was treated with ethanol to precipitate the fucoidan in it. Finally, alginate was extracted using a 0.2 M Na_2CO_3 solution at 45°C for 2 h (Lorbeer et al., 2015). The extraction blend was centrifuged and the liquid fraction, whereas alginate was in the soluble state was treated with anhydrous ethanol to make it precipitate. Final biorefinery residue was disposed at a municipal waste outside the system boundaries.

2.4. Techno-economic analysis

The mass and energy balance outputs from the biorefinery cascading sequence models were used to evaluate the capital and operating costs. All currency used in the models was pounds sterling (£) adjusted to the year 2016.

2.4.1. Capital cost estimation

Equipment cost information was obtained from quotes by equipment suppliers, and from BioSolve Process 7 software database. Due to the fact equipment size required may be different than that available from different resources, the exponential scaling expression (**Eq. 4-1**) was used according to Towler and Sinnott (2008).

$$New\ cost = (Base\ cost) \times \left(\frac{New\ size}{Base\ size}\right)^{0.6} \quad \textbf{(Eq. 4-1)}$$

The total FCI was calculated by the Lang factor, which is the ratio of the fixed capital investment to the total purchase cost of the equipment (**Table A-3**). The Lang factor was set to be 3.0, which is a consensus for a solids processing plant (Towler and Sinnott, 2008). The FCI cost includes the direct costs, e.g., raw materials, utilities, labour, and indirect costs, e.g., facility maintenance, local taxes, insurance, depreciation. The working capital in this assessment was set to be 5% of the FCI (Huang et al., 2016). The total capital investment is the result between the FCI, the working capital, and the contingency percentage, which in this case was set in 10%.

2.4.2. Total operating costs

A list of key assumptions of how these figures were derived can be observed in **Appendix A**. The total operating costs include both variable and fixed operating costs. Variable operating costs, which include raw material costs and utilities, are incurred only when the process is operating. The quantities of raw materials were determined by the

material and energy balances. The unit price of materials was determined by their market value in the current year. Water consumption includes the process water, and the make-up water for the heat exchangers. Fixed operating costs are generally incurred in full, regardless of whether the plant is producing at full capacity. These costs include labour and various overhead items.

2.5. Life cycle assessment

2.5.1. Goal, scope, and system boundaries

The primary goal of this assessment was to develop a gate-to-gate life cycle inventory and estimate the environmental impacts of a multi-product cascading biorefinery process using *A. nodosum*. The scope of this assessment was to quantify and compare the environmental impacts of multi-product cascading extraction sequence of different biorefinery technology scenarios, in order to adhere to Blue Economy development strategies. The functional unit used was 1 kg of dried and milled *A. nodosum* fed into the process. The different unit processes and its inputs were defined in the system boundaries for an LCA (**Fig 4-5**). The biomass pre-treatment inputs such as transportation, electricity, milling machinery were not included in the system boundaries. Within the extraction processes, chemicals used such as H_2SO_4, ethanol, electricity were considered within the system boundaries. SimaPro (version 8.5.2.0) software was used to run the life cycle assessments and Ecoinvent database (version 3.5) (Wernet et al., 2016) was used for integrating the life cycle inventory, ReCiPe impact assessment methods (version 1.13) were used for conducting the impact assessments using the Midpoint impact categorisation under a Hierarchist perspective, this means that the impacts produced to the environment by the process were analysed under the most common policy principles and a timeframe of 100 years (Huijbregts et al., 2017).

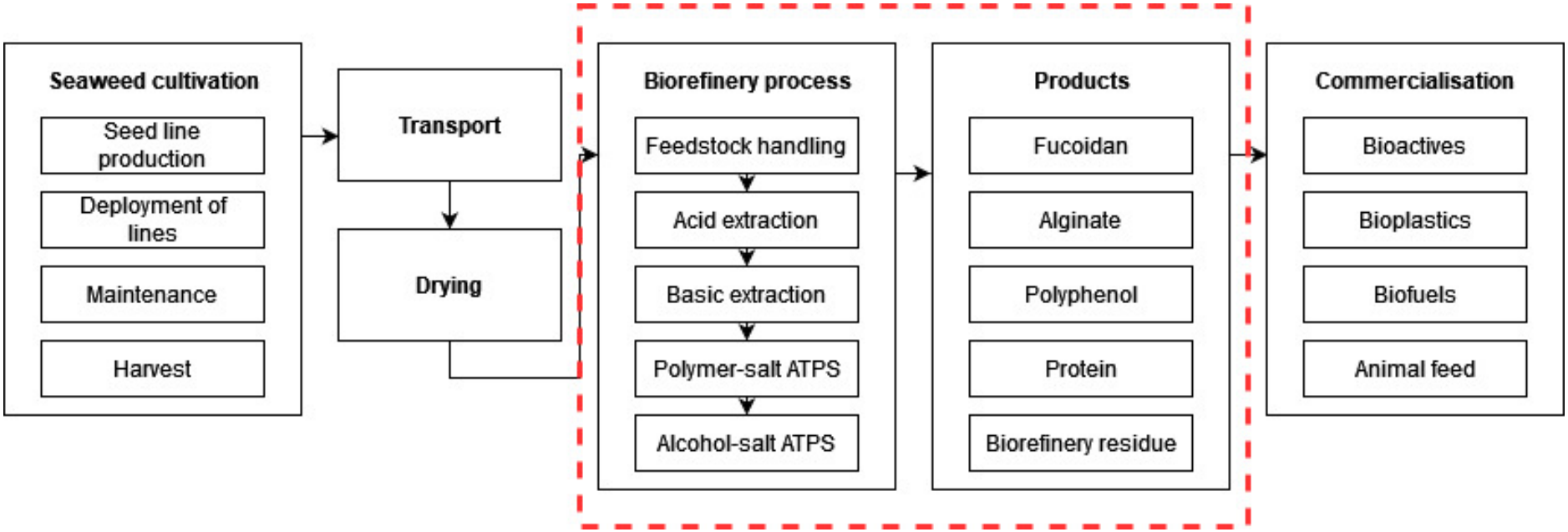

Fig 4-5. Supply chain diagram of the biorefinery process evaluated in this project. The red-dashed box indicates the gate-to-gate system boundaries considered for the development of this study.

2.5.2. Life cycle inventory

The results from the techno-economic evaluation for all different biorefinery scenarios were imported for LCI. The explanation of the different process descriptions and its inventories were given in **Section 2.3** from this **Chapter**. The inputs and outputs were obtained from the modelling including raw materials such as PEG 2000, methanol, outputs such as the amount of every co-product, and utilities such as the electricity consumed. All the other processes' inputs and outputs were obtained from the process flowsheet built for the economic evaluation. All the data were imported into an Ecoinvent database and integrated for conducted LCIA.

2.5.3. Life cycle impact assessment and selected impact categories

Seven impact categories were selected in order to analyse different aspects of the processes with a view to a Blue Economy approach, these categories were selected because they emit to the air and water, and to aim to a Blue Economy approach the understanding of how the emissions might affect this body of water and atmosphere needed to be understood, and to see how they affect them . The methodology selected for the impact assessment was with the Midpoint categories from the ReCiPe 2016 methodology under a Hierarchist perspective and a normalisation approach compared against the average European citizen at year 2010. Climate change impacts quantified in kg CO_2-eq., stratospheric ozone depletion impacts quantified in kg CFC–11-eq., terrestrial acidification impacts quantified kg SO_2-eq. released to air; freshwater eutrophication impacts quantified in kg P-eq., marine eutrophication impacts quantified in kg N-eq. released to water; water depletion impacts quantified in m^3-eq. water that will not return to its original body of water, and fossil fuel depletion quantified in kg oil-eq. consumed were selected to identify critical aspects of the environmental burdens of the scenarios modelled.

3. Results and discussion

3.1. Selection of the cascading sequence order of extractions

The different concentrations observed in **Table 4-1** between the compounds reported by the commercial supplier and the values obtained in the previous chapter might be due to geographical and seasonal variations in the harvesting process and time of analyses (Schmid et al., 2017; Tanniou et al., 2013). Before the assessment of different biorefinery scenarios, the cascading sequence order had to be selected; for this reason, the main biological compounds from *A. nodosum* with potential and/or actual commercial values were identified in **Table 4-1**. As seen in **Fig 4-2**, **4-3** and **4-4** pigments, specifically fucoxanthin, was chosen to be extracted first, due to the lower thermolabile properties (degradation around 30 – 40°C) of the compound (Shannon and Abu-Ghannam, 2018). Lipids were the next extraction in the cascading sequence, due to the interference these compounds produce in further extractions down the cascading sequence train (Sánchez-Machado et al., 2004), e.g., being co-extracted in the polyphenol step (Koivikko et al., 2007). After the extraction of lipids, the next extraction step was to recover polyphenols; this compound was selected because its thermolabile properties, degrading at around 55°C, and potential issues interfering in the next extraction steps (Zhang et al., 2018). Finally, fucoidan was selected to be extracted due to its thermolabile properties, its degradation happens at 80°C (Torres et al., 2019); and alginate was last, due to the bulk amount present in *A. nodosum*, allowing the prioritisation of other high-value compounds present in the macroalga.

3.2. Techno-economic analysis of different biorefinery scenarios

After deciding the order of the extractions in the cascading sequence producing the respective process flowsheets (**Fig 4-2**, **4-3** and **4-4**), techno-economic analyses were performed. TEA was used to quantify some of the important economic indicators such as capital investment/expenditure (CAPEX), operational expenditure (OPEX), total yearly revenue, production cost, internal rate of return (IRR), and NPV. A preliminary estimate

of the capital investment, including fixed and working capital can be seen in **Table 4-2**. The Lang factor was calculated according to Towler and Sinnott (2008). For a seaweed-based biorefinery using solvents with a 1,000 MT of dry biomass per year of capacity, the total capital investment was approximately £178 million, where most of the investment came from the polyphenol, alginate, and fucoxanthin sections. The total capital investment for the *Novel Tech* scenario with a capacity of 1,000 MT of dry biomass per year was £244 million. Thirdly, the total CAPEX for a biorefinery concept based in the use of green chemistry extraction techniques with a processing capacity of 1,000 MT per year was £30 million approximately. The differences of total CAPEX between the three scenarios were due to the more expensive and energy-intensive specialised equipment required for the *Novel Tech* scenario; in contrast with *Green Chem* scenario, where the use of low-heat and low-pressure equipment dropped the initial expenditure. Additionally, the total footprint of the *Solvent-based*, *Novel Tech*, and *Green Chem* scenario facilities for the process line was 105.93 m^2, 74.42 m^2, and 74.3 m^2 respectively. A breakdown of the costings of the three scenarios can be observed through **Sections 3.2.1** to **3.2.3** in this sub chapter.

Table 4-2. Total capital investment for the three different biorefinery scenarios.

Capital investment	Unit	*Solvent-based*	*Novel Tech*	*Green Chem*
Contingency	%	10	10	10
Lang factor	-	3.0	3.0	3.0
Total equipment purchase cost	£	56,382,837	77,555,641	7,977,512
Fixed capital investment	£	169,148,510	232,666,922	23,932,537
Working capital	£	8,457,426	11,633,346	1,196,627
Total capital investment	**£**	**177,605,936**	**244,158,836**	**29,813,062**

Table 4-3. Direct and indirect costs in the two biorefineries proposed.

Item	Unit	*Solvent-based*	*Novel Tech*	*Green Chem*
Direct costs				
Raw materials cost	£/y	1,113,323	185,569	928,500
Utilities cost	£/y	141,579	5,455,668	2,330
Labour cost	£/y	3,720,000	3,720,000	3,720,000
Total direct costs	**£/y**	**4,974,902**	**9,361,236**	**4,650,830**
Indirect costs				
Maintenance	£/y	16,914,851	23,253,222	2,839,339
Local taxes	£/y	3,382,970	4,650,644	567,868
Insurance	£/y	1,691,485	2,325,322	283,934
Depreciation	£/y	16,914,851	23,253,222	2,839,339
Total indirect costs	**£/y**	**38,904,157**	**53,482,412**	**6,530,480**
Total costs	**£/y**	**43,879,059**	**62,843,648**	**11,181,311**
CoG*/kg biomass	£	0.31	0.45	0.08
Production cost/kg biomass	£	0.04	0.07	0.03

*CoG: cost of goods

3.2.1. Solvent-based biorefinery scenario

The total CAPEX breakdown across the different extraction steps of the cascading sequence of the *Solvent-based* biorefining scenario can be observed in **Fig 4-6**, and a breakdown of the main components in each stage can be seen in **Appendix B** (**Table B-1**). The most expensive steps were lipids, polyphenols, and alginate stages, with figures rounding the £11, £15, and £16 million respectively, while fucoxanthin and fucoidan extraction stages CAPEX was around £4-5 million for both. The high CAPEX in the lipids, polyphenol, and alginate stages was due to the bigger processed volumes at them, 68, 620, and 301 m^3, respectively; compared to fucoxanthin and fucoidan steps with 38 and 62 m^3, respectively. *Solvent-based* scenario total CAPEX was lower than

other biorefinery concepts from lignocellulosic industry costings studies, with total capital investments figures around £267 million equivalent at 2016, for a concept using hot water pre-treatment, £278 - £283 million for biorefinery scenarios using dilute acid pre-treatment, and up to £371 million for a pervaporation-distillation scenario (Kazi et al., 2010), while the total CAPEX of this scenario was £178 million, around 1.5 – 2.1times lower of the overall initial expenditure.

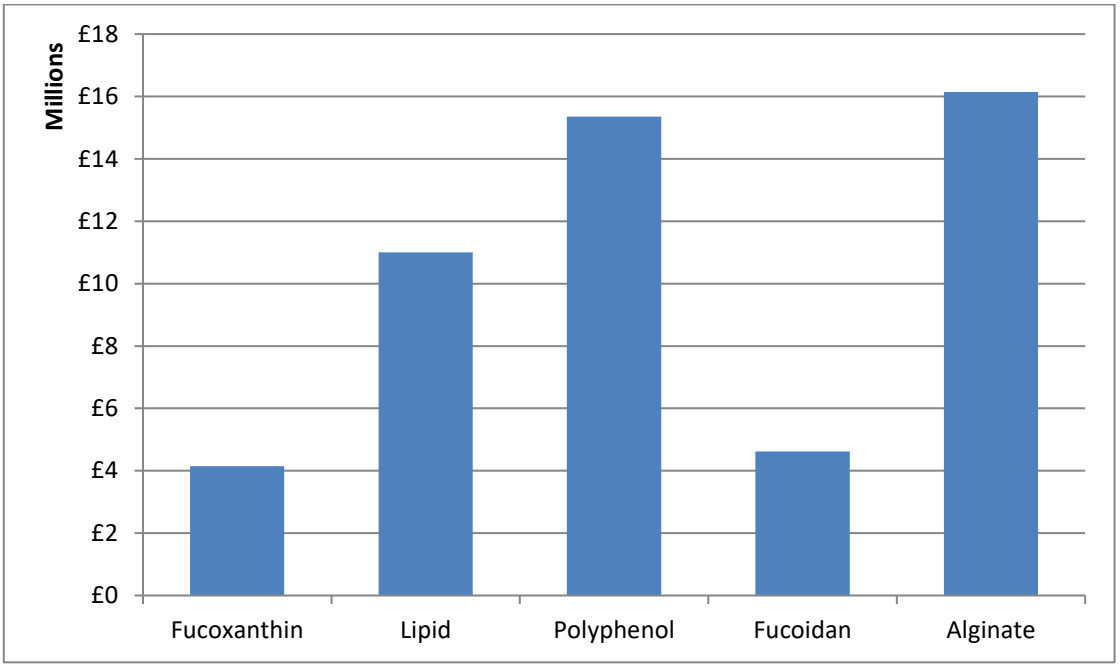

Fig 4-6. Total capital investment categorisation of a solvent-based biorefinery concept using *A. nodosum* as feedstock.

The breakdown of the operation cost for *Solvent-based* scenario is in **Fig 4-7**. Indirect costs, namely maintenance, taxes, insurance, and depreciation are the major drivers in this scenario with an 89% of the total OPEX, while direct costs e.g., raw materials, utilities, and labour covers only an 11% of the overall. Display of the items considered in the operation costs can be observed in **Table 4-3.** Analysing direct costs, the most expensive item is labour with £3,720,000, followed by raw materials with £1,113,323 to purchase the solvents required, specified in **Section 2.3.1** from this **Chapter** in each step of the cascading sequence, and lastly utilities costs with £141,579, this value was

due to the energy usage in the scenario, considering traditional extraction equipment, e.g., agitation tanks, centrifuges, filters, and pumps.

The operation costs across the different steps in the cascading sequence for *Solvent-based* scenario can be seen in **Fig 4-7**. Following the trend observed in **Fig 4-7** the most expensive extraction stages were lipids, polyphenol, and alginate. In the case of indirect costs these were derived from the FCI, thus its breakdown through the biorefining process is proportional to the CAPEX breakdown (**Fig 4-6**); on the other hand, direct costs were influenced by the purchase of extraction solvents, energy use, and labour. Polyphenol extraction process showed the highest direct costs (£1.7 million), due to higher raw materials consumption than the other stages, this elevated use of solvents means materials cost of £862,177, an energy consumption of 12,451 kWh, meaning an energy cost of £78,113, and a labour cost of £744,000. The OPEX of the remaining processing steps in the cascading sequence were £793,798, £812,610, £852,557, and £831,648 for fucoxanthin, lipids, fucoidan, and alginate, respectively.

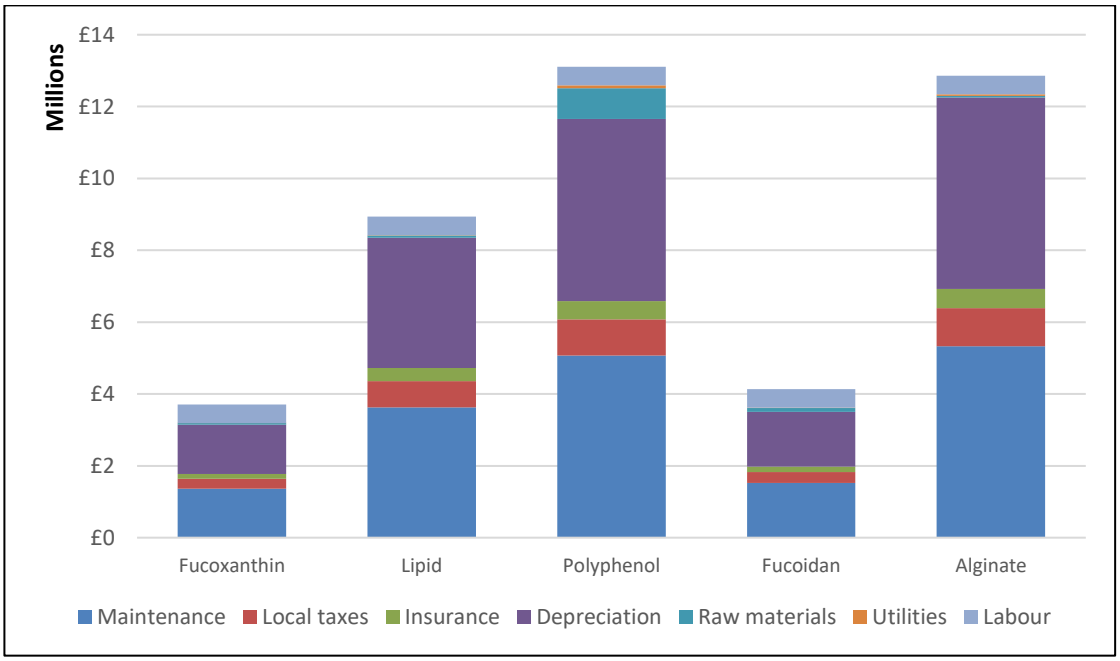

Fig 4-7. Breakdown of the total operation costs across the sequential extraction steps in a biorefinery scenario based in the use of solvents for *A. nodosum* as feedstock.

The breakdown for the costs of goods (CoG) (**Table 4-3**) is observed in **Fig 4-8**. The main factors affecting the CoG/kg were maintenance and depreciation, both with a 38.6% of contribution (£17 million), followed by labour and taxes with 8.5% and 7.7% of contribution (£3-4 million) to the CoG, not to be mistaken with the 2% FCI calculated for income taxes in the general assumptions of the TEA (see **Section 2.2** from this **Chapter**); the final contributions were insurance (3.9%, £1.7 million), raw materials (2.5%, £1.1 million), and utilities (0.3%, £141,579), respectively. With these values calculated the CoG/kg for the *Solvent-based* biorefinery scenario was £0.31, and the production costs were £0.04/kg. Huang et al. (2016) reported production costs of $0.59/L for biodiesel produced from sugarcane, and $0.4/L for bioethanol obtained from the same feedstock, the latter value is similar to the results obtained for this scenario, this is due to the use of well-established processing technologies, i.e., maceration, a conventional unit operation, where the uncertainty of the process is smaller than facilities using technologies with a smaller TRL. The implementation of green solvents has been discussed in recent years to develop more sustainable solvent-based biorefineries, with ionic liquids being suggested to utilise in lignocellulosic biorefineries (Soh and Eckelman, 2016), but TEA studies have shown that the high costs of ionic liquids hinder their application in these biorefinery concepts (Klein-Marcuschamer et al., 2011).

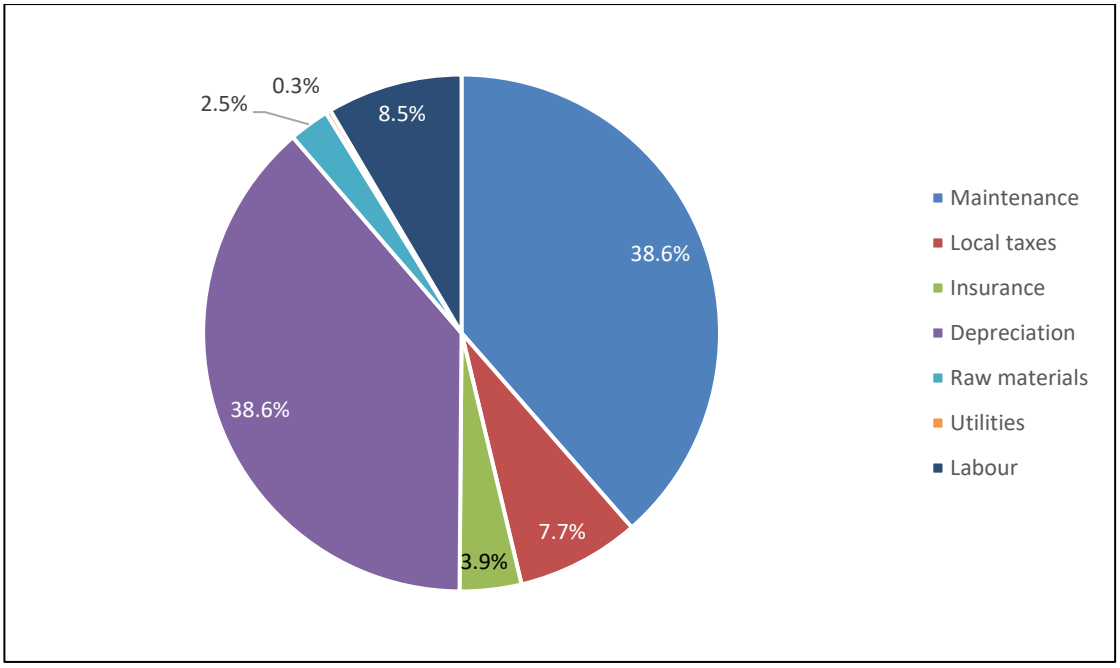

Fig 4-8. Analysis of the cost of goods of the solvent-based biorefining cascading sequence scenario using *A. nodosum* as a feedstock.

3.2.2. Novel technologies biorefinery scenario

The total CAPEX breakdown across the different extraction steps of the cascading sequence of the *Novel Tech* biorefining scenario can be observed in **Fig 4-9,** and an itemization of the main constituents in each stage can be seen in **Appendix B** (**Table B-2**). The most expensive steps were polyphenols, fucoidan, and alginate stages, with figures rounding the £17, £23, and £21 million respectively, while fucoxanthin and lipids extraction stages CAPEX was around £7.7 million, and £ 1.4 million, respectively for both. The high initial investment in the polyphenol, fucoidan, and alginate platforms was due to the need for specialised equipment, specifically microwave extractors in each step, with prices varying around £11 - £17 million per unit; compared with fucoxanthin and lipid, using ultrasound-assisted extraction and requiring less expensive specialised equipment, rounding £1 - £2 million. *Novel Tech* scenario total CAPEX was the highest from all scenarios analysed in the study, but still lower than the other biorefinery concepts from the lignocellulosic industry costings studies performed by Kazi et al. (2010), with total CAPEX around £267 million equivalent in 2017, and up to £371 million,

while the total CAPEX of this biorefinery concept was £244 million, around a 1.1 – 1.5-fold decrease of the overall initial expenditure.

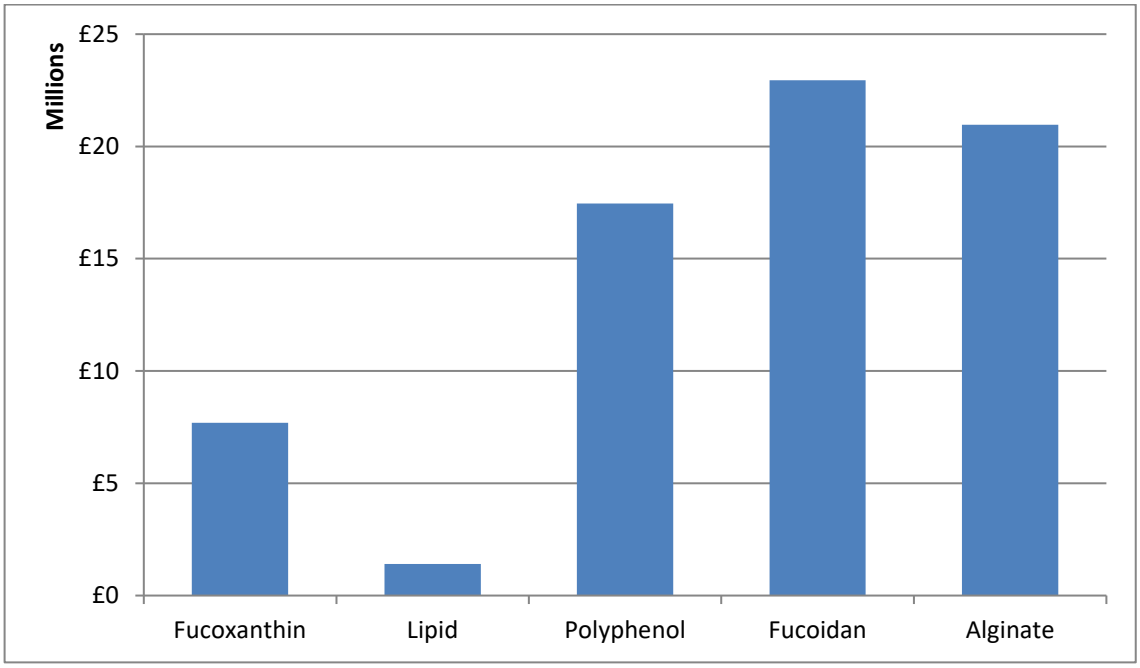

Fig 4-9. Total capital investment categorisation of a biorefinery concept implementing novel technologies to obtain high-value compounds from *A. nodosum*.

The breakdown of the operation cost for *Novel Tech* scenario is in **Fig 4-10.** Indirect costs, specifically maintenance, taxes, insurance, and depreciation are the main overhead in this scenario with an 85% of the total OPEX, while direct costs (raw materials, utilities, and labour) cover only a 15% of the overall. The display of the items considered in the calculation of the operation costs can be observed in **Table 4-3.** Analysing the direct costs, the most expensive item is utilities with £5,455,668, this figure was due to the high energy requirements of the specialised extraction pieces of equipment in this scenario; raw materials costs had the smallest contribution to the direct costs with £185,569 due to the smallest volumes of solvent required to perform the extractions and water-based extractions, detailed in **Section 2.3.2** from this **Chapter**, and lastly labour costs with £3,720,000.

The operation costs across the different steps in the cascading sequence for *Novel Tech* cascading sequence can be seen in **Fig 4-10**. Following the tendency observed in **Fig 4-9** the most expensive extraction stages were polyphenol, fucoidan, and alginate. In the case of indirect costs these were derived from the fixed capital investment, thus its breakdown through the biorefining process is proportional to the CAPEX breakdown (**Fig 4-10**); on the other hand, direct costs were influenced by the purchase of extraction reagents, energy use, and labour. Lipid and polyphenol extraction process showed the highest direct costs (£2.6 million), due to the elevated utilities needed for the extraction of these compounds, with a total cost in both processes of £1.8 million, attributable to an average energy consumption of 436,000 kWh per process; a labour cost of £744,000, and materials costs of £38,962 for the lipid stage and £108 for polyphenols, this value is the smallest because the modelled extraction use only water. The OPEX of the remaining processing steps in the cascading sequence were £789,963, £1.75 million, and £1.65 million for fucoxanthin, fucoidan, and alginate, respectively.

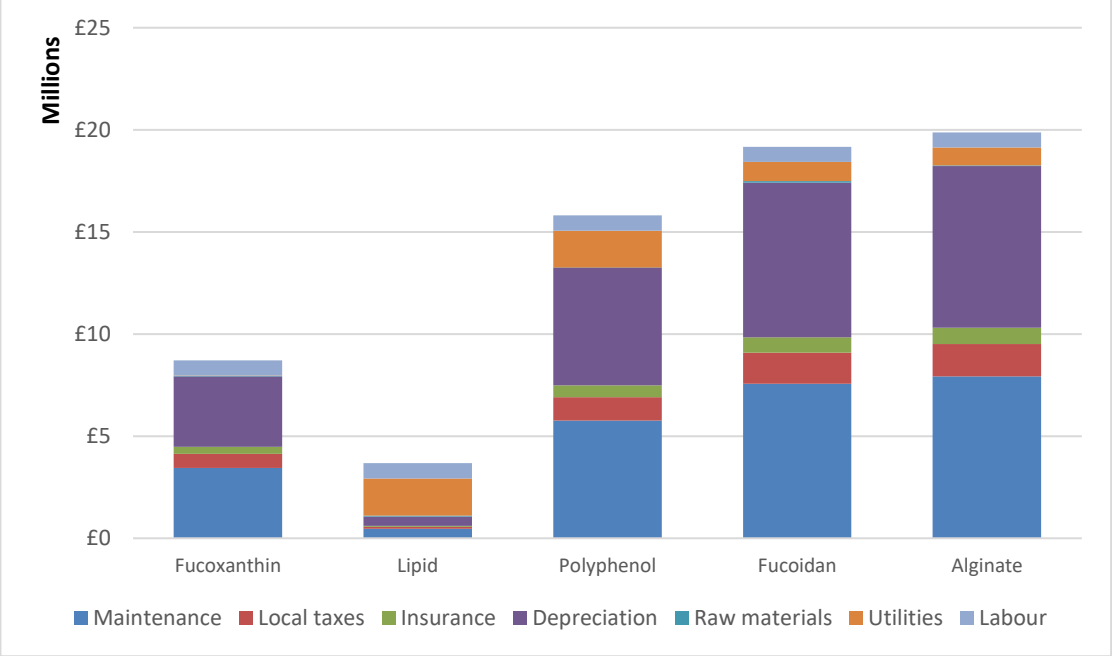

Fig 4-10. Breakdown of the total operation costs across the sequential extraction steps in a biorefinery scenario based in the use of MAE and UAE for *A. nodosum* as feedstock.

The breakdown for the CoG (**Table 4-3**) is observed in **Fig 4-11**. The main factors affecting the CoG/kg were maintenance and depreciation, both with a 37.0% of contribution (£23 million), followed by utilities and taxes with 8.7% and 7.4% of contribution (~£5 million); the final contributions were labour (5.9%, £3,720,000), insurance (3.7%, £2.3 million), and raw materials (0.3%, £185,569), respectively. With these values calculated the CoG/kg for the *Novel Tech* biorefinery scenario was £0.45, and the production costs were £0.07/kg. Comparing with the results obtained by (Huang et al., 2016), their production costs were similar than results for this scenario, this is due to, as explained previously, the high energy requirements calculated for the cascading stages used for this scenario and the high initial capital expenditure allocated for the purchase of microwave extractors.

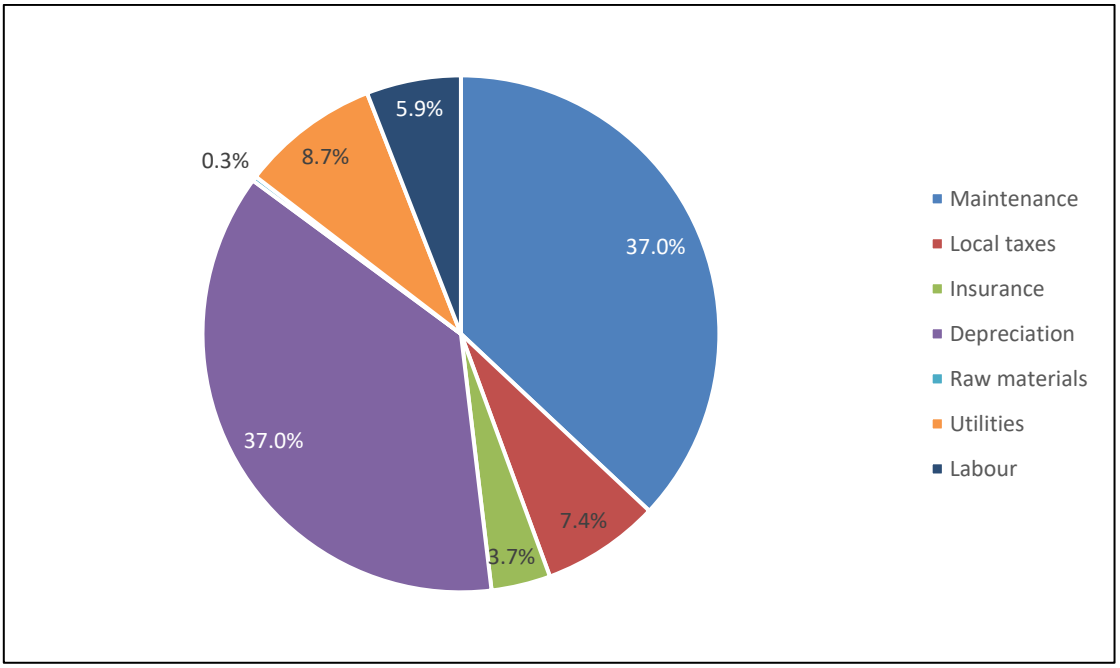

Fig 4-11. Analysis of the cost of goods of the MAE- and UAE-based biorefining cascading sequence scenario using *A. nodosum* as a feedstock.

3.2.3. Green chemistry biorefinery scenario

The total CAPEX breakdown across the different extraction steps of the cascading sequence of the *Green Chem* biorefining scenario can be observed in **Fig 4-12,** and a

breakdown of the main components in each stage can be seen in **Appendix B** (**Table B-3**). The most expensive steps were fucoidan and protein, with figures rounding the £2.82 million and £2.66 respectively, while polyphenol, fucoxanthin, and alginate extraction stages CAPEX was around £1.34 million, £1.18 million, and £600,557, respectively. The low initial investment in all extraction platforms was due to the use for low pressure, low temperature equipment was used, with agitation tanks, and centrifuges being the most used equipment. *Green Chem* scenario total CAPEX was the lowest from all scenarios analysed in the study, and substantially lower than other biorefinery concepts from the lignocellulosic industry costings studies rising as a promising candidate for biorefinery developments (Kazi et al., 2010), while the total CAPEX of this biorefinery concept was £244 million, around a 14.9 – 10.7-fold decrease of the overall initial expenditure.

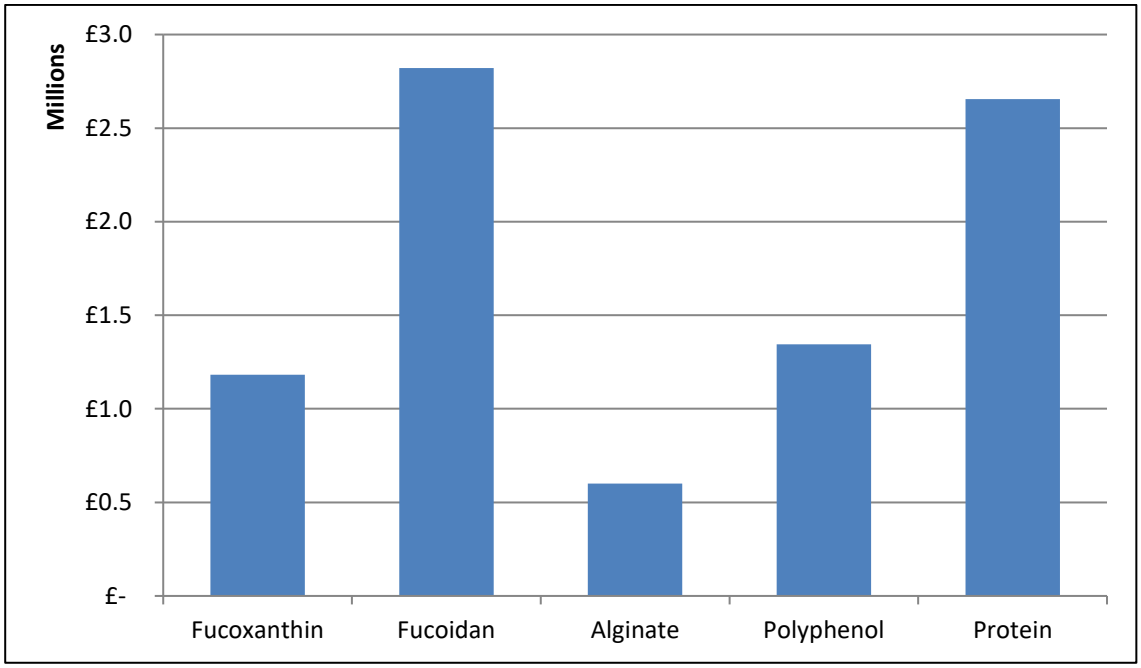

Fig 4-12. Total capital investment categorisation of a biorefinery concept implementing green chemistry technologies to obtain high-value compounds from *A. nodosum*.

The breakdown of the operation cost for the *Green Chem* scenario is in **Fig 4-13.** There is a more even distribution of the costs in this scenario, with the indirect costs, defined as maintenance, taxes, insurance and depreciation being the main contributors with a 58%

of the total OPEX, while direct costs (raw materials, utilities, and labour) covered the remaining 42%. The display of the items considered in the calculation of the operation costs can be observed in **Table 4-3.** When examining the direct costs, it is noted that the most expensive item was labour with £3,720,000, this figure was due to the salaries considered for the correct operation of the facility at all stages and all the supervisory personnel as well as the quality control/quality assurance (QC/QA); utilities costs had the smallest contribution to the direct costs with £2,330 due to the smaller energy requirements in all stages of the scenario, detailed in **Section 2.3.2** from this **Chapter**, and finally raw materials costs with £928,500.

The operation costs across the different steps in the cascading sequence for *Green Chem* cascading sequence can be seen in **Fig 4-13**. Following the trend examined in **Fig 4-12** the most expensive extraction stages were fucoidan and protein. In the case of indirect costs these were derived from the FCI, thus its breakdown through the biorefining process is proportional to the CAPEX breakdown (**Fig 4-12**); on the other hand, direct costs were influenced by the purchase of extraction reagents and phase forming components, energy use, and labour. Protein extraction process showed the highest direct costs (£1.6 million), due to the raw materials needed for the extraction of it (£858,259); a labour cost of £744,000, and utilities of £1,013. The OPEX of the remaining processing steps in the cascading sequence were £745,063, £766,200, £744,373, and £795,840 for fucoxanthin, polyphenol, fucoidan, and alginate, respectively.

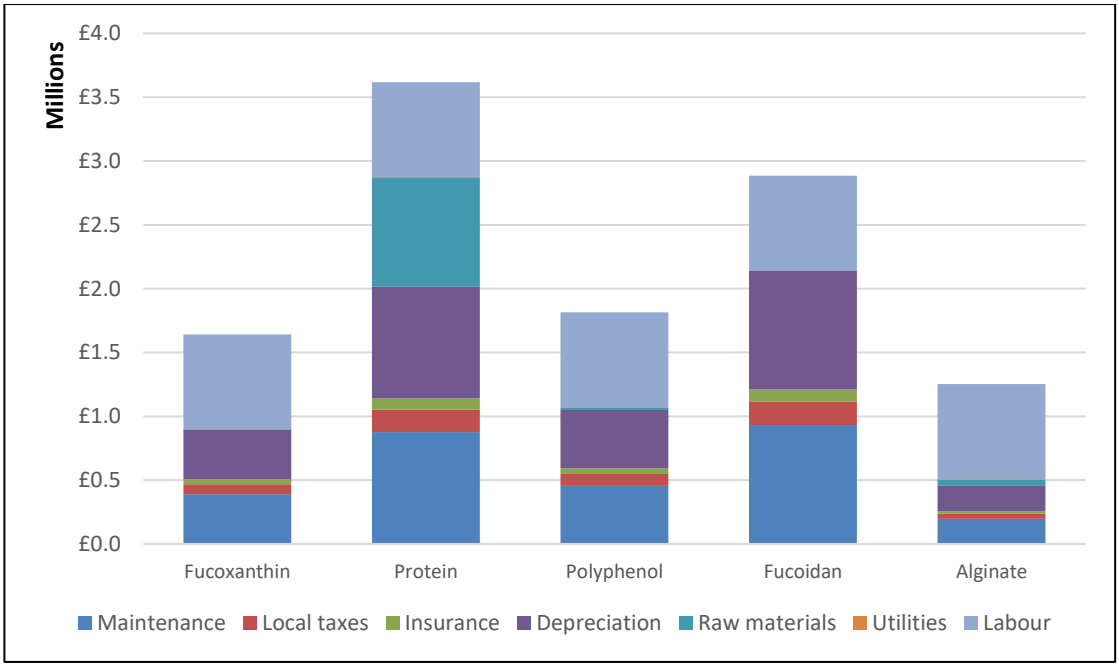

Fig 4-13. Breakdown of the total operation costs across the sequential extraction steps in a biorefinery scenario based in the use of green techniques for *A. nodosum* as feedstock.

The breakdown for the CoG (**Table 4-3**) is observed in **Fig 4-14**. The main factors affecting the CoG/batch was labour with a 33.3% of contribution, with a value of £3.7 million, followed by maintenance and depreciation, both with a 25.4% of contribution (£2.8 million), next raw materials (£928,500) and taxes (£567,868) with 8.3% and 5.1% of contribution, respectively; the final contributions were insurance (2.5%, £283,934), and utilities (0.1%, £6,247), respectively. With these values calculated the CoG/kg for the *Green Chem* biorefinery scenario was £0.08, and the production costs were £0.03/kg, rising as the cheapest option of all the scenarios analysed in this study. Huang et al. (2016) reported production costs of $0.59/L for biodiesel produced from sugarcane, and $0.4/L for bioethanol obtained from the same feedstock, these values are higher than the results for this scenario, this highlights the profitability of this cascading sequence and the further exploration of this scenario for the development of a sustainable biorefinery.

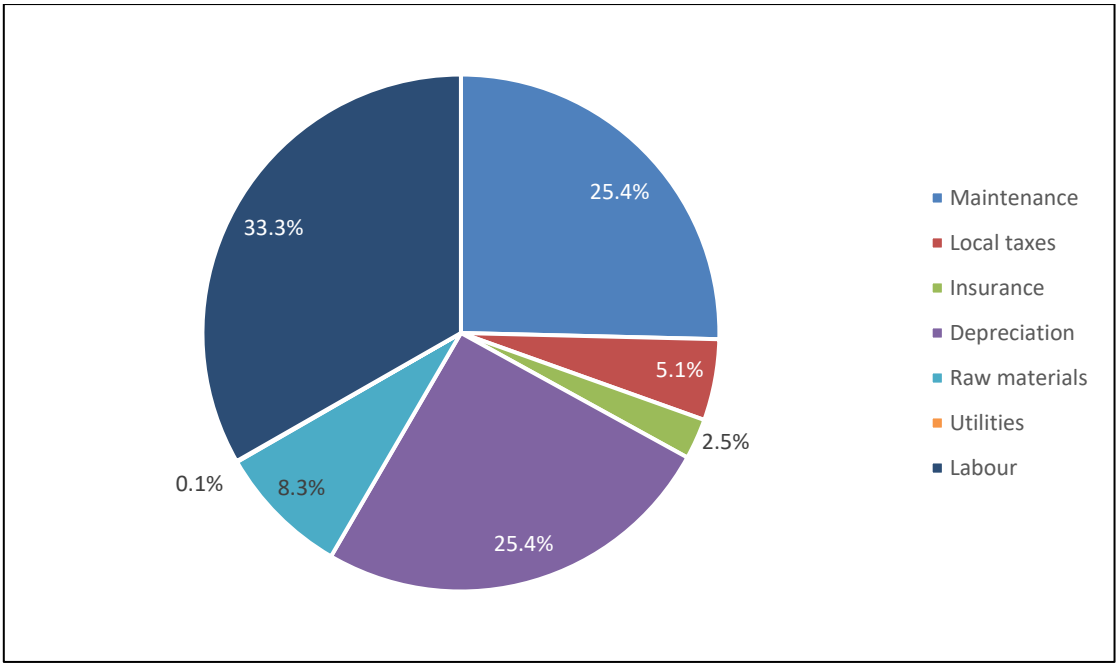

Fig 4-14. Analysis of the cost of goods of a green chemistry-compliant biorefining cascading sequence scenario using *A. nodosum* as a feedstock.

3.2.4. Comparison of biorefinery scenarios economic metrics

In **Table 4-3** are summarised the direct and indirect costs for the three biorefineries concepts analysed. Raw materials costs in *Solvent-based* scenario were 6 times higher than *Novel Tech* scenario and 1.6 times higher than *Green Chem* scenario; additionally, *Green Chem* biorefinery raw materials costs were 3.7 times higher than *Novel Tech* scenario (**Fig 4-15**). Labour cost was estimated to be the same in all scenarios. Labour was estimated considering two production operators per section, with five extraction section considered in all processes, one production supervisor in each section, and with QC/QA personnel in each step. Utilities were cheaper in *Green Chem* biorefinery, meanwhile *Novel* Tech scenario utilities were the highest in all scenarios analysed, this is due to the more energy-requiring equipment (microwave extractors) used. The OPEX to CAPEX ratio for *Solvent-based* and *Novel Tech* biorefining scenario pathways was 0.25 and 0.26, respectively, and *Green Chem* scenario was around 0.39. This increase could be attributed to a decrease in the total capital investment of the cascading sequence, requiring less energy intensive pieces of equipment, compared to the other

processes. The CAPEX for *Novel Tech* scenario was 9.7 times higher when is compared with *Green Chem* scenario, on the other hand *Solvent-based* scenario was 1.4 times lower than *Novel Tech* and 7 times higher than *Green Chem* scenario. The high initial investment in *Novel Tech* scenario was due to the purchase of microwave and ultrasound extractors, compared to the non-specialised equipment used in *Green Chem* scenario and the smaller volumes used in it. The greatest amount of process uncertainties across all scenarios analysed were found in the extraction yield of the recovery stages, which affected the sales price of the compounds, as well as the design of the extraction stages, influencing the sizing of the equipment and the volume handles for the operation. These uncertainty factors were identified by Tang et al. (2015) as well in a modelled biodiesel production facility, where in their case the main drivers for uncertainty were capital cost, feedstock price, and biodiesel conversion efficiency. The utilities costs associated to run the microwave extractors, as well as the utilities of the ultrasound-assisted extraction processes elevated the total OPEX of *Novel Tech* scenario, while the large amounts of volume required in the *Solvent-based* scenario and the costs of the solvents utilised elevated the operating costs, while the smaller volumes used in *Green Chem* scenario, due to the use of ATPS, produced the smallest OPEX of them all. Following the trend observed in CAPEX and OPEX *Novel Tech* scenario exhibited the highest total revenues of all scenarios analysed (**Fig 4-15**).

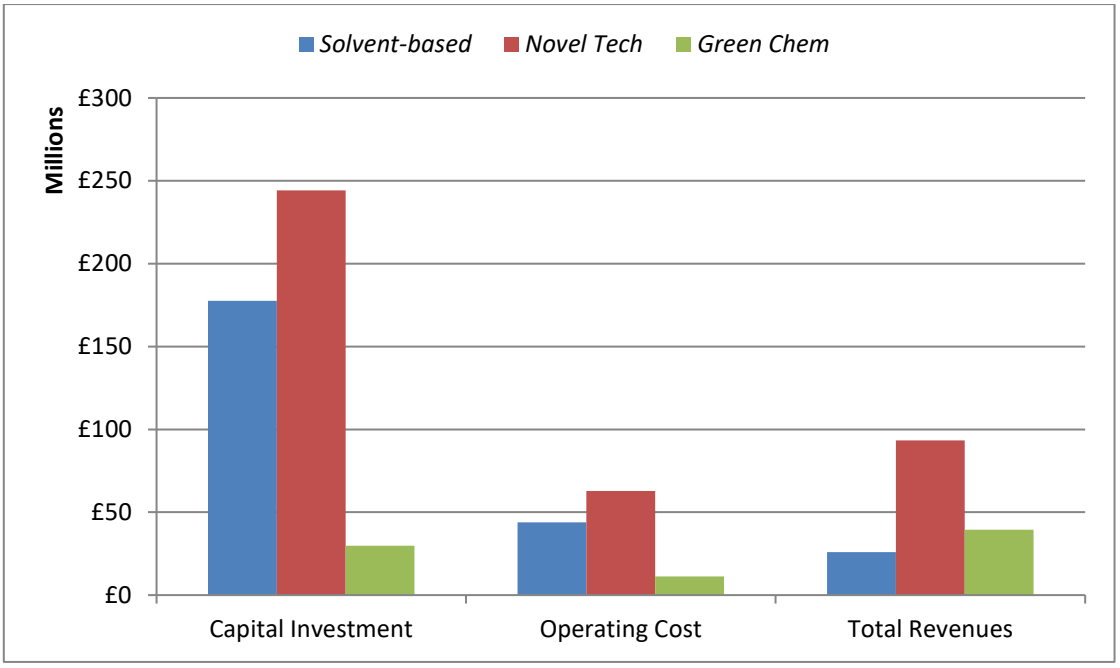

Fig 4-15. Economic metrics for different biorefinery scenarios using *A. nodosum* as a feedstock. Operating costs and total revenues are displayed based on one year of operation.

The production cost per kg of *A. nodosum* biomass utilised in *Green Chem* scenario was £0.03, the lowest of all scenarios analysed, with an IRR of 75.2% (**Fig 4-16**), highlighting this scenario as promising to undertake further TFT on it. *Novel Tech* scenario exhibited the highest production cost/kg (£0.07) and showed the second highest IRR value (30.5%), while *Solvent-based* scenario presented a production cost/kg and IRR values of £0.04 and 21.4%, respectively.

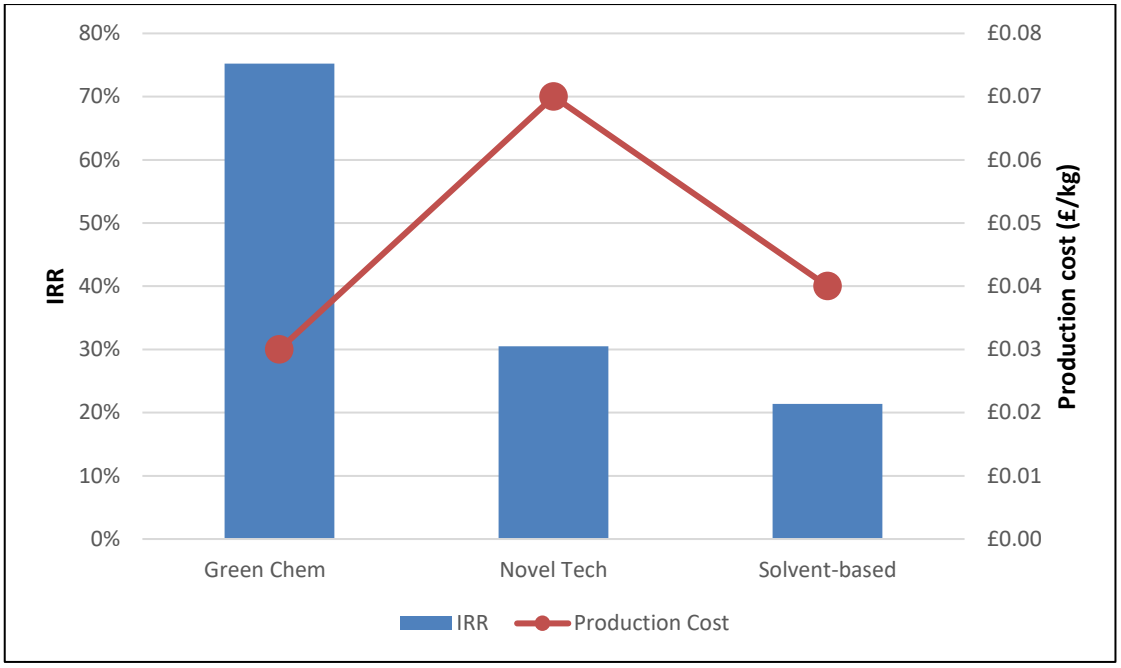

Fig 4-16. Internal rate of return and production cost per kg of biomass of the different scenarios assessed using *A. nodosum* as a feedstock.

The discounted cumulative cash flow in **Fig 4-17** showed that *Green Chem* scenario had the shortest break-even point at the first year of operation with a cash flow at year 1 of £11,840,641 a total cash flow after 10 years of operation of £251 million, with a NPV of £4,165,370. *Novel Tech* scenario break-even point occurred at third year of operation with a cash flow of £43 million, a total cash flow after ten years of operation of around £466 million and an NPV of £10,508,918. *Novel Tech* presented a steep increase after break-even point since the recovery yields in key compounds like polyphenols and fucoidan were higher than the other models; hence the profitability of its sales was higher (**Table 4-4**). Finally, *Solvent-based* scenario displayed a break-even point at fourth year, with a cash flow at that moment of £9 million, an NPV of £3,904.486, and a total cash flow after 10 years of operation of £137 million.

Table 4-4. Total yearly sales revenue of the three cascading scenarios analysed in this chapter.

Sales revenue	Unit	*Solvent-based*	*Novel Tech*	*Green Chem*	Average price/kg*
Fucoxanthin	£/y	165,310	267,652	706,374	459.55
Lipid	£/y	13,050	80,727	-	1.37
Protein	£/y	-	-	23,925,705	229.78
Polyphenol	£/y	17,729,254	45,295,705	5,121,446	459.55
Fucoidan	£/y	6,989,631	46,986,416	8,557,994	459.55
Alginate	£/y	942,496	662,457	1,153,977	5.01
Total sales	**£/y**	**25,839,741**	**93,292,957**	**39,465,496**	**-**

*: Prices derived from Andersen (2017)

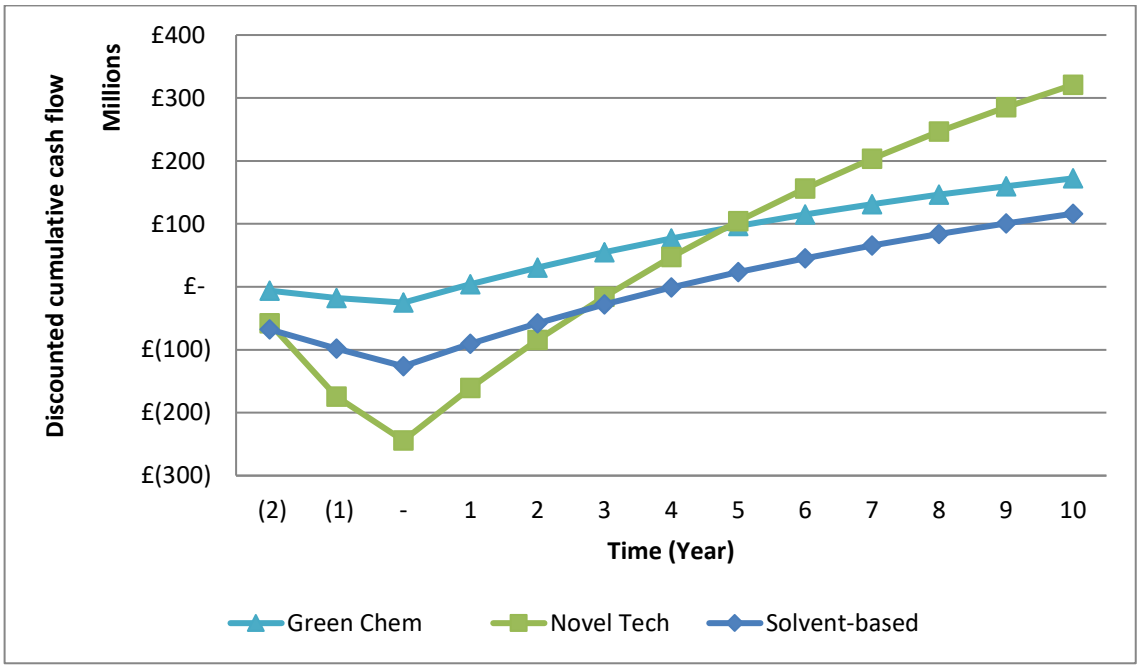

Fig 4-17. Discounted cumulative cash flow of three biorefinery scenarios using *A. nodosum* as initial feedstock.

3.3. Life cycle assessment of different biorefinery scenarios

Based on the inputs from the process flowsheets, the LCI inputs were obtained (**Table 4-5**). LCA was assessed with LCI using SimaPro v8.5.2 and ReCiPe v1.13 was used as an impact assessment method. Seven different environmental indicators were compared between the three scenarios. The functional unit was set at 1 kg of *A. nodosum* processed biomass.

Table 4-5. Life cycle inventory data used in each stage of the updated cascading sequence per batch.

				Solvent-based	*Novel Tech*	*Green Chem*
Extraction stage	Materials/Utilities	Eco-invent process	Unit	Amount	Amount	Amount
Fucoxanthin	Acetone	Acetone, liquid {GLO} | market for | Cut-off, S	m^3	21.3	-	-
	Ethanol	Ethanol, without water, in 99.7% solution state, from ethylene {GLO} | market for | Cut-off, S	m^3	-	-	151.18
	K_2HPO_4	Potassium hydroxide {GLO} | market for | Cut-off, S	kg	-	-	79,309
	KH_2PO_4	Phosphoric acid, industrial grade, without water, in 85% solution state {GLO} | market for | Cut-off, S				
	Water	Water, ultrapure {GLO} | market for | Cut-off, S	m^3	12.9	12.9	158.62
	Electricity	Electricity, medium voltage {GB} | market for | Cut-off, S	kWh	1,164.2	830.4	221.2
Lipid	Ethanol	Ethanol, without water, in 99.7% solution state, from ethylene {GLO} | market for | Cut-off, S	m^3	140.32	-	-
	Hexane	Hexane {GLO} | market for | Cut-off, S	m^3	-	34.22	-
	Electricity	Electricity, medium voltage {GB} | market for | Cut-off, S		1,450.6	211,752	-
	Heating	Heat, from steam, in chemical industry {RoW} | market for | Cut-off, S		2,259	1,128	-
Protein	Methanol	Methanol {GLO} | market for | Cut-off, S	m^3	-	-	335.14
	K_3PO_4	Potassium hydroxide {GLO} | market for | Cut-off, S	kg	-	-	502,704
		Phosphoric acid, industrial grade, without water, in 85% solution state {GLO} | market for | Cut-off, S				
	NaCl	Sodium chloride, powder {GLO} | market for | Cut-off, S	kg	-	-	50,270
	Water	Water, ultrapure {GLO} | market for | Cut-off, S	m^3	-	-	787,570
	Electricity	Electricity, medium voltage {GB} | market for | Cut-off, S	kWh	-	-	395.1
Polyphenol	Acetone	Acetone, liquid {GLO} | market for | Cut-off, S	m^3	432.25	-	-

	PEG 2000	Ethylene glycol {GLO} | market for | Cut-off, S	kg	-	-	15,031
	KH_2PO_4	Phosphoric acid, industrial grade, without water, in 85% solution state {GLO} | market for | Cut-off, S	kg	-	-	21,522
	Water	Water, ultrapure {GLO} | market for | Cut-off, S	m^3	185.25	86.28	46.11
	Electricity	Electricity, medium voltage {GB} | market for | Cut-off, S	kWh	12,450	434,630	10.03
Fucoidan	HCl	Hydrochloric acid, without water, in 30% solution state {RER} | market for | Cut-off, S	m^3	2.1	1.5	0.1
	NaOH	Sodium hydroxide, without water, in 50% solution state {GLO} | market for | Cut-off, S	kg	2,103	1,552	-
	Ethanol	Ethanol, without water, in 99.7% solution state, from ethylene {GLO} | market for | Cut-off, S	m^3	111.12	-	54.50
	Water	Water, ultrapure {GLO} | market for | Cut-off, S	m^3	55.57	40.99	27.25
	Electricity	Electricity, medium voltage {GB} | market for | Cut-off, S	kWh	1,253.7	224,264	21.3
Alginate	NaOH	Soda ash, dense {GLO} | market for | Cut-off, S	kg	4,825	455.5	-
	Ethanol	Ethanol, without water, in 99.7% solution state, from ethylene {GLO} | market for | Cut-off, S	m^3	120.6	-	-
	$CaCl_2$	Calcium chloride {GLO} | market for | Cut-off, S	kg	-	-	275
	Water	Water, ultrapure {GLO} | market for | Cut-off, S	m^3	60.3	42.98	27.5
	Electricity	Electricity, medium voltage {GB} | market for | Cut-off, S	kWh	603.11	209,615	6.1

3.3.1. Solvent-based biorefinery scenario

The impact contribution of each step of the cascading sequence for the *Solvent-based* scenario can be observed in **Fig 4-18**.

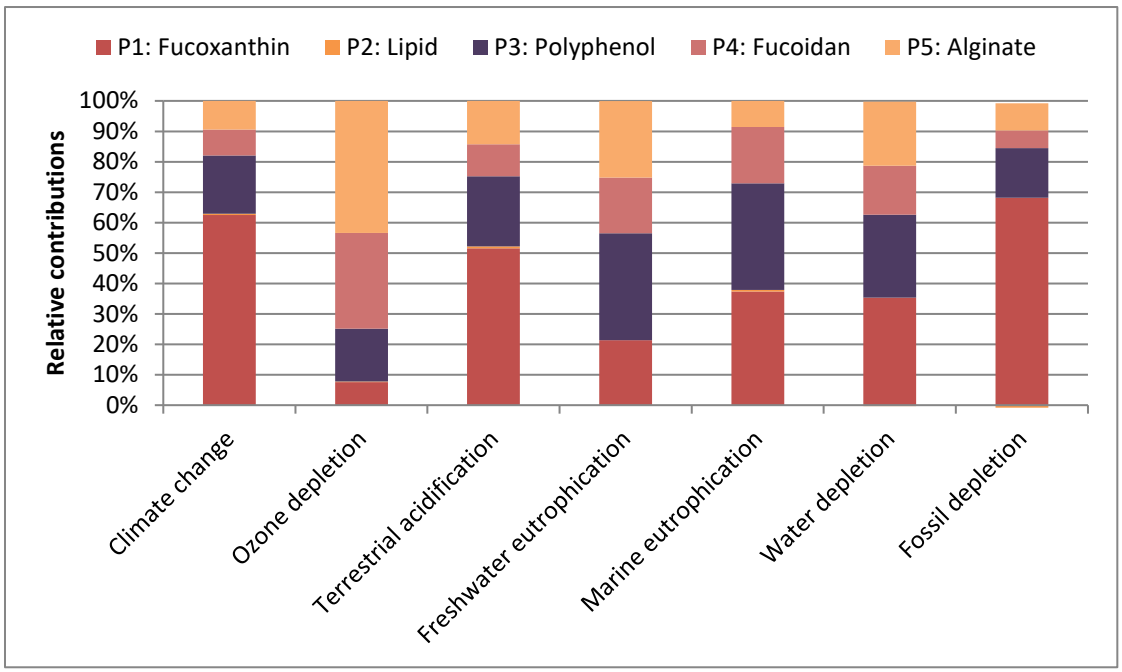

Fig 4-18. Breakdown of the impact contribution across different categories of each extraction step involved in the processing of 1 kg of *A. nodosum* using techniques based in the use of solvents.

Solvent-based scenario produced a total of 38.21 kg CO_2-eq., where the major contributors were fucoxanthin, and polyphenol extraction steps with 23.9 kg CO_2-eq. (62.4% total contribution) and 7.3 kg CO_2-eq. (19.1%) respectively. The high contribution in both stages was due to the use of acetone for their respective extractions. A total of 2.88×10^{-6} kg CFC-11-eq. were produced in this scenario, with the main contributors being polyphenol (4.99×10^{-7} kg CFC-11-eq.; 17.3%), fucoidan (9.08×10^{-7} kg CFC-11-eq.; 31.5%) and alginate (1.25×10^{-6} kg CFC-11-eq.; 43.4%). Again, the use of acetone in polyphenol stage contributes to the impacts in this category, while the use of ethanol in fucoidan and alginate increased their impact. Fucoxanthin, polyphenols and alginate were the stages with the biggest impact in the terrestrial acidification category, with

contributions of 51.5% (0.054 kg SO_2-eq.), 23% (0.024 kg SO_2-eq.), and 14.3% (0.015 kg SO_2-eq.), respectively, and a total contribution of this cascading sequence of 0.104 kg SO_2-eq. Fucoxanthin and polyphenol recovery were the most impactful processes in freshwater and marine eutrophication categories with $1.93x10^{-3}$ kg P-eq. and $3.29x10^{-2}$ kg N-eq. for fucoxanthin, and $3.17x10^{-3}$ kg P-eq. and $3.09x10^{-2}$ kg N-eq. for polyphenol. Alginate extraction stage contributed with $2.28x10^{-3}$ kg P-eq. in freshwater eutrophication, and fucoidan step contributed with around 18% in both categories, $1.65x10^{-3}$ kg P-eq. and $1.63x10^{-2}$ kg N-eq., respectively. A total of 0.47 m^3-eq. of water was depleted in this scenario to process 1 kg of *A. nodosum*, with fucoxanthin process being the most impactful contributor (35.5%; 0.17 m^3-eq.), followed by polyphenol (27.4%) and alginate (21.1%) with 0.13 m^3-eq., and 0.1 m^3-eq., respectively. Fucoxanthin stage was the main contributor for fossil depletion with 69.3% of the impact from a total of 7.7 kg oil-eq to process 1 kg of *A. nodosum* in this scenario. The high impacts across all categories of fucoxanthin and polyphenol extraction stages was due to the use of acetone in their recovery operations, while the use of ethanol in fucoidan and alginate steps was the main driver for their contributions.

3.3.2. Novel technologies biorefinery scenario

The process contribution of each step of the cascading sequence of the *Novel Tech* scenario can be seen in **Fig 4-19**. Polyphenol extraction step was the most contributing process in all categories assessed, contributing with 102.9 kg CO_2-eq. (34.3%) in climate change, $3.5x10^{-6}$ kg CFC-11-eq. (29.4%) for ozone depletion, 0.42 kg SO_2-eq. (35.4%) released in terrestrial acidification, freshwater and marine eutrophication values of $2.9x10^{-2}$ kg P-eq. (37.3%) and $4.1x10^{-2}$ kg-N eq. (36.3%), respectively. This extraction process is depleting 0.27 m^3-eq. with a contribution of 30.9% of the total impact; and finally, fossil depletion with 26.8 kg oil-eq. (32.3%). Following, lipid extraction step was the next most contributing process in all impact categories, with 81.2 kg CO_2-eq. (27.1%) in climate change, $4.2x10^{-6}$ kg CFC-11-eq. (34.9%) for ozone depletion, 0.29 kg SO_2-eq.

(24.7%) released in terrestrial acidification, freshwater and marine eutrophication values of $1.75x10^{-2}$ kg P-eq. (22.4%) and $2.62x10^{-2}$ kg-N eq. (23.3%), respectively. This extraction process is depleting 0.13 m^3-eq. with a contribution of 15.5% of the total impact; and finally, fossil depletion with 21.6 kg oil-eq. (26.1%). The next process contributing to the impact categories assessed was fucoidan extraction, with an average of 18.9% across all categories. This process was releasing 54.02 kg CO_2-eq. (18.03%) as climate change potential, $2.4x10^{-6}$ kg CFC-11-eq. (19.8%) for ozone depletion, 0.22 kg SO_2-eq. (18.7%) released in terrestrial acidification; freshwater and marine eutrophication values of $1.6x10^{-2}$ kg P-eq. (20%) and $2.2x10^{-2}$ kg-N eq. (19.4%), respectively. The calculated water depletion for this extraction stage was 0.17 m^3-eq. with a contribution of 19.2% of the total impact; and finally, fossil depletion with 14.1 kg oil-eq. (17%).

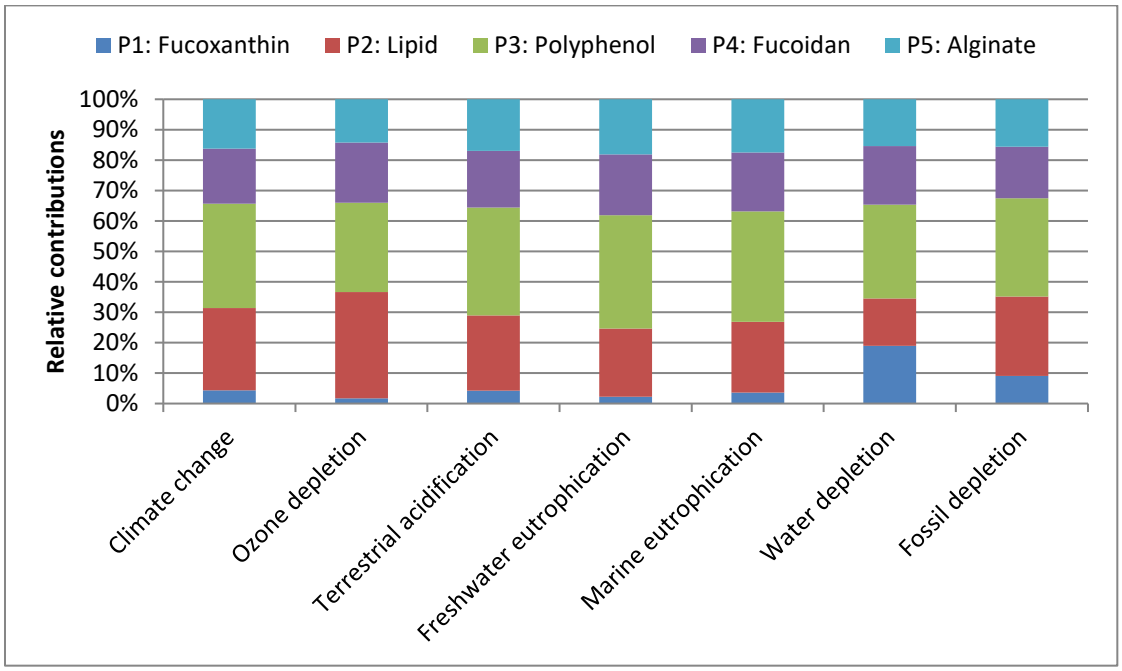

Fig 4-19. Breakdown of the impact contribution across different categories of each extraction step involved in the processing of 1 kg of *A. nodosum* using physicochemical techniques based in the application of ultrasound and microwave principles.

Next, alginate cascading step was the most contributing process, with 48.7 kg CO_2-eq. (16.2%) in climate change potential, $1.7x10^{-6}$ kg CFC-11-eq. (14.3%) for stratospheric ozone depletion, 0.2 kg SO_2-eq. (17%) released in terrestrial acidification, freshwater, and marine eutrophication values of $1.42x10^{-2}$ kg P-eq. (18.1%) and $1.96x10^{-2}$ kg-N eq. (17.5%), respectively. This extraction process depleted 0.13 m^3-eq. with a contribution of 15.4% of the total impact; and lastly, fossil depletion with 12.9 kg oil-eq. (15.6%). At last, fucoxanthin was the least contributing extraction process of this scenario, with 12.9 kg CO_2-eq. (4.3%) for climate change potential, $2.1x10^{-7}$ kg CFC-11-eq. (1.8%) for ozone depletion, 0.05 kg SO_2-eq. (4.3%) released in terrestrial acidification, freshwater, and marine eutrophication values of $1.8x10^{-3}$ kg P-eq. (2.3%) and $4x10^{-3}$ kg N-eq. (3.6%), respectively. This extraction process is depleting 0.16 m^3-eq. with a contribution of 19% of the total impact; and finally, fossil depletion with 7.5 kg oil-eq. (9.1%). The high energy usage of all stages was the main driver for the contributions across all impact categories (**Table 4-5**), with the high amount of electricity utilised by polyphenol the most contributing factor, followed by lipid recovery stage.

3.3.3. Green chemistry biorefinery scenario

In **Fig 4-20** the process contributions for the *Green Chem* biorefinery scenario can be observed. The global warming potential of this scenario produced a total impact of 20.22 kg CO_2-eq., where the major contributors were fucoxanthin, protein, polyphenol, and alginate extraction steps with 5.49 kg CO_2-eq. (27.2% total contribution), 4.93 kg CO_2-eq. (24.4%), 4.89 kg CO_2-eq. (24.2%) and 4.7 kg CO_2-eq. (23.2%) respectively. The total process contribution can be observed in **Appendix D** (**Table D-1**). A total of $4.48x10^{-7}$ kg CFC-11-eq. were produced for stratospheric ozone depletion in this scenario, where the main contributions were fucoxanthin ($9.8x10^{-8}$ kg CFC-11-eq.; 22.0%), polyphenol ($9.4x10^{-8}$ kg CFC-11-eq.; 21.1%), fucoidan ($9.3x10^{-8}$ kg CFC-11-eq.; 20.7%), alginate ($8.1x10^{-8}$ kg CFC-11-eq.; 18.5%), and protein ($8.1x10^{-8}$ kg CFC-11-eq.; 18.1%). Fucoxanthin and alginate were the stages with the biggest impact in terrestrial

acidification, with contributions of 23.4% ($3.91x10^{-3}$ kg SO_2-eq.), and 23.1% ($3.85x10^{-3}$ kg SO_2-eq.) respectively, and a total contribution of the cascading sequence of $1.67x10^{-2}$ kg SO_2-eq.

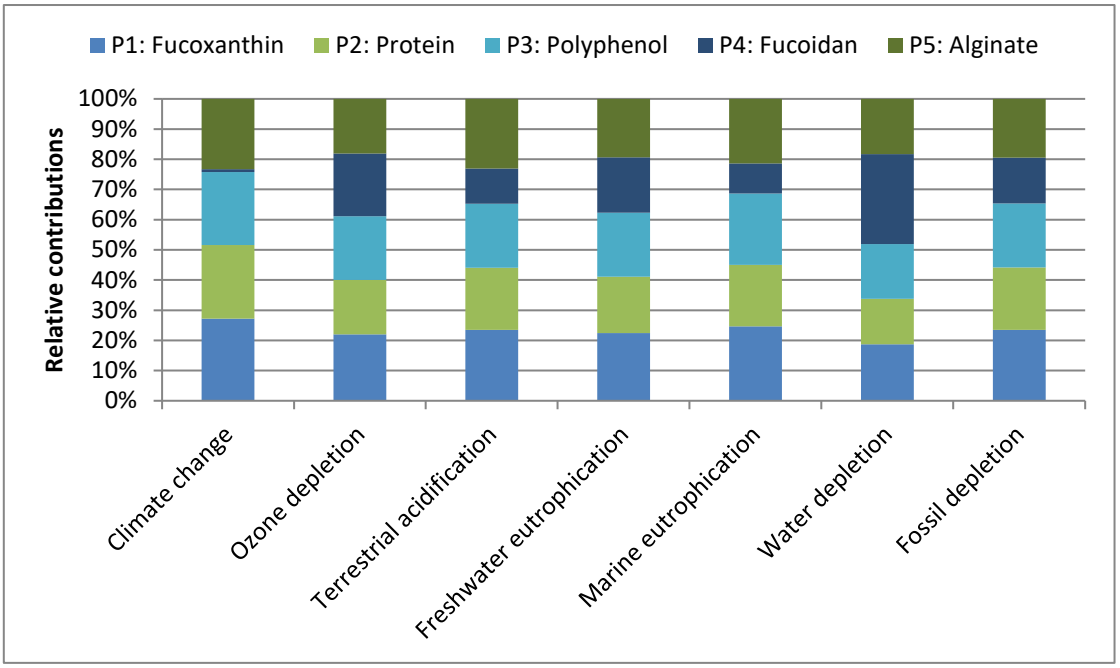

Fig 4- 20. Breakdown of the impact contribution across different categories of each extraction step involved in the processing of 1 kg of *A. nodosum* using techniques compliant to green chemistry strategies.

Contribution to freshwater eutrophication was even across all processes with an average of 20% per process. Fucoxanthin exhibited the highest value with 22.4% ($5.55x10^{-4}$ kg P-eq.), followed by polyphenols with 21.2% ($5.25x10^{-4}$ kg P-eq.), alginate with 19.4% ($4.81x10^{-4}$ kg P-eq.), proteins with 18.7% ($4.64x10^{-4}$ kg P-eq.), and fucoidan with 18.3% ($4.53x10^{-3}$ kg P-eq.). Biggest impacts in marine eutrophication were observed in the fucoxanthin and polyphenol steps with contributions of 0.021 kg N-eq. for fucoxanthin, and 0.020 kg N-eq. for polyphenol. Alginate followed in the overall contribution in this category releasing 0.018 kg N-eq., for a contribution of 21.4%. From a total of 0.08 m^3-eq. depleted in this scenario, fucoidan stage contributes with 29.8% of it (0.024 m^3-eq.), followed by fucoxanthin (18.7%), alginate (18.3%), and polyphenol (18.2%) with 0.0148

m^3-eq., 0.0145 and 0.0144 m^3-eq., respectively. Finally, fucoxanthin, polyphenol, and protein stages were the main contributors for fossil depletion with 23.5% (0.23 kg oil-eq.), 21.2% (0.21 kg oil-eq.), and 20.7% (0.2 kg oil-eq.) respectively.

3.3.4. Comparison of biorefinery scenarios environmental metrics

Comparing the three modelled scenarios (**Fig 4-21**) *Novel Tech* biorefinery exhibited the highest environmental impacts of the three, while *Green Chem* scenario showed the lowest impact contributions. *Green Chem* scenario climate change potential impact contributions were 16 times lower than *Novel Tech* scenario, and 2 times lower than *Solvent-based* scenario; additionally, *Solvent-based* scenario was 7.8 times lower than *Novel Tech* scenario.

The big impact contribution of *Novel Tech* was due to the higher energy consumption in the overall process, with energy-associated carbon dioxide emissions of 241 kg CO_2-eq., while *Solvent-based* and *Green Chem* carbon dioxide emissions associated to electricity consumption were 5 kg CO_2-eq. and 0.1 kg CO_2-eq., respectively. Ozone depletion was 27 times lower in *Green Chem* compared to *Novel Tech* scenario; meanwhile *Solvent-based* was 4 times lower when compared against *Novel Tech*. Terrestrial acidification in *Novel Tech* scenario main contribution was electricity usage with an impact of 1 kg SO_2-eq. released, while *Solvent-based* and *Green Chem* scenarios with 0.02 kg SO_2-eq. and $6.2x10^{-4}$ kg SO_2-eq. respectively. Freshwater eutrophication was 32 times higher in *Novel Tech* scenario when is compared against *Green Chem*, while *Solvent-based* scenario was 3.6 times higher compared to *Green Chem* and 8.7 lower than *Novel Tech* scenario. Marine eutrophication impacts where similar in all scenarios analysed, with *Solvent-based* and *Green Chem* scenarios being 1.27 and 1.33 times lower than *Novel Tech* scenario. These circumstances were due to the water utilisation across all processes.

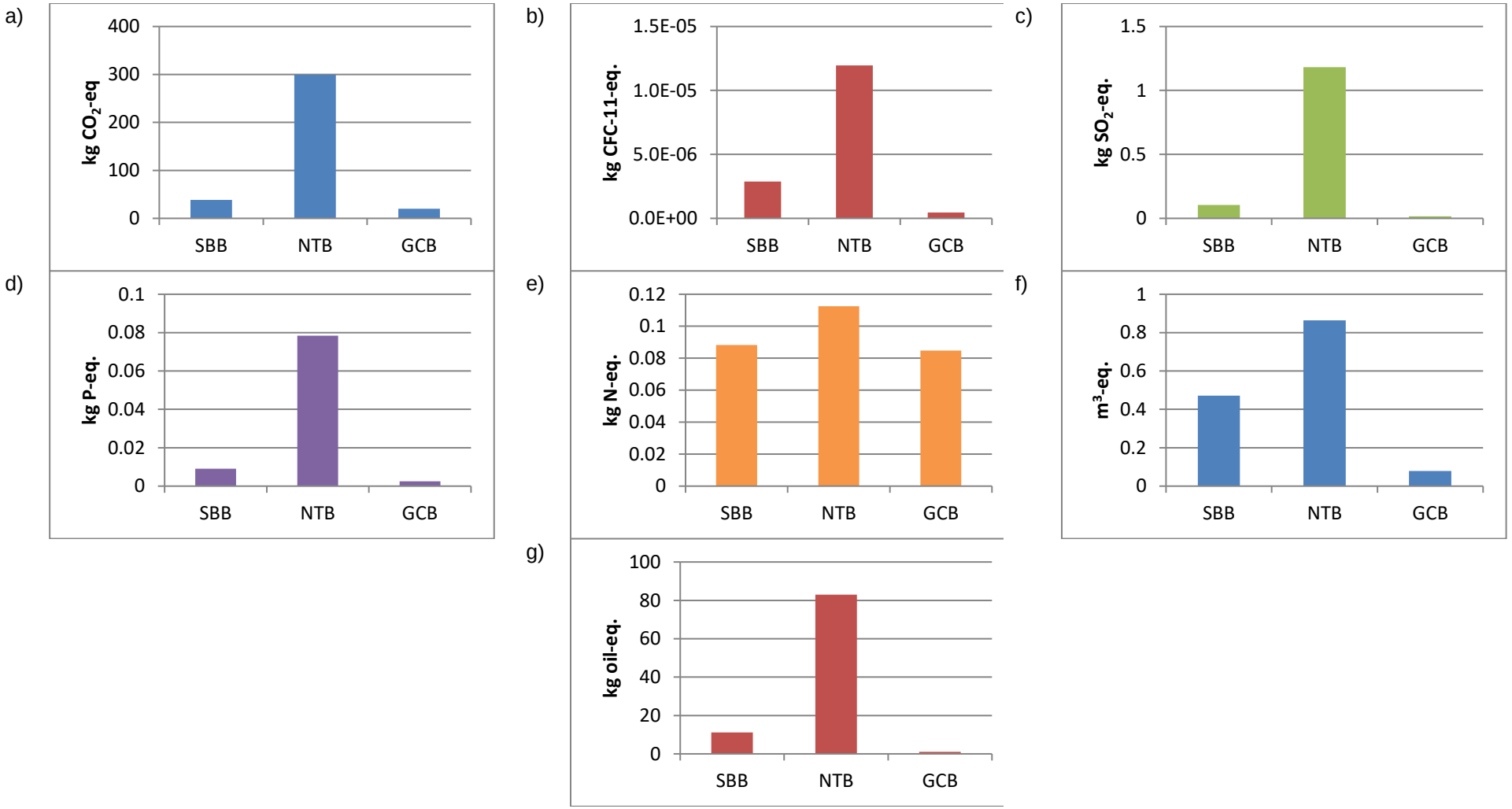

Fig 4-21. Environmental impacts for the different scenarios analysed using ReCiPe v1.13 as impact assessment method. The functional unit was 1 kg of *A. nodosum* as feedstock. SBB: Solvent-based. NTB: Novel Tech. GCB: Green Chem. a) Climate change; b) Stratospheric ozone depletion; c) Terrestrial acidification; d) Freshwater eutrophication; e) Marine eutrophication; f) Water depletion; g) Oil consumption.

Water resource depletion of *Green Chem* was 10- and 5 times lower than *Novel Tech* and *Solvent-based* respectively. Finally, *Novel Tech* scenario fossil fuel depletion impacts were the highest among all scenarios, due to the high energy consumption of the specialised equipment used; it was 91 times higher than *Green Chem* and 7.5 times higher than *Solvent-based* scenario. All process contributions in all impact categories assessed in this chapter are displayed in **Appendix D**.

The method utilised to perform the LCA was based in the black-box model, due to the widespread application of this methodology in the LCA modelling tools available in the market. This approach is beneficial because of the easy access to environmental flows and the comprehensive libraries with embedded data inventories this software possesses, allowing the rapid assembly and evaluation of a bioprocess. These embedded data inventories are one of the major drawbacks of this approach, limiting the researcher to the technology assumptions the black box set for them, leading to differences in LCA results due to the inventories used, technical assumptions, and technology types set by the LCA tool (Gentil et al., 2010). This shortcoming is particularly detrimental for biorefinery assessment, where the detailed data of the feedstock, e.g., biochemical composition is needed, the transformation of materials or substances during process, and the transition of mass and energy from one operation to another are necessary to model the bioprocess accurately (Lodato et al., 2020).

The environmental impacts of the scenarios and their initial capital expenditure are depicted together in **Fig 4-22**. It is observed that *Novel Tech* had the highest contribution in all metrics evaluated. *Green Chem* scenario presented a similar score in marine eutrophication with *Solvent-based* scenario. This can be explained due to the municipal solid waste disposal of the final residue, containing structural carbohydrates, lipids, and compounds not recovered in the cascading sequence operation, for both processes. Despite that score, *Green Chem* had the smallest contributions in all the other categories, emphasising this biorefining scenario as a potential candidate for the further investigation and development of a multi-product biorefinery utilising *A. nodosum*.

The early-design study results showed the potential of *Green Chem* scenario as a biorefinery concept to be further explored; it was for that reason that the theoretical green chemistry-based cascading sequence was tested in the lab to assess its actual process performance, e.g., to confirm that the cascading order of the extraction was functional, and to identify areas of improvement for a next iteration of the models.

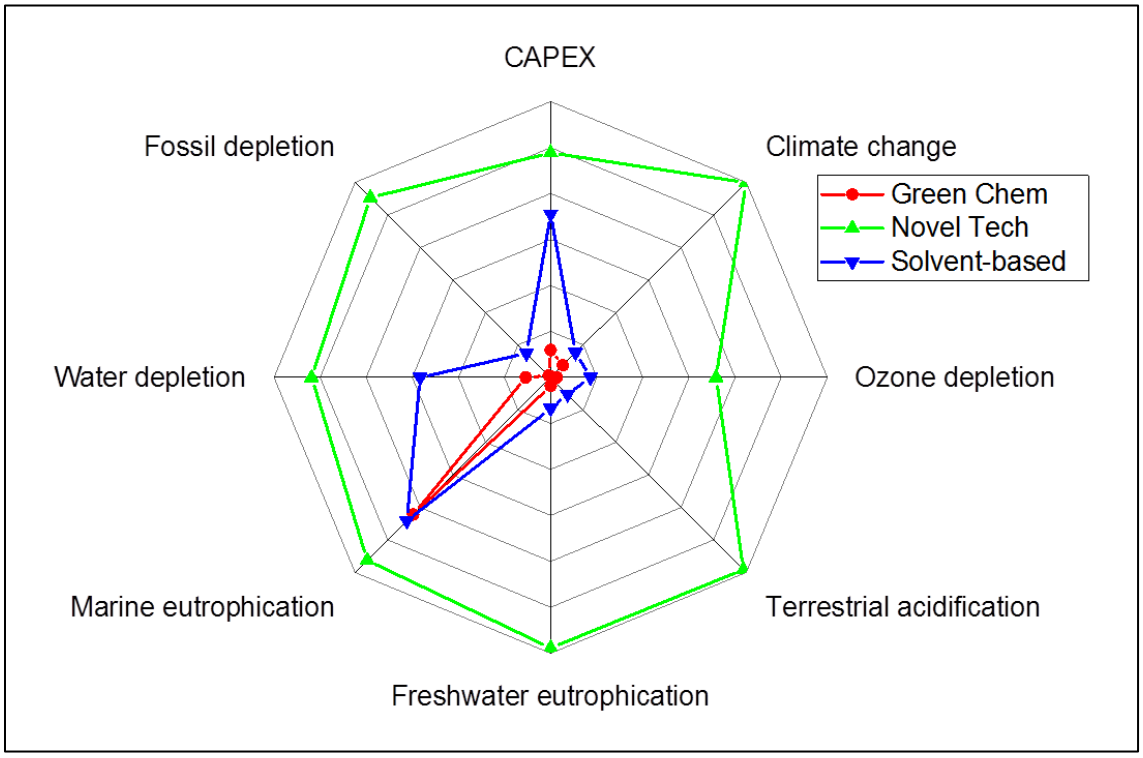

Fig 4-22. Combined environmental impacts together with initial capital investment of three biorefinery scenarios using *A. nodosum*. CAPEX was expressed in pound sterling (£) while the impact categories were quantified as described in **Section 2.5.3** in **Chapter 4**.

4. Technical feasibility of a green chemistry compliant cascading sequence

With the TEA and LCA results obtained in **Sections 3.2** and **3.3** from this **Chapter** *Green Chem* scenario demonstrated to be the most economically viable and environmentally sound biorefinery process, but this process was highly theoretical. Therefore, technical feasibility trials of the cascading sequence were performed. The first assembly of the cascading sequence, modelled in TEA and LCA studies, was conformed of fucoxanthin, protein, polyphenols, fucoidan, and alginate extraction steps. The protein

extraction step was prioritised at the expense of fucoxanthin step. Fucoxanthin step was eliminated, decision based on the facts of to the poor economic performance in the TEA of the latter (**Table 4-4**), the lower recovery yield of the pigment compared with proteins yield, and the higher environmental impacts of the fucoxanthin step than proteins. Therefore, the first re-iteration performed in the cascading sequence left it with four extraction operations, proteins, polyphenols, fucoidan, and alginate. Process complications regarding to alginate co-extraction and interference on the preceding polyphenol extraction step were qualitatively identified during the first trials of this cascading assembly (**Fig 4-23**), where the biopolymer was contaminating the process and making the recovery of polyphenols not feasible. Resolution of this technical hotspot was achieved by re-iterating the cascading sequence order again, placing the extraction of fucoidan and alginate first in the biorefining extraction train, followed by polyphenols and protein steps. In **Fig 4-24** a polyphenol extraction after extracting fucoidan and alginate can be observed, qualitatively confirming that the presence of alginate and alginic acids was minimised in the subsequent cascading extraction train. The new order of the cascading sequence can be observed in **Fig 4-25.**

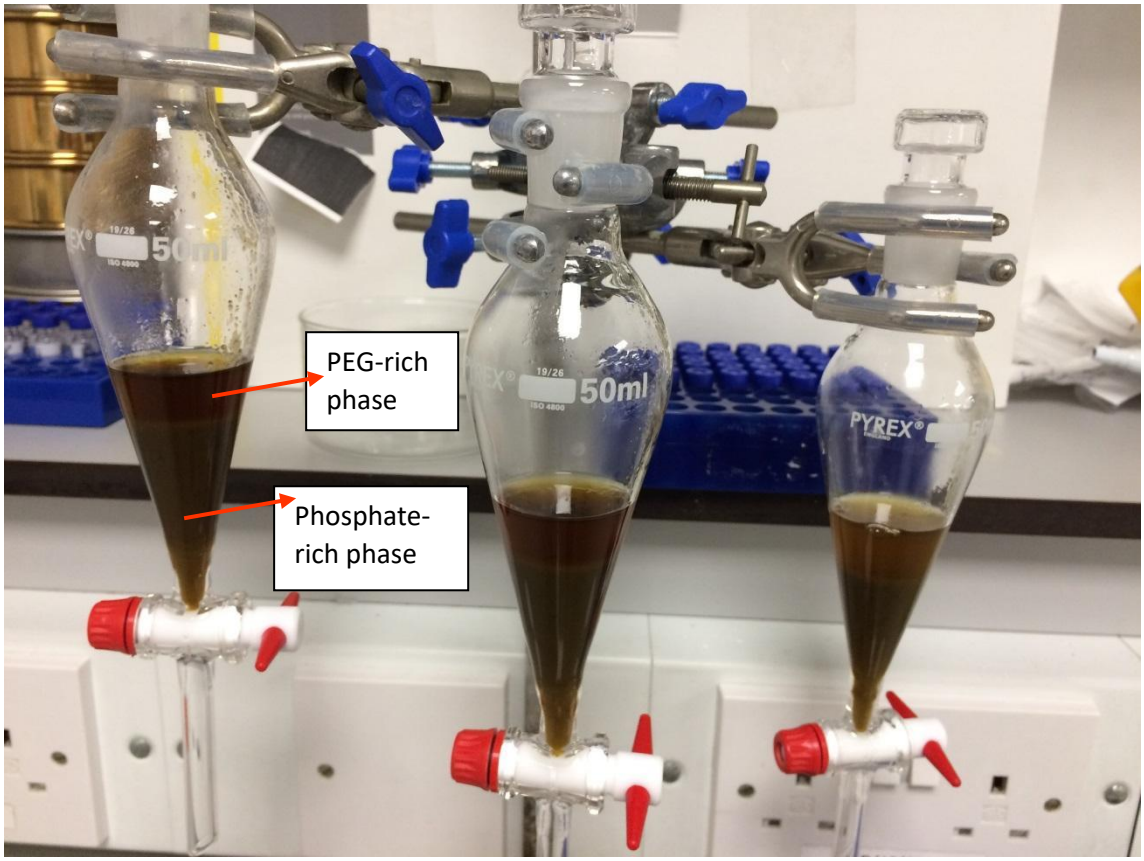

Fig 4-23. Extraction of polyphenols using ATPS before extracting alginate and fucoidan first in a cascading sequence approach. The ATPS used for the extraction in all flasks was PEG 2000-potassium phosphate buffer (22:10.5 %w/w). The presence of alginate and alginic acid in the top phase of the two-phase system can be observed as a brownish colouration.

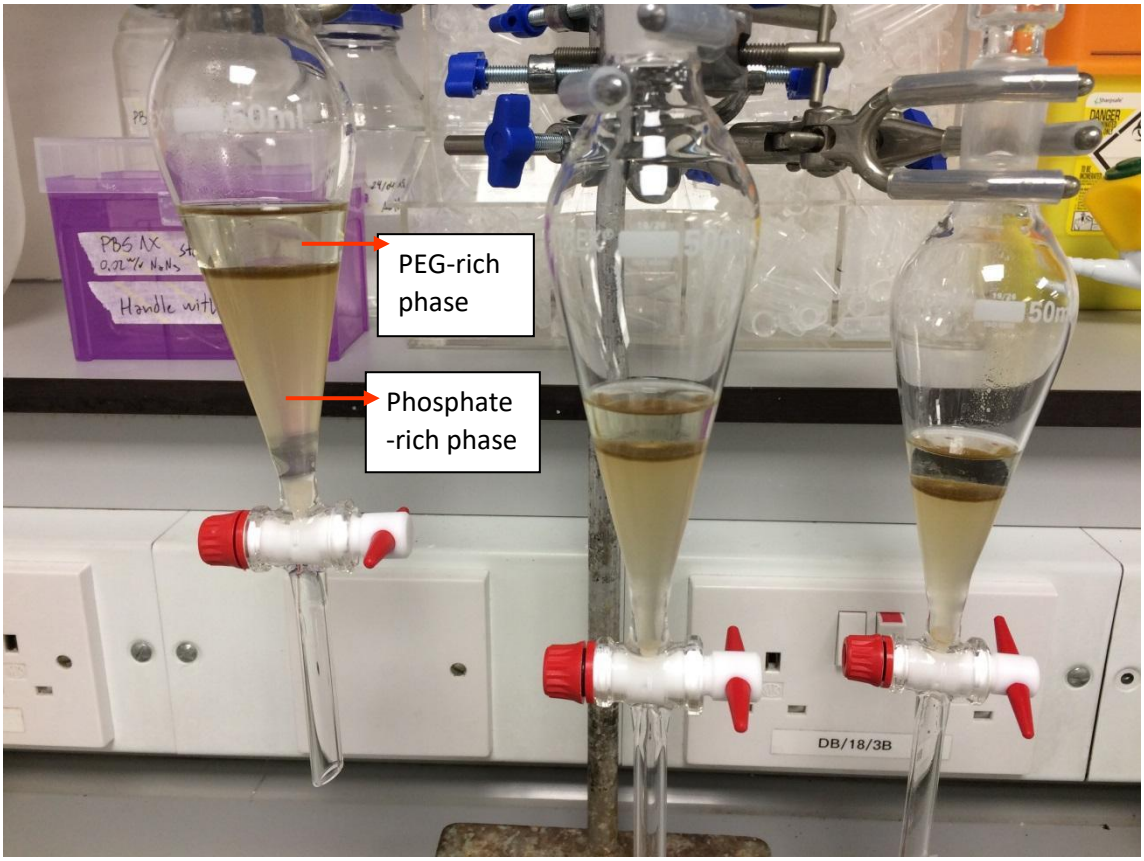

Fig 4-24. Extraction of polyphenols using ATPS after extracting fucoidan and alginate in a cascading sequence approach. The ATPS used for the extraction in all flasks was PEG 2000-potassium phosphate buffer (22:10.5 %w/w). The presence of alginate and alginic acid is no longer observed in the top phase of the polyphenol extraction step.

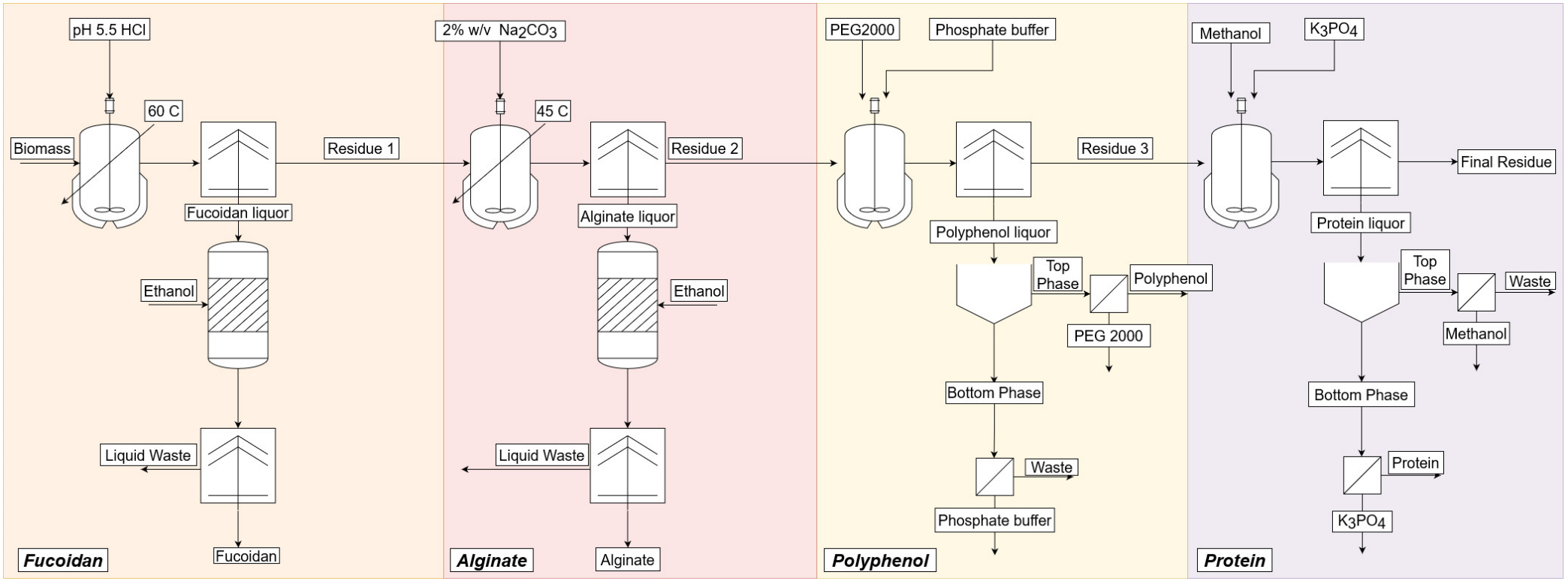

Fig 4-25. New order of extractions in the green chemistry-compliant cascading sequence.

The yields and process performance of the selected products obtained via cascading sequence were compared with extraction from primary biomass of fucoidan, alginate, polyphenols, and proteins using green chemistry techniques. Extraction of fucoidan and alginate as standalone process is observed in **Fig 4-26a**, fucoidan recovery was 16.9% of total carbohydrates, analogous to 5.78% DW in *A. nodosum*, while alginate yield was 15.1% of total carbohydrate content (TCC) present in *A. nodosum*, or 3.83% DW. Fucoidan and alginate co-extracted further down the cascading train were considered as impurities, this "contamination" added up to 15.1% carbohydrates lost in subsequent steps, a total of 5.17% DW; finally, 56.8% TCC present in *A. nodosum* were not extracted with the process. The cascading process performance of fucoidan and alginate recovery in **Fig 4-26b** showed that the recovery of fucoidan and alginate was lower than control process, 6.8% (2.32% DW) and 7.8% (2.67% DW) total carbohydrates, respectively, while the carbohydrates extracted as impurities in the subsequent processes was 11.9% TCC. Lastly, 73.5% TCC was not extracted at any step of the cascading sequence. The extraction process used in this cascading sequence was from Lorbeer et al. (2015), using *E. radiata* as a model feedstock; best extraction conditions on this study (same conditions used in this chapter) recovered 3.21% DW of fucoidan and 38.2% DW of alginate. Comparing these values with the results obtained in **Fig 4-26a** and **4-26b**, fucoidan recovery on the standalone process was higher but integrated extraction was lower (5.78% DW and 2.32% DW, respectively), whereas alginate recovery was around ten-fold lower in both processes; these differences might be due to the different species used in both studies, meaning that the best selected conditions in *E. radiata* did not reflect when used in *A. nodosum*.

a)

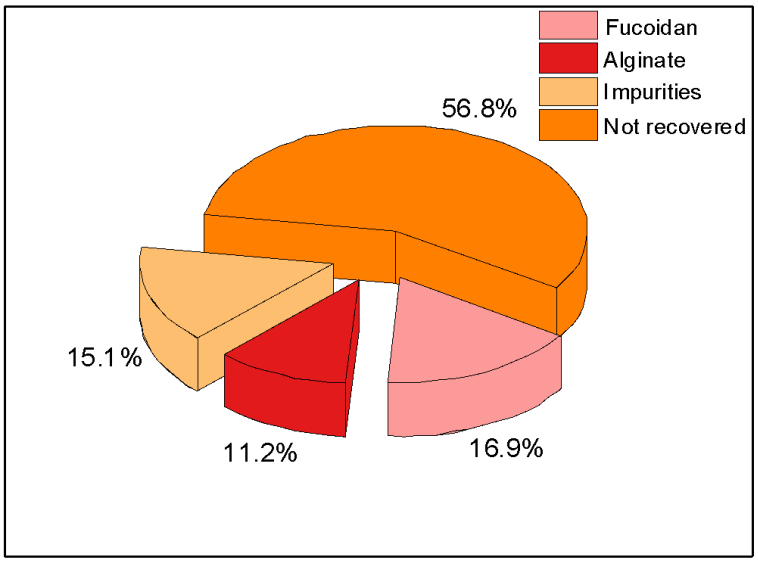

b)

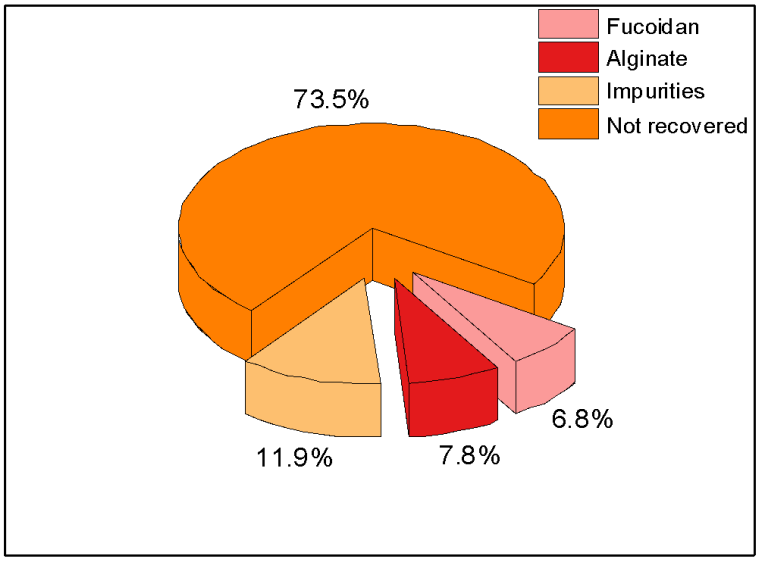

Fig 4-26. Extraction performance of fucoidan and alginate from *A. nodosum* in a) standalone extraction process and b) integrated cascading extraction indicating recovery yields, portion of carbohydrates not extracted, and carbohydrates co-extracted as impurities on the other standalone recovery steps or in the subsequent cascading recovery steps.

Standalone polyphenol recovery performance is shown in **Fig 4-27a**. 30.8% total polyphenols content (TPoC), analogous to 1.42% DW, was recovered using the process developed by Xavier et al. (2017), while 14.5% TPoC was lost as impurities, 54.7% TPoC was not extracted (2.53% DW). On the other hand, process performance of the integrated cascading polyphenol step (**Fig 4-27b**), recovered only 0.5% TPoC (0.23% DW), 34.2% total polyphenols lost as impurities in other extraction steps, while 65.3% TPoC (3.02% DW) was not extracted. Xavier et al. (2017) recovered 1.89% DW of polyphenols with the same process conditions used in this trial. These differences between processes might be due to the different origin of the biomass used in the extraction, since the information about ATPS applied to polyphenols at the moment when this study was performed was scarce, one of the few studies at that moment was Xavier et al. (2017), recovering polyphenolic compounds from wood waste. Another cause can be the integrated nature of the cascading sequence where previous treatments of the feedstock with acid and basic solutions might affect the properties of the cell wall, hence affecting the release of polyphenols to the top phase of the ATPS.

a)

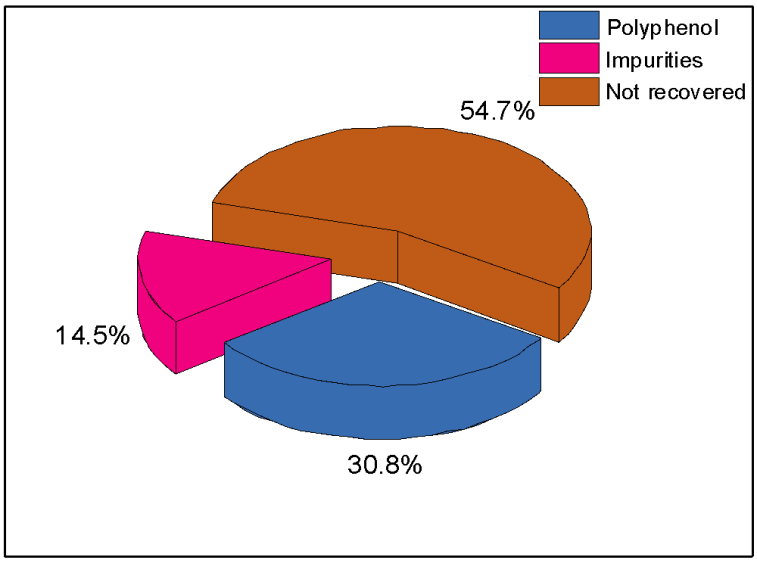

b)

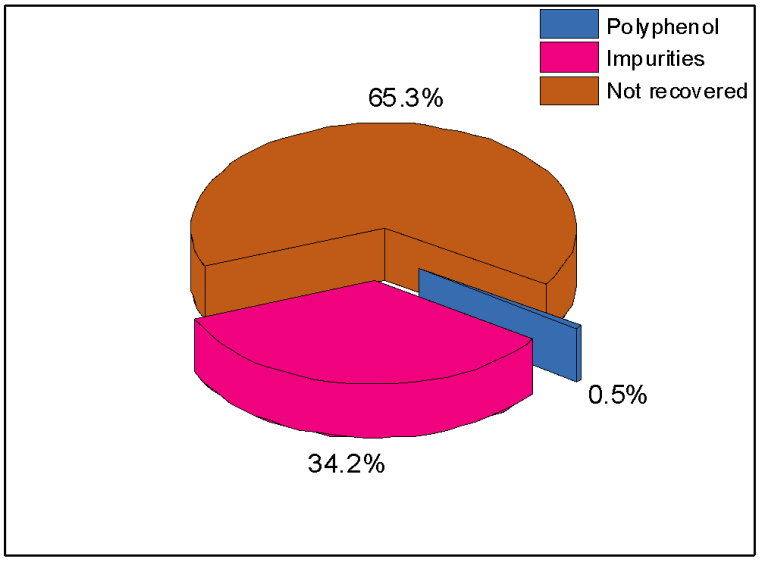

Fig 4-27. Extraction performance of polyphenols from *A. nodosum* in a) standalone extraction process and b) integrated cascading extraction indicating recovery yields, portion of polyphenols not extracted, and polyphenols co-extracted as impurities on the other standalone recovery steps or in the previous or subsequent cascading recovery steps.

Protein process performance of the standalone operation (**Fig 4-28a**) recovered 8.7% total protein content (TPrC) (0.99% DW), whereas 29% TPrC was co-extracted as impurities in the other standalone processes; lastly, 62.3% TPrC (7.06% DW) was not recovered using the extraction conditions developed by Phong et al. (2017). In contrast, integrated protein cascading recovery performance (**Fig 4-28b**) exhibited a recovery of 37.8% TPrC (4.28% DW), better performance than the standalone process, 19.3% TPrC lost as impurities, almost one third less than the standalone process, and 42.9% TPrC (4.86% DW) not recovered, 31% less than the standalone operation. Contrasting these values with Phong et al. (2017), they recovered 84.23% TPrC using the same conditions as this feasibility trial. The differences observed in this extraction step might be due to the treatments of the previous steps affected the cell wall and improving the recovery in the cascading scenario. Another point to consider is the lack of ATPS applied to non-specific protein from plant sources, with Phong et al. (2017) using *Chlorella sorokiniana* as a model species.

a)

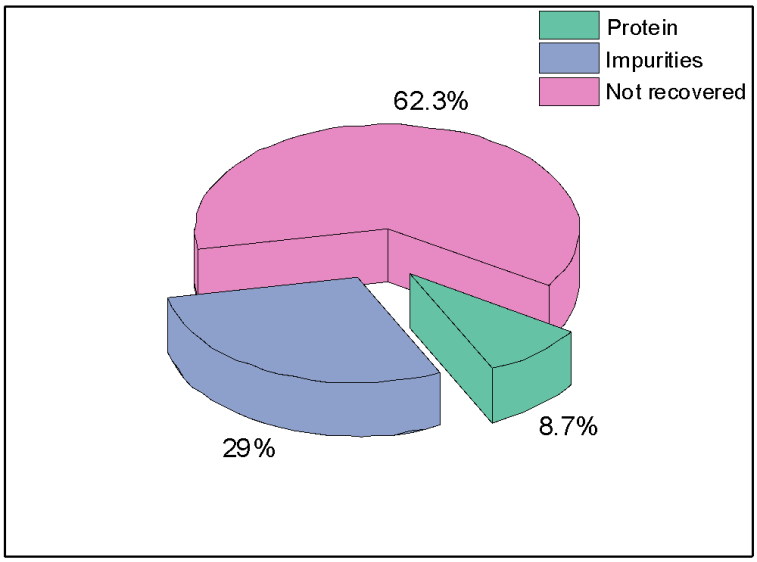

b)

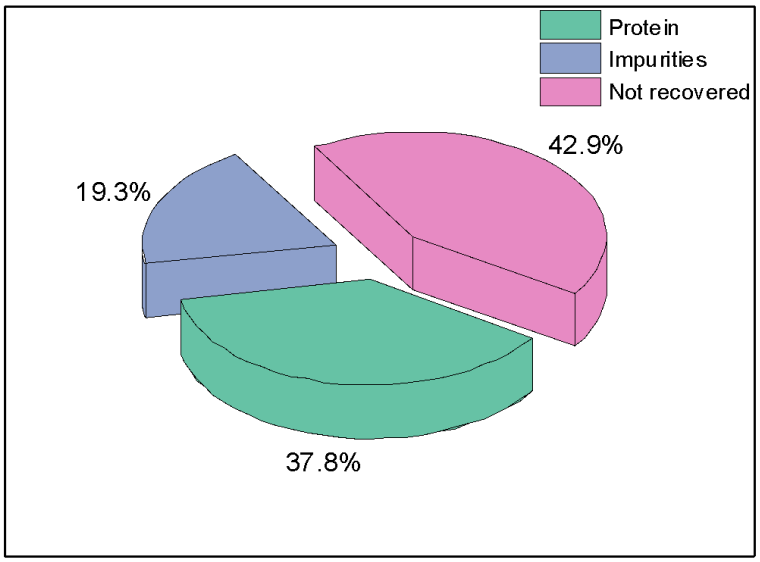

Fig 4-28. Extraction performance of proteins from *A. nodosum* in a) standalone extraction process and b) integrated cascading extraction indicating recovery yields, portion of proteins not extracted, and proteins co-extracted as impurities on the other standalone recovery steps or in the previous cascading recovery steps.

Completed all technical feasibility assessments of the different integrated extraction steps, processing hotspots were identified, with carbohydrate and polyphenol extraction steps requiring further exploration to successfully recover these compounds in a viable manner to comply with future economic and environmental requirements. These results help to give a more holistic view to the results produced using TEA and LCA, by putting the “dry-lab” cascading sequence produced with previously reported publications in a “wet-lab” context. This approach is beneficial because it allows the analysis of the real-time process performance of a process with a TRL around 1-2, and to start generating first-hand data that can help to re-iterate the models and update them. The addition of technical feasibility trials after an early design assessment allows identifying improvements along the bioprocess and to resolve them accordingly, in order to avoid a larger economic and environmental impact by passing them onto subsequent stages. Thomassen et al. (2020) suggested the integration of the technical dimension with the economic and environmental dimension when a new prospective technology is evaluated. The authors stated that by using this approach allows using similar system boundaries and assumptions to forecast both the economic and environmental potential of the potential bioprocess. Nadeau et al. (2010) also suggested the use of this approach, suggesting that the integration of the technical dimension in the early design will influence the performance in all three dimensions.

5. Conclusions

Three biorefinery scenarios using the brown macroalga *A. nodosum* as feedstock were evaluated for technical feasibility, economic viability, and the environmental impacts. The process models developed were designed based on 1,000 MT/year biomass processing facility. TEA revealed that green chemistry scenario was the most economical overall with a break-even point on the first year of operation (IRR = 75.0%), while solvent-based biorefinery was the most unprofitable due to larger volumes of solvents used and low yields of the extracted compounds (IRR = 21.5%). Novel technologies scenario required the highest CAPEX, OPEX, as well as total revenues; although this scenario presented the highest total revenues, the purchase of specialised equipment and the high energy usage of them, lowered its IRR (28.2%) and increased the production cost/kg (£0.07) and CoG/kg (£0.48). Environmental impact analyses revealed that green chemistry scenario exhibited the lowest environmental footprint in all impact categories assessed; on the other hand, novel technologies biorefinery was the most impactful scenario in all categories assessed, due to the energy-intensive processes used on it, with lipids, polyphenol, fucoidan, and alginate stages being the most energy-intensive cascading stages. With these results green chemistry biorefinery scenario proved being the most economically sound and environmentally viable process, hence technical feasibility trials were performed to analyse the process actual viability. Performance of each cascading sequence step was lower than their respective control standalone process, only with protein cascading extraction step having a better recovery than its control process (37.8%). Process hotspots were identified in this cascading sequence, specifically fucoidan and polyphenol step, therefore further optimisation of both operations was suggested to produce.

Chapter 5: High-throughput screening of aqueous two-phase systems for polyphenol extraction from *A. nodosum* – a green chemistry approach.

1. Introduction

Current developments in the biorefinery industry are transitioning towards more environmentally sustainable processes, given the need to reduce the environmental footprint of their operations, and the consideration of additional dimensions besides the technical feasibility of a new technique. The transition of promising technologies from bench-scale to commercial level is often difficult and expensive, such as ATPS; though in ATPS the high concentrations of salts and the cost of the polymers used are reasons claimed to be the limitation for the industrial application (Torres-Acosta et al., 2019), thus scale-down approaches have appeared in recent years to analyse these systems in a more resource-efficient way. ATPS are governed by their phase diagrams and can be considered as a unique fingerprint of a two-phase system under a given set of conditions, namely pH, temperature, salt concentration, among others. Information then can be derived from such diagrams includes the concentration of the phase-forming components necessary to form an ATPS in equilibrium, the subsequent concentration of phase components in the top and bottom phases, and the ratio of phase volumes (Kaul, 2000). Embedded in the phase diagram is the binodal curve, which divides a region of component concentrations that will form two immiscible aqueous two-phases, located above the curve, from those that will form one homogeneous phase, at and below the curve. The determination of the binodal curve can be calculated and fitted by least squares regression to the empirical relationship developed by Merchuk et al. (1998) (**Eq. 5-1**):

$$\boxed{y = A \times exp\,(Bx^{0.5} - Cx^{3})} \quad \textbf{(Eq. 5-1)}$$

Where, ***y***: polymer concentration, ***x:*** salt concentration, ***A***, ***B***, and ***C***: regression parameters.

There are no reports to date on the application of ATPS for the recovery of high-value products from brown macroalgae, although there are publications using polymer-salt ATPS to recover R-PE from red seaweeds (Denis et al., 2009; Mittal et al., 2019; Vicente et al., 2019), and one report also using salt-polymer ATPS to recover sulphated polysaccharides from the green seaweed *Enteromorpha* sp. (Du et al., 2018) hence, these compounds together with other high-value products are interesting options to evaluate the use of ATPS to extract them from brown algae. Polyphenols from seaweeds can be extracted by different methods, solvents (Koivikko et al., 2005), MAE (Yuan et al., 2018), EAE (Soto-Maldonado and Zúñiga-Hansen, 2017), SFE (Santos et al., 2019), among others; the main drawback of these methods is either economic scale-up or environmental performance. Recovery of polyphenols from macroalgae using ATPS have not been reported until the submission of this document, but there are reports on the recovery of polyphenolic compounds from lignocellulosic material (Xavier et al., 2017, 2014), thus is interesting to explore the extraction of these compounds applying green chemistry strategies, summarised in the use of ATPS for their extraction.

The mechanism of separation in ATPS is complex and not easy to predict. In general, the partition of high-value products is a result of Van der Waals and ionic interactions of the natural compounds with the surrounding phase. Some of the key mechanisms have been identified: electrostatic, hydrophobic, and steric hindrance interactions between the phases and the compound of interest. Considering a conventional polymer-salt aqueous two-phase systems for industrial production, the substances and equipment needed for its preparation are rather inexpensive compared to initial capital expenditures of previously mentioned methods, and recycling of phase-forming components is simpler than recycling or disposal of solvents (Bensch et al., 2011). Also, is important to consider

that limitations in the processing speed, equipment intricacy and thus scalability concerns are minimal since simple apparatus like stirred tanks or disc stack centrifuges, and mixer-settlers can be used (Torres-Acosta et al., 2019). Unluckily, the apparent technical simplicity of the setup of the process is not paralleled by the complex and still unresolved parameter predictability for an industrial purification step. When there is a gap in the knowledge about a certain molecule or process, the experimental approach in terms of high-throughput process development is a solution for a broad exploration of the design space. High-throughput process development is a methodology for the use of large number of parallelised, miniaturised, and automated experiments (Baumann and Hubbuch, 2017). High-throughput technologies can be used for characterisation of ATPS, for the determination of binodal curves for different salts and polymers (Bensch et al., 2011). In ATPS, the first step to consider as previously explained, is the determination of the binodal curve, but the process to determine or estimate this curve is cumbersome and require extensive analytical work and time, thus a rapid evaluation is needed. Reports in the purification of protein compounds, antibodies, plasmid deoxyribonucleic acid, among others have been described, yet a high-throughput procedure for polyphenols has not been defined yet (Oelmeier et al., 2012; Wiendahl et al., 2012; Zimmermann et al., 2017). Since theoretical or model-based solutions for this dilemma have not been developed, the only practical solution lies in a rapid and automated screening approach allowing parameter evaluation of a multi-parameter space within a short period of time. The method of choice for such a screening approach is found in the use of HTS platforms. These platforms are already used on a routine basis in the field of high throughput analytics. HTS applications in the development of ATPS and downstream process development in general have received attention in recent years (Baumann and Hubbuch, 2017; Effio and Hubbuch, 2015; Rakel et al., 2014), but it has never been used for the rapid screening of extraction systems for polyphenols from brown seaweeds.

In this chapter, the development of a methodology for a rapid evaluation of ATPS for polyphenol recovery using an automated HTS approach was used for the preparation, characterisation, and application of 384 different polymer-salt ATPS using a commercially available pipetting robot TECAN Freedom Evo™ 200. Preparation was simply established by liquid pipetting in combination of adequate mixing of the two-phase systems. Characterisation of the obtained systems was carried out by an automated determination of binodal curves and further estimation of regression parameters. Finally, polyphenol partitioning had been investigated, first by rapid proxy quantification of a model molecule for polyphenols, and later with scale-up trials of selected two-phase systems using two complex polyphenolic samples from brown seaweeds. The approach presented in this chapter is based on a screening only varying potassium phosphate buffer and polymer concentrations, being able to process close to 770 samples per day, and it offers a rapid screening method for the study of the partitioning behaviour of high-value compounds from macroalgae with potential economic breakthrough using ATPS.

2. Results and discussion

The section of the project covered in this chapter can be observed in **Fig 5-1**. ATPS can generally be characterised by the determination of the binodal curve, and the respective K_p for a given system. On the condition that all these parameters are known for various ATPS a rapid evaluation of their feasibility in a potential bio-purification process becomes possible. The strategies followed to reach this goal are summarised in **Fig 5-2**.

2.1. Method development and validation

Prior to its use, the method was optimised in terms of sample volume, ease of handling, accuracy, and reproducibility. Generally, the most convenient way of mixing on liquid handling stations lies in the use of orbital shakers. However, many applications of orbital shaking systems reported are hampered by insufficient power input, low shaking orbit, or non-optimised parameters (Oelmeier et al., 2011). For this reason, mixing process on the robotic system was conducted in deep well plates where disposable tips were used for aspirating and re-dispensing 800 µL of the phase system. ATPS are firstly characterised by determining the binodal curve, which is the boundary condition for the development of the two-phase systems between the polymer and the salts involved.

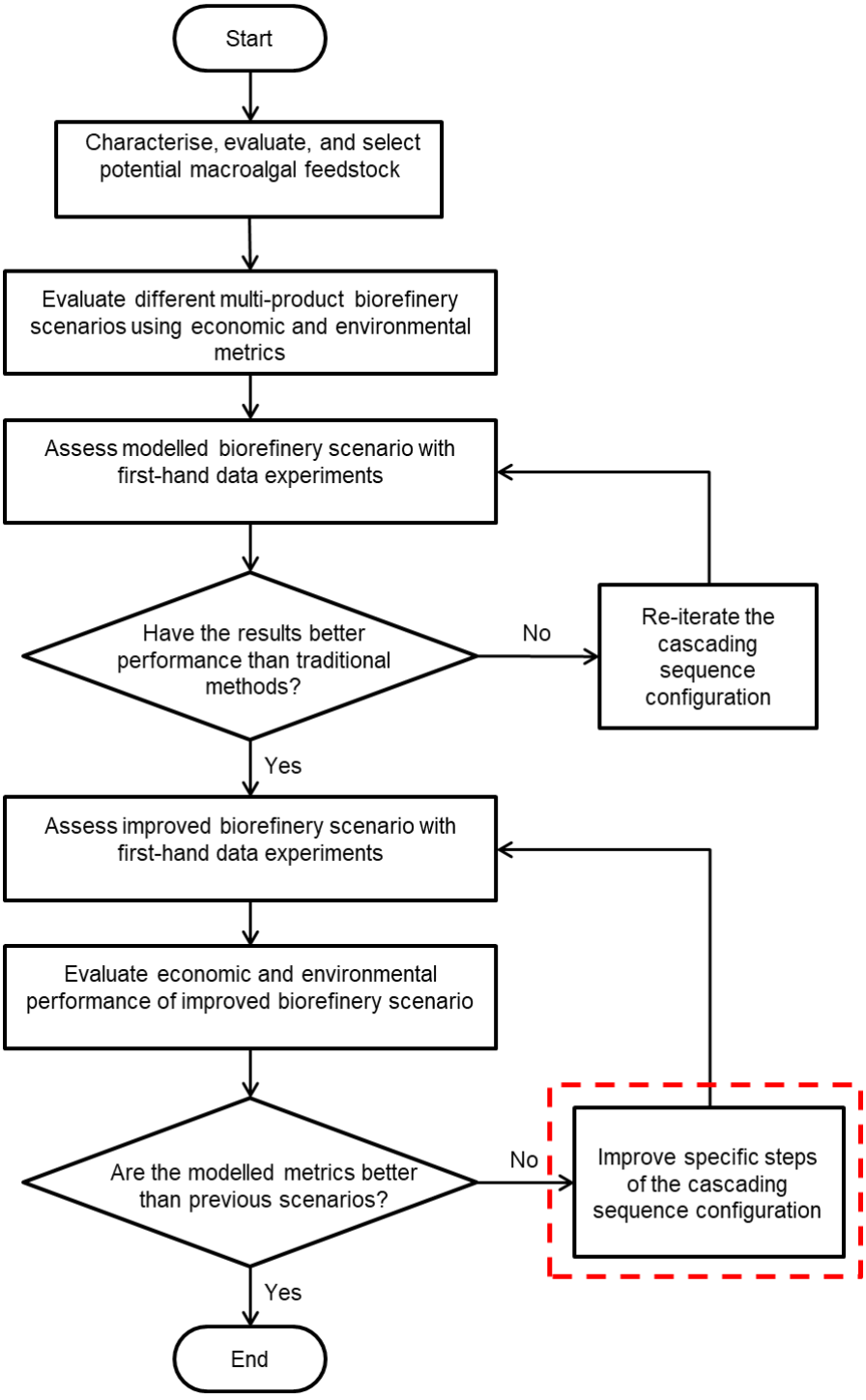

Fig 5-1. Proposed overall methodology for the development of a multi-product macroalgal biorefinery. In the red dashed box, the process optimisation step covered in this chapter is highlighted.

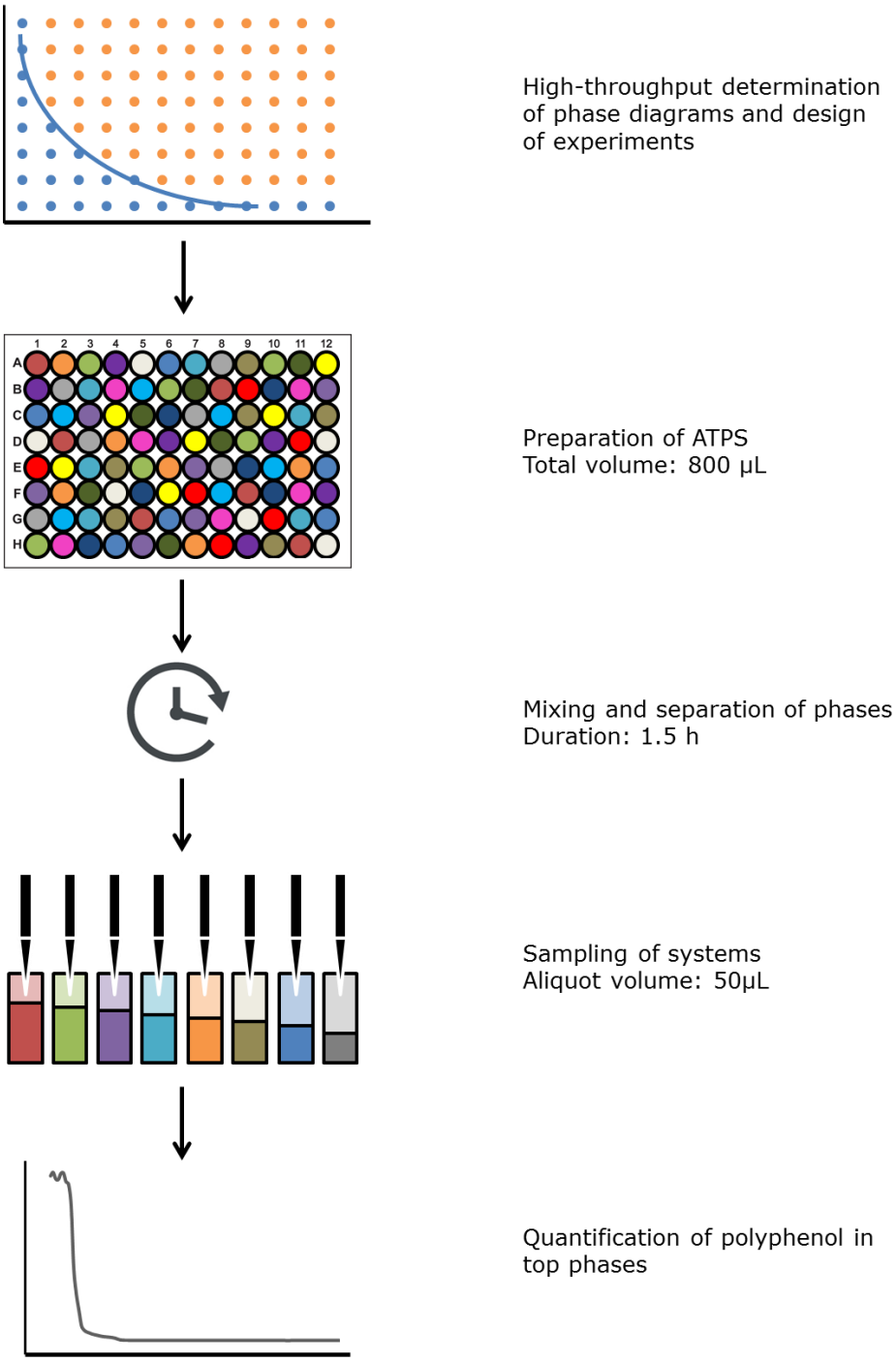

Fig 5-2. Overview of the developed high-throughput screening platform. After phase diagrams were determined in high-throughput, ATPS were selected for the partitioning screening. ATPS were prepared in deep-well plates, and phloroglucinol was added from a stock solution. After mixing and settling, samples were taken from the top phase, and polyphenols were quantified through absorbance.

Before the determination of the binodal curves and the screening methodology, a rapid quantification of polyphenols was assessed. To accomplish this, phloroglucinol was selected as a model molecule for the recovery tests. Phloroglucinol was used because is the building block of mostly all the polyphenols found in brown macroalgae (Li et al., 2011), therefore, an absorbance screening of all the components involved in the formation of any ATPS was assessed. Screening of the components showed that phloroglucinol had an absorbance peak at 245 and 265 nm (**Fig 5-3**). At 245 nm all PEGs showed an absorbance peak as well, making the construction of a polyphenol calibrations curve less accurate.

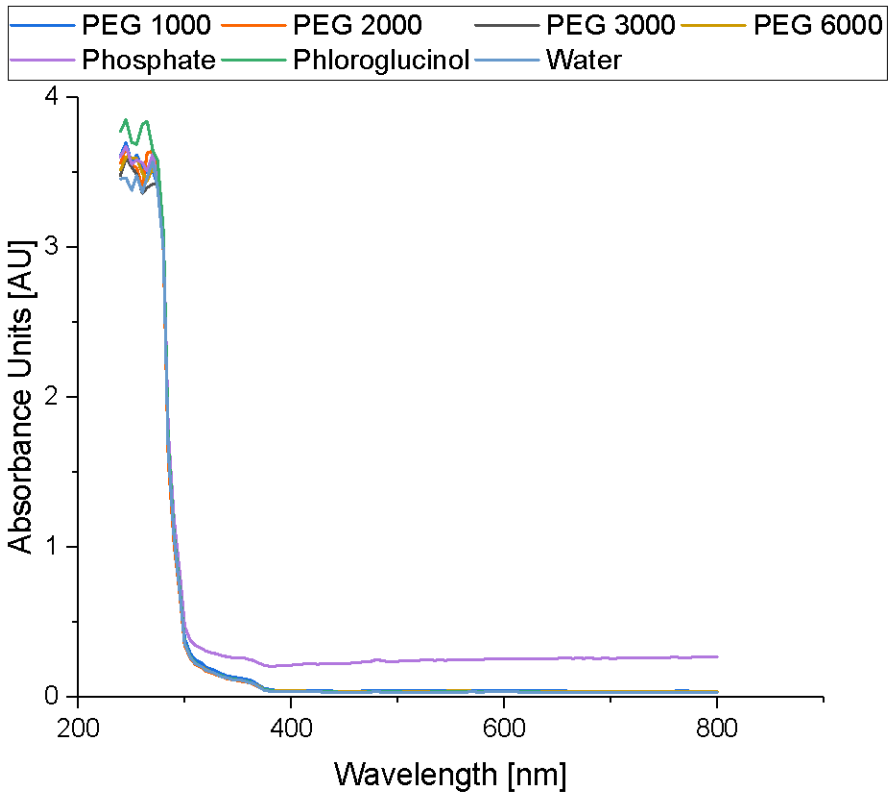

Fig 5-3. Absorbance screening of all the components involved in the aqueous two-phase system model for the high-throughput partition screening.

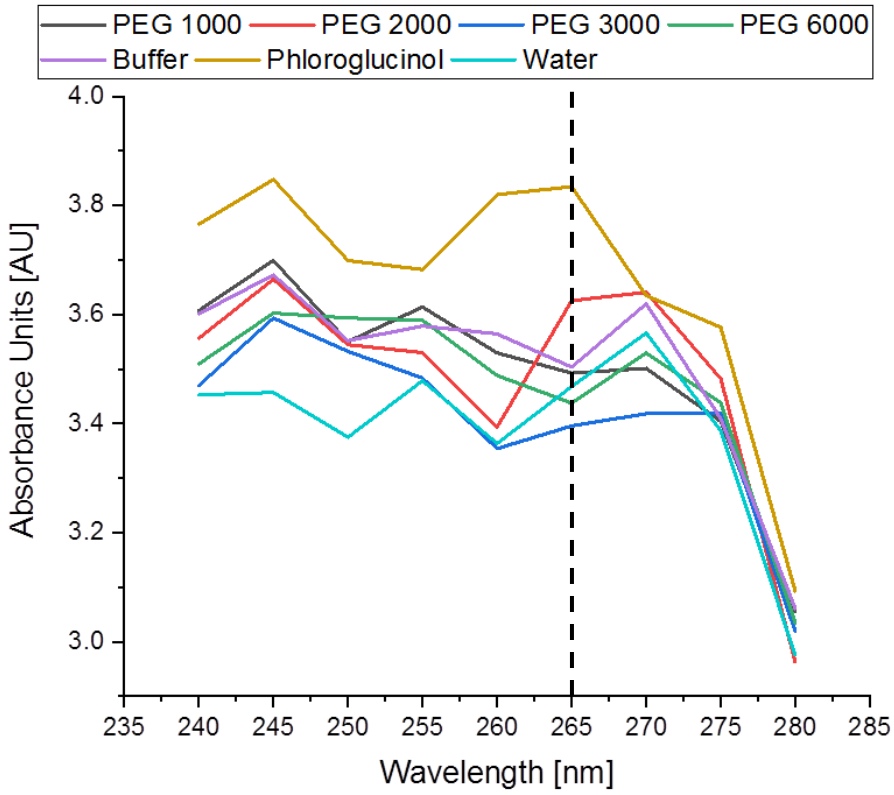

Fig 5-4. Focus of the absorbance screening in the 240 – 280 nm range of all the components involved in the aqueous two-phase system model for the high-throughput partition screening. The dashed line at 265 nm indicates the difference between absorbances of the different components.

At a wavelength of 265 nm the phloroglucinol peak can be differentiated from the other components involved in the ATPS formation, and the gap between the absorbances can be seen in **Fig 5-4**. Thus, this absorbance was selected to construct a calibration curve (**Fig 5-5**) to be used as an on-site proxy rapid quantification of polyphenols.

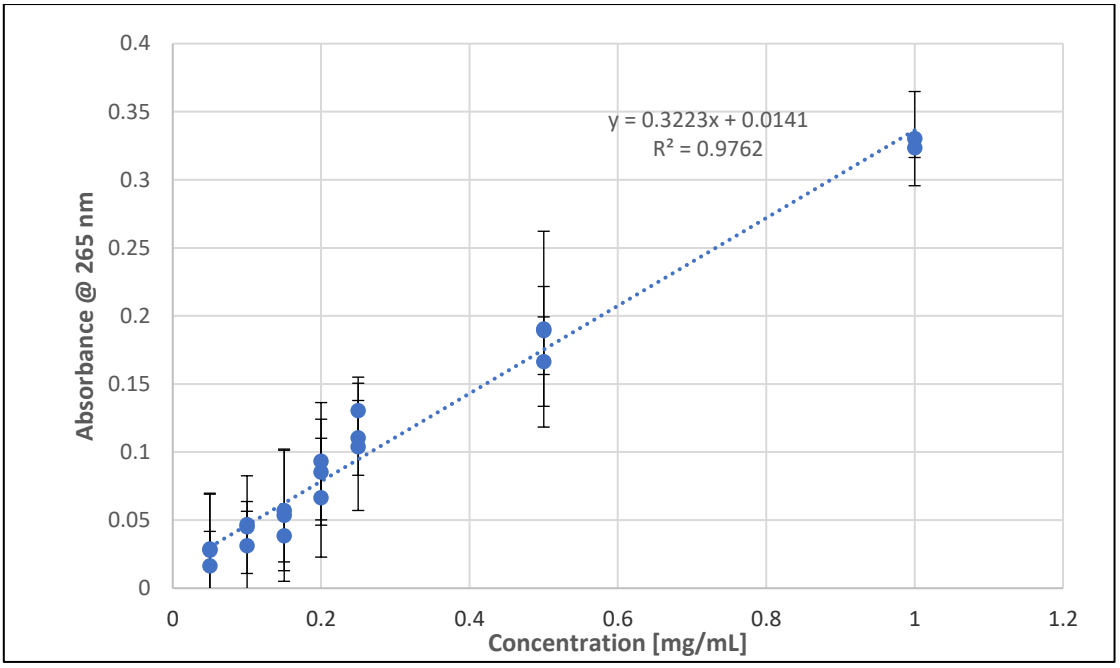

Fig 5-5. Calibration curve for the on-site proxy quantification of polyphenols for the high-throughput partitioning screening.

2.2. Determination of binodal curves

To validate the high throughput methodology, ATPS were determined both manually and by use of the LHS. The determination of the binodal curve represents the boundary conditions for the formation of a two-phase system and is a necessary prerequisite for any partitioning study. When it is done manually, these determinations are performed using a turbidimetric titration assay or by analysing the PEG/salt concentrations in the top and bottom phase of a series of two-phase systems. Both methods are difficult to adapt to an automated environment or require high analytical effort, e.g., labour, reagents, and time. To determine the formation of the two-phase systems a hydrophilic dye was used, methyl orange, that always partition to the top phase and in one-phase systems the dye is distributed homogenously over the entire system (Patel, 2017); therefore, the sample aspirated from the bottom phase showed an orange colouration. Binodals were determined for the PEG-potassium phosphate systems by use of the LHS. The experimental parameter space was initially covered by a matrix of 96 PEG-salt mixtures, as the position of the binodal is unknown a rather wide matrix was used, a

sampling space of 4% w/w of phase-forming components between points was selected. A regression fitting using Merchuk's equation (**Eq. 5-1)** has shown accurate goodness of fit in previous reports (Amrhein et al., 2014; Oelmeier et al., 2011)The estimation parameters for the binodal line and their 95% confidence bounds with the liquid handling station are displayed in **Table 5-1** and the coefficient of determination (R^2) of the fit for the curves were, PEG 1000-potassium phosphate: 0.9802, PEG 2000-potassium phosphate: 0.9904; PEG 3000-potassium phosphate: 0.9902, and PEG 6000-potassium phosphate: 0.9777. As can be seen in **Fig 5-6**, the binodal regression curves are in good fitting between both phases sampling points. The square points represent one-phase systems where the methyl orange dye was distributed homogenously across the sample, whereas the circle points represent the complete partition of the dye to the top phase indicating the formation of the two phases.

Table 5-1. Regression coefficients of binodal curves estimation from Merchuk's equation (**Eq. 5-1**) built using the liquid handling station method and their 95% confidence bounds.

Phase components	A (±95% CI)	B (±95% CI)	C (±95% CI)
PEG 1000-Phosphate	47.48 (44.12, 50.83)	-0.25 (-0.30, -0.20)	-3.3×10^{-4} (-4.6×10^{-4}, -2.1×10^{-4})
PEG 2000-Phosphate	47 (44.06, 49.94)	-0.34 (-0.41, -0.27)	-1.1×10^{-3} (-1.7×10^{-3}, -6.1×10^{-4})
PEG 3000-Phosphate	47.03 (43.98, 50.07)	-0.25 (-0.32, -0.18)	-1.6×10^{-3} (-2.2×10^{-3}, -9.9×10^{-4})
PEG 6000-Phosphate	47.08 (43.18, 50.98)	-0.47 (-0.58, -0.36)	-1.0×10^{-3} (-1.8×10^{-3}, -1.8×10^{-4})

Table 5-2. Regression coefficients of binodal curves estimation Merchuk's equation (**Eq. 5-1**) built using a manual determination process and the confidence limits of each regression parameter.

Phase components	A (±95% CI)	B (±95% CI)	C (±95% CI)
PEG 1000-Phosphate	47.95 (40.39, 55.51)	-0.18 (-0.29, -0.065)	-1.2×10^{-3} (-1.9×10^{-3}, -5.2×10^{-4})
PEG 2000-Phosphate	48.17 (42.25, 54.1)	-0.23 (-0.35, -0.12)	-2.4×10^{-3} (-4.1×10^{-3}, -7.1×10^{-4})
PEG 3000-Phosphate	47.41 (44.34, 50.49)	-0.25 (-0.32, -0.19)	-2.8×10^{-3} (-3.6×10^{-3}, -2.0×10^{-3})
PEG 6000-Phosphate	42.24 (34.93, 49.55)	-0.14 (-0.30, -0.027)	-5.2×10^{-3} (-8.7×10^{-3}, -1.7×10^{-3})

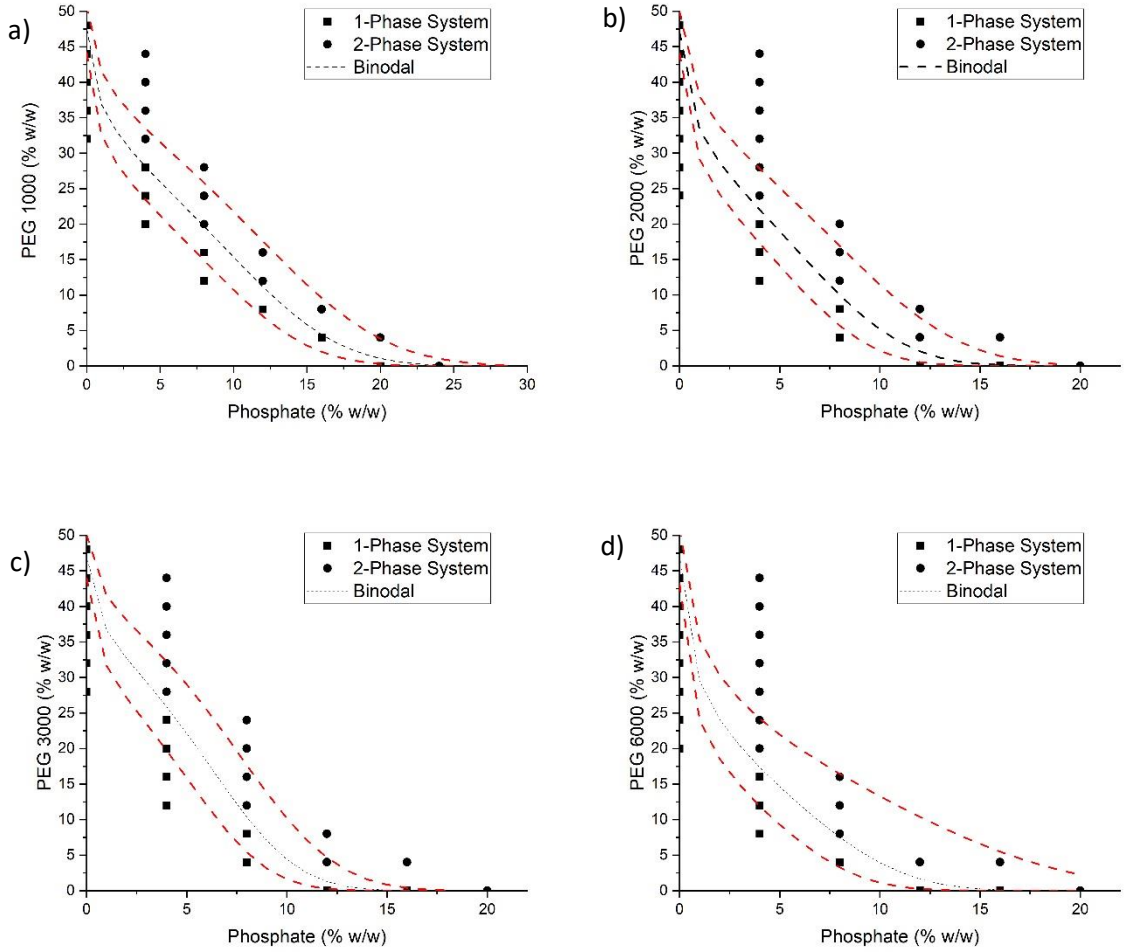

Fig 5-6. Breakdown of the binodal curve fitting of curves performed with the automated process, square points indicate one-phase systems, circular points indicate the formation of a two-phase system. Red-dashed curves indicate the 95% confidence intervals of the regression fit. A) PEG 1000, B) PEG 2000, C) PEG 3000, D) PEG 6000

After the automated determination of the binodal curves was completed, a manual determination was performed, in order to compare both procedures and validate the robustness of the LHS approach. The experimental parameter space, as well as the LHS approach, was initially covered by a matrix of 96 PEG-salt mixtures, as the position of the binodal is unknown a rather wide matrix was used, a sampling space of 4% w/w of phase-forming components between points was selected to assess the transition of a one- and two-phase system.

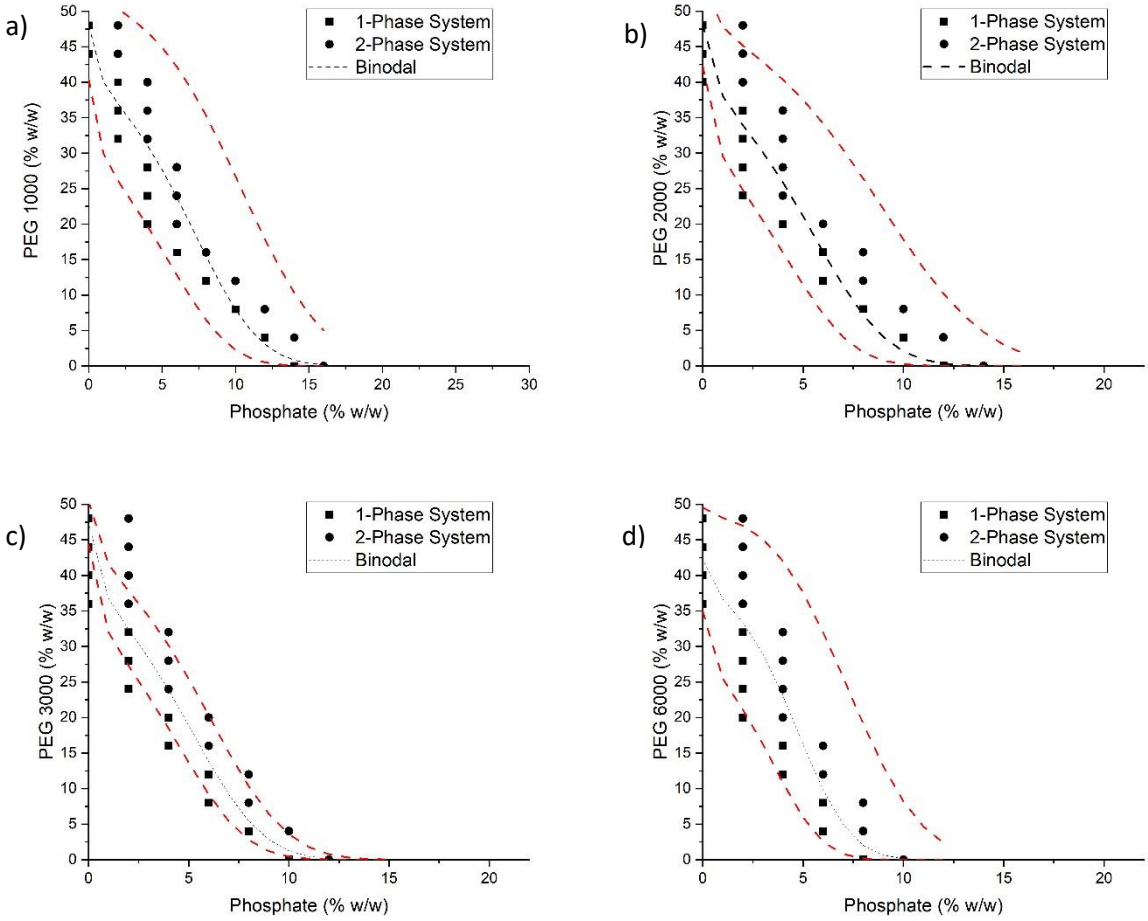

Fig 5-7. Breakdown of the binodal curve fitting of curves performed with the manual process, square points indicate one-phase systems, circular points indicate the formation of a two-phase system. Red-dashed lines indicate the 95% confidence intervals of the regression fit. A) PEG 1000, B) PEG 2000, C) PEG 3000, D) PEG 6000

The estimated parameters of **Eq. 5-1** from the manual determination with their 95% confidence bounds are exhibited in **Table 5-2**. The fitting of the binodal regression curves can be observed in **Fig 5-7**. Goodness of fit of the binodal curves from the manual determination exhibited an R^2 around 0.80 – 0.99 for the manual method, with PEG 1000-potassium phosphate showing a R^2 = 0.8856, PEG 2000-potassium phosphate R^2 = 0.953, PEG 3000-potassium phosphate R^2 = 0.9847 and PEG 6000-potassium phosphate R^2 = 0.7998, being more variable than the automated determination. The square points in **Fig 5-7** represent one-phase systems where the

methyl orange dye was distributed homogenously across the system, while the circle points represent the complete partition of the dye to the top phase indicating the formation of the two phases.

Completed both, manual and automated determinations, the methods were compared between them. All regression fittings showed binodal data similar with phase systems published previously, except from Huddleston et al. (2003): Huddleston et al., (2003) have worked with PEG 1000-K_3PO_4 systems at 25°C, Bensch et al., (2011) have worked with PEG 200, 1000, 1540, and 4000 with potassium phosphate buffer systems at 25°C, and Lei et al. (1990) have worked with PEG 400, 600, 1000, 1500, 3400, 8000, and 20000 and potassium phosphate systems at 4°C instead of 25°C and at pH 7 instead of 7.5. The values obtained by Huddleston et al. (2003) differ from the values obtained in the current work; this may be because they did not use a buffered solution but only added K_3PO_4, a salt which is expected to yield a much higher pH value than the 7.5 used within this work. The difference between manual and automated determination was between ~1.25 – 2.15% with the lowest value in the PEG 3000-potassium phosphate systems and the highest with PEG 6000-potassium phosphate systems (**Table 5-3**). The binodal fitting of all the automated approach curves exhibited a goodness of fit within the 95% confidence limits of the averaged fitted curve. The comparison between the two methods is shown in **Fig 5-8**. The most accurate automated fitting was in the PEG 3000-potassium phosphate system, with an error in the comparison of 1.26±0.28%; it can be noted as well that the automated binodal in each point of the regression is above the manual binodal, overlapping this curve. This situation was desirable because any error between the methods is negligible due to any two-phase system formed above the actual binodal curve is contained in the LHS determination. Following, PEG 2000-potassium phosphate systems displayed an error between the regressions of 1.47%±0.30%, while PEG 1000-potassium phosphate, and PEG 6000-potassium phosphate systems binodal regressions showed an error of 2.09±0.29% and 2.14±0.27%, respectively.

Table 5-3. Error between manual and automated determinations of the binodal curve.

Systems	Error (%)
PEG 1000-Potassium phosphate	2.09±0.29
PEG 2000- Potassium phosphate	1.47±0.30
PEG 3000- Potassium phosphate	1.26±0.28
PEG 6000- Potassium phosphate	2.14±0.27

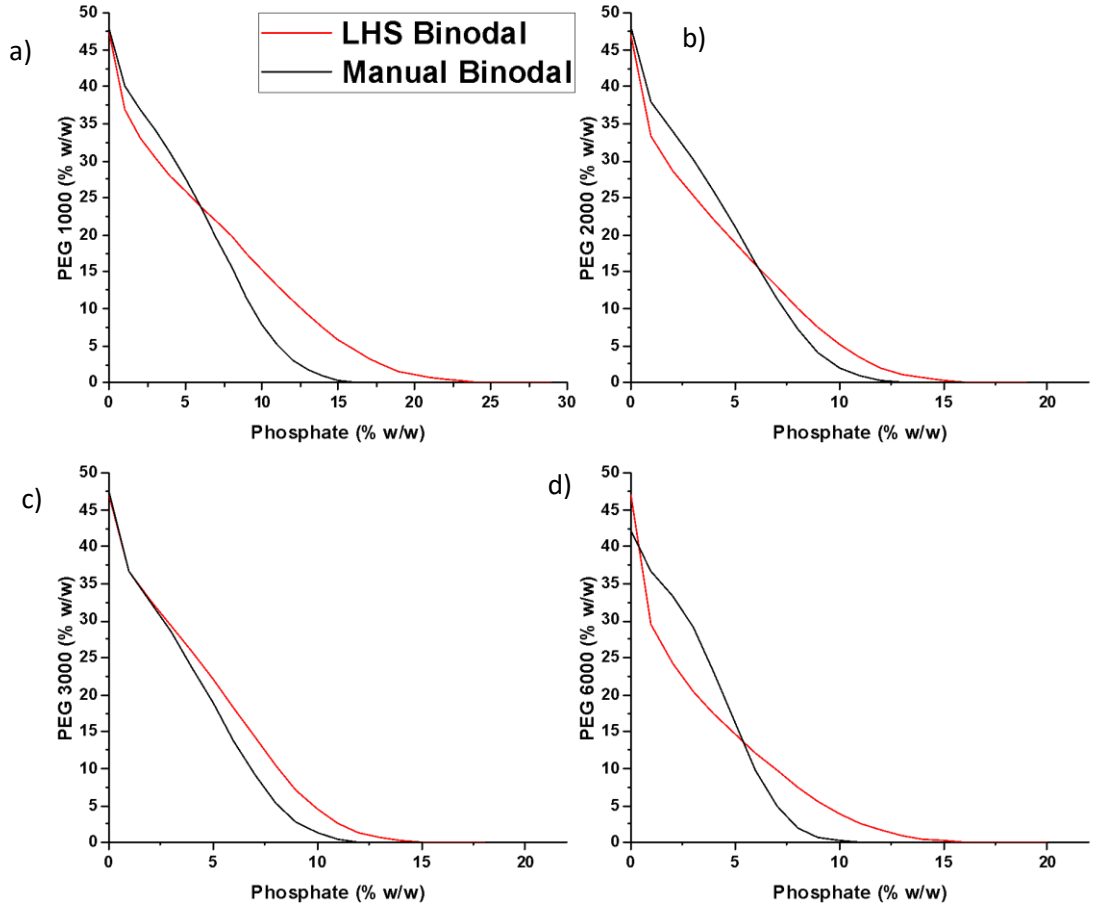

Fig 5-8. Comparison of binodal curves determination of 4 phase-forming systems: (A) PEG 1000, (B) 2000, (C) 3000, and (D) 6000; with phosphate buffer using an automated method and a manual determination process.

Differently from PEG 3000-potassium phosphate system, in all the other curve comparisons there was an intersection point between the regression approaches located

in (6, 15.99) for PEG 2000-potassium phosphate, (6, 23.84) for PEG 1000-potassium phosphate, and (6, 10.95) in PEG 6000-potassium phosphate system, this means there was an over- and underlapping in different portions of the fitting of the automated method with the manual approach. These slight deviations might arise from incorrect readings when performing the titration manually or from a too-high distance between two system points evaluated using the hydrophobic dye marker, and thus leading to a deviation when performing the regression. The accuracy of the latter can be enhanced by choosing a smaller step value by a second run focusing on the binodal region (Bensch et al., 2011). Nevertheless, from a processing perspective, both the experimental parameter space and accuracy shown in **Fig 5-5**, **5-6** and **5-7** can be considered as sufficient since system points close to the binodal curve do not express the necessary process robustness needed in industrial purification procedures. This outcome confirmed that automated construction of the binodal curve is equally reliable than manual determination and is a suitable method to assess polyphenol partitioning.

2.3. High-throughput screening of polyphenol partitioning

After the validation of the automated screening method was demonstrated, a HTS for partitioning of polyphenols was performed. Absorbance of phloroglucinol at 265 nm was used as seen in **Fig 5-3**. The above methodology represents a tool for the characterisation of system properties describing the respective ATPS and thus prepares the stage for the actual polyphenol partitioning. The LHS was used to make 384 different ATPS and subsequently analyse the recovery of polyphenols. For the preparation of the phase systems generally four pipetting steps for water, buffer, a fixed concentration of phloroglucinol of 0.25 mg/mL and PEG solution were required (see **Fig 5-2**). Phloroglucinol was selected as a model polyphenol to assess the partitioning due to participation as the main building block in the synthesis of polyphenols in brown macroalgae (Li et al., 2011). Analysis using direct absorbance at 265 nm required one additional pipetting step for sampling of the top phase, and transfer into a 96-well microplate. In order to reach a statistical robustness in the determination of the polyphenol partitioning, nine independent samplings were performed for each system, the measured absorption values when using the direct absorbance method showed an overall standard error of the mean (SEM) of: SEM = 0.0068 mg/mL for PEG 1000-potassium phosphate systems, SEM = 0.0052 mg/mL for PEG 2000-potassium phosphate, SEM = 0.0056 mg/mL for PEG 3000-potassium phosphate, and SEM = 0.0038 mg/mL for PEG 6000-potassium phosphate. This suggests both, a high precision during the pipetting steps, as well as the accuracy of the overall assay. The results of the polyphenol recovery can be seen in **Fig 5-9**. The first it can be observed is that mostly all the systems constructed with PEG 1000-potassium phosphate buffer at pH 7.5 did not partition phloroglucinol at all. This might be due to the shorter hydrophilic end group with shorter polymer chains that reduces the hydrophobicity of the top phase (Goja et al., 2013). Similarly, PEG 6000-potassium phosphate buffer systems did not recover phloroglucinol, a possible explanation of this might be the steric hindrance of PEG 6000 with water, not allowing the transport of phloroglucinol to the top phase, as well as the

fact that PEG with higher molecular weights produce smaller coefficient factor between top and bottom phases (Raja et al., 2012). On the other hand, in PEG 2000-potassium phosphate buffer systems it was observed areas where the polyphenol partitioning occurred, highlighted in red colouration in the contour plots, in two areas with the highest partitioning in PEG2000-potassium phosphate (37:1) and (27:4), with 0.157±0.030 mg/mL and 0.155±0.066 mg/mL, respectively; and the total recovery yield of both systems was 62.9±12.0% and 61.8±26.6%, respectively. Finally, in PEG 3000-potassium phosphate buffer systems areas with high partitioning were also observed in the contour plot, in PEG 3000-potassium phosphate (9:10) and (1:13), with 0.154±0.070 mg/mL and 0.153±0.050 mg/mL, respectively; and 61.6±27.9% and 61.2±19.7%, respectively. Comparing with the results obtained in **Chapter 4**, where the ATPS used in the biorefinery cascading sequence exhibited a recovery yield of 0.05±0.01% and the control process 30.8±7.36%, the ATPSs obtained in PEG 2000-potassium phosphate systems showed a 2.04- and 2.01-fold increase for (37:1) and (27:4) systems, respectively. In PEG 3000-potassium phosphate the recovery yield was 2.00 and 1.99 times higher for (9:10) and (1:13) systems, respectively.

With these results, four prospective ATPS were identified to recover polyphenols from brown macroalgae using an automated HTS. From all these systems just PEG 2000-potassium phosphate buffer (27:4) and PEG 3000-potassium phosphate buffer (9:10) were selected for further scale-up trials, this was due to PEG 2000-potassium phosphate buffer (37:1) and PEG 3000-potassium phosphate buffer (1:13) system points were close to the binodal curve regression limit, thus the associated error with the formation of the two phases was higher and the extraction process cannot be considered robust enough to use it in an industrial setup. Finally, PEG 2000-potassium phosphate buffer (27:4) and PEG 3000-potassium phosphate buffer (9:10) systems were selected for subsequent 40-times scale-up experiments.

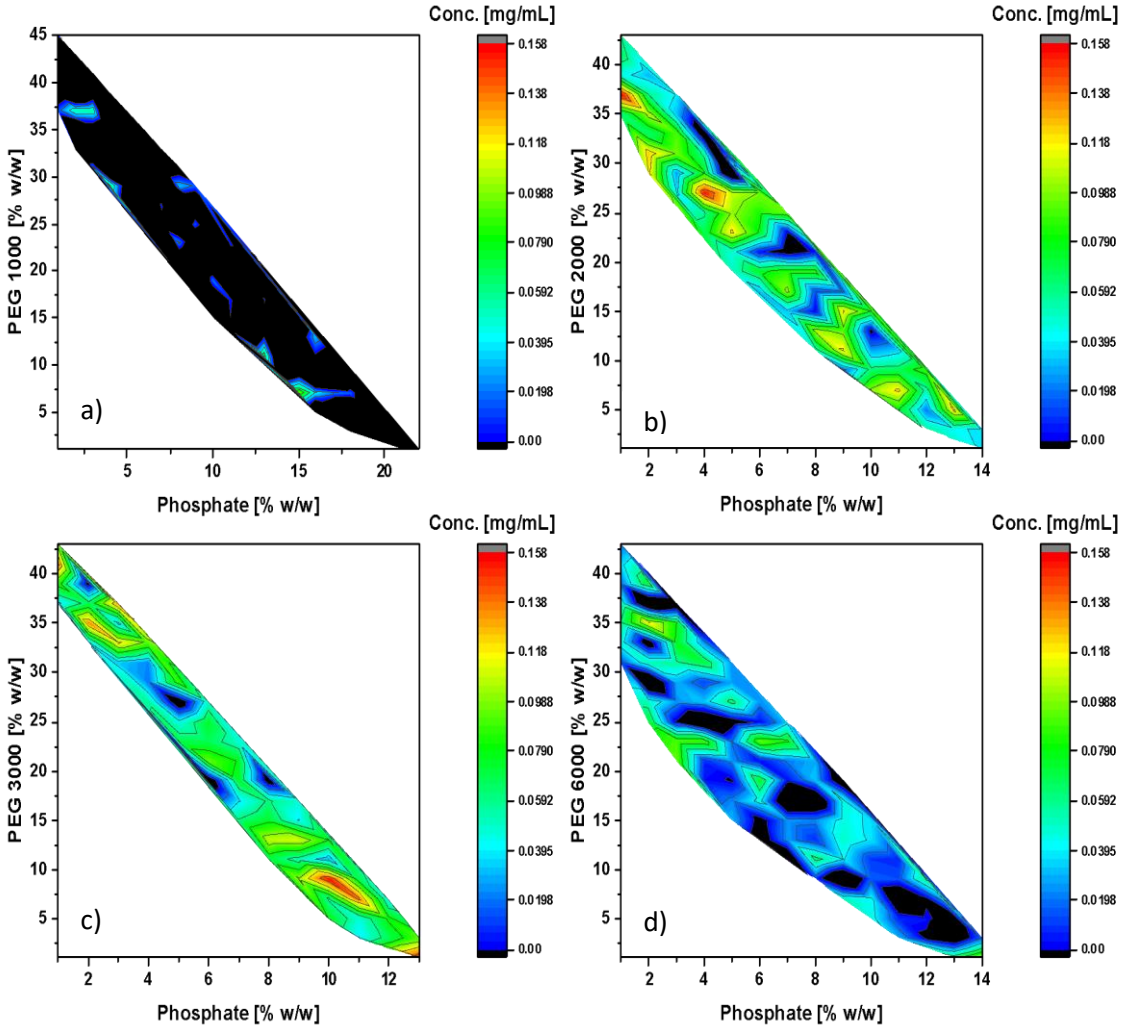

Fig 5-9. Contour plots of the partitioning of phloroglucinol in ATPS formed with A) PEG 1000, B) 2000, C) 3000, and D) 6000, with phosphate buffer.

2.4. Scale-up trials of selected ATPS

Before the scale-up trials, a modified version of the polyphenol quantification method using Folin-Ciocalteu reagent was developed (see **Section 4.6** from **Chapter 2**). This was decided due to the precipitation of this chemical in presence of non-ionic detergents, such as PEG (Dulley and Grieve, 1975). To be able to quantify the polyphenol content without the interference of PEG in the selected ATPS an aliquot of SDS was added to the samples to trap the polymer in an arrange of micellar aggregates (Bernazzani et al., 2004), in order to avoid the interaction between PEG and the Folin-Ciocalteu reagent,

because Folin-Ciocalteu is the chemical reagent in charge of bonding with polyphenols and produce a change of colouration that can be quantified via spectrophotometry. The calibration curve for this method can be observed in **Fig 5-10**, and the relative standard deviation (RSD) of the curve is within the 1.20% – 3.37% variation range and with a goodness of fit of R^2 = 0.95; thus, this modification in the protocol showed analytical robustness to quantify polyphenols in presence of PEG.

The interaction between SDS and PEG has been previously described in literature (Bernazzani et al., 2004; Dulley and Grieve, 1975), but the micellar aggregation between them has not been reported to aid the quantification of polyphenols in presence of detergents; this lack of information might be an indirect effect to explain the scarcity of ATPS reports on polyphenols recovery from any plant matrix. Interestingly to note, some of the few investigations reporting the use of ATPS to recover polyphenols (Xavier et al., 2017, 2015, 2014), the authors in their methods claimed using the regular method, without the addition of SDS as defined in **Section 4.5** from **Chapter 2**, but they do not discuss any step to avoid the interference of PEG or the difficulties they overcame to be able to quantify these compounds.

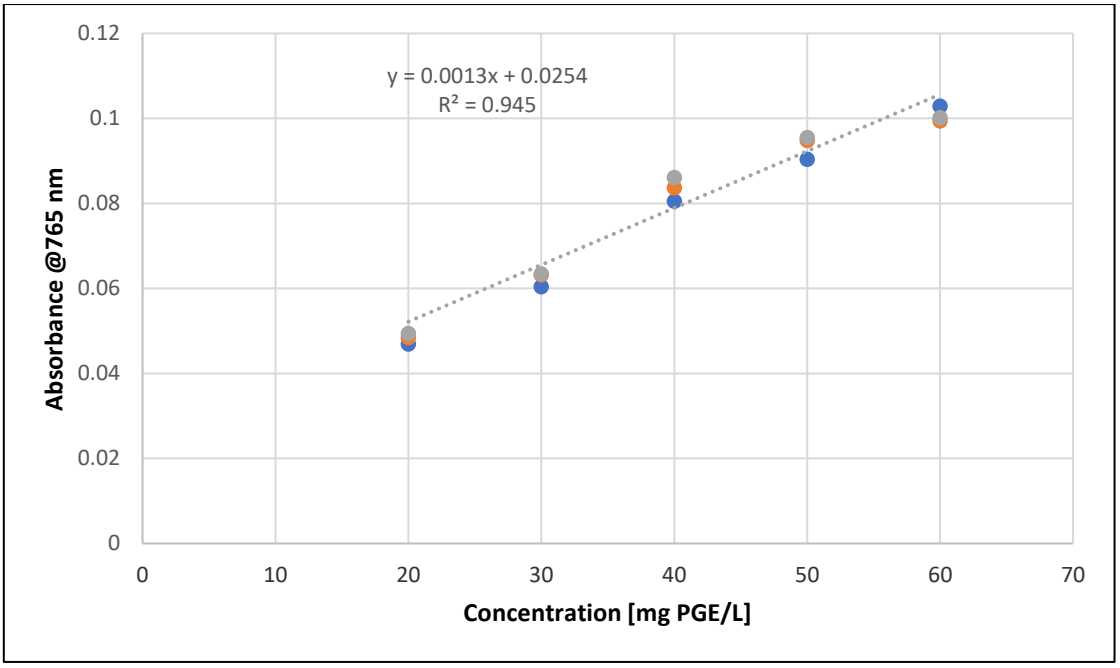

Fig 5-10. Calibration curve for the new developed protocol for the quantification of polyphenols in presence of polyethylene glycol.

With this updated method the selected ATPS from the partitioning screening were scaled-up 40 times and compared with the scaled-down systems to validate the process. The comparison of the two systems can be observed in **Table 5-4**. As stated above PEG 2000-potassium phosphate (27:4) scale-down system exhibited a recovery of 62.9±12.0%, while the partitioning of the scale-up system was 54.8±14.2%. On the other hand, PEG 3000-potassium phosphate (9:10) recovery of the scale-down ATPS was 61.6±27.9% compared to 40.4±14.6% of the scale-up system. In **Fig 5-11** the statistical comparison of both systems can be observed. While scale-up and scale-down approaches in both systems statistically speaking are not different, there is not a $p > 0.95$ of significance to determine the best scaled-up system. PEG 2000-potassium phosphate (27:4) exhibited a significance of $p > 0.70$ compared to a significance value of $p > 0.25$ of PEG 3000-potassium phosphate (9:10); thus, PEG 2000-potassium phosphate (27:4) exhibited a better statistical significance and therefore was selected for the final tests with two complex samples.

Table 5-4. Comparison of phloroglucinol partitioning in scale-down and scale-up systems.

PEG 2000 (% w/w)	PEG 3000 (% w/w)	Phosphate (% w/w)	Scale-down concentration (mg/mL)	Scale-up concentration (mg/mL)
27	-	4	0.155±0.0665	0.137±0.0656
-	9	10	0.154±0.0697	0.101±0.0364

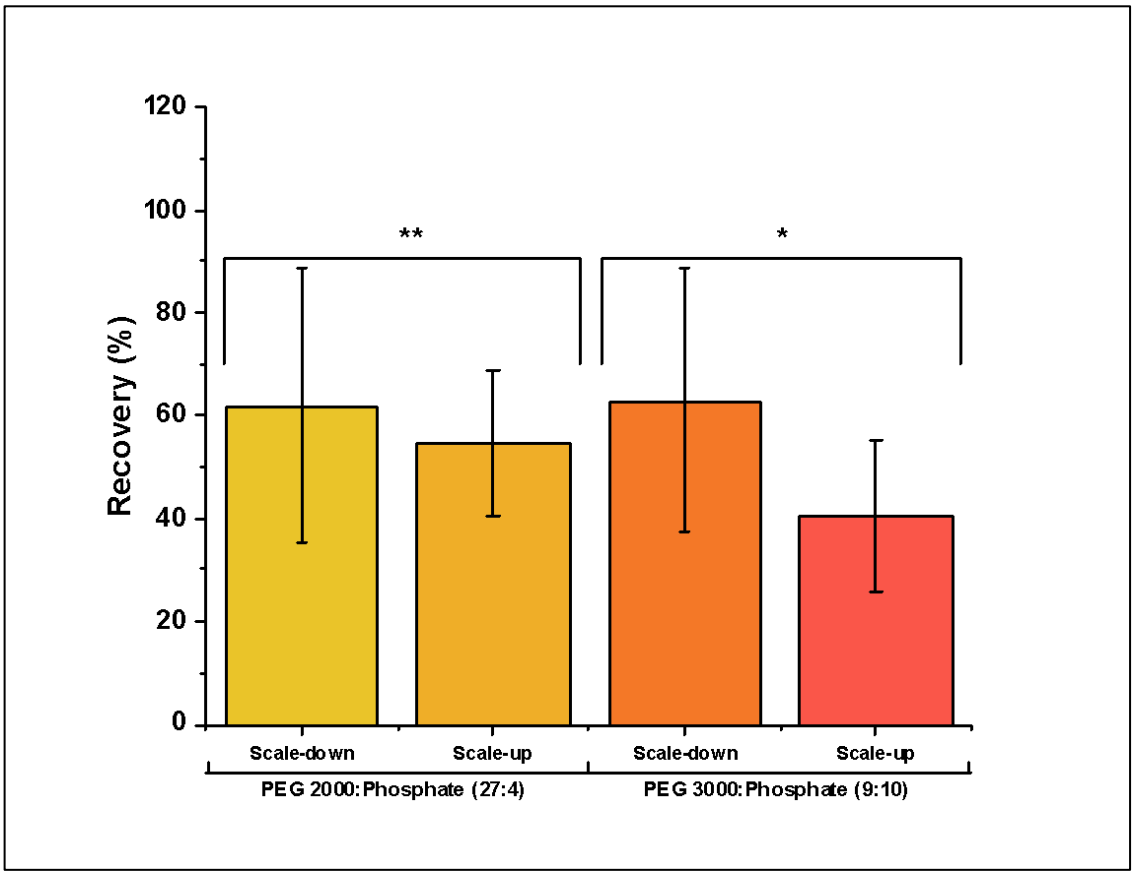

Fig 5-11. Comparison of the recovery between selected scale-down systems (800 µL) and scale-up tests (50 mL). Values grouped with "**" showed a significance of $p > 0.70$, and values grouped under "*" showed a significance of $p > 0.25$.

Thus, PEG 2000-potassium phosphate (27:4) was selected to test two case studies to confirm the optimisation of the processing step, a polyphenol partitioning trial from an aqueous polyphenol extract from *A. nodosum*, and another test recovering polyphenols

from a biorefinery residue that extracted fucoidan and alginate first. In **Table 5-5** the results from the scale-up test using the polyphenol aqueous extract can be observed. Polyphenols partitioned almost entirely to the top phase, with a 93.62±8.24% recovery, compared to the bottom phase which exhibited a 12.25±0.49% recovery. In **Table 5-6** it can be observed the comparison of the aqueous polyphenol extract and the biorefinery residue, as stated above the recovery of the extract was 93.6±8.24%, and the recovery of the residue was 87.8±3.51%. When compared with the few results that exists in literature PEG 2000-potassium phosphate (27:4) exhibited a 10-fold increase in the partitioning, with 11.38±1.00 g PGE/100 g DW alga and 10.76±0.56 g PGE/100 g DW alga for polyphenol extract and biorefinery residue respectively, while Xavier et al. (2014) showed a partitioning yield of 1.88±0.04 mg GAE/100 g DW wood using a PEG 2000-ammonium sulphate (1.08% w/w) system from eucalyptus wood industrial wastes. Both partitioning trials did not show statistically significant differences ($p < 0.05$) between them, however both experiments exhibited differences with the phloroglucinol model (**Fig 5-12**), demonstrating a better performance with complex samples and polyphenol samples with more than one polyphenol, this might be due to the pI of the polyphenols within the raw extract and biorefinery residue are closer to the pI of the ATPS (pI = ~7.5 – 8.5).

Table 5-5. Partitioning of polyphenol from complex seaweed extract.

PEG 2000/Phosphate (27:4)	Concentration (mg/mL)	Recovery (%)
Top phase	0.569±0.050	93.62±8.24
Bottom phase	0.0745±0.0029	12.25±0.49

These results confirm that PEG 2000-potassium phosphate (27:4) is the optimal ATPS for polyphenol partitioning from *A. nodosum*.

Table 5-6. Partitioning of polyphenol from biorefinery residue.

Source of polyphenol	Concentration (mg/mL)	Recovery (%)
Polyphenol extract	0.569±0.050	93.62±8.24
Biorefinery residue	0.538±0.028	88.40±4.59

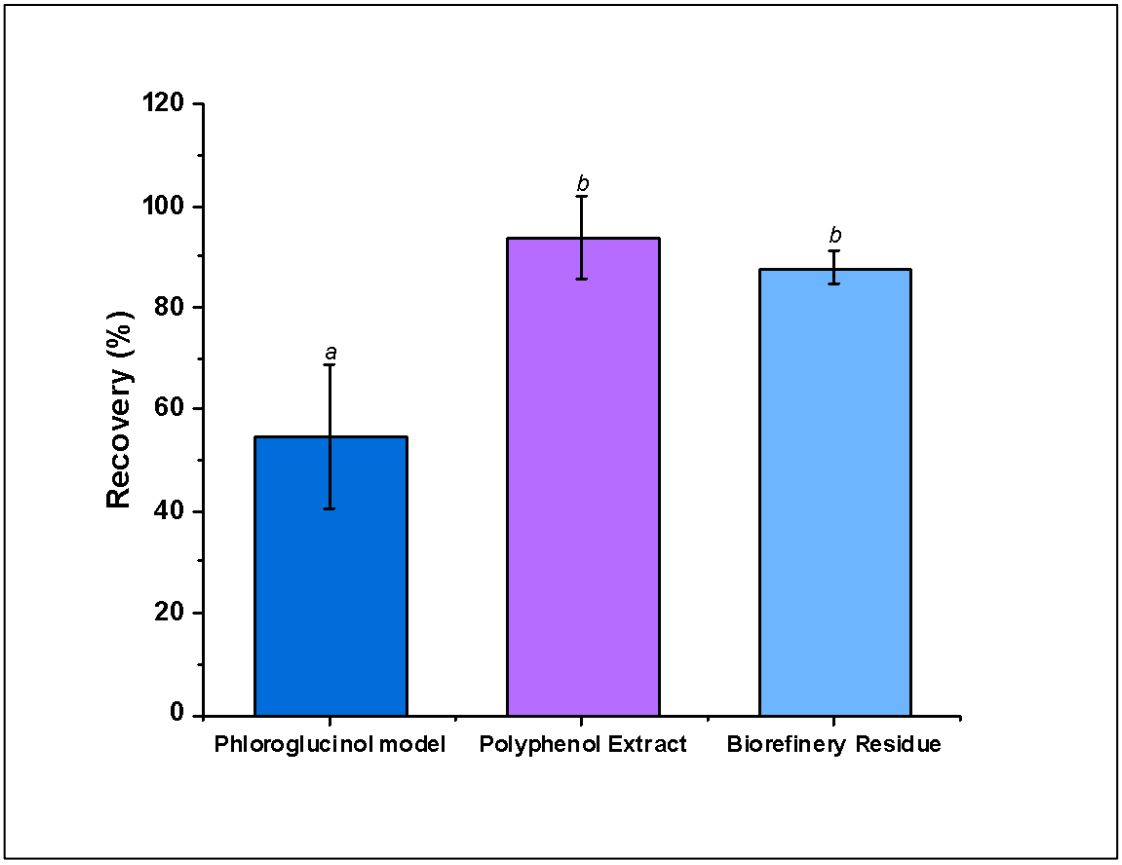

Fig 5-12. Comparison of the recovery of the scale-up model and two case studies: a polyphenol extract, and a carbohydrate biorefinery residue. Values are means ± standard deviation (n=3). Values with different letters are significantly different, as determined by a post hoc Tukey's HSD test ($p < 0.05$).

3. Conclusions

The main aim of this work was to develop a platform for HTS experimentation to select a suitable ATPS extraction processing step to separate polyphenols from its macroalgal matrix. The use of a HTS approach was chosen so that a rapid and robust methodology for process development could be obtained.

Partitioning of polyphenols was investigated with four different polymers, PEG 1000, 2000, 3000, and 6000 using an automated LHS in a scale down approach. Binodal curves for every system were built with the automated system and compared with a manual determination, proving being equally reliable than a manual binodal curve determination. Partition of polyphenols was affected by polymer molecular weight, were the smallest and largest weights (PEG 1000 and 6000) did not partition polyphenols, while intermediate weights (PEG 2000 and 3000) exhibited 62.9±12.0% and 61.6±27.9% recovery values in the scale-down method. Finally, during the scale up trials PEG 2000-potassium phosphate buffer (27:4) showed the highest recovery of all 384 systems analysed with ~91% of polyphenols in the top polymer-rich phase.

The benefit of the use of the high-throughput approach presented in this chapter is that resource intensive experiments and/or potential new processing steps such as application of ATPS for polar compounds extraction can be instead assessed in a scale-down manner to see whether a separation is feasible based on process performance requirements. In addition, this methodology allows the exploration of process robustness issues, based on a fast and reliable assessment of the binodal curve determination. The main limitation of the approach presented in this chapter is that the method is a high-throughput assessment that allows the possibility to design ATPS processes while screening a broad range of parameters, by only varying the concentration of the phase-forming components but does not consider any process optimisation regarding to temperature or different settling times. This issue could be addressed in future work by making use of a combined procedure of HTS and DoE to define the optimum ATPS while optimising the process parameters.

Chapter 6: Assessment and selection of a green extraction method for fucoidan from *A. nodosum* – a DoE-based procedure.

1. Introduction

There has been a growing interest in the use of natural products in the development of several products, such as cosmeceuticals, nutraceuticals, biopharmaceuticals, and biopolymers. Brown macroalgae (Phaeophyceae) contain soluble carbohydrates in their composition with well-defined markets for bulk chemicals i.e., alginate, and high-value biomolecules with potential breakthrough in new markets, such as fucoidan (Gomaa et al., 2018). Within brown seaweeds, fucoidan denotes a group of fucose-containing sulphated polysaccharides. Fucoidan may differ considerably in chemical composition, molecular mass and structure, depending on the algal species, spatial and temporal variation, or on the type of tissue sampled. What has emerged from research to date is the knowledge that a single algal species can contain more than one type of fucoidan polymer in terms of molecular size and composition (Rioux et al., 2007). These polysaccharides have been extracted from several species of marine algae and from some marine echinoderms such as sea urchins and sea cucumber (Song et al., 2018). Fucoidan polymers can be found in the fibrillary extracellular wall and intercellular spaces in brown macroalgae. It has been described that the method of extraction can affect the monosaccharide composition, sulphation patterns, fine structure and size of compound (Honya et al., 1999), therefore it is imperative the development of milder recovery processes to avoid undesired changes in the composition of fucoidan that can affect its bioactivity. Although the interest in developing new products from fucoidan, there has been few endeavours to optimise the extraction method of this compound, where most processes involve the use of strong acids and high temperature (Lorbeer et al., 2015). Current industrial extraction operations from seaweeds often suffer from low efficiencies of biomass utilisation, and the generation of waste streams. The

development of an integrated multi-product biorefinery concept from the starting process might help mitigating this issue, while also improving the economic viability of the macroalgae processing industry. A number of biorefinery strategies have been devised for Phaeophyceae, involving the use of new technologies such as supercritical CO_2 (Pérez-López et al., 2014), ultrasound-assisted (Kadam et al., 2015b), autohydrolysis (Balboa et al., 2013), and enzyme-assisted (Sanjeewa et al., 2019) extraction. Such approaches have the potential to extract fucoidan, reduce chemicals, and water use, and valorise post-extraction residues. However, industry may be slow to adopt these techniques due to the need for comprehensive and expensive infrastructure upgrades and difficulties associated with the scale-up of novel extraction technologies. In the meantime, parallels between existing processing technologies for different products reveal immediate opportunities for a progression toward macroalgae biorefineries. Common procedures involve the use of HCl to disrupt hydrogen bonds between polysaccharides, resulting in the release of fucoidan, while simultaneously preventing alginate contamination by converting it into insoluble alginic acid. In addition, in conventional alginate production processes, acid pre-treatments are used before alginate extraction in order to remove potential contaminants e.g., fucoidan, laminarin, and some polyphenols, while converting insoluble alginate salts into alginic acid, which is then more easily converted into soluble sodium alginate. Therefore, the development of a cascading sequence process involving the simultaneous extraction of fucoidan, and pre-treatment of alginate is attractive for industry. Hot acid-water extraction for fucoidan recovery is usually associated with long extraction time and high temperatures. The application of diluted acid solutions at ambient temperature may give higher yields of crude fucoidan, but could result in the extraction of undesirable impurities, such as alginic acid or polyphenols (Pomin, 2011). Thus, a middle point in the use of these extraction methods is necessary in a holistic approach of this simultaneous two-step initial extraction. Protonation behaviour is what defines the strengths of different types of acids, with strong acids ionising completely by losing a proton in an aqueous solution,

i.e., HCl, and H_2SO_4; while weak acids only dissociate partially in solution, i.e., acetic and oxalic acid. Thus, the use of a hot acid-water extraction using a mildly strong acid was hypothesised in this chapter to be the most suitable extraction process for fucoidan. Regardless its use in fucoidan and alginate extraction, HCl can be a strong acid driver when it is used in industrial application settings, and therefore can affect wetlands, more than sulphates or nitrates, and it is suggested that can be contributing to increase dissolved organic carbon leaching to surface waters (Evans et al., 2011), so greener options for the further scale up of these processes has been deemed as required. Citric acid on the other hand, is a biodegradable mild organic acid that is widely used in the food industry as a food additive; its use in fucoidan extraction had been reported previously (Hifney et al., 2016), but overall information is still scarce. Nonetheless, it can be a desirable economic, environmental, and effective method of extraction of polysaccharides and preserve the native structures of fucoidan and avoid impurities in both, fucoidan and alginate.

The aim of this chapter was to first, optimise the recovery of the fucoidan and alginate extraction stages of the cascading sequence developed in **Chapter 4** without jeopardising the extraction performance of the subsequent stages first, by comparing two different extraction methods for fucoidan recovery using different acid types and concentration, and analyse their infrared spectra and sulphate content to determine the less destructive process to extract fucoidan and alginate; and second, to develop a green process using a mild acid to extract fucoidan from *A. nodosum* improving the extraction conditions using Design of Experiments to leverage the acquisition of data and define an optimised extraction step, to diminish the existing knowledge gap in process optimisation focused in the extraction of fucoidan with greener methods.

2. Results and discussion

The section of the project covered in this chapter can be seen in **Fig 6-1**. A two-step extraction process was developed in order to obtain fucoidan and alginate from *A. nodosum*. Firstly, a screening of different acid types, varying their acid power, was executed to select the best reagent for the fucoidan extraction step, considering the effect of the extraction conditions in both, fucoidan and alginate.

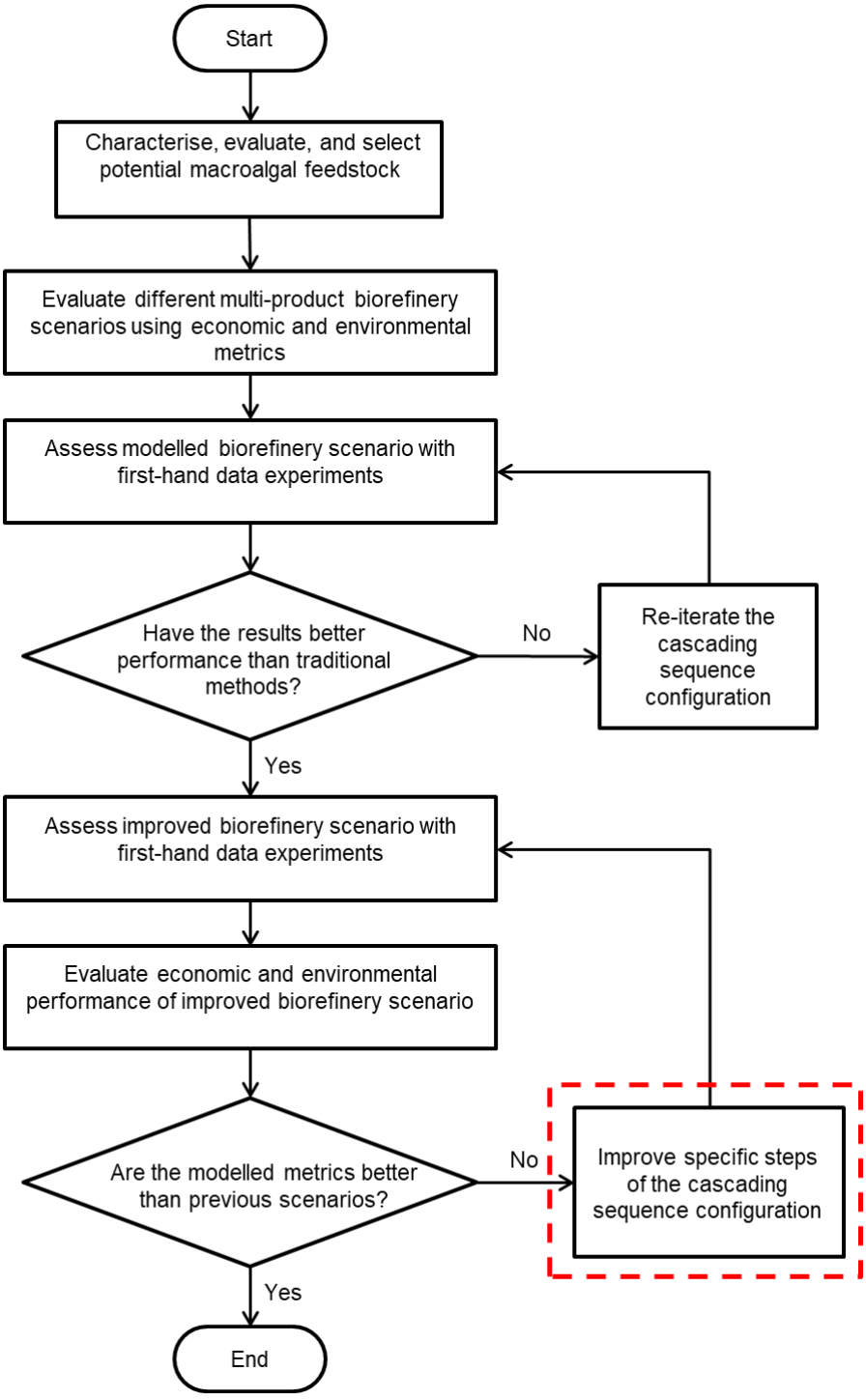

Fig 6-1. Proposed overall methodology for the development of a multi-product macroalgal biorefinery. In the red dashed box, the process optimisation step covered in this chapter is highlighted.

2.1. Comparison of yields with different acidic extraction methods

The gravimetric yield of the fucoidan extracts was first analysed using H_2SO_4, HCl, and citric acid, on two different extraction conditions, one with an acid concentration of 0.2 M (Hifney et al., 2016), and the second using an acidic solution with pH 5.5 (Lorbeer et al., 2015); these methods were selected because both offer a sequential approach extracting fucoidan and alginate. The fucoidan recovery can be observed in **Fig 6-2** where the highest recovery was obtained using the pH 5.5 method, with concentrations for citric acid, H_2SO_4, and HCl of 89.2±2.7, 87.8±3.3, and 90.5±5.1 mg Fucoidan/g DW, respectively; these results did not show statistically significant differences ($p < 0.05$). On the other hand, 0.2 M method showed statistically significant differences of HCl with the other two acid types ($p > 0.05$), and exhibited a fucoidan recovery of 78.7±1.4, 77.3±14.6, and 27.8±2.7 mg Fucoidan/g DW, for citric acid, H_2SO_4, and HCl respectively. Recovery of HCl extracts from 0.2 M method was lower than the other acid type extracts of the same method, this results might be due to the acid strength of the acid used that could be causing hydrolysation of the sulphated polysaccharides of the extracts; another explanation could be that the acid treatment using HCl is not releasing the fucoidan attached to the cell wall, due to the high concentration of the acid and high temperature that can produce harsh reactions conditions in the extraction environment that could result in the epimerisation and dehydration of polysaccharides (Fernando et al., 2019). These results support the proposed role of acids in extracting fucoidan while preventing co-extraction with alginate. Besides the results of any method tried here, mostly all samples had better fucoidan yield (**Table 6-1**) than some studies published in literature using the same methods; Lorbeer et al. (2015a) showed fucoidan yield results varying of 2.31 – 3.19% DW, similar to HCl 0.2 M extracts yield, 2.78±0.27% DW, while citric acid and H_2SO_4 showed a recovery yield of 7.87±0.14% DW and 7.73±1.45% DW, respectively; In addition, extracts from the pH 5.5 method also exhibited higher recovery yields than results published by Lorbeer et al. (2015a), with yields for citric acid, H_2SO_4 and HCl of 8.92±0.27% DW, 8.78±0.33% DW, and 9.05±0.51% DW respectively. When

extracting alginate, the use of different acid types did not show differences in the recovery yields (**Fig 6-3**), indicating the preliminary suitability of citric acid to recover fucoidan and alginate in a sequential approach.

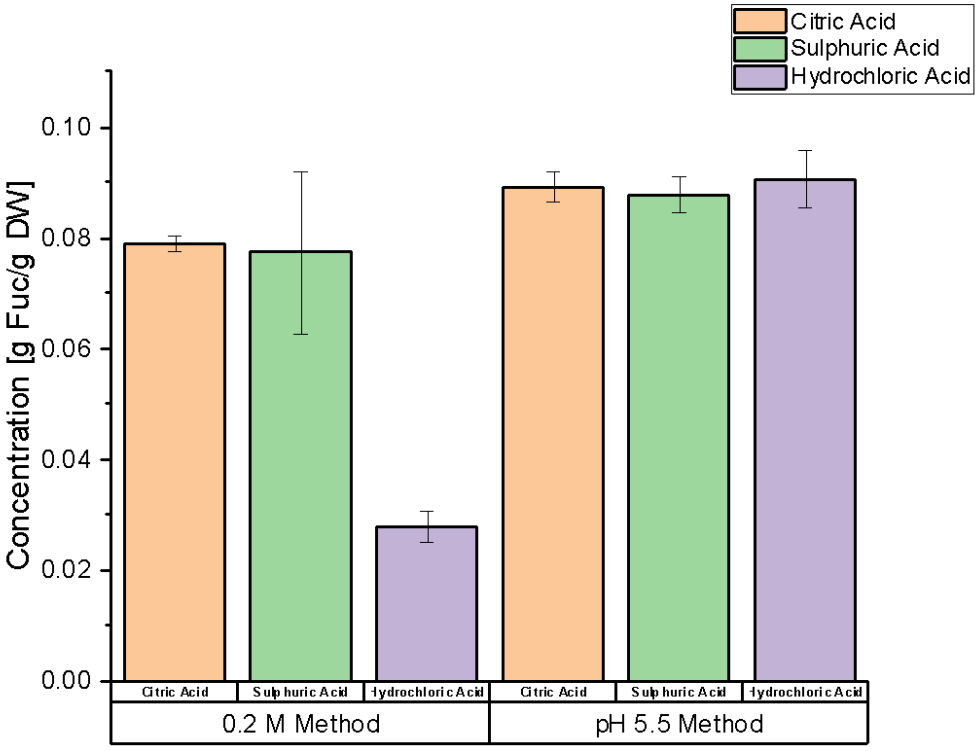

Fig 6-2. Comparison of different acid conditions and methods for fucoidan extraction within a biorefinery context.

Table 6-1. Recovery yield of the different extracts obtained by two different methods of extraction.

	0.2 M method (% DW)	pH 5.5 method (% DW)
Equivalences	pH ~1.0-2.0	~$3.2x10^{-6}$-$3x10^{-2}$ M
Citric acid	7.87±0.14	8.92±0.27
H_2SO_4	7.73±1.45	8.78±0.33
HCl	2.78±0.27	9.05±0.51

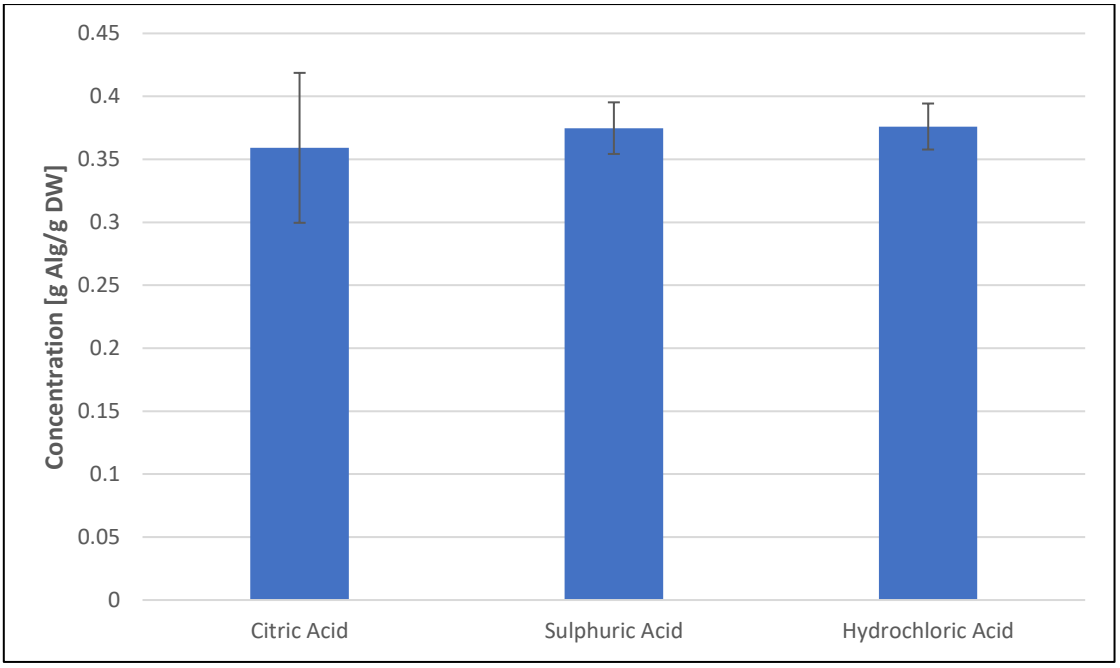

Fig 6-3. Comparison of alginate extraction after an acid extraction step to obtain fucoidan in a cascading sequence approach.

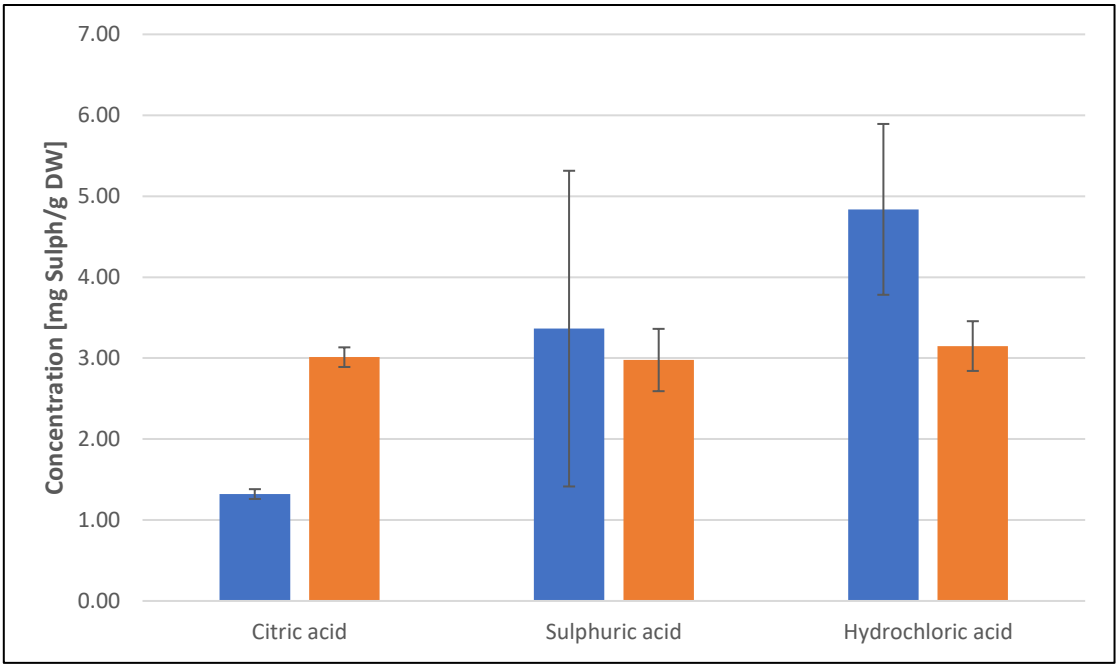

Fig 6-4. Sulphate content of extracts obtained using different acid types and different concentrations. Blue bars: 0.2 M extraction method. Orange bars: pH 5.5 extraction method.

The sulphate content (**Fig 6-4**) did not exhibit statistically significant differences in the pH 5.5 method and showed similar sulphate content in the three acid type extracts. Sulphate

content in the 0.2 M method showed differences, but sulphate concentration was inversely correlated with recovery, where HCl showed the highest sulphate content. Yields of the 0.2 M method showed statistically significant differences between them, while pH 5.5 method did not, thus this method was selected for further improvement due to the higher yields obtained compared to the 0.2 M method, and because the robustness of the results, indicating that the HCl and citric acid method obtained the same yields. HCl is the most used chemical to extract fucoidan, so having obtained similar results with citric acid is promising in order to develop a green cascading sequence step for a multi-product biorefinery process. An acid pre-treatment is industrially used to release the alginate before the alkaline extraction, so it is a desirable outcome to extract fucoidan first and alginate later. Nonetheless, extraction using strong acids is the most commonly used extraction method to obtain fucoidan, in recent years there have been several efforts using different techniques to obtain these sulphated polysaccharides, e.g., solvent extraction using ethanol (Foley et al., 2011), ultrasound-assisted extraction (Kadam et al., 2015b), enzyme-assisted extraction (Sanjeewa et al., 2019). While these processes have shown good recovery yields, the initial capital expenditure is higher than the standard strong acid method, and the environmental footprint is not well defined in any of these processes, for this reason it was attractive to explore different weaker acid types to assess the extraction performance of fucoidan.

2.2. Universal attenuated total reflectance Fourier transform infrared (UATR-FTIR) spectroscopy analysis

Vibrational spectroscopy has been applied as a rapid non-destructive technique in order to identify the quality of fucoidan and alginate extracts. The UATR-FTIR spectra of the different fucoidan extracts can be observed in **Fig 6-5**. UATR-FTIR spectra of citric acid (**Fig 6-5a**) and HCl (**Fig 6-5b**) from the pH 5.5 method showed the same spectra than the fucoidan standard (**Fig 6-5d**), while H_2SO_4 extracts did not (**Fig 6-5c**); these results might suggest hydrolysation of the extracts to some extent. This analysis was conducted

to determine whether the extracts have similar infrared absorption properties to those identified in published data. All extracts exhibited similar signals, with two bands in the 4000 – 2000 cm^{-1} region (defined as *(i)* in **Fig 6-5**) and numerous signals with similar wavenumbers within the 2000 – 800 cm^{-1} region (defined as *(ii)*, *(iii)*, and *(iv)* in **Fig 6-5**). Common to all polysaccharides and seaweed polysaccharides, two bands appeared in the 4000 – 2000 cm^{-1} region of the UATR-FTIR spectra. There was a broad band centred at 3378 cm^{-1} (citric acid), 3403 cm^{-1} (H_2SO_4), and 3383 cm^{-1} (HCl), which was assigned to hydrogen bonded O–H symmetrical and asymmetrical stretching vibrations (Lim et al., 2014). These peaks were also caused by the presence of moisture in the sample, as H_2O contains O–H bonds that give a stretching vibration signal (Saravana et al., 2018). In section *(ii)* there was another weak signal at 2944 cm^{-1} (citric acid), 2987 cm^{-1} (H_2SO_4), and 2941 cm^{-1} (HCl) due to C–H stretching vibrations, associated to all polysaccharides. The signals at 1619 cm^{-1} (citric acid), 1621 cm^{-1} (H_2SO_4), and 1616 cm^{-1} (HCl) were due to the bending vibrations of HOH, which indicate the presence of moisture in the samples. Main differences in section *(iii)* were observed in the H_2SO_4 extracts spectra compared to the others occurred in the 1200 – 970 cm^{-1} regions, which has been defined as the medium to strong IR absorption area. In this region the C–C and C–O stretching occurs in pyranoid rings and the C–O–C stretching in glycosidic bonds (Lim et al., 2014), thus the differences in the spectra occurred with the appearance of higher bands in the C–O–C stretching band than in the C–C and C–O bands (**Fig 6-5c *(iii)***). Absorption in this spectral region is common for all polysaccharides, which suggests that hydrolysation of fucoidan happened in H_2SO_4 extracts. The typical absorption bands of fucoidan are the bands that indicate the presence of sulphate (SO_4) and methyl (CH_3) groups, as fucoidan is a sulphated polysaccharide and contains mainly fucose, a monosaccharide that has a methyl group attached to the C_5 position (Ale et al., 2011). There was a strong signal at 1025 cm^{-1}, 1021 cm^{-1} and 1024 cm^{-1} (citric acid, HCl, and H_2SO_4 respectively) and a shoulder signal at 1076 cm^{-1} (citric acid), 1075 cm^{-1} (HCl) and 1073 cm^{-1} (H_2SO_4), which were assigned to the stretching vibrations of sulphoxides

(S–O). The strong signals for sulphoxides indicate that there were significant amounts of sulphate groups in the fucoidan. In section *(iv)* of **Fig 6-5** a rather sharp signal at 963 cm^{-1} (citric acid), 958 cm^{-1} (HCl) and 960 cm^{-1} (H_2SO_4) indicates the presence of the asymmetrical stretching vibration of C–O–S bonds, while the signals at 822 cm^{-1} (citric acid) and 837 – 849 cm^{-1} (H_2SO_4 and HCl) were assigned to the symmetrical stretching vibrations of C–O–S bonds.

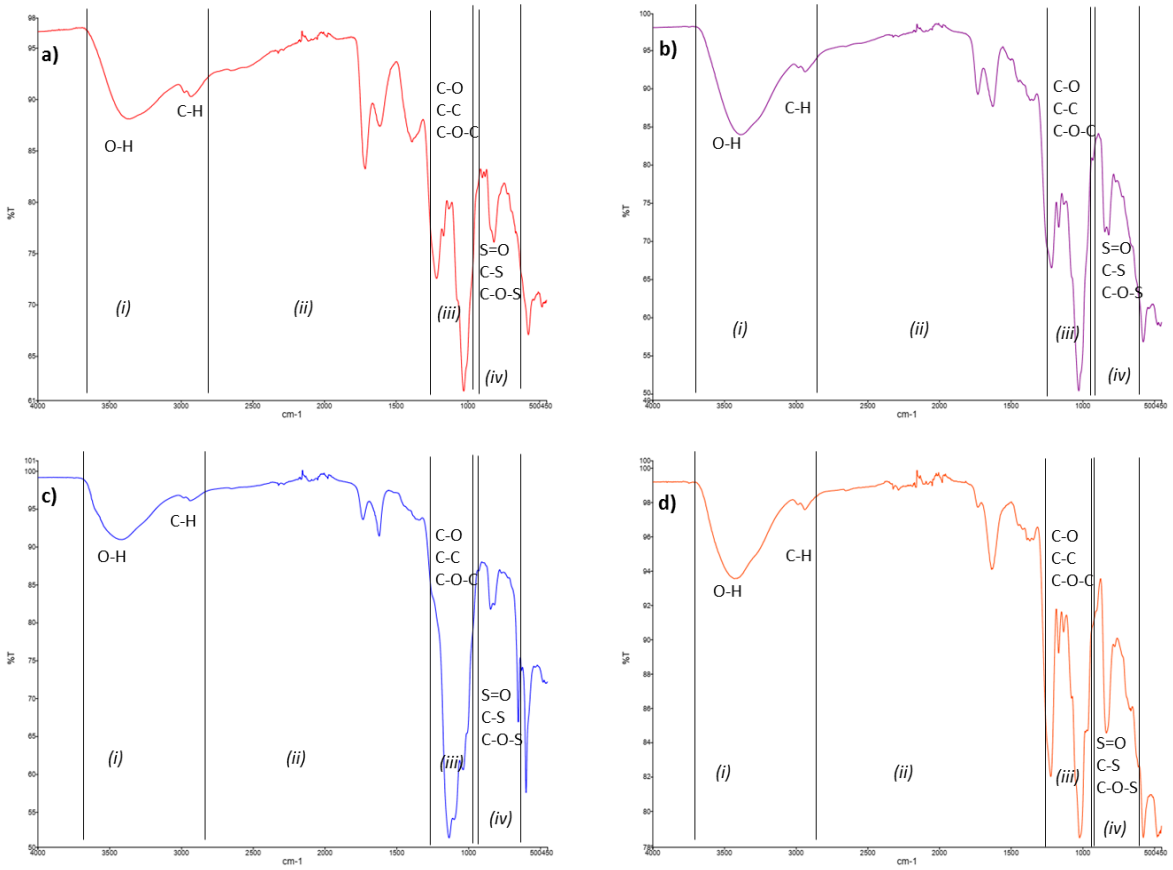

Fig 6-5. UATR-FTIR spectra of fucoidan extracts obtained with different acid types a) citric acid, b) HCl, c) H_2SO_4, and d) fucoidan standard.

In the UATR-FTIR spectra of the alginate extracts (**Fig 6-6**) showed the same broad bands centred at around 3400 – 3200 cm^{-1} (O–H stretching) and 3000 – 2870 cm^{-1} (C–H stretching) found in fucoidan extracts, the first one associated to moisture in the sample and the latter referred common to all polysaccharides, as mentioned above (section *(i)* in **Fig 6-6**). A broad band at 3420 cm^{-1} and a weak signal at 2932 cm^{-1} in the citric acid

sample were assigned to hydrogen bonded O–H, and C–H stretching vibrations, respectively. These O–H stretching vibrations were observed in the other samples as well at 3397 cm^{-1} and 3405 cm^{-1} for H_2SO_4 and HCl respectively, but not as pronounced as the standard and citric acid sample. In section *(ii)* the major difference between H_2SO_4 (**Fig 6-6c**) and HCl (**Fig 6-6b**) extracts and the standard (**Fig 6-6d**) was in the band at around 1600 cm^{-1} which indicate the asymmetric stretching vibration of COO^-, indicating that the polysaccharides are in the form of sodium alginate rather than alginic acid, this can also be observed in the citric acid extracts (**Fig 6-6a**), but to a lesser extent; citric acid extract spectrum also exhibited a higher band around 1700 – 1720 cm^{-1} were the carboxylic acid ester form, C=O was found indicating the presence of alginic acid in the extract (El Atouani et al., 2016), this band is observed as well in the other extracts but in a small vibrational peak. In section *(iii)* signals at 800 cm^{-1} were assigned to the α–L-gulopyranuronic acid asymmetric ring vibration and to the mannuronic acid residues (Rostami et al., 2017) in all the extracts obtained. The asymmetric and symmetric stretching vibrations of carboxylate groups (COO^-) on the polymeric backbone of alginate appeared at 1616 cm^{-1} and 1415 cm^{-1}, respectively, with the contribution of C–OH deformation to the signal at 1415 cm^{-1} (Leal et al., 2008). The bands at 1125 cm^{-1}, 1118, and 1122 cm^{-1} for citric acid, H_2SO_4, and HCl, respectively may be assigned to C–O stretching vibrations; and bands at 1094 cm^{-1} 1087 cm^{-1} and 1096 cm^{-1} were associated to C–O (and C–C) stretching vibrations of pyranose rings, for citric acid, H_2SO_4, and HCl, respectively, with the band at 1028 cm^{-1} may be also due to C–O stretching vibrations. The spectrum shows an indicative band of uronic acid at 945 cm^{-1} which attributed to C–O stretching vibrations. Additionally, the weak signals at 904 cm^{-1} and 814 cm^{-1} were related to the α-L-guluronic acid asymmetric ring vibration and to the β-mannuronic acid, respectively, with the one at 880 cm^{-1} indicating the C1–H deformation vibration of the β-mannuronic acid (Leal et al., 2008). Finally, according to the literature signals at around 1650 and 1550 cm^{-1} are assigned to the amide I and amide II bands, proposed for

identification of proteins. These absorption bands gave well defined signals in the UATR-FTIR spectra of all extracts. The signal at around 1600 cm^{-1} in all samples may appear overlapped with the strong vibrational peak of carbonyl group. Protein content in these brown algae, which has been reported by Gómez-Ordóñez and Rupérez (2011) fairly agrees with these results. These results showed that citric acid extracts using the pH 5.5 method of both, fucoidan and alginate, had the most similar spectra to the standard of each compound, qualitatively implying the purity of the materials extracted, by means of avoiding the co-extraction of other carbohydrates or proteins with them. Finally, with the FTIR analyses the comparison between different acid performances meant that pH 5.5 method using citric acid can be further evaluated as an option to extract fucoidan first and act as a pre-treatment for the further alginate extraction step in a cascading sequence for a biorefinery concept, hence additional evaluation of the extraction conditions was performed in the following section.

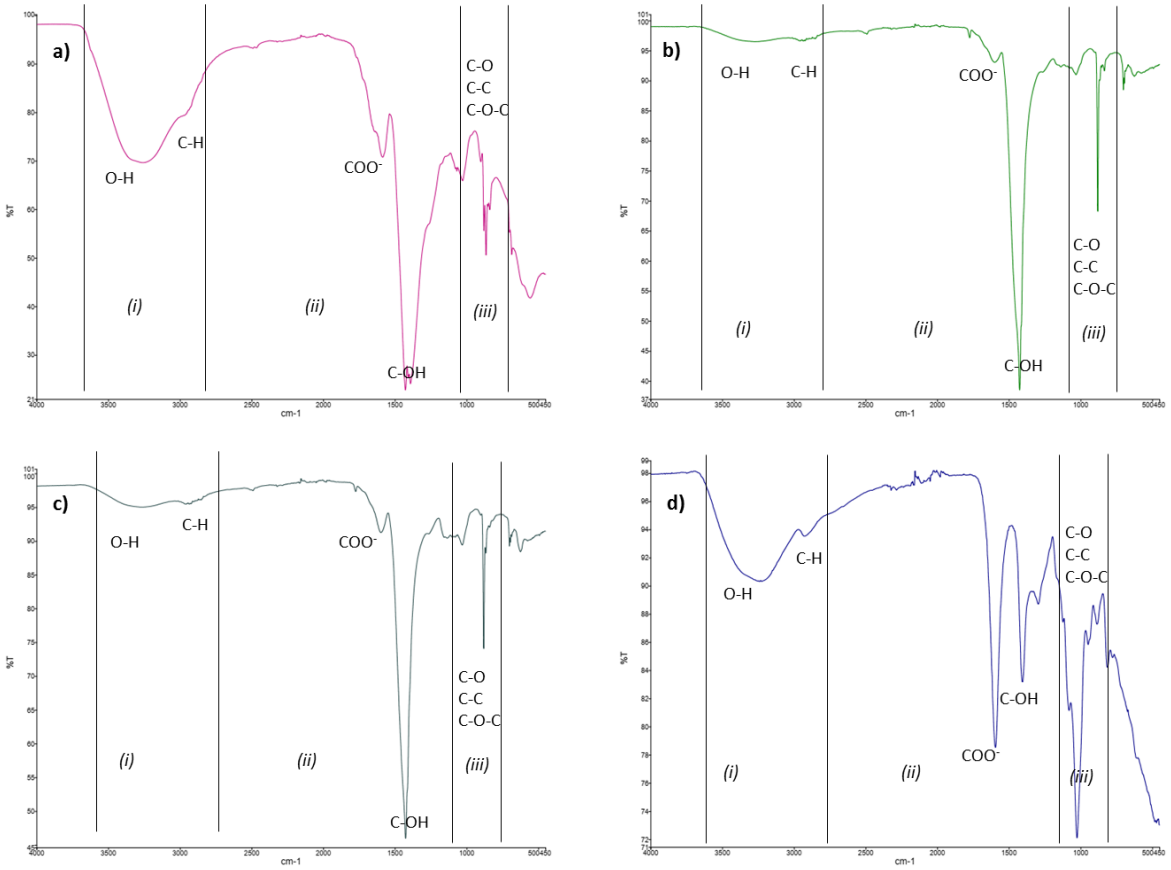

Fig 6-6. UATR-FTIR spectra of alginate extracts obtained after fucoidan extraction with different acid types a) citric acid, b) HCl, c) H_2SO_4, and d) alginate standard.

2.3. Improvement strategy of fucoidan extraction conditions

Finalised the integrity analysis of the extracts in the previous step, citric acid was decided to be used in an improvement strategy, in order to enhance the recovery yield of fucoidan using a pH 5.5 methodology. Two different conditions were identified to test further improvement, initial biomass, and temperature, both in three different levels and with one expected response (fucoidan recovery), while the volume of the experiments' solution was kept constant at 150 mL. For this reason, a simple 2^2 factorial design using DoE was employed and this experimental layout can be observed in **Table 6-2**.

Table 6-2. Experimental layout for improvement strategy in the extraction process of fucoidan using citric acid pH 5.5.

Temperature (°C)		Initial biomass (g)		
		(-1)	(0)	(+1)
(-1)	30	2.25	5.00	7.50
(0)	40	2.25	5.00	7.50
(+1)	50	2.25	5.00	7.50

Within the conditions tested temperature and initial biomass were directly correlated with the recovery of fucoidan (**Fig 6-7**), with the highest recovery of 11.92% DW obtained at 50°C and 7.50 g of initial biomass, while the lowest yield (8.38% DW) was obtained at 30°C and 2.25 g of initial biomass. There was a 33% increase in the recovery of fucoidan compared with the initial extraction conditions of citric acid tested in the comparison method screening in the previous section.

An increase in the co-extraction of alginate had been reported beforehand when the pH increases in the fucoidan extraction step (Lorbeer et al., 2015), which is why a pH 5.5 was selected in contrast to the other 0.2 M method, which showed a pH ~1.0 – 2.0 depending on the acid type (**Table 6-1**). The area located in between the best and worst recovery yields in **Fig 6-7** also presented a higher recovery than the previous extractions, varying from 9.71 to 10.59% DW, within the experimental borders of 40°C and 2.25 g, 30°C and 5.0 g, 30°C and 7.50 g, 42°C and 7.50 g, 50°C and 4.50 g, and 50°C and 2.25 g. Considering the potential application of this process in an industrial setup, is a positive outcome having a robust extraction area in case the scale-up conditions change or if it is not possible to reach the optimal conditions.

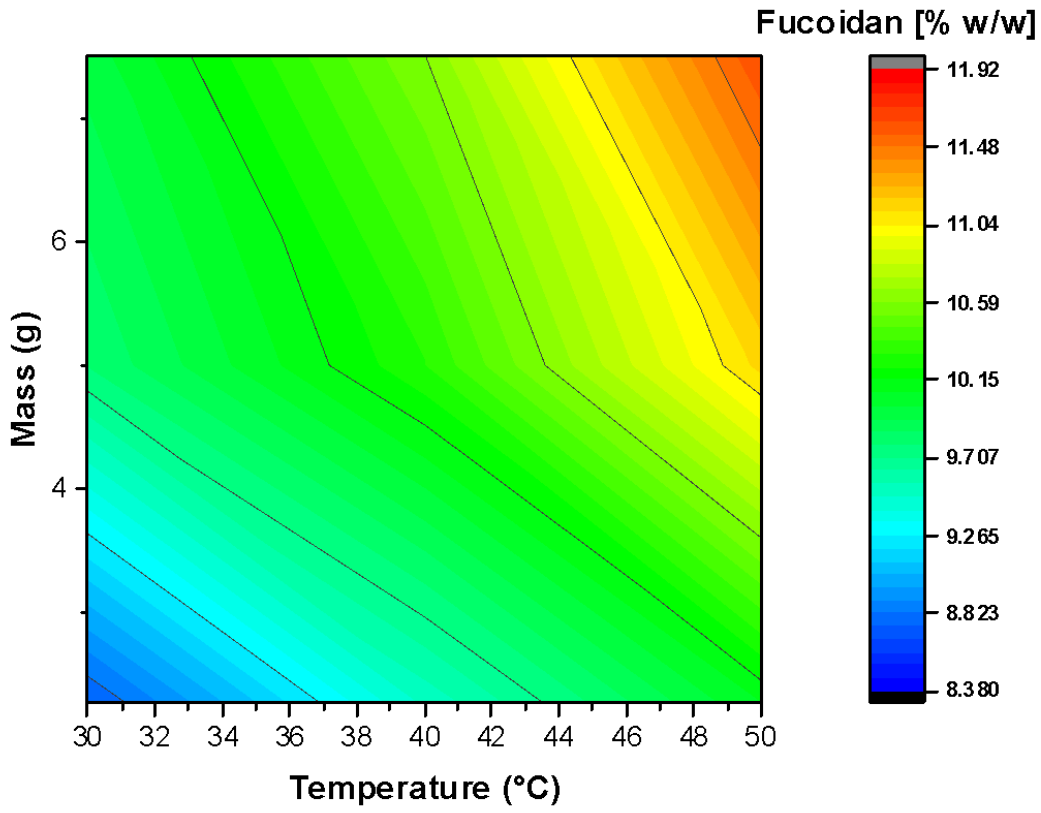

Fig 6-7. Contour plot of the extraction of fucoidan in citric acid pH 5.5 under different temperature and solids loading conditions.

In order to confirm the optimal conditions for fucoidan recovery showed in **Fig 6-7** an expanded domain was used to analyse the recovery performance of the process. An extra level of 10.0 g on the initial biomass extraction condition was added to assess if the fucoidan recovery yield obtained with 50°C and 7.50 g of extraction conditions was an artefact of the experimental domain or if these results are the improved conditions to extract fucoidan. In **Fig 6-8** the updated contour plot of the expanded domain can be observed, and it can be confirmed that the previous extraction conditions were the optimal to obtain fucoidan using citric acid. Interestingly, a higher initial biomass used at 30°C exhibited a similar behaviour with the previous lowest recovery conditions (30°C, 2.25 g). The equation associated with these experiments can be observed in **Eq. 6-1**, where all the terms are involved in a linear relation with the expected response.

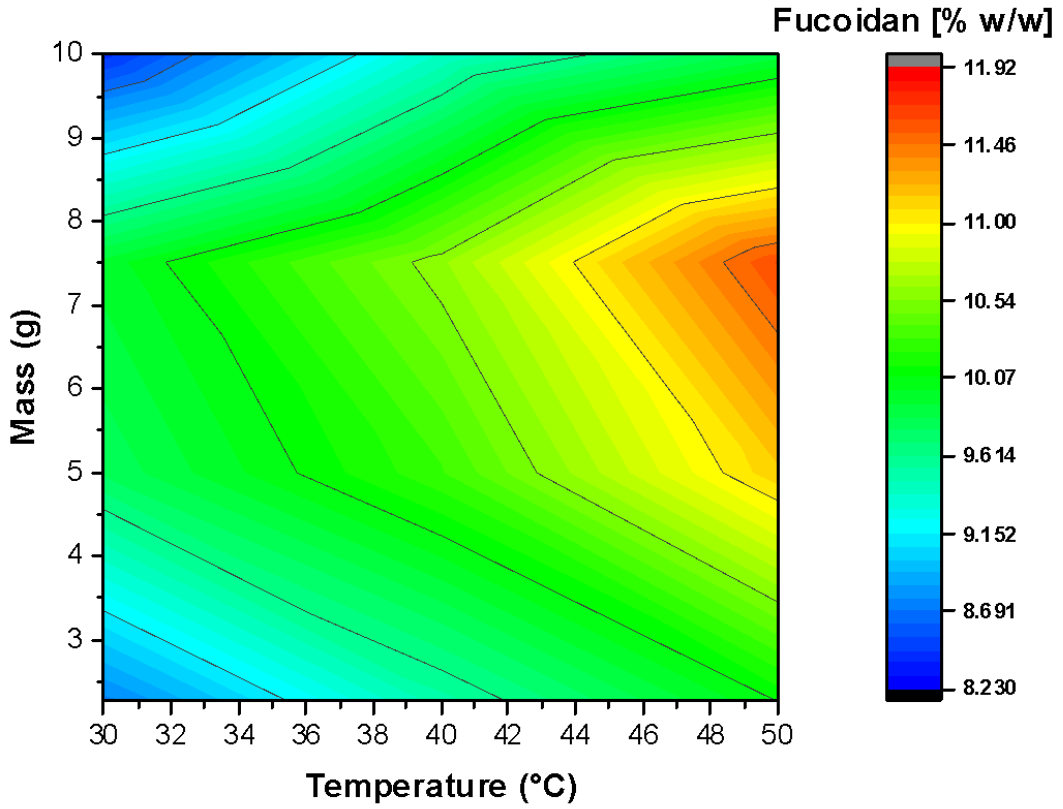

Fig 6-8. Updated contour plot of the extraction of fucoidan in citric acid pH 5.5 under different temperature and solids loading conditions.

$$Recovery = 10.13 + 0.75 * \left(\frac{(Temp - 40)}{10}\right) + 0.69 * \left(\frac{(Mass - 4.87)}{2.63}\right) \quad \textbf{(Eq. 6-1)}$$

Where, **Recovery**: Amont of fucoidan recovered, **Temp**: Temperature of the operation, **Mass**: initial biomass.

It has been reported that laminarin can be co-extracted with fucoidan in a pH 5.5 HCl method from *E. radiata* (Lorbeer et al., 2015), that can increase the overall yield; in this study however, laminarin content remained constant through all the conditions analysed in both, the experimental and expanded domain experiments, using glucose content as an indicative of laminarin presence (**Fig 6-9** and **6-10**) impurities.

2.4. Monosaccharide profiles of fucoidan extracts obtained using citric acid

The characterisation of the monosaccharide profile present in the fucoidan extracts was executed in order to confirm the hydrolysis mildness of the citric acid extraction step, i.e., avoiding the hydrolysis of the fucoidan extracts and its monosaccharide composition. In **Fig 6-9** the profile of the six main monosaccharide that are present in fucoidan extracts can be observed, and in **Fig 6-10** the profile of the monosaccharide profile obtained with expanded domain of the extraction conditions can be seen. Monosaccharide content did not show differences between the different extraction conditions in both, experimental and expanded domain, indicating that regardless the recovery conditions the extraction process is not hydrolysing the extracts, thus the potential bioactivities of the fucoidan shall remain the same. Bioactivities reported from fucoidan are extensive e.g., anticancer (Gutiérrez-Rodríguez et al., 2018), antioxidant (Zhao et al., 2018), and antiviral, with recent studies reporting the blocking of the new SARS-CoV-2 infectious process that causes COVID-19 (Kwon et al., 2020), among others. Extracts from all conditions were predominantly composed of fucose followed by xylose. Fucose content was similar in all extraction conditions when compared to literature reports, with values ranging between 38.40 – 40.24% g Fucose/g Fucoidan. Kostas et al. (2017) presented extracts with a fucose content of 42.5%±2.2% g Fucose/g Fucoidan, while Sugiono and Ferdiansyah (2019) showed values ranging between 16.41 – 35.21% g Fucose/g Fucoidan. Xylose content reported in this chapter was in between 19.99 – 22.86% g Xylose/g Fucoidan, being the second highest monosaccharide in the extracts; these results were different than other reports in literature. Sanjeewa et al. (2019) presented a xylose content of 9.14% g Xylose/g Fucoidan, and along the same lines Kostas et al. (2017) reported a xylose content of 2.6±.01% g Xylose/g Fucoidan; these differences might be due to the use of different seaweed species and extraction conditions, with Kostas et al. (2017) using *L. digitata* and a 0.1 M HCl extraction step at 70°C, and Sanjeewa et al. used *Sargassum horneri* and a Celluclast enzymatic hydrolysis step at 50°C; the geographic and seasonal harvesting differences also might affect the xylose content of the fucoidan

extract. Mannitol and glucose were the next highest monosaccharide contents in all extracts with values of 8.98 – 12.23% and 9.19 – 11.51%, respectively. Mannitol, glucose and rhamnose can be considered impurities indicators in the extracts, as mannitol is a sugar alcohol present in macroalgae that does not interact with fucoidan (Fernando et al., 2019). While glucose bonds with fucose to form fucoidan, this monosaccharide can indicate the presence of laminarin in the extract, while rhamnose does not interact with fucose so their presence it can be considered an impurity indicator. The combined content of all impurity monosaccharides is 18.58 – 24.43% g Impurities/g Fucoidan which is a desirable outcome with a purity of the extracts of 75.57 – 81.42% g Pure Fucoidan/g Raw Extract, while Kostas et al. (2017) reported a lower purity of fucoidan extracts than the extracts obtained in this chapter with 65±2.1%. Finally, galactose is also a monosaccharide that can interact with fucose to produce fucoidan and exhibited a concentration of 5.46 – 6.19% g Galactose/g Fucoidan. All monosaccharides did not show statistically significant differences ($p < 0.05$) between different extraction conditions indicating the robustness of the pH 5.5 citric acid extraction method to do not hydrolyse the fucoidan in the extracts.

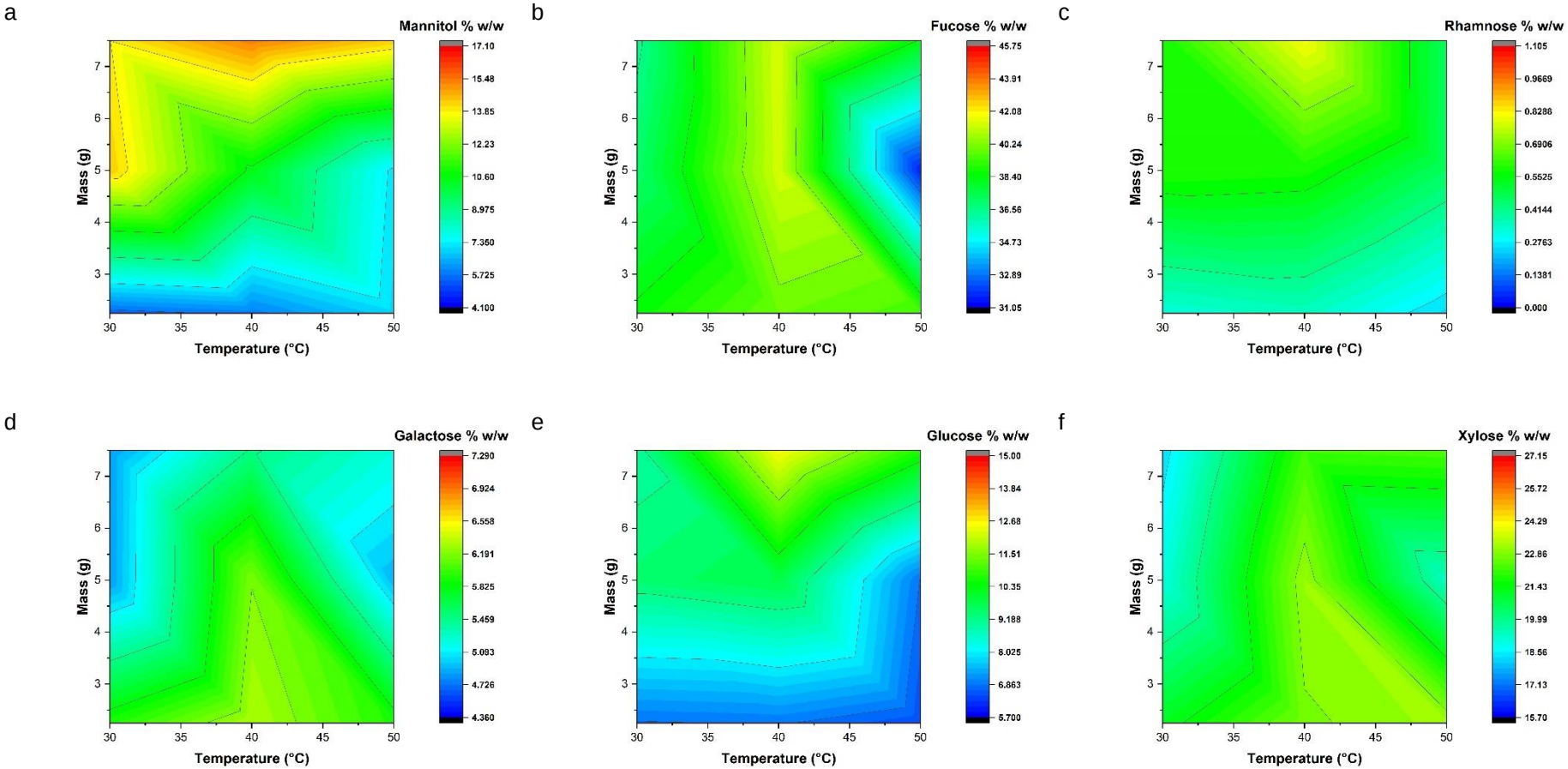

Fig 6-9. Comparison of the monosaccharide profiles of fucoidan extracts in different temperature and initial biomass conditions. A) Mannitol content; B) Fucose content; C) Rhamnose content; D) Galactose content; E) Glucose content; F) Xylose content.

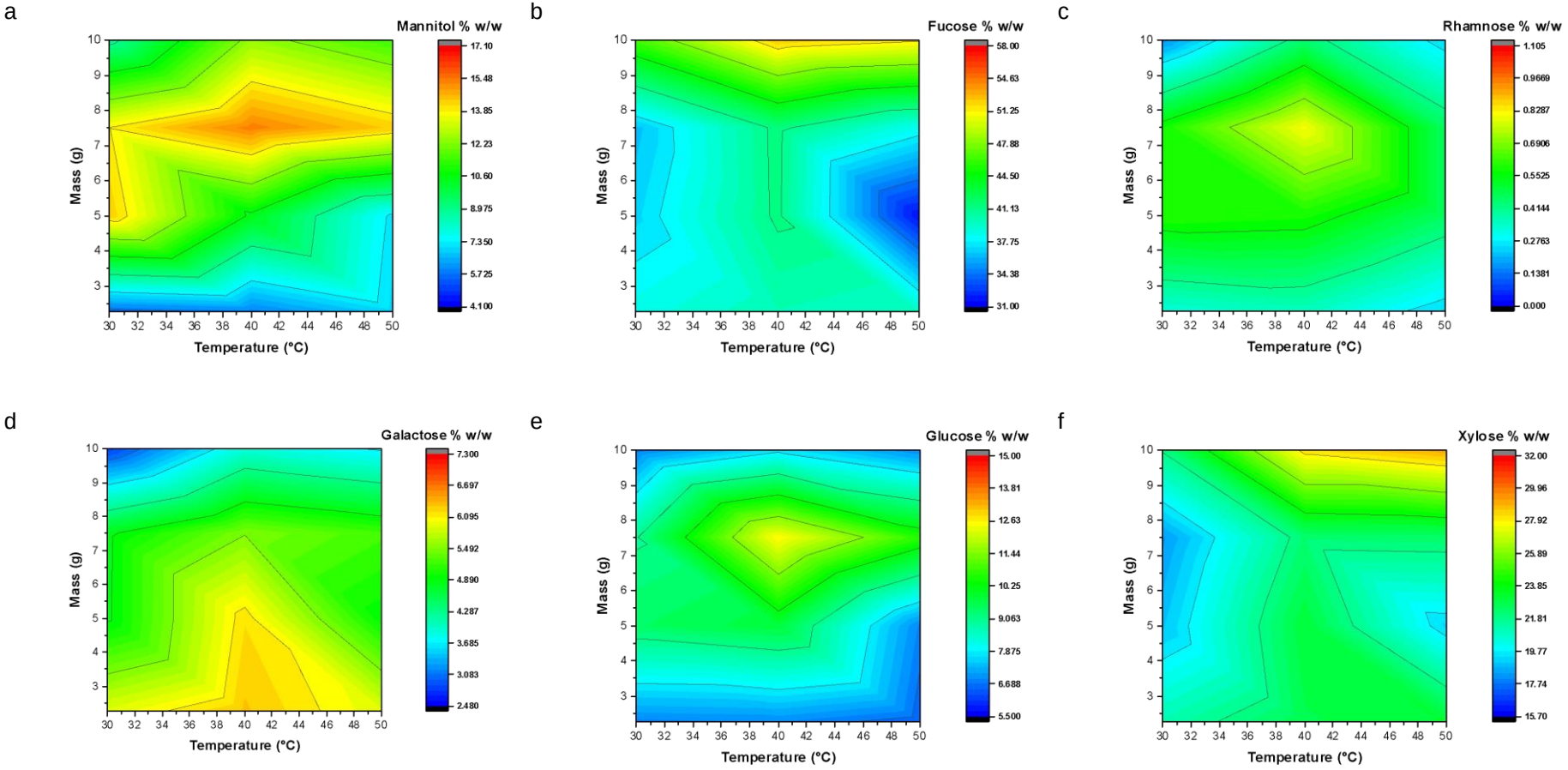

Fig 6-10. Comparison of the monosaccharide profiles of fucoidan extracts of the expanded domain of different temperature and initial biomass conditions.

A) Mannitol content; B) Fucose content; C) Rhamnose content; D) Galactose content; E) Glucose content; F) Xylose content.

A breakdown in the monosaccharide profile allowed the observation that fucose content at 30, 40, and 50°C showed statistically significant differences of initial biomass condition of 10.0 g with the rest of the initial conditions (2.25 g, 5.00 g, and 7.50 g) in all temperatures tested. At 30°C, 10.0 g condition, extracts showed a fucose content of 46.3% g Fucose/g Fucoidan, at 40°C the fucose content was around 52.3% g Fucose/g Fucoidan, and finally at 50°C the fucose concentration was 51.4% g Fucose/g Fucoidan (**Fig 6-11**). Fucose content at 10.0 g of initial biomass did not exhibit statistically significant differences ($p < 0.05$) across the different temperature conditions analysed. Kostas et al. (2017) reported fucose content in their *L. digitata* extracts of 42.5±2.2% g Fucose/g Fucoidan; differently, Foley et al. (2011) reported a fucose content in their *A. nodosum* fucoidan extracts similar to the values reported in this work, 52.1% g Fucose/g Fucoidan. Xylose content did not show statistically significant differences ($p < 0.05$) between all conditions tested, with a notorious trend of higher concentrations at higher temperatures. On the other hand, Foley et al. (2011) reported a lower concentration of xylose, 16.5% g Xylose/g Fucoidan, but higher than the values reported by Kostas et al. (2017), this might be due to the species used in all studies, Foley et al. (2011) and this work used *A. nodosum*, while Kostas et al. (2017) studied *L. digitata* fucoidan extracts. Finally, mannitol (**Fig 6-12**) did not show statistically significant differences between all the conditions tested and glucose content at 50°C using 7.50 g of initial biomass showed differences with the rest of the conditions analysed, with a concentration of 10.7% g Glucose/g Fucoidan. All the remaining monosaccharide content comparison graphs of the monosaccharide profiles can be observed in **Appendix E.** Considering all the variables analysed, i.e., robustness in the monosaccharide profile in all the extraction conditions, use of a mild extraction process using a biodegradable chemical, and a highest recovery yield than other reports, the selected extractions conditions were 7.50 g initial biomass, at 50°C using citric acid at pH 5.5.

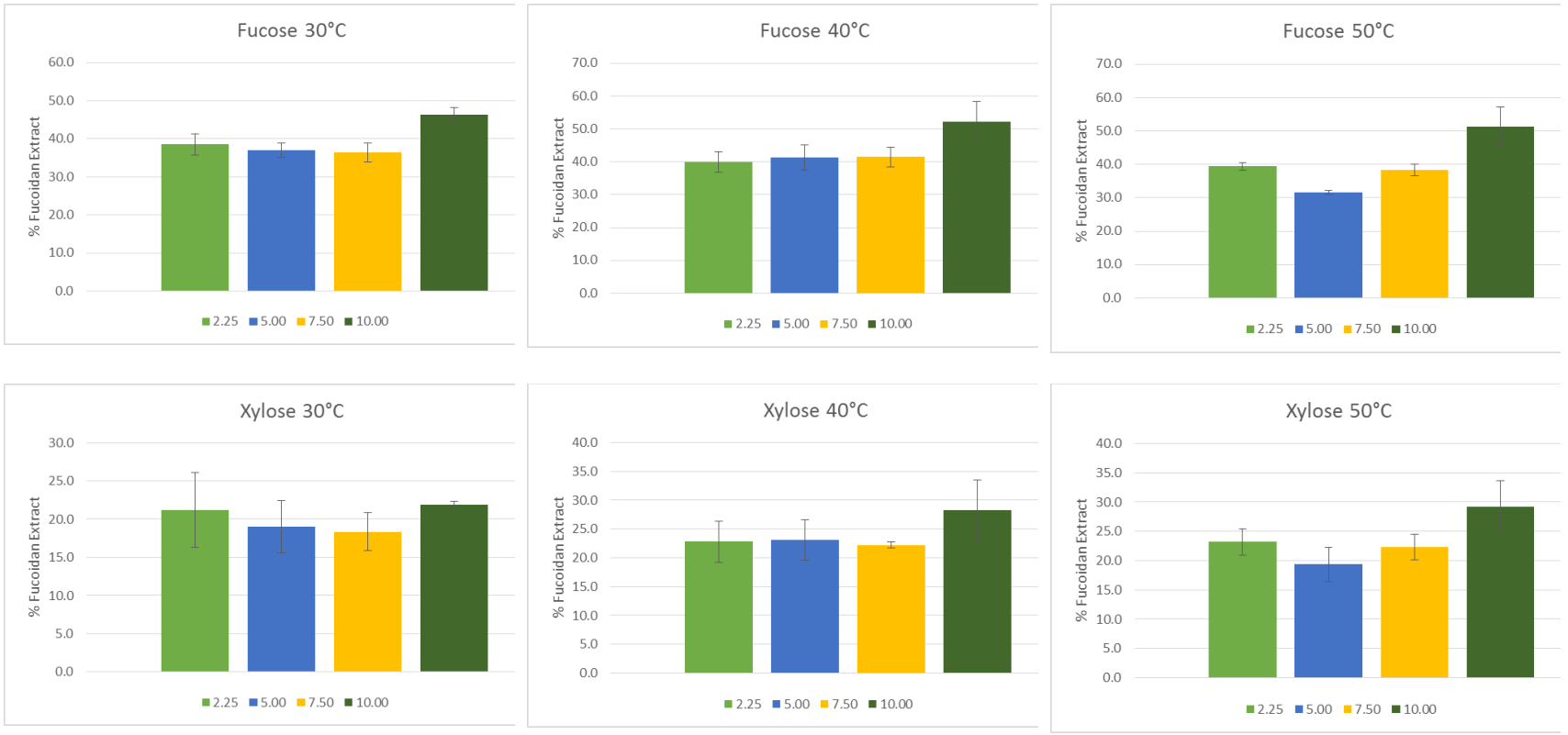

Fig 6-11. Comparison of the fucose and xylose content in the different conditions analysed for fucoidan extracts using citric acid pH 5.5.

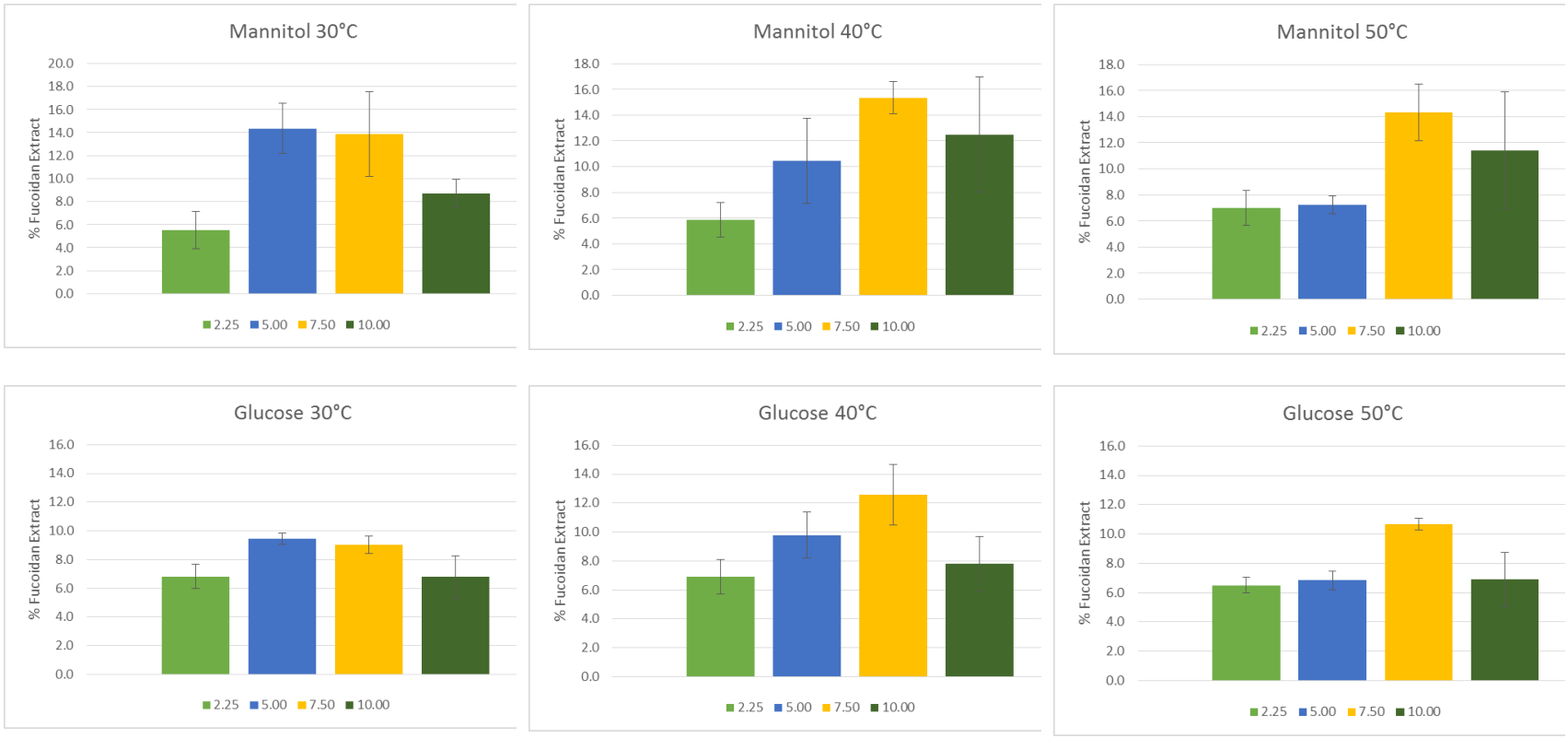

Fig 6-12. Comparison of the mannitol and glucose content in the different conditions analysed for fucoidan extracts using citric acid pH 5.5.

3. Conclusions

The main objective of this chapter was to develop a green extraction process for fucoidan that did not jeopardise the subsequent extraction yields in the cascading sequence, e.g., alginate, polyphenols, and proteins for a multi-product biorefinery concept.

In order to achieve this, two different extraction approaches comparing the use of citric acid, HCl, and H_2SO_4 were considered. A comparison of the recovery yields was performed using two different extraction methods, an extraction at 0.2 M acid concentration and the second with an extraction using acid solutions at pH 5.5.

Comparison of both methods showed that the acidic treatment of *A. nodosum* using citric acid at pH 5.5 was the most effective extraction method to obtain high recovery yields of fucoidan and alginate that are less hydrolysed according to qualitative assessments, with recovery yields of 8.92±0.27% DW and 35.91±5.95% DW, respectively and with a sulphate content of 3.01±0.12 mg Sulphate/g Fucoidan.

After selected the best extraction method a DoE-based approach was used to improve the extraction performance of the process varying the conditions of the method. Thus, the optimum extraction process conditions were 10.0 g of initial biomass, 50°C, pH 5.5 for 2 hours, with an improved yield of 11.92% DW, increasing a 33% the amount of fucoidan extracted when compared to the initial conditions of the process. This improved protocol was further confirmed by characterisation of the monosaccharide profile of the extracts to confirm the mildness of the process, reflected in the non-significant statistical differences of the monosaccharides content between the different concentration, meaning the process did not hydrolyse the fucoidan extracted and confirming a high purity of the extracts of 75.57 – 81.42 % g Pure Fucoidan/g Raw Extract. All these results confirmed the development of a new greener extraction process to obtain fucoidan with minimal impurities during the extraction and not affecting the following extraction steps in the cascading sequence of a multi-product seaweed biorefinery.

Chapter 7: Final assessment of the technical, economic, and environmental performance of an optimised cascading sequence following green chemistry principles.

1. Introduction

One of the grand challenges in sustainability is the fast evaluation of new technologies that help mitigate the environmental emergency we are facing; by means of devising new biorefinery concepts that allow us to move towards a bio-based economy. The need for more sustainable processes in all economic areas has been advised as a result of the increased global environmental problems. The combination of the technical, economic and environmental dimension has been recommended to improve the learning effects in prospective technology assessment and to comply with the Triple Bottom Line guidelines of sustainability (Thomassen et al., 2020). In **Chapter 4** an initial performance assessment of a multi-product third generation biorefinery using green technologies was performed. Though this approach supports the early bioprocess decisions by identifying process, economic, and environmental hotspots and to provide further optimisation in following chapters, the main obstacle of this method was the use of second-hand data, and consequently the difficulties to obtain reliable data, due to the lack of background information of these new processes (Julio et al., 2017). The iterative nature of the LCA framework (International Organization for Standardization, 2006) and the evaluation of the technology readiness level of new processes (Buyle et al., 2019), propose that the repetition of the technical, economic, and environmental studies after their respective hotspots had been identified and resolved is necessary to confirm the robustness and viability of a new technology pathway developed. The overall goal of this chapter was to reassess the cascading sequence built in **Chapter 4**, and further optimised in **Chapter 5** and **6** to develop a framework to conduct TEA and LCA combined with first-hand data results to assess the implications of the chosen technology pathway on the economic

viability and environmental impact metrics when compared to the early-design model of the cascading sequence.

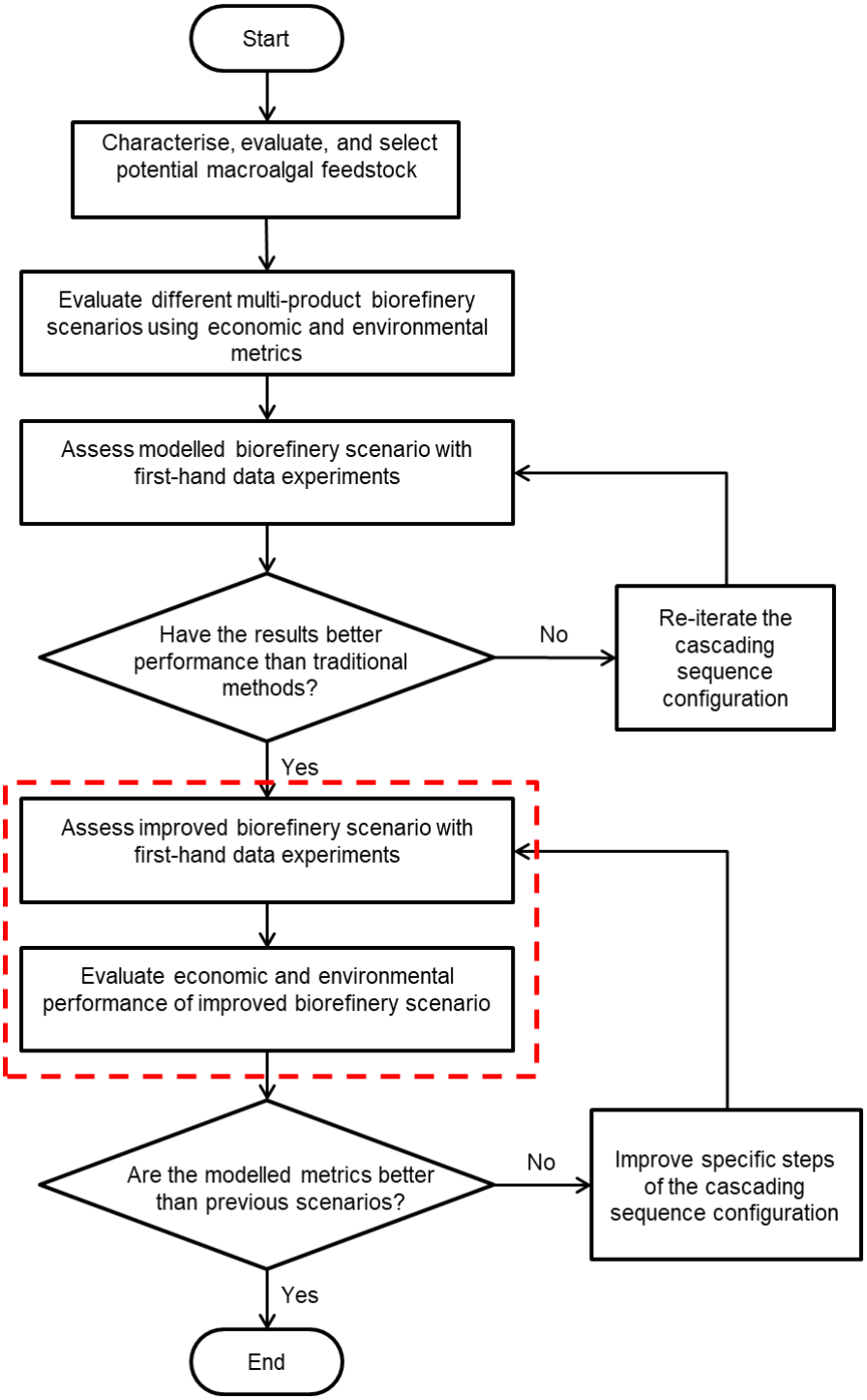

Fig 7-1. Proposed overall methodology for the development of a multi-product macroalgal biorefinery. The red-dashed box highlights the portion covered in this chapter.

2. Results and discussion

2.1. Technical feasibility trial of the integrated optimised cascading sequence

The section of the project covered in this chapter can be observed in **Fig 7-1**. Completed all the optimisation experiments to improve the recovery of fucoidan and polyphenols in **Chapter 5** and **6**, and collaterally aiding the recovery of alginate, the new version of the green chemistry-compliant biorefinery cascading sequence was assembled. The extraction conditions of the cascading sequence are summarised in **Table 7-1**.

Table 7-1. Summary of the recovery conditions in the updated biorefinery cascading sequence.

Compound	Solid-liquid ratio	Method	Time
Fucoidan	5%	Citric acid solution pH 5.5 at 50°C, mixing at 200 rpm, followed by ethanol precipitation.	2 h
Alginate	3.3%	Na_2CO_3 2% w/v solution at 45°C, mixing at 200 rpm, followed by ethanol precipitation	2 h
Polyphenol	2%	ATPS composed of PEG 2000-potassium phosphate buffer pH 7.5 (27:4 %w/w) at room T	1.5 h
Protein	0.02%	ATPS composed of methanol-K_3PO_4 (20:30 %w/w) at room T.	1.5 h

The cascading order selected at the end of **Chapter 4**, observed in **Fig 7-1**, was maintained for this feasibility trial, thus fucoidan, alginate, polyphenols, and protein were sequentially extracted. Consequently, the recovery yields and process performance of the high-value compounds obtained with the optimised cascading sequence were compared against the original cascading extraction train (**Fig 7-2**).

The improved extraction process of fucoidan and alginate inserted in the cascading sequence is observed in **Fig 7-3a**, fucoidan recovery was 11.92% DW in *A. nodosum* compared to the original cascading extraction stage (**Fig 4-26b**) that recovered 2.32% DW of fucoidan; while alginate yield was 35.91% DW compared against the original

cascading stage in **Fig 4-26b** that recovered 2.67% DW. Due to the current events of the COVID-19 global pandemic and the following lockdown measures undertaken at the time, it was not possible to quantify the amount of carbohydrates, polyphenols, and proteins co-extracted as impurities, as seen in **Fig 4-26** to **4-28**, in the respective previous and/or subsequent steps of the improved cascading sequence, hence in **Fig 7-3** these "impurities" fractions were merged into the corresponding "not recovered" fraction, and the compound is considered just as not extracted by this method. Thus, impurities/not recovered carbohydrates accumulate up to 52.17% DW. Comparing these results with the original cascading sequence (**Fig 4-26**) the optimised fucoidan cascading process had a 2-fold increase in the recovery; additionally, alginate recovery in the improved sequence was 9.4 times higher when compared to the original extraction process. Fucoidan recovery obtained with the updated cascading sequence was higher than previous reports, Lorbeer et al. (2015) reported a recovery yield of 3.21% DW from dried and milled *E. radiata*, while Gomaa et al. (2018) showed a recovery of 10.1±0.2% DW in *S. latifolium* milled and dried. On the other hand, alginate recovery, was lower than reported, 38.2% DW and 44.26±1.5% DW, by Lorbeer et al. (2015) in *E. radiata* and Gomaa et al. (2018) in *S. latifolium*, respectively. Although alginate recovery is lower than those studies, the process was maintained because published literature about alginate extraction using different methods range between 18% DW up to 44% DW (Gomaa et al., 2018; Hifney et al., 2016; Yuan and Macquarrie, 2015b; Zubia et al., 2008).

a)

b)

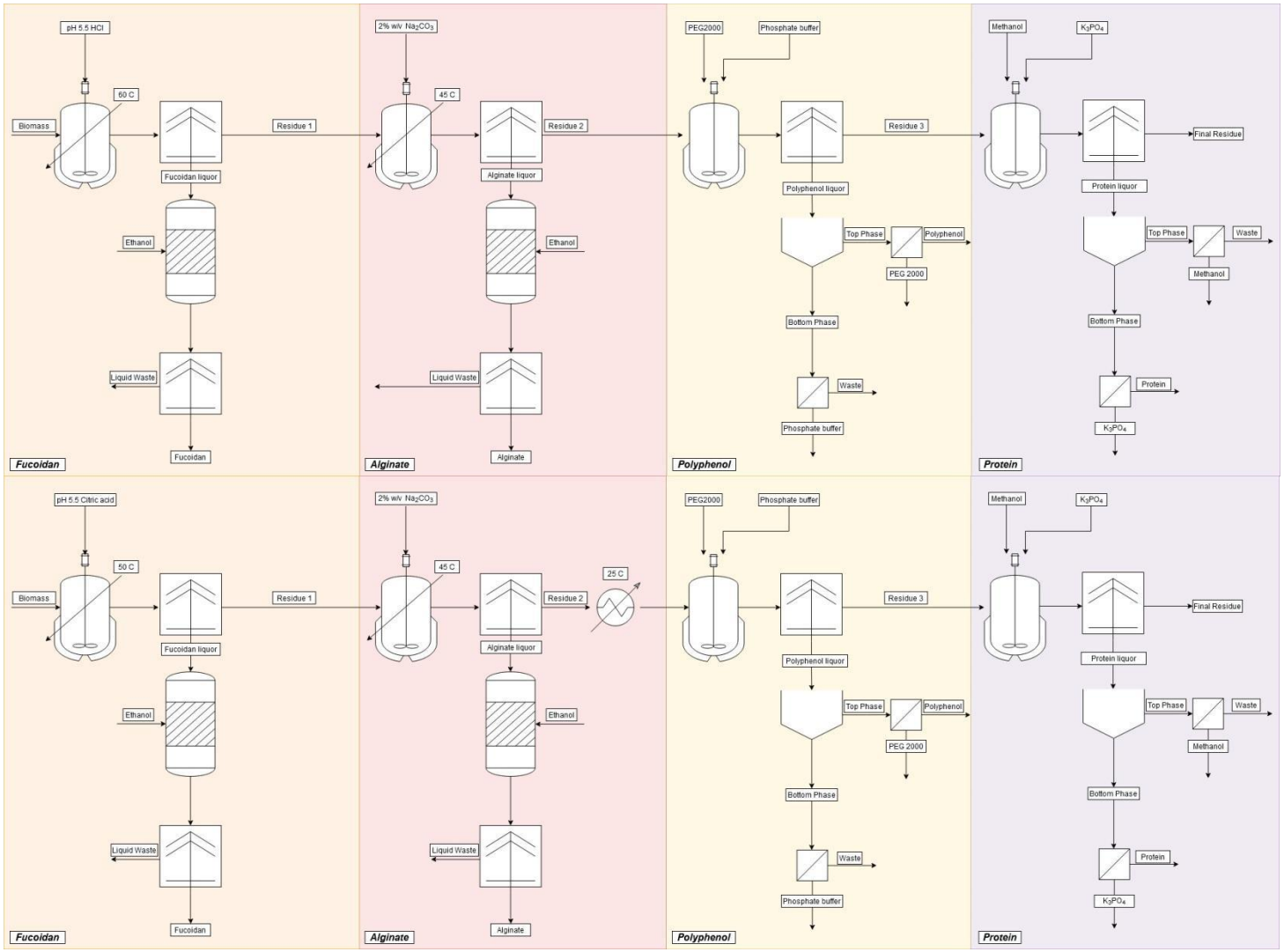

Fig 7-2. Process flowsheet of the newly optimised cascading sequence for *A. nodosum* compared with the original cascading sequence at the end of **Chapter 4**. a) Cascading sequence after technical assessment in **Chapter 4**; b) Re-iterated cascading sequence after optimisation steps.

The optimised cascading ATPS extraction process performance for polyphenols is shown in **Fig 7-3b**. In total, 87.8% of total polyphenol content (TPoC) was recovered, analogous to 4.06% DW, while 12.2% TPoC was either lost as impurities or not recovered, using the total polyphenol concentration in obtained in **Chapter 3** as a benchmark (**Table 3-1**). Comparing this process with the original cascading step analysed in **Chapter 4** (**Fig 4-27b**), the improved cascading recovery process had an 18-fold increase; these results were also higher than reported in literature, Xavier et al. (2017) reported polyphenols recovery of 1.89% DW from wood chips, 2.15 times lower than results obtained in this chapter.

Lastly, protein recovery performance on the optimised cascading sequence (**Fig 7-3c**) recovered 33.35% total protein content (TPrC) (3.78% DW), whereas 66.65% (7.55% DW) was co-extracted as impurities in the previous steps or not recovered at all. When this extraction stage was compared with the original cascading protein step (4.28% DW) from **Chapter 4** (**Fig 4-28b**); it was observed that the improved cascading process for protein recovery exhibited a 0.12-fold lower content, the difference between yields is statistically significant ($p < 0.05$). Albeit these results were lower than the original cascading process it was satisfactory for the further techno-economic analysis and life cycle assessment considering the improved recovery yields of the previous stages, improving the overall economic performance of the process, observed in **Section 2.2** from this **Chapter**.

Having completed the technical feasibility trials of the new iteration of the cascading sequence biorefinery, the process robustness was evaluated, and first-hand data was obtained to update the values of the process flowsheet produced in **Chapter 4** to re-iterate the TEA and LCA models to re-check and validate the performance of the multi-product biorefinery concept based in green chemistry principles (**Fig 7-1**).

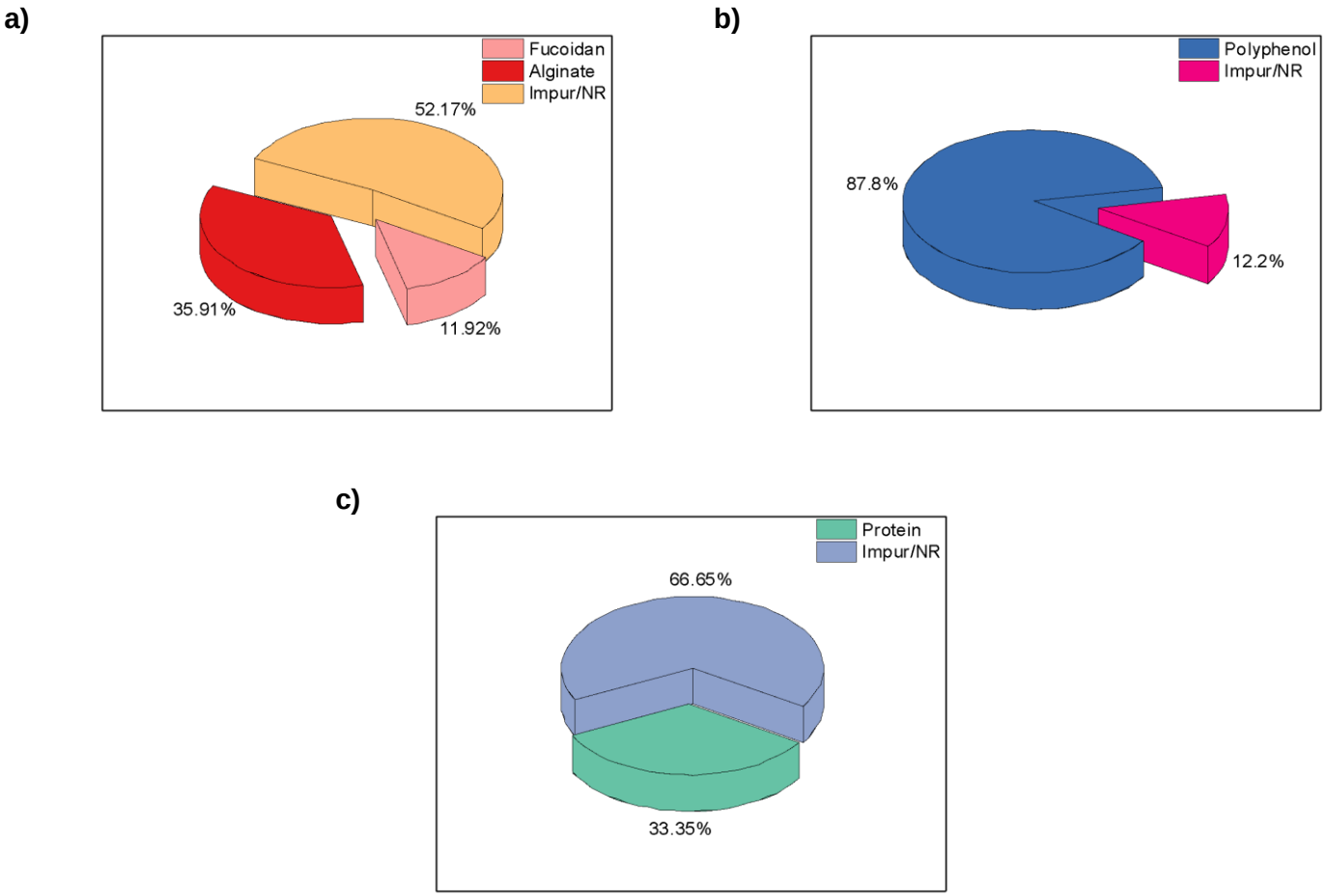

Fig 7-3. Improved extraction process performance of a) fucoidan and alginate b) polyphenols and c) proteins from *A. nodosum* indicating recovery yields, and fraction of carbohydrates, polyphenols or proteins not extracted or lost as impurities on the previous or subsequent cascading steps.

2.2. Techno-economic analysis of the optimised green chemistry-based biorefinery scenario

A list of the key assumptions used to build the TEA can be seen in **Appendix A**. The total CAPEX (**Table 7-2**) breakdown across the cascading sequence steps of the updated *Green Chem* biorefining scenario can be observed in **Fig 7-4**, where the most expensive steps were fucoidan and alginate, with figures rounding the £5.30 and £5.81 million respectively; while polyphenol and protein extraction stages capital expenditure was around £1.53 and £1.74 million respectively, the breakdown of this stages can be seen in **Table B-4** in **Appendix B**. the low initial investment in the two latter extraction platforms was due to the use of low pressure, room temperature equipment, with agitation tanks, settling tanks, and centrifuges being the most commonly used equipment, in addition to the lowest utilities costs used by these stages.

Table 7-2. Total capital investment of the updated biorefinery scenario based on a system processing 1,000 metric tonnes per annum using green chemistry techniques.

Capital investment	Unit	*Green Chem v2*
Contingency	%	10
Lang factor	-	3.00
Total equipment purchase cost	£	15,822,507
Fixed capital investment	£	47,467,520
Working capital	£	2,373,376
Total capital investment	**£**	**49,840,896**

Table 7-3. Direct and indirect costs in the updated biorefinery using green chemistry principles.

Item	Unit	*Green Chem v2*
Direct costs		
Raw materials costs	£/y	682,363
Utilities costs	£/y	8,674
Labour costs	£/y	2,976,000
Total direct costs	**£/y**	**3,667,038**
Indirect costs		
Maintenance	£/y	4,746,752
Local taxes	£/y	949,350
Insurance	£/y	474,675
Depreciation	£/y	4,746,752
Total indirect costs	£/y	**10,917,530**
Total costs	£/y	**14,584,567**
CoG/kg biomass	£	0.05
Production cost/kg biomass	£	0.01

Updated *Green Chem* scenario total CAPEX was higher than the first iteration of the cascading sequence modelled in **Chapter 4** (£29.8 million), due to higher volumes processed in the optimised extraction fucoidan, alginate and polyphenol steps; on the other hand, CAPEX of this scenario was still lower than the other technology pathways analysed in **Chapter 4** (*Solvent-based*: £177 million, and *Novel Tech*: £244 million), and biorefinery concepts from the lignocellulosic industry (Kazi et al., 2010), with total CAPEX of this concepts around £244 million, hence the updated *Green Chem* scenario exhibited a ~10 – 3-fold decrease of the overall initial expenditure of these case studies.

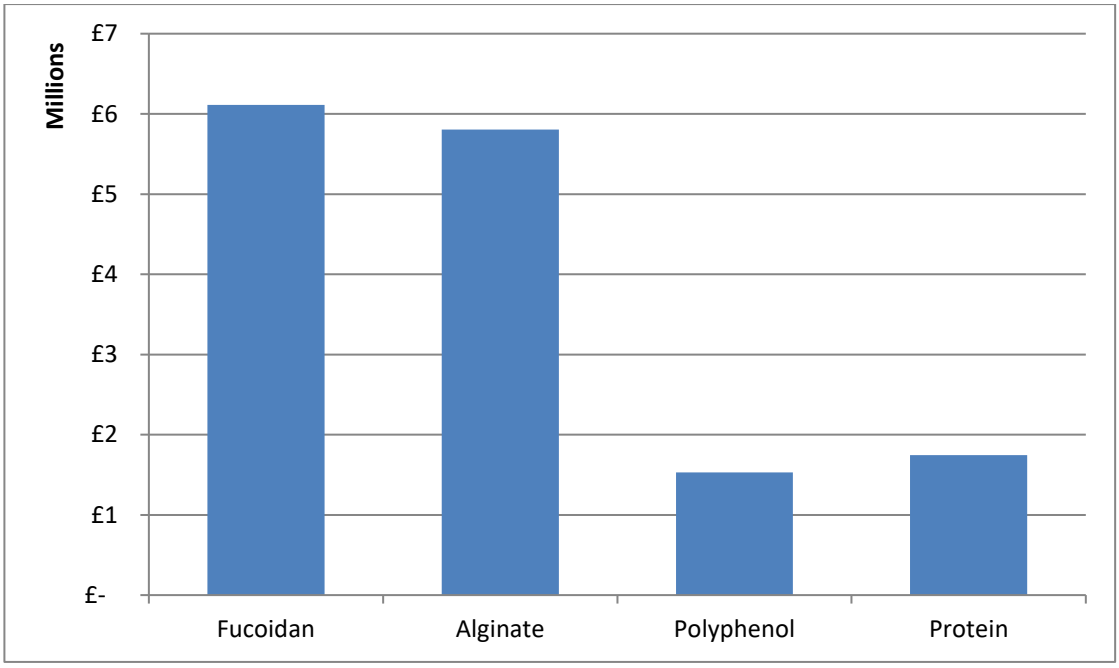

Fig 7-4. Total capital investment categorisation of the updated green chemistry biorefinery concept using *A. nodosum* as feedstock.

The breakdown of the operation costs for the enhanced *Green Chem* cascading sequence is in **Fig 7-5**. Indirect costs, defined as maintenance, taxes, insurance and depreciation were the main contributors of total OPEX with a 76% of total input, while direct costs (raw materials, utilities, and labour) covered the remaining 24%. The display of the items considered in the calculation of the operation costs can be observed in **Table 7-3**. When analysing the direct costs, it is noted that the most expensive item was labour with £2,976,000, this figure was the highest due to the parameters considered for the correct operation of the facility at all stages and all the supervisory personnel, as well as QC/QA, utilities costs had the smallest contribution to the direct costs with £8,674 due to the smaller energy requirements in all stages of the cascading sequence, and finally raw materials costs with £682,363.

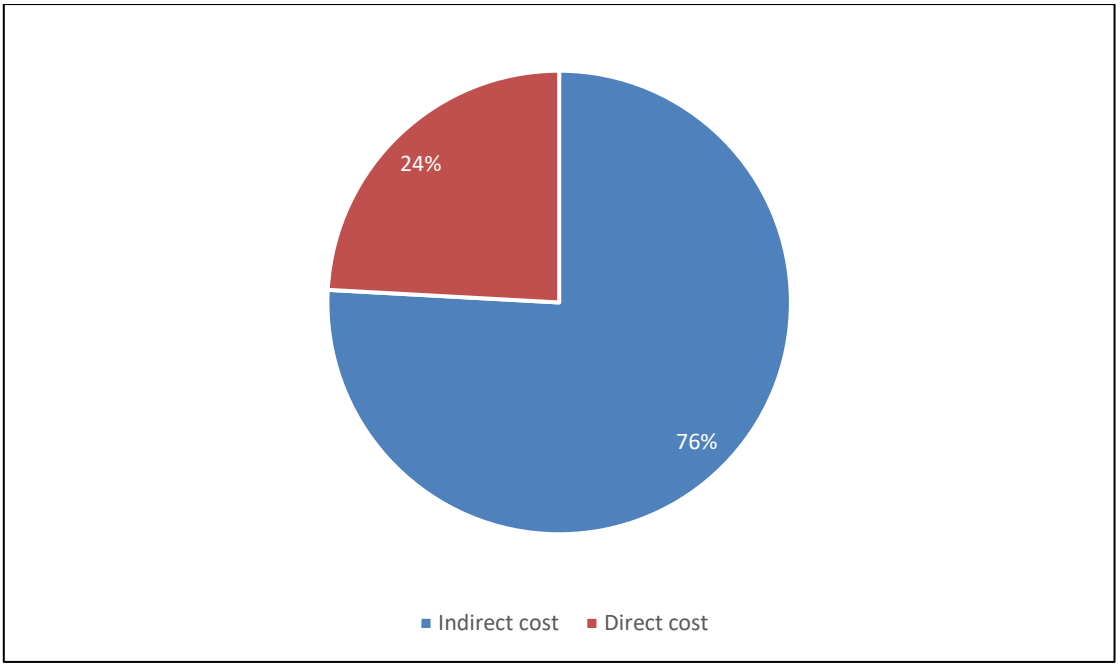

Fig 7-5. Analysis of the direct and indirect costs of the optimised biorefinery scenario using green chemistry as the primary strategy on *A. nodosum* as model feedstock.

The operation costs across the different steps in the cascading sequence for the improved *Green Chem* cascading sequence biorefinery scenario can be observed in **Fig 7-6**. Following the trend examined in **Fig 7-4**, the most expensive extraction stages were fucoidan and alginate. In the case of indirect costs these were derived from the FCI, thus its breakdown through the biorefining process is proportional to the CAPEX breakdown (**Fig 7-4**); on the other hand, direct costs were influenced by the purchase of extraction of extraction reagents and phase-forming components, energy use, and labour. Protein extraction process showed the highest direct costs (£1.1 million), due to the raw materials needed for the extraction of it (£370,428); a labour cost of £744,000, and utilities of £549. The OPEX of the remaining processing steps in the cascading sequence were £873,217, £907,433, and £771,410 for fucoidan, alginate, and polyphenol respectively.

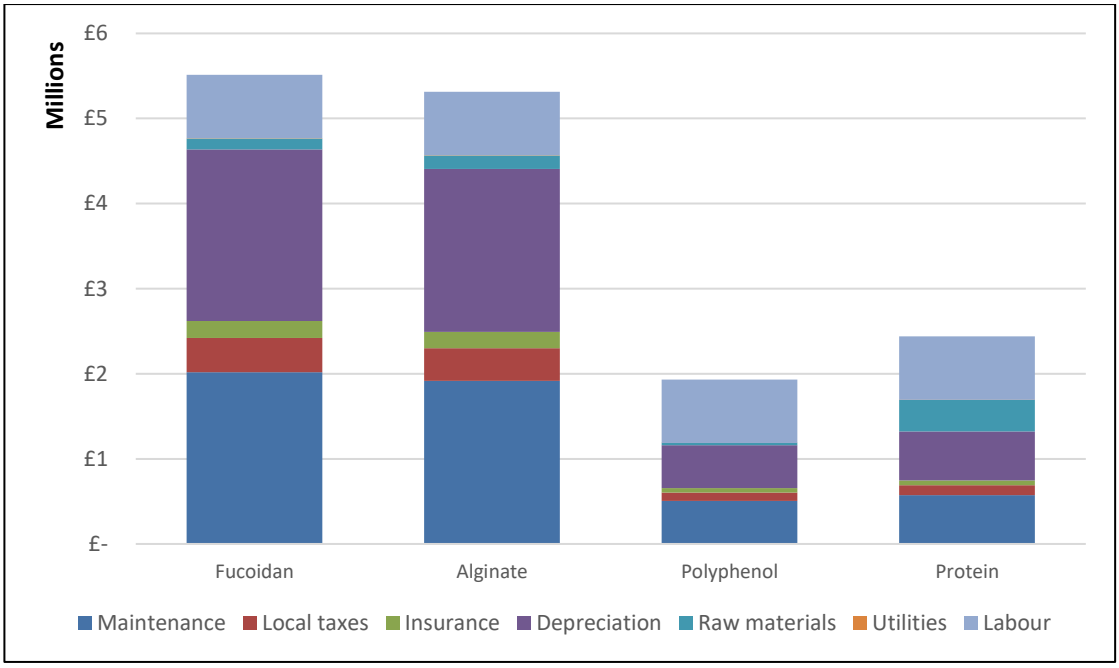

Fig 7-6. Breakdown of the total operation costs across the sequential extraction steps in the optimised biorefinery scenario based in the use of green chemistry for *A. nodosum* as feedstock.

The breakdown for the CoG (**Table 7-3**) is observed in **Fig 7-7**. The main factors affecting the CoG/batch was maintenance and depreciation, both with a 32.5% of contribution, with a value of £4.7 million, followed by labour, with a 20.4% of contribution (3.0 million), taxes (£949,350) and raw materials (£682,363) were next with 6.5% and 4.7% of contribution, respectively. The final contributions were insurance (3.3%, 474,675), and utilities (0.1%, £8,674). With these values calculated the CoG/kg for the optimised cascading sequence was £0.05, and the production costs were £0.01/kg, rising as the cheapest option of all the scenarios analysed in this study. Huang et al. (2016) reported production costs of $0.59/L for biodiesel produced from sugarcane, and $0.4/L for bioethanol obtained from the same feedstock. These values are higher than the results for this scenario, highlighting this cascading sequence as a promising candidate for the development of third generation biorefineries specialised in high-value products.

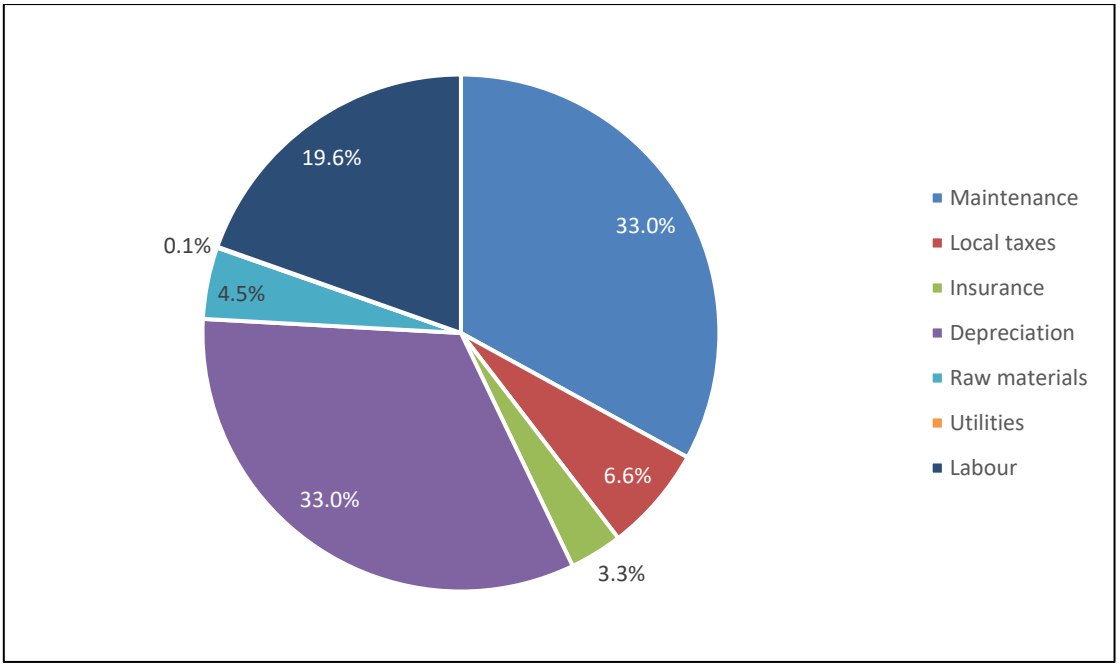

Fig 7-7. Analysis of the cost of goods of the optimised green chemistry biorefining cascading sequence scenario using *A. nodosum* as a feedstock.

In **Table 7-3** are summarised the direct and indirect costs for this new iteration of the green chemistry-compliant biorefinery. Raw materials costs in this scenario were lower than the original scenario (**Table 4-3**) with a difference of £246,137 due to the increased processing volumes of the original iteration. Labour costs were lower because one operation stage was removed from the previous iteration (fucoxanthin recovery stage); hence, labour was estimated considering two production operators per section, with four extraction sections considered, one production supervisor in each section, and with QC/QA personnel in each step. Utilities were 3.7 times more expensive in this new iteration than the original *Green Chem* biorefinery. This was due to the biggest equipment needed for the re-iterated volumes used in the fucoidan and alginate stages. The OPEX to CAPEX ratio for the re-iterated technology pathway was 0.29, smaller than the original version of the *Green Chem* (0.38). This decrease could be attributed to the increase in the total capital investment and indirect costs of this cascading sequence.

The CAPEX for the re-iterated *Green Chem* scenario 1.6 times higher when compared with the original *Green Chem* scenario (**Fig 7-8**), on the other hand *Solvent-based*

scenario was 3.6 times higher than the new iteration, and *Novel Tech* scenario was 4.9 times higher than the new scenario. The higher initial investment of the optimised *Green Chem* scenario when compared with the original model was due to, as explained previously, the higher volumes processed in the fucoidan and alginate stages. The extraction of fucoidan and alginate in the original and the re-iterated scenario considered a solid-liquid ratio for the extraction of 5% and because in the original cascading setup the fucoidan and alginate stages were allocated in the final portion of the operation, this meant a smaller amount of the initial feedstock (79.8% of the initial biomass) was entering into the process, hence smaller volumes were utilised in the original sequence; on the other hand the re-iterated cascading sequence allocated the fucoidan and alginate stages at the beginning of the process, this meant the 100% of the initial biomass was fed into the process, therefore bigger volumes were utilised and this turned into bigger pieces of equipment used to process and extract *A. nodosum*. The utilities costs associated to run this optimised scenario along the increased indirect costs elevated the total OPEX of *Green Chem v2* scenario, relative to the original iteration of this scenario. The smaller volumes and phase-forming components used in the ATPS stages, namely polyphenol and protein, kept the OPEX lower than *Novel Tech* and *Solvent-based* scenarios. The optimised cascading sequence presented the second highest total revenues of all the scenarios analysed (**Table 7-4**) behind *Novel Tech* scenario, this increased profitability of the process was due to the increased recovery yields of the fucoidan and polyphenol extraction stages, with around £60 million and £20 million respectively. The return of investment of this re-iterated scenario was 81.77%, highlighting the economic viability of this model.

Table 7-4. Total yearly sales revenue of the cascading scenario analysed for this project.

Sales revenue	Unit	*Green Chem v2*	Average price/kg
Fucoidan	£/y	59,758,211	459.55
Alginate	£/y	1,960,686	5.01
Polyphenol	£/y	20,404,020	459.55
Protein	£/y	9,475,085	229.78
Total sales	**£/y**	**91,598,002**	**-**

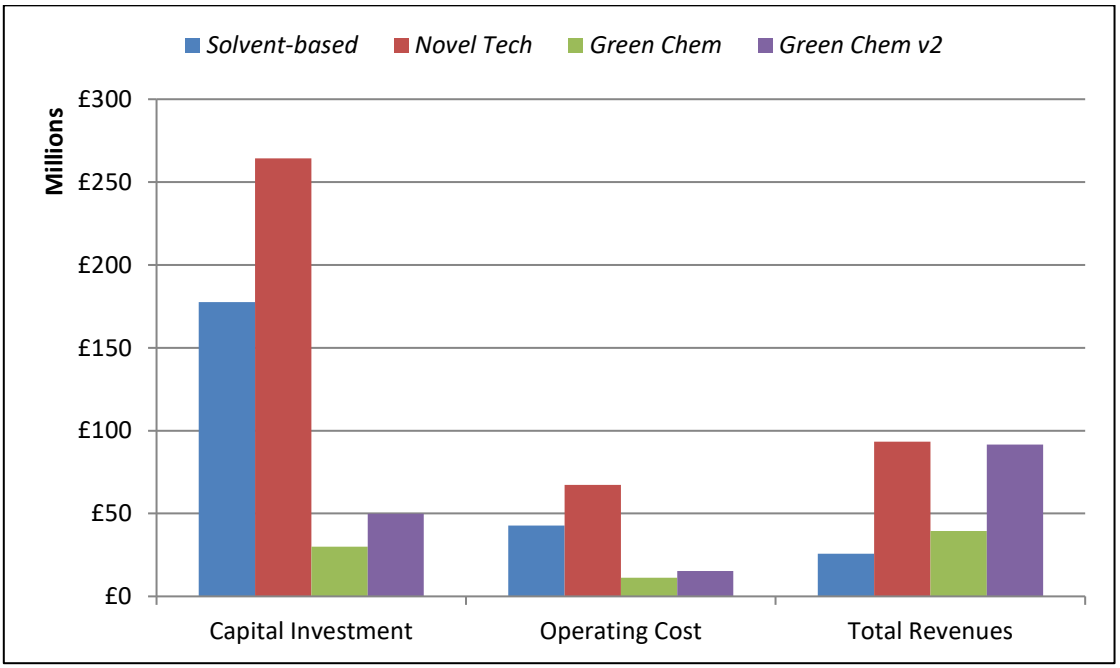

Fig 7-8. Economic metrics of the different biorefinery cascading sequences analysed in this project using *A. nodosum* as a model feedstock.

The production costs of process 1 kg of *A. nodosum* biomass utilised in the improved *Green Chem* scenario was £0.01, the lowest of all scenarios analysed in this project (**Table 4-3**), with an internal rate of return of 82.1% (**Fig 7-9**), emphasising the economic possibility of this biorefinery technology pathway.

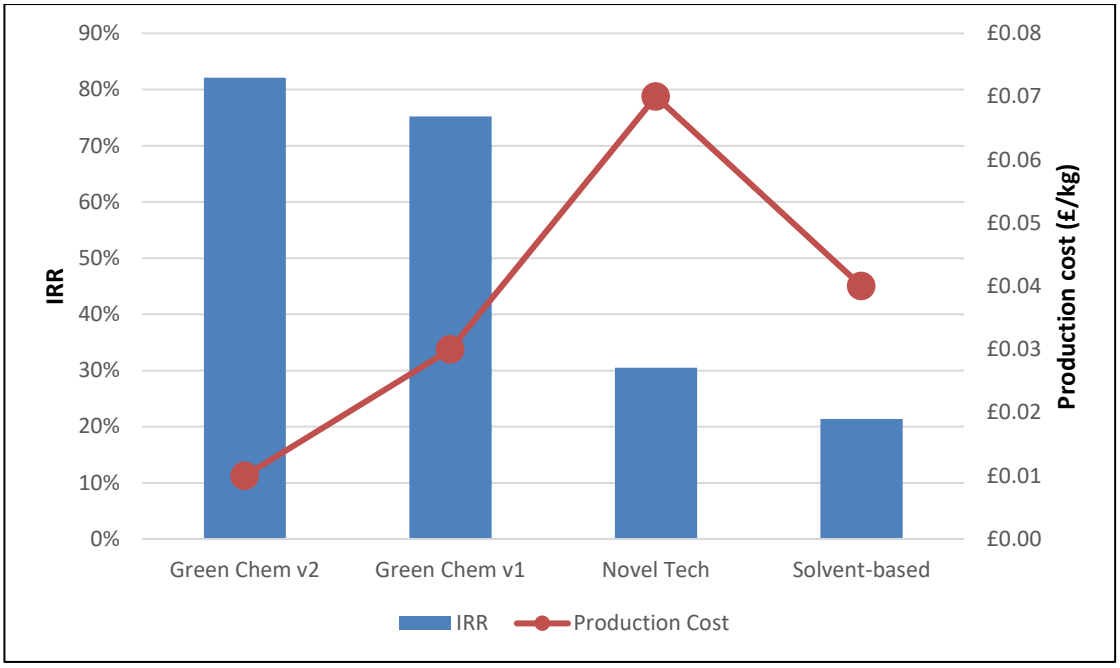

Fig 7-9. Internal rate of return (IRR) and production costs per kg of biomass of the different technology pathway assessed in this project using *A. nodosum* as feedstock.

The discounted cumulative cash flow in **Fig 7-10** showed that the improved *Green Chem* cascading sequence had the same break-even point of the original *Green Chem* scenario occurring at the first year of operation. The cash flow of the improved scenario at year 1 was £41,225,645 and a total cash flow after 10 years of operation of £579 million, with a NPV of £9,343,992. Finally, after evaluating all these indicators it was observed that the optimised cascading sequence was the most profitable scenario from all scenarios analysed in this project.

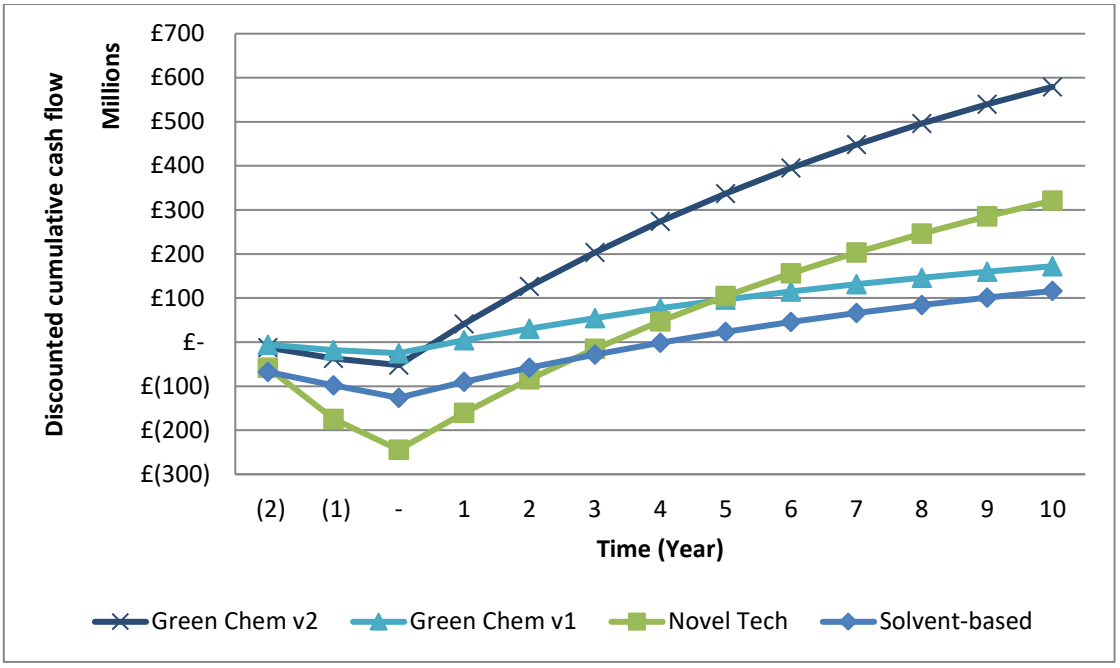

Fig 7-10. Discounted cumulative cash flow of all biorefinery scenarios evaluated in this project.

2.3. Life cycle assessment of the optimised green chemistry-based biorefinery scenario

Based on the inputs from the process flowsheet re-iterated with the first-hand data obtained in the previous chapters of this project (**Fig 7-1**), the LCI inputs were obtained (**Table 7-5**). LCA was assessed with LCI using SimaPro v.8.5.2 and ReCiPe v1.13 was used as an impact assessment method. Following the impact assessment performed in **Section 3.3** from **Chapter 4**, seven different environmental indicators were evaluated and compared against the three previous scenarios. The functional unit was kept as 1 kg of biomass of *A. nodosum* used as input in the cascading sequence.

Table 7-5. Life cycle inventory data used in each stage of the updated cascading sequence per batch.

Extraction stage	Materials/Utilities	Ecoinvent process	Unit	Amount
Fucoidan	Citric acid	Citric acid {GLO} | market for | Cut-off, S	kg	788
	Water	Water, ultrapure {GLO} | market for | Cut-off, S	m^3	68.5
	Ethanol	Ethanol, without water, in 99.7% solution state, from ethylene {GLO} | market for | Cut-off, S	m^3	143.8
	Electricity	Electricity, medium voltage {GB} | market for | Cut-off, S	kWh	1458.36
Alginate	Sodium carbonate	Neutralising agent, sodium hydroxide equivalent {GLO} | soda ash, dense, generic market for neutralising agent | Cut-off, S	kg	2,285
	Water	Water, ultrapure {GLO} | market for | Cut-off, S	m^3	91.4
	Ethanol	Ethanol, without water, in 99.7% solution state, from ethylene {GLO} | market for | Cut-off, S	m^3	182.8
	Electricity	Electricity, medium voltage {GB} | market for | Cut-off, S	kWh	1458.21
Polyphenol	PEG 2000	Ethylene glycol {GLO} | market for | Cut-off, S	kg	24,120
	K_2HPO_4	Potassium hydroxide {GLO} | market for | Cut-off, S	kg	2,383
	KH_2PO_4	Phosphoric acid, industrial grade, without water, in 85% solution state {GLO} | market for | Cut-off, S	kg	1,179
	Water*	Water, ultrapure {GLO} | market for | Cut-off, S	kg	61,639
	Electricity	Electricity, medium voltage {GB} | market for | Cut-off, S	kWh	207.5
Protein	Methanol*	Methanol {GLO} | market for | Cut-off, S	kg	164,726
	K_3PO_4	Potassium hydroxide {GLO} | market for | Cut-off, S Phosphoric acid, industrial grade, without water, in 85% solution state {GLO} | market for | Cut-off, S	kg	247,089
	Water*	Water, ultrapure {GLO} | market for | Cut-off, S	kg	823,630
	Electricity	Electricity, medium voltage {GB} | market for | Cut-off, S	kWh	207.5

*: ATPS phase-forming components are usually denoted in mass quantities.

In **Fig 7-11** the process contributions for the updated cascading sequence biorefinery process can be observed. Climate change potential of this scenario produced a total

impact of 16.3 kg CO_2-eq., where the major contributors were fucoidan stage, with 8.16 kg CO_2-eq. (50.1% total contribution), followed by polyphenol, alginate, and protein, with 3.96 kg CO_2-eq. (24.3%), 3.00 kg CO_2-eq. (18.4%), and 1.18 kg CO_2-eq. (7.22), respectively. A total of $1.19x10^{-6}$ kg CFC-11-eq. were produced for stratospheric ozone depletion in this scenario, where the main contributions were fucoidan ($7.77x10^{-7}$ kg CFC-11-eq., 65.2%), alginate ($2.81x10^{-7}$ kg CFC-11-eq., 23.6%), polyphenol ($9.94x10^{-8}$ kg CFC-11-eq., 8.4%), and proteins ($3.45x10^{-8}$ kg CFC-11-eq., 2.9%).

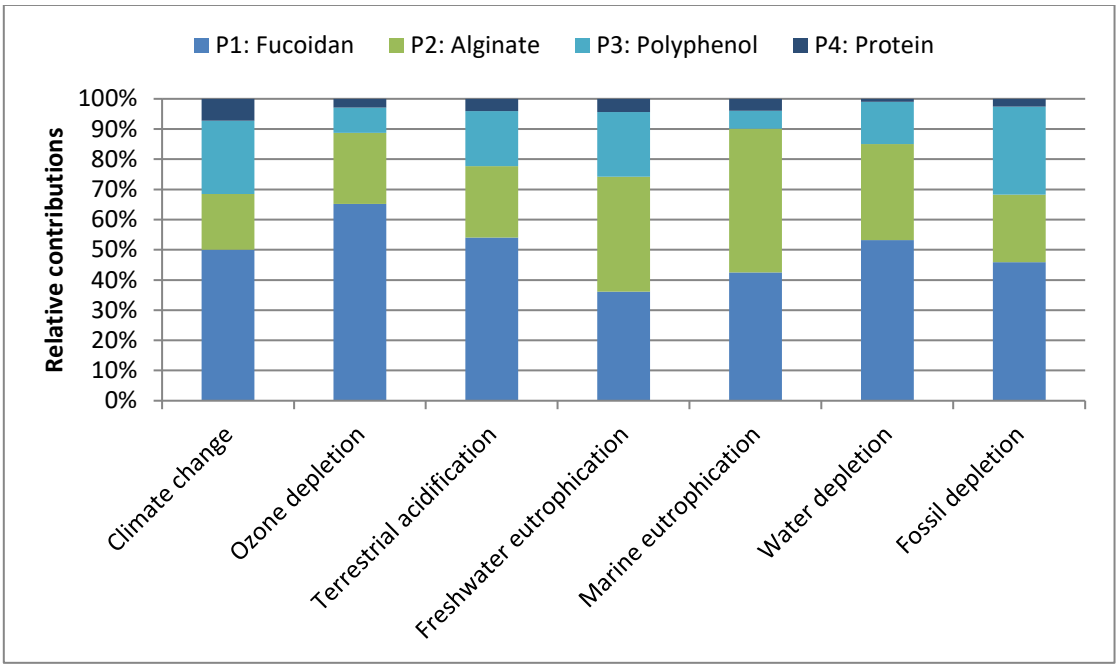

Fig 7-11. Breakdown of the impact contribution across different categories of each extraction step involved in the processing of 1 kg of *A. nodosum* using first-hand data from a green chemistry-based cascading sequence.

Fucoidan and alginate were the stages with the biggest impact in terrestrial acidification, with contributions of 54.1% (0.022 kg SO_2-eq.), and 23.6% (0.0097 kg SO_2-eq.) respectively, and a total contribution of the cascading sequence of 0.041 kg SO_2-eq. Contribution to freshwater eutrophication had the highest inputs from alginate and fucoidan stages, $1.49x10^{-3}$ kg P-eq. (38.1% total contribution), and $1.41x10^{-3}$ kg P-eq. (36.1% total contribution), followed by polyphenol ($8.4x10^{-4}$ kg P-eq., 21.5%) and protein

step ($1.7x10^{-4}$ kg P-eq., 4.3%). Biggest impacts in marine eutrophication were observed in the alginate and fucoidan steps with contributions of 0.025 kg N-eq. for alginate, and 0.022 kg N-eq. for fucoidan. Polyphenol and protein stages emitted 0.003 kg N-eq. (5.9%), and 0.002 kg N-eq. (3.9%) respectively. Fucoidan is the process that contributed the most to water depletion with 0.13 m^3-eq. from a total of 0.25 m^3-eq. consumed in this scenario, followed by alginate (31.8%) and polyphenol (14.0%) with 0.079 m^3-eq. and 0.035 m^3-eq., respectively. Protein contributed with 1.03% (0.003 m^3-eq.). Finally, fucoidan, polyphenol and alginate stages were the main contributors for fossil depletion with 45.9% (1.47 kg oil-eq.), 29.2% (0.93 kg oil-eq.), and 22.3% (0.71 kg oil-eq.), respectively. The use of ethanol to precipitate fucoidan and alginate in their respective cascading stages increased their impact contributions in all categories, and the small quantities of phase-forming compounds used in polyphenol and protein stages helped to alleviate their contributions.

Comparing the updated cascading sequence with the three previous scenarios from **Chapter 4** (**Fig 7-12**), this new scenario had the smallest contributions from all of scenarios in climate change and marine eutrophication, in the five remaining contributions the optimised *Green Chem* scenario had the second to last smallest contributions. Comparing the cascading sequence with other studies analysing the extraction of high-value products was difficult due to the different functional units these studies had chosen and the single-product extraction approach used in their LCAs, for example Barjoveanu et al. (2020) assessed the extraction of polyphenols from wood products, however, the functional unit chosen was 1 mg of polyphenol product; Rodríguez-Meizoso et al. (2012) on the other hand, performed an LCA on antioxidants compounds from rosemary leaves, choosing a functional unit of 10 mg of rosemary extracts. The selection of the appropriate functional unit is one of the drawbacks the LCA methodology exhibits, making the comparison between different systems or technology pathways difficult to perform. Although these difficulties, it can be observed in both studies that one of the most impactful drivers in the environmental performance of an

extraction process of high-value compounds is energy usage, with a scenario based in UAE in the study of Barjoveanu et al. (2020) exhibiting the highest environmental contributions of all scenarios studied. In the study of Rodríguez-Meizoso et al. (2012) changing the country where the theoretical facility would be deployed changed the environmental impacts, showing that Sweden was the least impactful scenario, due to the greener energy matrix of the country, highlighting that the energy use when extracting high-value products is one of the main contributors.

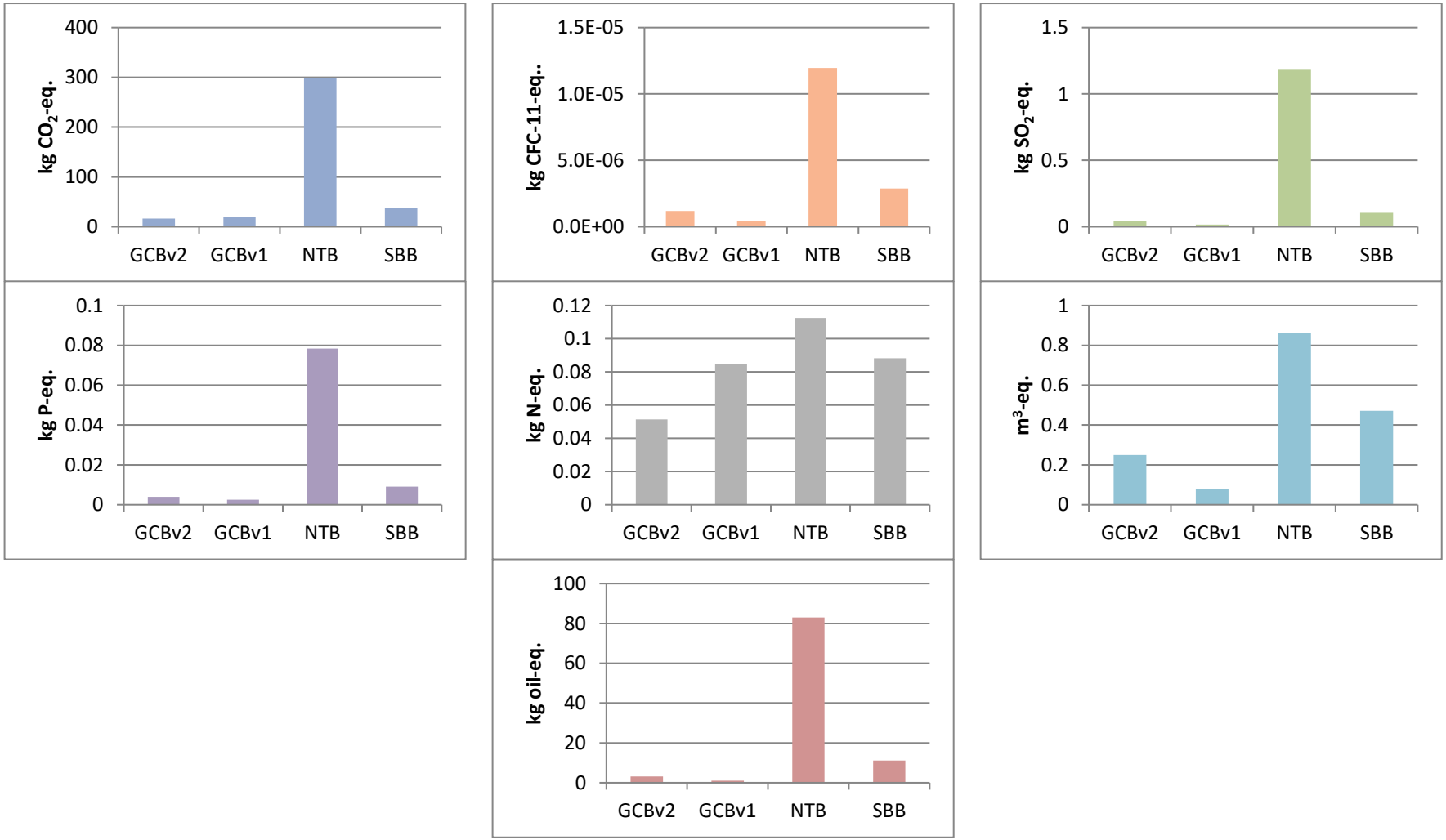

Fig 7-12. Environmental impacts for the different scenarios analysed using ReCiPe v1.13 as impact assessment method. The functional unit was 1 kg of *A. nodosum* as feedstock. SBB: Solvent-based. NTB: Novel Tech. GCBv1: Green Chem v1. GCBv2: Green Chem v2. a) Climate change; b) Stratospheric ozone depletion; c) Terrestrial acidification; d) Freshwater eutrophication; e) Marine eutrophication; f) Water depletion; g) Fossil depletion.

Finally, all the environmental impacts of processing 1 kg of *A. nodosum* were depicted together with total CAPEX in **Fig 7-13**. The re-iterated cascading sequence, as described previously, presented almost the smallest impact contributions of all scenarios, even in marine eutrophication, category that was the highest in its previous iteration. The highest value in the original scenario was due to the final disposal of the biorefinery residue compared to the updated version (**Appendix D**, **Table D-5**). The improved *Green Chem* scenario occupy a smaller portion of the radar than all scenarios evaluated, indicating that after the re-iteration and with the use of experimental data in this scenario the economic and environmental performance of the cascading sequence was improved.

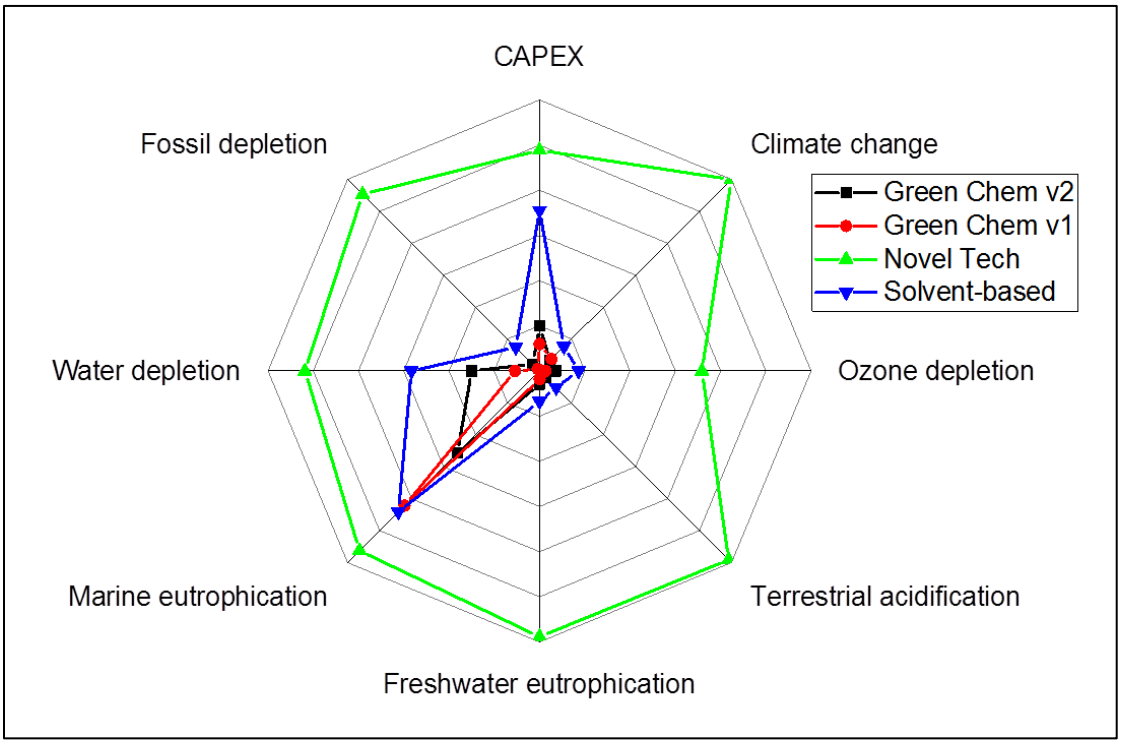

Fig 7-13. Combined environmental impacts together with initial capital investment of three biorefinery scenarios using *A. nodosum*. CAPEX was expressed in pound sterling (£) while the impact categories were quantified as described in **Section 2.5.3** in **Chapter 4**.

3. Conclusions

The optimised biorefinery cascading scenario using the brown macroalga *A. nodosum* as feedstock was evaluated to confirm its technical feasibility, and to re-assess the economic viability, and the environmental impacts of the model developed with first-hand data. The TFT for the optimised cascading sequence showed improvements in the process hotspots identified in **Chapter 4**. Fucoidan and polyphenol steps enhanced their process performance, recovering 11.92% DW and 4.06% DW, respectively, and a 2-fold increase for fucoidan stage and 18-fold increase for the polyphenol stage. Re-iteration of the process flowsheet developed in **Chapter 4** with first-hand data obtained via experiments from **Chapter 5** and **6** was utilised to re-evaluate the economic and environmental performance of the cascading sequence. TEA revealed that the updated green chemistry-based scenario was the most economical overall from all scenarios studied in this project, with a break-even point on the first year of operation (IRR = 82.1%), with a yearly sales revenue of £91,598,002, this was due to the increased extraction yields of the fucoidan and polyphenol stages, improving the economic performance of the cascading sequence, even though total capital investment and operating costs were higher than the previous operation £49,840,896 and £14,584,567, respectively. Lastly, this updated scenario exhibited the lowest CoG/kg (£0.05) and production costs/kg (£0.01) of all scenarios analysed in this study. With these results, it was confirmed the technical feasibility of the optimised green chemistry biorefinery cascading sequence and proved being the most economically sound and environmentally viable project of all biorefinery scenarios assessed in this study. Demonstrating the effectiveness of the use of early-design tools together with TFT in the development of new sustainable multi-product third generation biorefineries.

Chapter 8: Conclusions and future work

1. Review of project objectives

The aim of this thesis was to develop a third-generation multi-product biorefinery based in the use of green chemistry principles to obtain high-value products and commodity chemicals from macroalgae populating the coasts of the UK. Before starting the assessment of the biorefinery cascading sequence the model feedstock had to be selected, it was thus performed a biochemical characterisation of three macroalgal candidates to pick the most suitable model organism for the following biorefinery concept. From all candidates the brown macroalga *A. nodosum* was selected to perform the subsequent process development studies. In order to select the best biorefining scenario three process flowsheets using different technology pathways were built using previous published reports and the application of TEA and LCA as early-design tools were utilised to assess the commercial and environmental performance of the bioprocesses. After selected the best theoretical biorefining scenario, a green chemistry-compliant cascading sequence, the pathway was trialled in the laboratory to assess the actual process performance, with the objective to confirm the process technical viability or to identify process hotspots along the extraction sequence. The fucoidan and polyphenol extractions steps underperformed in the cascading sequence approach when compared with the standalone extraction process, thus optimisation steps were performed to enhance the overall cascading sequence operation. Polyphenol was decided during the construction of the process flowsheets to be recovered using ATPS. To optimise the performance of ATPS for polyphenol recovery a series of high-throughput experimental techniques were employed which used automated liquid-handling and followed by a scale-up corroboration test to confirm process robustness. Fucoidan was modelled in the process flowsheet to be extracted using a solution with HCl. To optimise this process a milder acid was selected, in the form of citric acid, and

using DoE an improvement in the extraction conditions was obtained. By optimising the recovery performance of fucoidan with mild acids the alginate recovery performance was benefited as well. Finally, these new optimised processes were inserted in the new iteration of the green chemistry cascading sequence, where their combined cascading extraction performance was analysed to confirm the process viability. These results were used to re-iterate the previously built process flowsheet and to update the TEA and LCA, in order to confirm environmental feasibility and commercial profitability of the biorefinery. The motivation to use a combined approach was to address the issue of resource intensive process development for new prospective sustainable bioprocesses. This is because the development of new sustainable prospective biorefineries is affected by several factors, e.g., TRL or process uncertainties of new techniques, which might be detrimental in further stages of development of a new technology pathway. The use of process early-design models can help gain insights into the impacts of process decisions in early stages and how this might affect the subsequent stages of development, aid in the decision-making process by using a holistic approach and help develop robust processes at the same time as optimising the use of experimental assets.

This chapter aims to review the key contributions of the thesis and outline directions for future work and translation of the findings for the development of macroalgal biorefineries.

2. Macroalgal biomass as a resource for a multi-product biorefinery in the UK

In **Chapter 3** the selection of an appropriate feedstock for the development of a multi-product third generation biorefinery was executed. From three species present in the UK coasts, one was selected as a model feedstock in the subsequent chapters of this thesis. The motivation for evaluating different species was to explore the different feedstock options present in the UK for the potential development of a biorefinery concept based in the use of marine macroalgae. The selection criterion for the appropriate seaweed candidate was based on the high accumulation of biological compounds with potential

economic revenues after extraction. The results revealed that *A. nodosum* was the most suitable candidate, due to its accumulation of high-value compounds with potential application in several industries, as well as bulk chemicals with well-defined market applications. The benefits of characterising the potential candidates' compounds are in order to help to get a snapshot of the composition of the biomass at the starting point of experimentation, and to guide the decision of the compounds to prioritise extractions, and to help in the selection of the most appropriate recovery techniques and to increase the yields of the selected natural products. This chapter considered the use of three potential candidates for biorefinery developments, two brown seaweeds and a red seaweed species, leaving green seaweeds out of the scope. In retrospective the analysis of a green seaweed candidate would have been beneficial to understand the context of biochemical compositions of macroalgae from the UK. The consideration of seaweed species with more advanced cultivation technologies such as *F. vesiculosus* or *L. digitata* would have been interesting to explore, but these organisms have been studied more intensively during the last years (Hermund et al., 2018; Kostas et al., 2017; Lopes et al., 2018), and for this reason this project wanted to focus on other algal candidates that can highlight the properties of other macroalgal feedstocks.

In terms of future work, it would be valuable to analyse the seasonal and geographical variation of macroalgal feedstock in order to understand the inherently variable nature of their composition, to look for insights of how certain key components are accumulated and to develop an extraction strategy depending on the seasonal and/or spatial variability. The work presented in this chapter looked at the characterisation and selection of a model species to develop a multi-product biorefinery concept using seaweeds as feedstock. One of the challenges of working with macroalgae biomass is the inherently variable nature of it, exhibiting variation in their compositions related to seasonal and geographical changes. For example, Beratto-Ramos et al. (2019) reported the seasonal variation of total polyphenolic content of *M. pyrifera* and *Lessonia spicata*, with polyphenol concentration increasing from summer to winter, and therefore

increasing the antioxidant capacity of the alga, they conclude that knowing these variations in composition will contribute to the development of more resource-efficient industries using seaweeds. Therefore, to fully understand the capabilities of a given feedstock in a biorefinery concept it will be necessary to perform biochemical characterisation of specimens collected at different seasons and from different locations, in order to understand how the chemical composition varies across time or place, and so to implement strategies along the cascading sequence to maximise the recovery of the interest compounds.

3. Combining TEA and LCA is a powerful method for early-stage evaluation of a cascading biorefinery sequence for *A. nodosum*

Chapter 4 aimed to analyse the economic and environmental performance of three different technology pathways for the extraction of several compounds from macroalgae in a cascading sequence approach. The motivation to perform these analyses was based in the lack of reports, at the time of the execution of the assessments, utilising macroalgae in a biorefinery context for the extraction of high-value and bulk chemicals using prospective extraction technologies, as usually reports using TEA and/or LCA on seaweed feedstocks are focused on the cultivation stages of the process, or the assessments are performed in adaptations of well-established processing technologies. Recent publications have reported the application of LCA in the recovery of polyphenols from wood waste (Barjoveanu et al., 2020). The authors reported a solvent-based extraction, a high-temperature alkali solution extraction, and a UAE process, where all the environmental profiles were dominated by the electricity use, followed using ethanol as extraction solvent. These results were like the results obtained in this project, with high utilities costs in *Novel Tech* scenario due to the electricity used to operate the microwave extractors, and the high costs of raw materials in *Solvent-based* scenario for the purchase of solvent to recover the different compounds. Alternative technology pathways to process the biomass for the release of carbohydrates that appeared after

this study was executed would have been interesting to investigate in a cascading sequence. Greetham et al. (2020) use of seawater to perform hydrolysis of macroalgae for release of carbohydrates appeared as a more efficient method to release carbohydrates from macroalgal matrices; this approach also might be cheaper than the use of novel technologies or biodegradable acids, due to the virtually untapped availability of seawater to use in the method, but a comprehensive analysis of the corrosive effects of saltwater in the equipment is an interesting approach to analyse in the future.

A biorefinery scenario based in the implementation of green chemistry principles was the most economically sound scenario and the least environmentally impactful of all analysed. For that reason, this cascading sequence was analysed in the lab to evaluate the real process performance of it, identifying hotspots in two stages, fucoidan and polyphenol, that required further development. The application of ATPS in the cascading sequence was another motivation in this chapter, due to the lack of published papers first, extracting polyphenols and proteins from seaweed with these systems, at the time of executed the studies; and second, because the use of ATPS in a cascading sequence context had not been reported.

One key area for future development of the TEA/LCA platform would be the application of sensitivity analysis. The early-design tools selected for this chapter were used to obtain a snapshot of the economic and environmental viability of prospective multi-product biorefinery scenarios, in order to understand and identify hotspots in their cascading sequences. Unfortunately, there was not the opportunity to test the models on different uncertainty scenarios and to test the robustness of the assumptions of the cascading sequence. Therefore, a proposal for short term future work would be to conduct sensitivity analyses under different uncertainty scenarios to test the economic and environmental viability of the multi-product biorefinery. Monte Carlo simulations can help to determine differences between scenarios within a comparative LCA by using stochastic calculations to evaluate the scenarios under uncertainty (Kralisch et al., 2015).

Application of Monte Carlo simulations have led to the development of more sophisticated tools for biorefinery assessment, Shi and Guest (2020) developed an integrated modelling framework for agile combined TEA and LCA in biorefineries developed in Python 3.7 that allows users to perform streamlined TEA/LCA of biorefineries.

Life cycle costing (LCC) is a tool like TEA, which uses economic metrics to aid in the decision-making process for products or processes. Differently than TEA, LCC not only considers the purchase costs and revenues of a process, but all the associated costs along the life cycle of the process (Swarr et al., 2011), while TEA is a framework to analyse the technical and economic performance of a process, and includes studies on the economic impacts of research, development, demonstration and deployment of technologies (Zimmermann et al., 2020). For this reason, the application of TEA in this study was selected, due to the 'gate-to-gate' approach of both, TEA and LCA to perform preliminary studies of new technology pathways.

Another interdisciplinary aspect that is more challenging to evaluate is the wider societal impact of bioprocess decision making. It is proposed that in order to fully comply with the triple bottom line of sustainable development the social aspect must be considered. A social life cycle assessment (S-LCA) is suggested as a long term proposal to be implemented along the other early-design tools to evaluate the social and sociological impacts of a product or process, in this case the execution of a type 2 S-LCA modelling the consequence of change (Macombe, 2020) to evaluate how the deployment of a multi-product biorefinery facility will affect the livelihood of a certain coastal community, analysing the stakeholders involved in the process, i.e. workers, consumers, local community, general society, and value chain actors, and the social impact categories, i.e. fair salary, working conditions, equal opportunities, health and safety of workers, transparency, etc. (Falcone et al., 2019) to give a fully holistic approach to the evaluation of prospective biorefineries. Reports including the social dimension in third generation biorefineries have been published recently (Sadhukhan et al., 2019), indicating that

producing protein, sugars, and minerals from seaweed to displace food, sugar and mineral products in countries from Southeast Asia makes an attractive value proposition to investigate macroalgal biorefineries further.

4. Demonstration of high-throughput screening as means to reduce process uncertainty in biorefinery process design

Chapter 5 looked at using high-throughput screening to improve the polyphenol extraction using ATPS from the cascading sequence developed in **Chapter 4** to improve the overall performance of the sequence in the next iteration of the assessments. An automated liquid-handling robot was used to obtain a rapid and robust methodology after calibration of the equipment. With the aid of the robot the binodal curves of four different systems were built and compared to binodal curves determined manually. The automated method proved being equally reliable than the manual determination. For that reason, the robot was used to assess the partitioning of polyphenols in ATPS. Phloroglucinol was selected as a model target compound for the partitioning experiments, decision since this molecule is the basic block for polyphenols synthesis. From 384 different two-phase systems two prospective ATPS were selected after the scale-down high-throughput screening was completed and were further scaled-up to analyse process robustness. Finally, the aqueous two-phase system with the highest recovery was selected, composed of PEG 2000-potassium phosphate buffer (27:4), to be inserted in the new iteration of the cascading sequence developed in **Chapter 4**. Some limitations of this approach were observed in the determination of the binodal curves because it was necessary to considerably reduce speeds of aspiration and dispense compared to guidelines recommended as standard. It was also necessary to ensure that dispensed droplets were fully disengaged from the liquid handling tips and that additional steps were taken to eliminate carry over and cross-contamination between the phases.

While the separation of polyphenols was demonstrated successfully, partitioning studies of other polar compounds in ATPS using HTS would enable a faster screening of natural products with potential breakthrough in the market. Future work should evaluate how automated HTS can be used to explore different ATPS to recover more compounds than just polyphenols in seaweeds i.e., pigments, specific peptides, among others. This platform could be expanded its use to different plant matrices i.e., microalgae, fruit waste, or even aquaculture waste to recover high-value compounds and to add valorisation to often discarded biomass in a modular biorefinery approach (Du et al., 2018; Nascimento et al., 2020; Xavier et al., 2017). This approach is proposed on account of the empirical nature of ATPS process development, making the evaluation of a new two-phase system a slow process. This piece of work aimed to assist in this task, developing a rapid method of evaluation of a bigger design space, allowing a faster sample processing. This rapid approach also offers the possibility to manage the natural heterogeneity of macroalgal feedstock, by being able to rapidly identify a best ATPS candidate if the concentration of the interest compound changes with time or location. Quantification of the impurities in the phase containing the compound of interest is also suggested to improve the high-throughput performance of the technique. Analytical technologies that could address this include the use of high-performance anion-exchange chromatography with pulsed amperometric detection (HPAEC-PAD), ultra-performance liquid chromatography (UPLC), microfluidic-based electrophoresis, and lab-on-a-chip devices that could be coupled with the liquid-handling station.

Other ultra-scale-down approaches have designed specialised equipment to overcome limitations of sample handling at small scale (Noyes et al., 2015; Rayat et al., 2016). Development of dedicated microwell platforms for the study of ATPS via HTS could facilitate this process. The study and assembly of dedicated labware would help to develop HTS of ATPS to allow sampling without cross-contamination minimising sample error. This proposal is suggested because of the challenges of the technique when sampling from the bottom phase is attempted, e.g., when the determination of binodal

curves is being studied, where the pipette tip has to travel through the top phase as well as potential precipitation at the interface. It is interesting to explore the design of 96-deep well plates with bottom valves which could be opened and/or accessed to sample the bottom phase as required.

5. Embedding DoE methods into bioprocess design facilitates the design of a green extraction method for fucoidan from *A. nodosum*

Chapter 6 examined the use of citric acid as a green extraction method for fucoidan, in order to improve the performance of said process in the cascading sequence built in **Chapter 4**. The motivation for explore different acid types to recover fucoidan arises from the lack of information of different options in published literature, with most of them using HCl, and optimising the extraction conditions without inquiring if the action of this strong acid might affect the biological activities of the fucoidan extracted, or how the action of the acid would affect other compounds of interest in a cascading context (Abraham et al., 2019; Lorbeer et al., 2015; Widjanarko et al., 2014). After selected the best extraction method, a DoE-based approach was used to improve the extraction performance of the process varying the conditions of the method, and the monosaccharides profile was obtained to confirm the mildness of the process, which meant that the action of citric acid to recover fucoidan was not hydrolysing it but extracting it with a 76 – 81% purity. These results confirmed the establishment of a green extraction process to recover fucoidan with minimal impurities during the extraction, meaning the recovery yields of the subsequent extraction stages in the re-iterated cascading sequence might not be affected by means of co-extraction of undesired products. One critical aspect of this investigation includes the absence of more quantitative techniques to characterise the alginate extract, only a qualitative determination using UATR-FTIR was performed, but the MW distribution, the β-D-mannuronic (M) to α-L-guluronic (G) acid (M/G) ratio, and gel strength determinations

were not considered in this chapter, because the extraction performance in an industrial cascading environment was prioritised.

In the DoE-based improvement strategy undertaken to increase the fucoidan recovery performance the influence of extraction conditions such as time, mixing strategy, among others were not assessed. In the short term the evaluation of these extraction conditions it is proposed using of DoE to expand the experimental domain used in this chapter. Therefore, recovery conditions such as, extraction time, pH of the extraction solution, mixing regime, particle size of the feedstock should be studied to understand the underlying principles involved in this process in a more detailed way, and to attempt to increase the recovery yields to a higher extent. This future work should also consider the inclusion of mass transfer experiments, in order to understand the fucoidan mass flux in presence of different concentrations of acid, due to the proposition that different temperatures, acid concentrations, or even microwave irradiation affect the mass transfer (Dobrinčić et al., 2020; Rodriguez-Jasso et al., 2011; Saravana et al., 2017), but there are not published reports quantifying this phenomenon; this proposal should be accompanied by modelling of all these parameters to develop a detailed description that can help to select the best extraction conditions with minimal experimental effort required.

Recent literature (Fitton et al., 2015; Kwon et al., 2020) has indicated that fucoidan may have important anti-viral properties. Future work should assess the biological activities of fucoidan extracted via citric acid solution pH 5.5. This proposal suggests the evaluation of the biological activities of the fucoidan extracted with this method, such as antioxidant properties, anti-cancer activities, and anti-microbial properties, and compare them against previously reported publications, with the purpose of identify an increase or decrease in the biological activities of the fucoidan recovered with this technique, and thus explore further investigations, using this compound as the main driver for new biopharmaceuticals, for example the exploration of the viability of a biopharmaceutical

that helps to mitigate COVID-19 effects in the following years after inoculation, given the reported anti-SARS-CoV-2 properties of this compound (Kwon et al., 2020).

6. Feedback loops at an early stage have major implications for improvement of the technical, economic, and environmental performance of cascading biorefinery sequence following green chemistry principles

Chapter 7 employed the improved extraction methods developed in **Chapter 5** and **6** to re-iterate the cascading sequence built in **Chapter 4** and analyse the process performance of the consolidated process. With this new iteration of recovery yields the process flowsheet was updated, and thus the previous TEA and LCA developed in **Chapter 4** were updated as well. TEA showed that the updated green chemistry cascading sequence was the most economically sound scenario from all analysed in this project, with the second highest total sales revenues and lowest production costs per kg of biomass processed. This scenario also had the lowest environmental impact contributions of them all. The motivation to re-iterate the cascading sequence with two updated extraction stages and re-evaluate its economic and environmental metrics arises from the absence of this kind of reports in literature, as explained previously, but also from the necessity to use first-hand data in order to model the biorefinery performance more accurately, and thus helping in the decision-making process. With these results, it was confirmed that the use of a mixed approach using early-design tools together with lab experimentation is effective in the development of new multi-product third generation biorefineries using prospective technology pathways such as green chemistry cascading sequences to extract high-value and bulk chemicals from *A. nodosum* to potentiate the development of an economy more focused in the use of marine renewable resources.

As mentioned previously, the use of early-design tools was adopted to obtain a snapshot of the economic and environmental viability of prospective multi-product biorefinery scenarios. In order to get a more accurate appraisal of this scenario, and adopting the

proposal of **Chapter 4,** the model should be expanded starting with a system boundaries expansion, as this scenario was considered on a gate-to-gate approach, hence a cradle-to-grave approach could be implemented to consider the seaweed aquaculture process and how this stage might affect the environmental footprint of the biorefinery, as well as inclusion of life cycle costing to analyse the process under the framework of a life cycle sustainability assessment (LCSA), considering the environmental, economic, and social life cycle of the process (Swarr et al., 2011). In addition, it is proposed that the updated cascading sequence is scaled-up to the order of 10 L working volume of each cascading step to evaluate the scale-up performance and to identify potential issues in a future pilot plant scale up operation.

Longer term, and with the aspiration to create a platform for more global macroalgal biorefineries, it would be advantageous to develop a consolidated early-design framework, considering the economic, environmental, and social (implementing the long-term proposal of **Chapter 4**) aspects. This framework is also suggested to assess biorefineries in a modular approach; this means the construction and evaluation of integrated biorefinery scenarios using a variety of macroalgal species as feedstock, for example in different seasons, to produce an optimal range of products, and selecting the optimum extraction technology depending on type of feedstock, accumulation of interest product in the organism, and other process variables. A big challenge in using macroalgae as feedstock for biorefinery operations is the lack of seaweed industrial aquaculture developments in the UK, with most of the brown macroalgae used for these experiments harvested from wild populations, raising an issue when industrial third generation biorefinery facilities become a reality. A long-term proposal to combat this is the development of advanced cultivation techniques that allows a competitive seaweed aquaculture industry that can successfully support the demand of future biorefinery facilities without compromising the sustainability of wild banks.

7. Concluding remarks

In line with the aims of this thesis, it can be concluded that the application of TEA and LCA in the early stages of prospective multi-product third generation biorefinery concepts is a powerful tool for the rapid evaluation of new sustainable bioprocessing options. This approach combined with the use of lab experimentation methods focused on the rapid acquisition of data, such as HTS and DoE, provide comprehensive process insights and facilitates the decision-making process of new technology pathways for macroalgal biorefineries. In a wider context, this piece of work aimed to develop a biorefinery concept based in green chemistry principles specialised in the sequential extraction of high-value compounds and commodity chemicals from macroalgae, together with the use of environmental and economic metrics to give a holistic approach to the evaluation of new technology developments. This work also advocates for the simultaneous experimentation of scale-down biorefinery cascading sequence concepts and theoretical models due to the iterative nature of the sustainable bioprocesses' development field, allowing a more resource-efficient approach to produce more robust processes. Overall, the work presented in this thesis encourages looking at the development of sustainable biorefineries from an interdisciplinary scope, with researchers working alongside policy makers, communities, and the private sector to accomplish the Blue Growth directives and move towards an ocean-based economy.

References

Abbati de Assis, C., Gonzalez, R., Kelley, S., Jameel, H., Bilek, T., Daystar, J., Handfield, R., Golden, J., Prestemon, J., Singh, D., 2017. Risk management consideration in the bioeconomy. Biofuels, Bioprod. Biorefining 11, 549–566.

Abraham, R.E., Su, P., Puri, M., Raston, C.L., Zhang, W., Su, P., Puri, M., 2019. Optimisation of biorefinery production of alginate, fucoidan and laminarin from brown seaweed Durvillaea potatorum. Algal Res. 38, 101389.

Adetunji, L.R., Adekunle, A., Orsat, V., Raghavan, V., 2017. Advances in the pectin production process using novel extraction techniques: A review. Food Hydrocoll. 62, 239–250.

Afonso, N.C., Catarino, M.D., Silva, A.M.S., Cardoso, S.M., 2019. Brown Macroalgae as Valuable Food Ingredients. Antioxidants 8, 365.

Ahluwalia, S., Shivhare, U.S., Basu, S., 2013. Supercritical CO 2 Extraction of Compounds with Antioxidant Activity from Fruits and Vegetables Waste -A Review. Focus. Mod. Food Ind. 2, 43–62.

Aitken, D., Bulboa, C., Godoy-Faundez, A., Turrion-Gomez, J.L., Antizar-Ladislao, B., 2014. Life cycle assessment of macroalgae cultivation and processing for biofuel production. J. Clean. Prod. 75, 45–56.

Akbar, M., Irohara, T., 2018. Scheduling for sustainable manufacturing: A review. J. Clean. Prod. 205, 866–883.

Alara, O.R., Abdurahman, N.H., Ukaegbu, C.I., Azhari, N.H., 2018. Vernonia cinerea leaves as the source of phenolic compounds, antioxidants, and anti-diabetic activity using microwave-assisted extraction technique. Ind. Crops Prod. 122, 533–544.

Alboofetileh, M., Rezaei, M., Tabarsa, M., 2019. Enzyme-assisted extraction of Nizamuddinia zanardinii for the recovery of sulfated polysaccharides with anticancer and immune-enhancing activities. J. Appl. Phycol. 31, 1391–1402.

Ale, M.T., Mikkelsen, J.D., Meyer, A.S., 2011. Important determinants for fucoidan

bioactivity: A critical review of structure-function relations and extraction methods for fucose-containing sulfated polysaccharides from brown seaweeds. Mar. Drugs 9, 2106–2130.

Almeida, M., Humanes, M., Melo, R., Silva, J.A., Fraústo Da Silva, J.J.R., Vilter, H., Wever, R., 1998. Saccorhiza polyschides (Phaeophyceae; Phyllariaceae) a new source for vanadium-dependent haloperoxidases. Phytochemistry 48, 229–239.

Alvarado-Morales, M., Boldrin, A., Karakashev, D.B., Holdt, S.L., Angelidaki, I., Astrup, T., 2013. Life cycle assessment of biofuel production from brown seaweed in Nordic conditions. Bioresour. Technol. 129, 92–99.

Amano, H., Noda, H., 1990. Proteins of Protoplasts from Red Alga Porphyra yezoensis. Nippon Suisan Gakkaishi 56, 1859–1864.

Amano, H., Noda, H., 1992. Proteins of Protoplasts from Several Seaweeds. Nippon Suisan Gakkaishi 58, 291–299.

Amrhein, S., Schwab, M.L., Hoffmann, M., Hubbuch, J., 2014. Characterization of aqueous two phase systems by combining lab-on-a-chip technology with robotic liquid handling stations. J. Chromatogr. A 1367, 68–77.

Anaëlle, T., Serrano, E., Laurent, V., Elena, I., Mendiola, J.A., Stéphane, C., Nelly, K., Stéphane, L.B., Luc, M., Stiger-Pouvreau, V., 2013. Green improved processes to extract bioactive phenolic compounds from brown macroalgae using Sargassum muticum as model. Talanta 104, 44–52.

Andersen, M., 2017. Opportunities and Risks of Seaweed Biofuels in Aviation, Bellona.org.

Arvidsson, R., Tillman, A.M., Sandén, B.A., Janssen, M., Nordelöf, A., Kushnir, D., Molander, S., 2018. Environmental Assessment of Emerging Technologies: Recommendations for Prospective LCA. J. Ind. Ecol. 22, 1286–1294.

Asenjo, J.A., Andrews, B.A., 2012. Aqueous two-phase systems for protein separation: Phase separation and applications. J. Chromatogr. A 1238, 1–10.

Ashokkumar, V., Salim, M.R., Salam, Z., Sivakumar, P., Chong, C.T., Elumalai, S.,

Suresh, V., Ani, F.N., 2017. Production of liquid biofuels (biodiesel and bioethanol) from brown marine macroalgae Padina tetrastromatica. Energy Convers. Manag. 135, 351–361.

Attard, T.M., McElroy, C.R., Hunt, A.J., 2015. Economic assessment of supercritical CO2 extraction of waxes as part of a maize stover biorefinery. Int. J. Mol. Sci. 16, 17546–17564.

Azmir, J., Zaidul, I.S.M., Rahman, M.M., Sharif, K.M., Mohamed, A., Sahena, F., Jahurul, M.H.A., Ghafoor, K., Norulaini, N.A.N., Omar, A.K.M., 2013. Techniques for extraction of bioactive compounds from plant materials: A review. J. Food Eng. 117, 426–436.

Backa, S., Andresen, M., Rojahn, T., 2012. Biorefineries using wood for production of specialty cellulose fibers, lignosulfonates, vanillin, bioethanol and biogas - the Borregaard Sarpsborg example. In: Dahlquist, E. (Ed.), Biomass as Energy Source: Resources, Systems and Apllications. Taylor & Francis, pp. 141–150.

Baghel, R.S., Trivedi, N., Gupta, V., Neori, A., Reddy, C.R.K.K., Lali, A., Jha, B., 2015. Biorefining of marine macroalgal biomass for production of biofuel and commodity chemicals. Green Chem. 17, 2436–2443.

Baghel, R.S., Trivedi, N., Reddy, C.R.K., 2016. A simple process for recovery of a stream of products from marine macroalgal biomass. Bioresour. Technol. 203, 160–165.

Balboa, E.M., Rivas, S., Moure, A., Domínguez, H., Parajó, J.C., 2013. Simultaneous extraction and depolymerization of fucoidan from Sargassum muticum in aqueous media. Mar. Drugs 11, 4612–4627.

Barjoveanu, G., Alexandra, O., Teodosiu, C., Volf, I., 2020. Life cycle assessment of polyphenols extraction processes from waste biomass 1–12.

Baumann, P., Hubbuch, J., 2017. Downstream process development strategies for effective bioprocesses: Trends, progress, and combinatorial approaches. Eng. Life Sci. 17, 1142–1158.

Belda, M., Sanchez, D., Bover, E., Prieto, B., Padrón, C., Cejalvo, D., Lloris, J.M., 2016. Extraction of polyphenols in Himanthalia elongata and determination by high performance liquid chromatography with diode array detector prior to its potential use against oxidative stress. J. Chromatogr. B 1033–1034, 334–341.

Benavides, J., Rito-Palomares, M., 2008. Practical experiences from the development of aqueous two-phase processes for the recovery of high value biological products. J. Chem. Technol. Biotechnol. 83, 133–142.

Bensch, M., Selbach, B., Hubbuch, J., 2011. High throughput screening techniques in downstream processing: Preparation , characterization and optimization of aqueous two-phase systems. Chem. Eng. Sci. 62, 2011–2021.

Beratto-Ramos, A., Castillo-Felices, R. del P., Troncoso-Leon, N.A., Agurto-Muñoz, A., Agurto-Muñoz, C., 2019. Selection criteria for high-value biomass: seasonal and morphological variation of polyphenolic content and antioxidant capacity in two brown macroalgae. J. Appl. Phycol. 31, 653–664.

Bernazzani, L., Borsacchi, S., Catalano, D., Gianni, P., Mollica, V., Vitelli, M., Asaro, F., Feruglio, L., 2004. On the interaction of sodium dodecyl sulfate with oligomers of poly(ethylene glycol) in aqueous solution. J. Phys. Chem. B 108, 8960–8969.

Bleakley, S., Hayes, M., 2017. Algal Proteins: Extraction, Application, and Challenges Concerning Production. Foods 6, 33.

Bligh, E.., Dyer, W.J., 1959. A rapid Method of Total Lipid Extraction and Purification. Can. J. Biochem. Physiol.

Bocanegra, A., Bastida, S., Benedí, J., Ródenas, S., Sánchez-Muniz, F.J., 2009. Characteristics and nutritional and cardiovascular-health properties of seaweeds. J. Med. Food 12, 236–58.

Bora, M.M., Borthakur, S., Rao, P.C., Dutta, N.N., 2005. Aqueous two-phase partitioning of cephalosporin antibiotics: Effect of solute chemical nature. Sep. Purif. Technol. 45, 153–156.

Brent, Z.W., Barbesgaard, M., Pedersen, C., 2018. The Blue Fix: Unmasking the politics

behind the promise of blue growth. Amsterdam.

Britton, G., Liaaen-Jensen, S., Pfander, H., 2009. Carotenoids: Nutrition and Health.

Brockmann, D., Pradinaud, C., Champenois, J., Benoit, M., Hélias, A., 2015. Environmental assessment of bioethanol from onshore grown green seaweed. Biofuels, Bioprod. Biorefining 9, 696–706.

Brown, T.R., 2018. Price uncertainty, policy, and the economic feasibility of cellulosic biorefineries. Biofuels, Bioprod. Biorefining 12, 485–496.

Bruhn, A., Janicek, T., Manns, D., Nielsen, M.M., Balsby, T.J.S., Meyer, A.S., Rasmussen, M.B., Hou, X., Saake, B., Göke, C., Bjerre, A.B., 2017. Crude fucoidan content in two North Atlantic kelp species, Saccharina latissima and Laminaria digitata—seasonal variation and impact of environmental factors. J. Appl. Phycol. 1–17.

Buyle, M., Audenaert, A., Billen, P., Boonen, K., Passel, S. Van, Van Passel, S., Passel, S. Van, 2019. The Future of Ex-Ante LCA? Lessons Learned and Practical Recommendations. Sustainability 11, 5456 1–24.

Camus, C., Ballerino, P., Delgado, R., Olivera-Nappa, Á., Leyton, C., Buschmann, A.H., 2016. Scaling up bioethanol production from the farmed brown macroalga Macrocystis pyrifera in Chile. Biofuels, Bioprod. Biorefining 10, 673–685.

Carbajales-Dale, M., Mahmud, R., High, K., Moni, S.M., Mahmud, R., High, K., Carbajales-Dale, M., 2020. Life cycle assessment of emerging technologies: A review. J. Ind. Ecol. 24, 52–63.

Cardona-Alzate, C.A., Serna-Loaiza, S., Ortiz-Sanchez, M., 2020. Sustainable biorefineries: What was learned from the design, analysis and implementation. J. Sustain. Dev. Energy, Water Environ. Syst. 8, 88–117.

Centi, G., Iaquaniello, G., Perathoner, S., 2019. Chemical engineering role in the use of renewable energy and alternative carbon sources in chemical production. BMC Chem. Eng. 1, 1–16.

Charoensiddhi, S., Lorbeer, A.J., Franco, C.M.M., Su, P., Conlon, M.A., Zhang, W.,

2018. Process and economic feasibility for the production of functional food from the brown alga Ecklonia radiata. Algal Res. 29, 80–91.

Chemat, F., Rombaut, N., Sicaire, A.G., Meullemiestre, A., Fabiano-Tixier, A.S., Abert-Vian, M., 2017. Ultrasound assisted extraction of food and natural products. Mechanisms, techniques, combinations, protocols and applications. A review. Ultrason. Sonochem. 34, 540–560.

Chemat, F., Tomao, V., Virot, M., 2009. Ultrasound-Assisted Extraction in Food Analysis. In: Handbook of Food Analysis Instruments. pp. 85–103.

Cheung, P.C.K., 1999. Temperature and pressure effects on supercritical carbon dioxide extraction of n-3 fatty acids from red seaweed. Food Chem. 65, 399–403.

Chrapusta, E., Kaminski, A., Duchnik, K., Bober, B., Adamski, M., Bialczyk, J., 2017. Mycosporine-Like Amino Acids: Potential health and beauty ingredients. Mar. Drugs 15, 1–29.

Cikoš, A.-M., Jerković, I., Molnar, M., Šubarić, D., Jokić, S., 2019. New trends for macroalgal natural products applications. Nat. Prod. Res. 0, 1–12.

Ciriminna, R., Carnaroglio, D., Delisi, R., Arvati, S., Tamburino, A., Pagliaro, M., 2016. Industrial Feasibility of Natural Products Extraction with Microwave Technology. Chem. Sel. Rev. 1, 549–555.

Cisneros-Montemayor, A.M., Moreno-Báez, M., Voyer, M., Allison, E.H., Cheung, W.W.L., Hessing-Lewis, M., Oyinlola, M.A., Singh, G.G., Swartz, W., Ota, Y., 2019. Social equity and benefits as the nexus of a transformative Blue Economy: A sectoral review of implications. Mar. Policy 109.

Clark, J.H., Luque, R., Matharu, A.S., 2012. Green chemistry, biofuels, and biorefinery. Annu. Rev. Chem. Biomol. Eng. 3, 183–207.

Clean Cities, 2021. Alternative Fuel Price Report July 2021.

Cofrades, S., López-Lopez, I., Bravo, L., Ruiz-Capillas, C., Bastida, S., Larrea, M.T.T., Jiménez-Colmenero, F., 2010. Nutritional and Antioxidant Properties of Different Brown and Red Spanish Edible Seaweeds. Food Sci. Technol. Int. 16, 361–370.

Craigie, J.S., Cornish, M.L., Deveau, L.E., 2019. Commercialization of Irish moss aquaculture: The Canadian experience. Bot. Mar. 62, 411–432.

Czyrnek-Delêtre, M.M., Rocca, S., Agostini, A., Giuntoli, J., Murphy, J.D., 2017. Life cycle assessment of seaweed biomethane, generated from seaweed sourced from integrated multi-trophic aquaculture in temperate oceanic climates. Appl. Energy 196, 34–50.

Dawczynski, C., Schubert, R., Jahreis, G., 2007. Amino acids, fatty acids, and dietary fibre in edible seaweed products. Food Chem. 103, 891–899.

De Jesus Raposo, M.F., De Morais, A.M.M.B., De Morais, R.M.S.C., 2016. Emergent sources of prebiotics: Seaweeds and microalgae. Mar. Drugs 14, 1–27.

Denis, C., Ledorze, C., Jaouen, P., Fleurence, J., 2009. Comparison of different procedures for the extraction and partial purification of R-phycoerythrin from the red macroalga Grateloupia turuturu. Bot. Mar. 52, 278–281.

DeRose, K., DeMill, C., Davis, R.W., Quinn, J.C., 2019. Integrated techno economic and life cycle assessment of the conversion of high productivity, low lipid algae to renewable fuels. Algal Res. 38, 101412.

Dey, P., Pal, P., Kevin, J.D., Das, D.B., 2020. Lignocellulosic bioethanol production: Prospects of emerging membrane technologies to improve the process - A critical review. Rev. Chem. Eng. 36, 333–367.

Dobrinčić, A., Balbino, S., Zorić, Z., Pedisić, S., Kovačević, D.B., Garofulić, I.E., Dragović-Uzelac, V., 2020. Advanced technologies for the extraction of marine brown algal polysaccharides. Mar. Drugs 18.

Du, L.P., Cheong, K.L., Liu, Y., 2018. Optimization of an aqueous two-phase extraction method for the selective separation of sulfated polysaccharides from a crude natural mixture. Sep. Purif. Technol. 202, 290–298.

DuBois, M., Gilles, K.A., Hamilton, J.K., Rebers, P.A., Smith, F., 1956. Colorimetric method for determination of sugars and related substances. Anal. Chem. 28, 350–356.

Dulley, J.R., Grieve, P.A., 1975. A simple technique for eliminating interference by detergents in the Lowry method of protein determination. Anal. Biochem. 64, 136–141.

Dutta, A., Talmadge, M., Nrel, J.H., Worley, M., Harris, D.D., Barton, D., Groenendijk, P., Ferrari, D., Chemical, B.S.D., Searcy, E.M., Wright, C.T., Idaho, J.R.H., 2011. Process Design and Economics for Conversion of Lignocellulosic Biomass to Ethanol Thermochemical Pathway by Indirect gasification and mixed alcohol synthesis. Renew. Energy.

Edwards, M.D., Watson, L., 2011. Cultivating Laminaria digitata, Aquaculture Explained.

Effio, C.L., Hubbuch, J., 2015. Next generation vaccines and vectors: Designing downstream processes for recombinant protein-based virus-like particles. Biotechnol. J. 10, 715–727.

El Atouani, S., Bentiss, F., Reani, A., Zrid, R., Belattmania, Z., Pereira, L., Mortadi, A., Cherkaoui, O., Sabour, B., 2016. The invasive brown seaweed Sargassum muticum as new resource for alginate in Morocco: Spectroscopic and rheological characterization. Phycol. Res. 64, 185–193.

Eom, S.-H., Lee, S.-H., Yoon, N.-Y., Jung, W.-K., Jeon, Y.-J., Kim, S.-K., Lee, M.-S., Kim, Y.-M., 2012. α-Glucosidase- and α-amylase-inhibitory activities of phlorotannins from Eisenia bicyclis. J. Sci. Food Agric. 92, 2084–2090.

Eriz, G., Sanhueza, V., Roeckel, M., Fernández, K., 2011. Inhibition of the angiotensin-converting enzyme by grape seed and skin proanthocyanidins extracted from Vitis vinífera L. cv. País. LWT - Food Sci. Technol. 44, 860–865.

Esquivel-Hernández, D.A., Ibarra-Garza, I.P., Rodríguez-Rodríguez, J., Cuéllar-Bermúdez, S.P., Rostro-Alanis, M. de J., Alemán-Nava, G.S., García-Pérez, J.S., Parra-Saldivar, R., 2017. Green extraction technologies for high-value metabolites from algae: a review. Biofuels, Bioprod. Biorefining 11, 215–231.

Evans, C.D., Monteith, D.T., Fowler, D., Cape, J.N., Brayshaw, S., 2011. Hydrochloric acid: An overlooked driver of environmental change. Environ. Sci. Technol. 45,

1887–1894.

Fabrowska, J., Ibañez, E., Łęska, B., Herrero, M., 2016. Supercritical fluid extraction as a tool to valorize underexploited freshwater green algae. Algal Res. 19, 237–245.

Fabrowska, J., Łeska, B., Schroeder, G., Messyasz, B., Pikosz, M., 2015. Biomass and Extracts of Algae as Material for Cosmetics. In: Marine Algae Extracts: Processes, Products, and Applications. pp. 681–706.

Falcone, P.M., Moreira, M.T., García, S.G., Imbert, E., Tani, A., Tartiu, V.E., Morone, P., 2019. Transitioning towards the bio - economy: Assessing the social dimension through a stakeholder lens. Corp. Soc. Responsib. Environ. Manag. 26, 1135–1153.

FAO, 2020. The State of World Fisheries and Aquaculture 2020. Sustainability in action., Fao.

Fernandes, F., Barbosa, M., Oliveira, A.P., Azevedo, I.C., Sousa-Pinto, I., Valentão, P., Andrade, P.B., 2016. The pigments of kelps (Ochrophyta) as part of the flexible response to highly variable marine environments. J. Appl. Phycol. 28, 3689–3696.

Fernando, I.P.S., Kim, K.N., Kim, D., Jeon, Y.J., Priyan Shanura Fernando, I., Kim, K.N., Kim, D., Jeon, Y.J., Fernando, I.P.S., Kim, K.N., Kim, D., Jeon, Y.J., 2019. Algal polysaccharides: potential bioactive substances for cosmeceutical applications. Crit. Rev. Biotechnol. 39, 99–113.

Filote, C., Santos, S.C.R., Popa, V.I., Botelho, C.M.S., Volf, I., 2021. Biorefinery of marine macroalgae into high-tech bioproducts: a review, Environmental Chemistry Letters. Springer International Publishing.

Fitton, J.H., Stringer, D.N., Karpiniec, S.S., 2015. Therapies from fucoidan: An update. Mar. Drugs 13, 5920–5946.

Foley, S.A., Szegezdi, E., Mulloy, B., Samali, A., Tuohy, M.G., Szegezdi, E., Mulloy, B., Samali, A., Tuohy, M.G., 2011. An Unfractionated Fucoidan from Ascophyllum nodosum: Extraction, Characterization, and Apoptotic Effects in Vitro. J. Nat. Prod. 74, 1851–1861.

Garcia-Vaquero, M, Lopez-Alonso, M., Hayes, M., 2017. Assessment of the functional

properties of protein extracted from the brown seaweed Himanthalia elongata (Linnaeus) S . F . Gray. Food Res. Int. 99, 971–978.

Garcia-Vaquero, M., Rajauria, G., O'Doherty, J.V. V., Sweeney, T., 2017. Polysaccharides from macroalgae: Recent advances, innovative technologies and challenges in extraction and purification. Food Res. Int. 99, 1011–1020.

Gavankar, S., Suh, S., Keller, A.A., 2015. The Role of Scale and Technology Maturity in Life Cycle Assessment of Emerging Technologies: A Case Study on Carbon Nanotubes. J. Ind. Ecol. 19, 51–60.

Gentil, E.C., Damgaard, A., Hauschild, M., Finnveden, G., Eriksson, O., Thorneloe, S., Kaplan, P.O., Barlaz, M., Muller, O., Matsui, Y., Ii, R., Christensen, T.H., 2010. Models for waste life cycle assessment: Review of technical assumptions. Waste Manag. 30, 2636–2648.

Ghatak, H.R., 2011. Biorefineries from the perspective of sustainability: Feedstocks, products, and processes. Renew. Sustain. Energy Rev. 15, 4042–4052.

Glasson, C.R.K.K., Sims, I.M., Carnachan, S.M., Nys, R. De, Magnusson, M., de Nys, R., Magnusson, M., Nys, R. De, Magnusson, M., de Nys, R., Magnusson, M., 2017. A cascading biorefinery process targeting sulfated polysaccharides (ulvan) from Ulva ohnoi. Algal Res. 27, 383–391.

Glyk, A., Scheper, T., Beutel, S., 2015. PEG–salt aqueous two-phase systems: an attractive and versatile liquid–liquid extraction technology for the downstream processing of proteins and enzymes. Appl. Microbiol. Biotechnol. 99, 6599–6616.

Goja, A.M., Yang, H., Cui, M., Li, C., 2013. Aqueous Two-Phase Extraction Advances for Bioseparation. J. Bioprocess. Biotech. 4, 1–8.

Golberg, A., Vitkin, E., Linshiz, G., Khan, S.A., Hillson, N.J., Yakhini, Z., Yarmush, M.L., 2014. Proposed design of distributed macroalgal biorefineries: thermodynamics, bioconversion technology, and sustainability implications for developing economies. Biofuels, Bioprod. Biorefining 8, 67–82.

Gomaa, M., Fawzy, M.A., Hifney, A.F., Abdel-Gawad, K.M., 2018. Use of the brown

seaweed Sargassum latifolium in the design of alginate-fucoidan based films with natural antioxidant properties and kinetic modeling of moisture sorption and polyphenolic release. Food Hydrocoll. 82, 64–72.

Gómez-Loredo, A., Benavides, J., Rito-Palomares, M., 2014. Partition behavior of fucoxanthin in ethanol-potassium phosphate two-phase systems. J. Chem. Technol. Biotechnol. 89, 1637–1645.

Gómez-Ordóñez, E., Jiménez-Escrig, A., Rupérez, P., 2012. Molecular weight distribution of polysaccharides from edible seaweeds by high-performance size-exclusion chromatography (HPSEC). Talanta 93, 153–159.

Gómez-Ordóñez, E., Rupérez, P., 2011. FTIR-ATR spectroscopy as a tool for polysaccharide identification in edible brown and red seaweeds. Food Hydrocoll. 25, 1514–1520.

Greetham, D., Adams, J.M., Du, C., 2020. The utilization of seawater for the hydrolysis of macroalgae and subsequent bioethanol fermentation. Sci. Rep. 10, 1–15.

Griffiths, M.J., Harrison, S.T.L., 2009. Lipid productivity as a key characteristic for choosing algal species for biodiesel production. J. Appl. Phycol. 21, 493–507.

Guo, H., Chang, Y., Lee, D.J., 2018. Enzymatic saccharification of lignocellulosic biorefinery: Research focuses. Bioresour. Technol. 252, 198–215.

Gutiérrez-Rodríguez, A.G., Juárez-Portilla, C., Olivares-Bañuelos, T., Zepeda, R.C., 2018. Anticancer activity of seaweeds. Drug Discov. Today 23, 434–447.

Güven, K.C., Percot, A., Sezik, E., 2010. Alkaloids in marine algae. Mar. Drugs 8, 269–284.

Hafting, J.T., Craigie, J.S., Stengel, D.B., Loureiro, R.R., Buschmann, A.H., Yarish, C., Edwards, M.D., Critchley, A.T., 2015. Prospects and challenges for industrial production of seaweed bioactives. J. Phycol. 51, 821–837.

Harnedy, P.A., FitzGerald, R.J., 2011. Bioactive proteins, peptides, and amino acids from macroalgae. J. Phycol. 47, 218–232.

Harvey, A.L., 2008. Natural products in drug discovery. Drug Discov. Today 13, 894–

901.

Hatti-Kaul, R., 2000. Aqueous Two-Phase Systems: Methods and Protocols, Journal of Chemical Information and Modeling.

Haugan, J.A., Liaaen-Jensen, S., 1994. Algal Carotenoids 54. Carotenoids of Brown Algae (Phaeophyceae). Biochem. Syst. Ecol. 22, 31–41.

He, Z., Chen, Y.Y.Y.Y., Chen, Y.Y.Y.Y., Liu, H., Yuan, G., Fan, Y., Chen, K., 2013. Optimization of the microwave-assisted extraction of phlorotannins from Saccharina japonica Aresch and evaluation of the inhibitory effects of phlorotannin-containing extracts on HepG2 cancer cells. Chinese J. Oceanol. Limnol. 31, 1045–1054.

Hemavathi, A.B., Raghavarao, K.S.M.S., 2011. Differential partitioning of β-galactosidase and β-glucosidase using aqueous two phase extraction. Process Biochem. 46, 649–655.

Heo, S.-J., Park, E.-J., Lee, K.-W., Jeon, Y.-J., 2005. Antioxidant activities of enzymatic extracts from brown seaweeds. Bioresour. Technol. 96, 1613–23.

Hermund, D.B., Plaza, M., Turner, C., Jónsdóttir, R., Kristinsson, H.G., Jacobsen, C., Nielsen, K.F., 2018. Structure dependent antioxidant capacity of phlorotannins from Icelandic Fucus vesiculosus by UHPLC-DAD-ECD-QTOFMS. Food Chem. 240, 904–909.

Hernández, V., Romero-García, J.M., Dávila, J.A., Castro, E., Cardona, C.A., 2014. Techno-economic and environmental assessment of an olive stone based biorefinery. Resour. Conserv. Recycl. 92, 145–150.

Hifney, A.F., Fawzy, M.A., Abdel-Gawad, K.M., Gomaa, M., 2016. Industrial optimization of fucoidan extraction from Sargassum sp. and its potential antioxidant and emulsifying activities. Food Hydrocoll. 54, 77–88.

Hoegh-Guldberg, O., Thezar, M., Boulos, M., Guerraoui, M., Harris, A., Graham, A., Llewellyn, G., Singer, S., Ath, W. De, Hirsch, D., Soede, L.P., 2015. Reviving the Ocean Economy: the case for action - 2015, WWF International.

Holdt, S.L., Kraan, S., 2011. Bioactive compounds in seaweed: Functional food

applications and legislation. J. Appl. Phycol. 23, 543–597.

Honya, M., Mori, H., Anzai, M., Araki, Y., Nisizawa, K., 1999. Monthly changes in the content of fucans, their constituent sugars and sulphate in cultured Laminaria japonica. Hydrobiologia 398–399, 411–416.

Hu, J., Yang, B., Lin, X., Zhou, X.-F.F., Yang, X.-W.W., Liu, Y., 2011. Bioactive Metabolites from Seaweeds. In: Handbook of Marine Macroalgae: Biotechnology and Applied Phycology. pp. 262–284.

Huang, H., Long, S., Singh, V., 2016. Techno-economic analysis of biodiesel and ethanol co-production from lipid-producing sugarcane. Biofuels, Bioprod. Biorefining 10, 299–315.

Huddleston, J.G., Willauer, H.D., Rogers, R.D., 2003. Phase diagram data for several PEG + salt aqueous biphasic systems at 25°C. J. Chem. Eng. Data 48, 1230–1236.

Huijbregts, M.A.J., Steinmann, Z.J.N., Elshout, P.M.F., Stam, G., Verones, F., Vieira, M., Zijp, M., Hollander, A., van Zelm, R., 2017. ReCiPe2016: a harmonised life cycle impact assessment method at midpoint and endpoint level. Int. J. Life Cycle Assess. 22, 138–147.

Humbird, D., Davis, R., Tao, L., Kinchin, C., Hsu, D., Aden, A., 2011. Process Design and Economics for Biochemical Conversion of Lignocellulosic Biomass to Ethanol.

Ingle, K., Vitkin, E., Robin, A., Yakhini, Z., Mishori, D., Golberg, A., 2018. Macroalgae Biorefinery from Kappaphycus alvarezii: Conversion Modeling and Performance Prediction for India and Philippines as Examples. Bioenergy Res. 11, 22–32.

International Organization for Standardization, 2006. ISO 14040-Environmental management - Life Cycle Assessment - Principles and Framework. Int. Organ. Stand. 3, 20.

Jeon, Y.-J., Wijesinghe, W.A.J.P.A.J.P., Kim, S.-K., 2012. Enzyme-assisted Extraction and Recovery of Bioactive Components from Seaweeds. In: Kim, S.-K. (Ed.), Handbook of Marine Macroalgae: Biotechnology and Applied Phycology. John Wiley & Sons, Ltd, pp. 221–228.

Jeon, Y., Wijesinghe, W.A.J.P., Kim, S., 2012. Recovery of Bioactive Components from Seaweeds. Handb. Mar. Macroalgae Biotechnol. Appl. Phycol.

Jerez, M., Selga, A., Sineiro, J., Torres, J.L., Núñez, M.J., 2007. A comparison between bark extracts from Pinus pinaster and Pinus radiata: Antioxidant activity and procyanidin composition. Food Chem. 100, 439–444.

Jeswani, H.K., Falano, T., Azapagic, A., 2015. Life cycle environmental sustainability of lignocellulosic ethanol produced in integrated thermo-chemical biorefineries. Biofuels, Bioprod. Biorefining 6, 661–676.

Jiao, G., Yu, G., Zhang, J., Ewart, H.S., 2011. Chemical structures and bioactivities of sulfated polysaccharides from marine algae. Mar. Drugs 9, 196–233.

Jiménez-Escrig, A., Gómez-Ordóñez, E., Rupérez, P., 2011. Brown and red seaweeds as potential sources of antioxidant nutraceuticals. J. Appl. Phycol. 24, 1123–1132.

Jiménez-González, C., Overcash, M.R., 2014. The evolution of life cycle assessment in pharmaceutical and chemical applications – a perspective. Green Chem. 16, 3392–3400.

Jordan, P., Vilter, H., 1991. Extraction of proteins from material rich in anionic mucilages: Partition and fractionation of vanadate-dependent bromoperoxidases from the brown algae Laminaria digitata and L. saccharina in aqueous polymer two-phase systems. BBA - Gen. Subj. 1073, 98–106.

Julio, R., Albet, J., Vialle, C., Vaca-Garcia, C., Sablayrolles, C., Vaca-Garcia, C., Sablayrolles, C., 2017. Sustainable design of biorefinery processes: existing practices and new methodology. Biofuels, Bioprod. Biorefining 11, 373–395.

Jung, K.A., Lim, S.-R.R., Kim, Y., Park, J.M., 2013. Potentials of macroalgae as feedstocks for biorefinery. Bioresour. Technol. 135, 182–190.

Kadam, S.U., Álvarez, C., Tiwari, B.K., O'Donnell, C.P., 2015a. Processing of seaweeds, Seaweed Sustainability: Food and Non-Food Applications. Elsevier Inc.

Kadam, S.U., Tiwari, B.K., O'Donnell, C.P., 2013. Application of novel extraction technologies for bioactives from marine algae. J. Agric. Food Chem. 61, 4667–75.

Kadam, S.U., Tiwari, B.K., Smyth, T.J., O'Donnell, C.P., 2015b. Optimization of ultrasound assisted extraction of bioactive components from brown seaweed Ascophyllum nodosum using response surface methodology. Ultrason. Sonochem. 23, 308–316.

Karagoz, P., Bill, R.M., Ozkan, M., 2019. Lignocellulosic ethanol production: Evaluation of new approaches, cell immobilization and reactor configurations. Renew. Energy 143, 741–752.

Kaul, A., 2000. The Phase Diagram. In: Aqueous Two-Phase Systems: Methods and Protocols. pp. 11–21.

Kazi, F.K., Fortman, J., Anex, R., 2010. Techno-Economic Analysis of Biochemical Scenarios for Production of Cellulosic Ethanol.

Keegan, D., Kretschmer, B., Elbersen, B., Panoutsou, C., 2013. Cascading use: a systematic approach to biomass beyond the energy sector. Biofuels, Bioprod. Biorefining 7, 193–206.

Kendel, M., Couzinet-Mossion, A., Viau, M., Fleurence, J., Barnathan, G., Wielgosz-Collin, G., 2013. Seasonal composition of lipids, fatty acids, and sterols in the edible red alga Grateloupia turuturu. J. Appl. Phycol. 25, 425–432.

Kerton, F.M., Liu, Y., Omari, K.W., Hawboldt, K., 2013. Green chemistry and the ocean-based biorefinery. Green Chem. 15, 860–871.

Kidgell, J.T., Magnusson, M., de Nys, R., Glasson, C.R.K., 2019. Ulvan: A systematic review of extraction, composition and function. Algal Res. 39, 101422.

Kim, S.-K., 2014. Marine cosmeceuticals. J. Cosmet. Dermatol. 13, 56–67.

Klein-Marcuschamer, D., Simmons, B.A., Blanch, H.W., 2011. Techno-economic analysis of a lignocellulosic ethanol biorefinery with ionic liquid. Biofuels, Bioprod. Biorefining 5, 562–569.

Koivikko, R., Loponen, J., Honkanen, T., Jormalainen, V., 2005. Contents of soluble, cell-wall-bound and exuded phlorotannins in the brown alga Fucus vesiculosus, with implications on their ecological functions. J. Chem. Ecol. 31, 195–212.

Koivikko, R., Loponen, J., Pihlaja, K., Jormalainen, V., 2007. High-performance liquid chromatographic analysis of phlorotannins from the brown alga Fucus vesiculosus. Phytochem. Anal. 18, 326–32.

Konda, N.V.S.N.M., Singh, S., Simmons, B.A., Klein-Marcuschamer, D., 2015. An Investigation on the Economic Feasibility of Macroalgae as a Potential Feedstock for Biorefineries. BioEnergy Res. 8, 1046–1056.

Kostas, E.T., White, D.A., Cook, D.J., 2017. Development of a bio-refinery process for the production of speciality chemical, biofuel and bioactive compounds from Laminaria digitata. Algal Res. 28, 211–219.

Kralisch, D., Ott, D., Gericke, D., 2015. Rules and benefits of Life Cycle Assessment in green chemical process and synthesis design: A tutorial review. Green Chem. 17, 123–145.

Kumari, P., Kumar, M., Gupta, V., Reddy, C.R.K., Jha, B., 2010. Tropical marine macroalgae as potential sources of nutritionally important PUFAs. Food Chem. 120, 749–757.

Kwon, P.S., Oh, H., Kwon, S.J., Jin, W., Zhang, F., Fraser, K., Hong, J.J., Linhardt, R.J., Dordick, J.S., 2020. Sulfated polysaccharides effectively inhibit SARS-CoV-2 in vitro. Cell Discov. 6, 4–7.

Laurienzo, P., 2010. Marine polysaccharides in pharmaceutical applications: An overview. Mar. Drugs 8, 2435–2465.

Leal, D., Matsuhiro, B., Rossi, M., Caruso, F., 2008. FT-IR spectra of alginic acid block fractions in three species of brown seaweeds. Carbohydr. Res. 343, 308–316.

Lee, O.K., Lee, E.Y., 2016. Sustainable production of bioethanol from renewable brown algae biomass. Biomass and Bioenergy 92, 70–75.

Lei, X., Diamond, A.D., Hsu, J.T., 1990. Equilibrium Phase Behavior of the Poly(ethylene glycol)/Potassium Phosphate/Water Two-Phase System at 4 °C. J. Chem. Eng. Data 35, 420–423.

Li, Y.-X., Wijesekara, I., Li, Y.-X., Kim, S.-K., 2011. Phlorotannins as bioactive agents

from brown algae. Process Biochem. 46, 2219–2224.

Lim, S.J., Wan Aida, W.M., Maskat, M.Y., Mamot, S., Ropien, J., Mazita Mohd, D., 2014. Isolation and antioxidant capacity of fucoidan from selected Malaysian seaweeds. Food Hydrocoll. 1–9.

Liu, W., Wang, J., Richard, T.L., Hartley, D.S., Spatari, S., Volk, T.A., 2017. Economic and life cycle assessments of biomass utilization for bioenergy products. Biofuels, Bioprod. Biorefining 11, 633–647.

Lodato, C., Tonini, D., Damgaard, A., Astrup, T.F., 2020. A process-oriented life-cycle assessment (LCA) model for environmental and resource-related technologies (EASETECH). Int. J. Life Cycle Assess. 25, 73–88.

Lopes, G., Andrade, P.B., Valentão, P., 2017. Phlorotannins: Towards new pharmacological interventions for diabetes mellitus type 2. Molecules 22, 1–21.

Lopes, G., Barbosa, M., Vallejo, F., Gil-Izquierdo, Á., Andrade, P.B., Valentão, P., Pereira, D.M., Ferreres, F., 2018. Profiling phlorotannins from Fucus spp. of the Northern Portuguese coastline: Chemical approach by HPLC-DAD-ESI/MSn and UPLC-ESI-QTOF/MS. Algal Res. 29, 113–120.

López Barreiro, D., Beck, M., Hornung, U., Ronsse, F., Kruse, A., Prins, W., 2015. Suitability of hydrothermal liquefaction as a conversion route to produce biofuels from macroalgae. Algal Res. 11, 234–241.

Lorbeer, A.J., Charoensiddhi, S., Lahnstein, J., Lars, C., Franco, C.M.M., Bulone, V., Zhang, W., 2017. Sequential extraction and characterization of fucoidans and alginates from Ecklonia radiata, Macrocystis pyrifera, Durvillaea potatorum, and Seirococcus axillaris. J. Appl. Phycol. 29, 1515–1526.

Lorbeer, A.J., Lahnstein, J., Bulone, V., Nguyen, T., Zhang, W., 2015. Multiple-response optimization of the acidic treatment of the brown alga Ecklonia radiata for the sequential extraction of fucoidan and alginate. Bioresour. Technol. 197, 302–309.

Lordan, S., Ross, R.P., Stanton, C., 2011. Marine bioactives as functional food ingredients: potential to reduce the incidence of chronic diseases. Mar. Drugs 9,

1056–100.

Lorenzo, J.M., Agregán, R., Munekata, P.E.S., Franco, D., Carballo, J., Şahin, S., Lacomba, R., Barba, F.J., 2017. Proximate composition and nutritional value of three macroalgae: Ascophyllum nodosum, Fucus vesiculosus and Bifurcaria bifurcata. Mar. Drugs 15, 360.

Loveday, S.M., 2019. Food Proteins: Technological, Nutritional, and Sustainability Attributes of Traditional and Emerging Proteins. Annu. Rev. Food Sci. Technol. 10.

Lowry, O.H., Rosebrough, N.J., Farr, A.L., Randall, R.J., 1951. Protein Measurement With The Folin Phenol Reagent. Anal. Biochem. 217, 265–275.

Macaya, E.C., Rothäusler, E., Thiel, M., Molis, M., Wahl, M., 2005. Induction of defenses and within-alga variation of palatability in two brown algae from the northern-central coast of Chile: Effects of mesograzers and UV radiation. J. Exp. Mar. Bio. Ecol. 325, 214–227.

Macombe, C., 2020. Social Life Cycle Assessment for Industrial Biotechnology. In: Fröhling, M., Hiete, M. (Eds.), Sustainability and Life Cycle Assessment in Industrial Biotechnology. Springer Nature Switzerland, pp. 205–232.

Magnusson, M., Yuen, A.K.L., Zhang, R., Wright, J.T., Taylor, R.B., Maschmeyer, T., de Nys, R., 2017. A comparative assessment of microwave assisted (MAE) and conventional solid-liquid (SLE) techniques for the extraction of phloroglucinol from brown seaweed. Algal Res. 23, 28–36.

Mandal, V., Mohan, Y., Hemalatha, S., 2008. Microwave assisted extraction of curcumin by sample–solvent dual heating mechanism using Taguchi L9 orthogonal design. J. Pharm. Biomed. Anal. 46, 322–327.

Martelli, F., Favari, C., Mena, P., Guazzetti, S., Ricci, A., Del Rio, D., Lazzi, C., Neviani, E., Bernini, V., 2020. Antimicrobial and fermentation potential of himanthalia elongata in food applications. Microorganisms 8, 1–15.

Masarin, F., Paz Cedeno, F.R., Gabriel, E., Chavez, S., Ezequiel De Oliveira, L., Gelli, V.C., Monti, R., 2016. Chemical analysis and biorefinery of red algae Kappaphycus

alvarezii for efficient production of glucose from residue of carrageenan extraction process. Biotechnol. Biofuels 9.

McCormick, K., Kautto, N., 2013. The Bioeconomy in Europe: An Overview. Sustain. 5, 2589–2608.

Mehrnoush, A., Mustafa, S., Sarker, M.Z.I., Yazid, A.M.M., 2012. Optimization of Serine Protease Purification from Mango (Mangifera indica cv. Chokanan) Peel in Polyethylene Glycol/Dextran Aqueous Two Phase System. Int. J. Mol. Sci. 13, 3636–3649.

Mehrnoush, A., Mustafa, S., Yazid, A.M.M., 2011. “Heat-treatment aqueous two phase system” for purification of serine protease from kesinai (streblus asper) leaves. Molecules 16, 10202–10213.

Menon, V.V., 2012. Seaweed Polysaccharides - Food Applications. In: Handbook of Marine Macroalgae: Biotechnology and Applied Phycology. pp. 541–555.

Merchuk, J.C., Andrews, B.A., Asenjo, J.A., 1998. Aqueous two-phase systems for protein separation: Studies on phase inversion. J. Chromatogr. B Biomed. Sci. Appl. 711, 285–293.

Messyasz, B., Michalak, I., Łęska, B., Schroeder, G., Górka, B., Korzeniowska, K., Lipok, J., Wieczorek, P., Rój, E., Wilk, R., Dobrzyńska-Inger, A., Górecki, H., Chojnacka, K., 2017. Valuable natural products from marine and freshwater macroalgae obtained from supercritical fluid extracts. J. Appl. Phycol. 30, 591–603.

Mestechkina, N.M., Shcherbukhin, V.D., 2010. Sulfated polysaccharides and their anticoagulant activity: A review. Appl. Biochem. Microbiol. 46, 267–273.

Mhatre, Apurv, Gore, S., Mhatre, Akanksha, Trivedi, N., Sharma, M., Pandit, R., Anil, A., Lali, A., 2019. Effect of multiple product extractions on bio-methane potential of marine macrophytic green alga Ulva lactuca. Renew. Energy 132, 742–751.

Michalak, I., Chojnacka, K., 2014. Algal extracts: Technology and advances. Eng. Life Sci. 14, 581–591.

Mishra, B.B., Tiwari, V.K., 2011. Natural products: An evolving role in future drug

discovery. Eur. J. Med. Chem. 46, 4769–4807.

Mittal, R., Sharma, R., Raghavarao, K.S.M.S., 2019. Aqueous two-phase extraction of R-Phycoerythrin from marine macro-algae, Gelidium pusillum. Bioresour. Technol. 280, 277–286.

Modahl, I.S., Brekke, A., Valente, C., 2015. Environmental assessment of chemical products from a Norwegian biorefinery. J. Clean. Prod. 94, 247–259.

Morais, A.R., Bogel-Lukasik, R., 2013. Green chemistry and the biorefinery concept. Sustain. Chem. Process. 1, 18.

Morrissey, J., Kraan, S., Guiry, M.D.., 2001. A Guide to Commercially Important Seaweeds on the Irish Coast. Irish Sea Fisheries Board.

Murugesan, T., Perumalsamy, M., 2005. Liquid-liquid equilibria of poly(ethylene glycol) 2000 + sodium citrate + water at (25, 30, 35, 40, and 45) °C. J. Chem. Eng. Data 50, 1392–1395.

Nadeau, M.C., Kar, A., Roth, R., Kirchain, R., 2010. A dynamic process-based cost modeling approach to understand learning effects in manufacturing. Int. J. Prod. Econ. 128, 223–234.

Nascimento, S.S., Santos, V.S.V., Watanabe, E.O., de Souza Ferreira, J., 2020. Assessment of the purification of phycobiliproteins in cyanobacteria through aqueous two-phase systems with different proportions of PEG/salt. Food Bioprod. Process. 119, 345–349.

Nezammahalleh, H., Adams, T.A., Ghanati, F., Nosrati, M., Shojaosadati, S.A., 2018. Techno-economic and environmental assessment of conceptually designed in situ lipid extraction process from microalgae. Algal Res. 35, 547–560.

Nguyen, P.H., Choi, I.-W., Kim, S.-K., Jung, W.-K., 2012. Immune Regulatory Effects of Phlorotannins Derived From Marine Brown ALgae (Phaeophyta). In: Kim, S.-K. (Ed.), Handbook of Marine Macroalgae: Biotechnology and Applied Phycology. John Wiley & Sons, Ltd, pp. 340–347.

Nguyen, T.H., Granger, J., Pandya, D., Paustian, K., 2019. High-resolution multi-

objective optimization of feedstock landscape design for hybrid first and second generation biorefineries. Appl. Energy 238, 1484–1496.

Noyes, A., Basha, J., Frostad, J., Cook, S., Millard, D., Mullin, J., LaCasse, D., Wright, R.S., Huffman, B., Fahrner, R., Godavarti, R., Titchener-Hooker, N., Sunasara, K., Mukhopadhyay, T., 2015. A modular approach for the ultra-scale-down of depth filtration. J. Memb. Sci. 496, 199–210.

Ochsenreither, K., Glück, C., Stressler, T., Fischer, L., Syldatk, C., 2016. Production strategies and applications of microbial single cell oils. Front. Microbiol. 7.

Oelmeier, S.A., Dismer, F., Hubbuch, J., 2011. Application of an aqueous two-phase systems high-throughput screening method to evaluate mAb HCP separation. Biotechnol. Bioeng. 108, 69–81.

Oelmeier, S.A., Ladd Effio, C., Hubbuch, J., 2012. High throughput screening based selection of phases for aqueous two-phase system-centrifugal partitioning chromatography of monoclonal antibodies. J. Chromatogr. A 1252, 104–114.

Ögmundarson, Ó., Sukumara, S., Herrgård, M.J., Fantke, P., 2020. Combining Environmental and Economic Performance for Bioprocess Optimization. Trends Biotechnol. 38, 1203–1214.

Olivares-Molina, A., Fernández, K., 2016. Comparison of different extraction techniques for obtaining extracts from brown seaweeds and their potential effects as angiotensin I-converting enzyme (ACE) inhibitors. J. Appl. Phycol. 28, 1295–1302.

Ortiz, J., Romero, N., Robert, P., Araya, J., Lopez-Hernández, J., Bozzo, C., Navarrete, E., Osorio, A., Rios, A., 2006. Dietary fiber, amino acid, fatty acid and tocopherol contents of the edible seaweeds Ulva lactuca and Durvillaea antarctica. Food Chem. 99, 98–104.

Pádua, D., Rocha, E., Gargiulo, D., Ramos, A.A., 2015. Bioactive compounds from brown seaweeds: Phloroglucinol, fucoxanthin and fucoidan as promising therapeutic agents against breast cancer. Phytochem. Lett. 14, 91–98.

Palma, M., Barroso, C.G., 2002. Ultrasound-assisted extraction and determination of

tartaric and malic acids from grapes and winemaking by-products. Anal. Chim. Acta 458, 119–130.

Pangestuti, R., Kim, S.-K.K., 2015. An Overview of Phycocolloids: The Principal Commercial Seaweed Extracts. Mar. Algae Extr. Process. Prod. Appl. 1–2, 319–330.

Papoutsis, K., Pristijono, P., Golding, J.B., Stathopoulos, C.E., Bowyer, M.C., Scarlett, C.J., Vuong, Q. V., 2018. Optimizing a sustainable ultrasound-assisted extraction method for the recovery of polyphenols from lemon by-products: comparison with hot water and organic solvent extractions. Eur. Food Res. Technol. 244, 1353–1365.

Parsons, S., Allen, M.J., Abeln, F., McManus, M., Chuck, C.J., 2019. Sustainability and life cycle assessment (LCA) of macroalgae-derived single cell oils. J. Clean. Prod. 232, 1272–1281.

Patel, N., 2017. Development of aqueous two - phase separations by combining high - throughput screening and process modelling.

Peñuela, A., Robledo, D., Bourgougnon, N., Bedoux, G., Hernández-Núñez, E., Freile-Pelegrín, Y., 2018. Environmentally friendly valorization of Solieria filiformis (Gigartinales, rhodophyta) from IMTA using a biorefinery concept. Mar. Drugs 16.

Pérez-López, P., Balboa, E.M., González-García, S., Domínguez, H., Feijoo, G., Moreira, M.T., 2014. Comparative environmental assessment of valorization strategies of the invasive macroalgae Sargassum muticum. Bioresour. Technol. 161, 137–148.

Pérez, M.J., Falqué, E., Domínguez, H., 2016. Antimicrobial action of compounds from marine seaweed. Mar. Drugs 14, 1–38.

Philp, J., 2018. The bioeconomy, the challenge of the century for policy makers. N. Biotechnol. 40, 11–19.

Phong, W.N., Le, C.F., Show, P.L., Chang, J.-S., Ling, T.C., 2017. Extractive disruption process integration using ultrasonication and aqueous two-phase system for

proteins recovery from Chlorella sorokiniana. Eng. Life Sci. 17, 357–369.

Phong, W.N., Show, P.L., Ling, T.C., Juan, J.C., Ng, E.P., Chang, J.S., 2018. Mild cell disruption methods for bio-functional proteins recovery from microalgae—Recent developments and future perspectives. Algal Res. 31, 506–516.

Pomin, V.H., 2011. Structure and Use of Algal Sulfated Fucans and Galactans. In: Handbook of Marine Macroalgae: Biotechnology and Applied Phycology. pp. 229–261.

Prabhu, M.S., Israel, A., Palatnik, R.R., Zilberman, D., Golberg, A., 2020. Integrated biorefinery process for sustainable fractionation of Ulva ohnoi (Chlorophyta): process optimization and revenue analysis. J. Appl. Phycol. 32, 2271–2282.

Prasanna, R., Sood, A., Suresh, A., Nayak, S., Kaushik, B.D., 2007. Potentials and applications of algal pigments in biology and industry. Acta Bot. Hung. 49, 131–156.

Preece, K.E., Hooshyar, N., Krijgsman, A.J., Fryer, P.J., Zuidam, N.J., 2017. Pilot-scale ultrasound-assisted extraction of protein from soybean processing materials shows it is not recommended for industrial usage. J. Food Eng. 206, 1–12.

Price, C.A., 1965. A membrane method for determination of total protein in dilute algal suspensions. Anal. Biochem. 12, 213–218.

Puri, M., Sharma, D., Barrow, C.J., 2012. Enzyme-assisted extraction of bioactives from plants. Trends Biotechnol. 30, 37–44.

Raja, S., Murty, V.R., Thivaharan, V., Rajasekar, V., Ramesh, V., 2012. Aqueous Two Phase Systems for the Recovery of Biomolecules – A Review. Sci. Technol. 1, 7–16.

Rajak, R.C., Jacob, S., Kim, B.S., 2020. A holistic zero waste biorefinery approach for macroalgal biomass utilization: A review. Sci. Total Environ. 716, 137067.

Rajendran, K., Murthy, G.S., 2017. How does technology pathway choice influence economic viability and environmental impacts of lignocellulosic biorefineries? Biotechnol. Biofuels 1–19.

Rakel, N., Baum, M., Hubbuch, J., 2014. Moving through three-dimensional phase

diagrams of monoclonal antibodies. Biotechnol. Prog. 30, 1103–1113.

Rayat, A.C., Chatel, A., Hoare, M., Lye, G.J., 2016. Ultra scale-down approaches to enhance the creation of bioprocesses at scale: impacts of process shear stress and early recovery stages. Curr. Opin. Chem. Eng. 14, 150–157.

Reisky, L., Préchoux, A., Zühlke, M.K., Bäumgen, M., Robb, C.S., Gerlach, N., Roret, T., Stanetty, C., Larocque, R., Michel, G., Song, T., Markert, S., Unfried, F., Mihovilovic, M.D., Trautwein-Schult, A., Becher, D., Schweder, T., Bornscheuer, U.T., Hehemann, J.H., 2019. A marine bacterial enzymatic cascade degrades the algal polysaccharide ulvan. Nat. Chem. Biol. 15.

Rioux, L.-E.E., Beaulieu, L., Turgeon, S.L., 2017. Seaweeds: A traditional ingredients for new gastronomic sensation. Food Hydrocoll. 68, 255–265.

Rioux, L.E., Turgeon, S.L., Beaulieu, M., 2007. Characterization of polysaccharides extracted from brown seaweeds. Carbohydr. Polym. 69, 530–537.

Rodrigues, D., Costa-Pinto, A.R., Sousa, S., Vasconcelos, M.W., Pintado, M.M., Pereira, L., Rocha-Santos, T.A.P., Costa, João P. da, Silva, A.M.S., Duarte, A.C., Gomes, A.M.P., Freitas, A.C., Da Costa, Joao P., Silva, A.M.S., Duarte, A.C., Gomes, A.M.P., Freitas, A.C., 2019. Sargassum muticum and Osmundea pinnatifida Enzymatic Extracts: Chemical, Structural, and Cytotoxic Characterization. Mar. Drugs 17, 209.

Rodrigues Gurgel da Silva, A., Errico, M., Rong, B.-G.G., 2018. Techno-economic analysis of organosolv pretreatment process from lignocellulosic biomass. Clean Technol. Environ. Policy 20, 1401–1412.

Rodriguez-Jasso, R.M., Mussatto, S.I., Pastrana, L., Aguilar, C.N., Teixeira, J.A., 2011. Microwave-assisted extraction of sulfated polysaccharides (fucoidan) from brown seaweed. Carbohydr. Polym. 86, 1137–1144.

Rodríguez-Meizoso, I., Castro-Puyana, M., Börjesson, P., Mendiola, J.A., Turner, C., Ibáñez, E., 2012. Life cycle assessment of green pilot-scale extraction processes to obtain potent antioxidants from rosemary leaves. J. Supercrit. Fluids 72, 205–212.

Roe, S., 2001. Protein Purification Techniques: A Practical Approach.

Rój, E., Dobrzynska-Inger, A., Debczak, A., Kostrzewa, D., Stepnik, K., Dobrzyńska-Inger, A., Dębczak, A., Kostrzewa, D., Stępnik, K., 2015. Algae Extract Production Methods and Process Optimization. In: Marine Algae Extracts: Processes, Products, and Applications. pp. 101–120.

Rosa, P.A.J., Azevedo, A.M., Sommerfeld, S., Mutter, M., Aires-Barros, M.R., Bäcker, W., 2009. Application of aqueous two-phase systems to antibody purification: A multi-stage approach. J. Biotechnol. 139, 306–313.

Rosa, P.A.J., Ferreira, I.F., Azevedo, A.M., Aires-Barros, M.R., 2010. Aqueous two-phase systems: A viable platform in the manufacturing of biopharmaceuticals. J. Chromatogr. A 1217, 2296–2305.

Rostami, Z., Tabarsa, M., You, S.G., Rezaei, M., 2017. Relationship between molecular weights and biological properties of alginates extracted under different methods from Colpomenia peregrina. Process Biochem. 58, 289–297.

Rozo, G., Rozo, C., Puyana, M., Ramos, F.A., Almonacid, C., Castro, H., 2019. Two compounds of the Colombian algae Hypnea musciformis prevent oxidative damage in human low density lipoproteins LDLs. J. Funct. Foods 60, 103399.

Ruangrit, K., Chaipoot, S., Phongphisutthinant, R., Duangjan, K., Phinyo, K., Jeerapan, I., Pekkoh, J., Srinuanpan, S., 2021. A successful biorefinery approach of macroalgal biomass as a promising sustainable source to produce bioactive nutraceutical and biodiesel. Biomass Convers. Biorefinery.

Ruiz, H.A., Rodríguez-Jasso, R.M., Fernandes, B.D., Vicente, A.A., Teixeira, J.A., 2013. Hydrothermal processing, as an alternative for upgrading agriculture residues and marine biomass according to the biorefinery concept: A review. Renew. Sustain. Energy Rev. 21, 35–51.

Sadhukhan, J., Gadkari, S., Martinez-Hernandez, E., Ng, K.S., Shemfe, M., Torres-Garcia, E., Lynch, J., 2019. Novel macroalgae (seaweed) biorefinery systems for integrated chemical, protein, salt, nutrient and mineral extractions and

environmental protection by green synthesis and life cycle sustainability assessments. Green Chem. 21, 2635–2655.

Samaraweera, A.M., Vidanarachchi, J.K., Kurukulasuriya, M.S., 2012. Industrial Applications of Macroalgae. In: Kim, S.-K. (Ed.), Handbook of Marine Macroalgae. John Wiley & Sons, Ltd, Chichester, UK, pp. 500–521.

Sampath-Wiley, P., Neefus, C.D., 2007. An improved method for estimating R-phycoerythrin and R-phycocyanin contents from crude aqueous extracts of Porphyra (Bangiales, Rhodophyta). J. Appl. Phycol. 19, 123–129.

Sánchez-Machado, D.I.I., López-Cervantes, J., López-Hernández, J., Paseiro-Losada, P., 2004. Fatty acids, total lipid, protein and ash contents of processed edible seaweeds. Food Chem. 85, 439–444.

Sanjeewa, K.K.A., Jayawardena, T.U., Kim, S.Y., Kim, H.S., Ahn, G., Kim, J., Jeon, Y.J., 2019. Fucoidan isolated from invasive Sargassum horneri inhibit LPS-induced inflammation via blocking NF-κB and MAPK pathways. Algal Res. 41, 101561.

Santos, C.I., Silva, C.C., Mussatto, S.I., Osseweijer, P., van der Wielen, L.A.M., Posada, J.A., 2018. Integrated 1st and 2nd generation sugarcane bio-refinery for jet fuel production in Brazil: Techno-economic and greenhouse gas emissions assessment. Renew. Energy 129, 733–747.

Santos, S.A.O., Félix, R., Pais, A.C.S., Rocha, S.M., Silvestre, A.J.D., 2019. The Quest for Phenolic Compounds from Macroalgae: A Review of Extraction and Identification Methodologies. Biomolecules 9, 847.

Saravana, P.S., Cho, Y.-N.N., Woo, H.-C.C., Chun, B.-S.S., 2018. Green and efficient extraction of polysaccharides from brown seaweed by adding deep eutectic solvent in subcritical water hydrolysis. J. Clean. Prod. 198, 1474–1484.

Saravana, P.S., Tilahun, A., Gerenew, C., Tri, V.D., Kim, N.H., Kim, G. Do, Woo, H.C., Chun, B.S., 2017. Subcritical water extraction of fucoidan from Saccharina japonica: optimization, characterization and biological studies. J. Appl. Phycol. 1–12.

Schiener, P., Atack, T., Wareing, R., Kelly, M.S., Hughes, A.D., 2016. The by-products

from marine biofuels as a feed source for the aquaculture industry: a novel example of the biorefinery approach. Biomass Convers. Biorefinery 6, 281–287.

Schiener, P., Zhao, S., Theodoridou, K., Carey, M., Mooney-McAuley, K., Greenwell, C., 2017. The nutritional aspects of biorefined Saccharina latissima, Ascophyllum nodosum and Palmaria palmata. Biomass Convers. Biorefinery 7, 221–235.

Schmid, M., Guihéneuf, F., Stengel, D.B., 2017. Ecological and commercial implications of temporal and spatial variability in the composition of pigments and fatty acids in five Irish macroalgae. Mar. Biol. 164.

Schmid, M., Stengel, D.B., 2015. Intra-thallus differentiation of fatty acid and pigment profiles in some temperate Fucales and Laminariales. J. Phycol. 51, 25–36.

Schoenwaelder, M., Wiencke, C., 1999. Phenolic Compounds in the Embryo Development of Several Northern Hemisphere Fucoids. Plant Biol. 2, 24–33.

Schubert, N., García-Mendoza, E., Pacheco-Ruiz, I., 2006. Carotenoid Composition of Marine Red Algae. J. Phycol. 42, 1208–1216.

Seghetta, M., Hou, X., Bastianoni, S., Bjerre, A.B., Thomsen, M., 2016. Life cycle assessment of macroalgal biorefinery for the production of ethanol, proteins and fertilizers ? A step towards a regenerative bioeconomy. J. Clean. Prod. 137, 1158–1169.

Seghetta, M., Romeo, D., D'Este, M., Alvarado-Morales, M., Angelidaki, I., Bastianoni, S., Thomsen, M., 2017. Seaweed as innovative feedstock for energy and feed – Evaluating the impacts through a Life Cycle Assessment. J. Clean. Prod. 150, 1–15.

Shannon, E., Abu-Ghannam, N., 2017. Optimisation of fucoxanthin extraction from Irish seaweeds by response surface methodology. J. Appl. Phycol. 29, 1027–1036.

Shannon, E., Abu-Ghannam, N., 2018. Enzymatic extraction of fucoxanthin from brown seaweeds. Int. J. Food Sci. Technol. 53, 1–10.

Shannon, E., Abu-Ghannam, N., 2019. Seaweeds as nutraceuticals for health and nutrition. Phycologia 58, 563–577.

Sharma, M., Prakash Chaudhary, J., Mondal, D., Meena, R., Prasad, K., 2015. A green

and sustainable approach to utilize bio-ionic liquids for the selective precipitation of high purity agarose from an agarophyte extract. Green Chem. 17, 2867–2873.

Sheldon, R.A., 2018. Metrics of Green Chemistry and Sustainability: Past, Present, and Future. ACS Sustain. Chem. Eng. 6, 32–48.

Shi, R., Guest, J.S., 2020. BioSTEAM-LCA: An Integrated Modeling Framework for Agile Life Cycle Assessment of Biore fi neries under Uncertainty. ACS Sustain. Chem. Eng. 8, 18903–18914.

Shirsath, S.R., Sonawane, S.H., Gogate, P.R., 2012. Intensification of extraction of natural products using ultrasonic irradiations-A review of current status. Chem. Eng. Process. Process Intensif. 53, 10–23.

Sinha, R.P., Singh, S.P., Häder, D.P., 2007. Database on mycosporines and mycosporine-like amino acids (MAAs) in fungi, cyanobacteria, macroalgae, phytoplankton and animals. J. Photochem. Photobiol. B Biol. 89, 29–35.

Slocombe, S.P., Ross, M., Thomas, N., McNeill, S., Stanley, M.S., 2013. A rapid and general method for measurement of protein in micro-algal biomass. Bioresour. Technol. 129, 51–57.

Smit, A.J., 2004. Medicinal and pharmaceutical uses of seaweed natural products: A review. J. Appl. Phycol. 16, 245–262.

Soares, R.R.G., Azevedo, A.M., Van Alstine, J.M., Raquel Aires-Barros, M., 2015. Partitioning in aqueous two-phase systems: Analysis of strengths, weaknesses, opportunities and threats. Biotechnol. J. 10, 1158–1169.

Soh, L., Eckelman, M.J., 2016. Green solvents in biomass processing. ACS Sustain. Chem. Eng. 4, 5821–5837.

Song, S., Wu, S., Ai, C., Xu, X., Zhu, Z., Cao, C., Yang, J., Wen, C., 2018. Compositional analysis of sulfated polysaccharides from sea cucumber (Stichopus japonicus) released by autolysis reaction. Int. J. Biol. Macromol. 114, 420–425.

Soto-Maldonado, C., Zúñiga-Hansen, M.E., 2017. Enzyme-Assisted Extraction of Phenolic Compounds. In: Water Extraction of Bioactive Compounds. Elsevier Inc.,

pp. 369–384.

Stengel, D.B., Connan, S., Popper, Z.A., 2011. Algal chemodiversity and bioactivity: Sources of natural variability and implications for commercial application. Biotechnol. Adv. 29, 483–501.

Stengel, D.B., Dring, M.J., 1998. Seasonal variation in the pigment content and photosynthesis of different thallus regions of Ascophyllum nodosum (Fucales, Phaeophyta) in relation to position in the canopy. Phycologia 37, 259–268.

Sugiono, S., Ferdiansyah, D., 2019. Biorefinery Sequential Extraction of Alginate by Conventional and Hydrothermal Fucoidan from the Brown Alga, Sargassum cristaefolium. Biosci. Biotechnol. Res. Commun. 12, 894–903.

Suleria, H., Osborne, S., Masci, P., Gobe, G., 2015. Marine-Based Nutraceuticals: An Innovative Trend in the Food and Supplement Industries. Mar. Drugs 13, 6336–6351.

Swarr, T.E., Hunkeler, D., Klöpffer, W., Pesonen, H., Ciroth, A., Brent, A.C., Pagan, R., 2011. Environmental life-cycle costing : a code of practice. Int. J. Life Cycle Assess. 16, 389–391.

Takaichi, S., Yokoyama, A., Mochimaru, M., Uchida, H., Murakami, A., 2016. Carotenogenesis diversification in phylogenetic lineages of Rhodophyta. J. Phycol. 52, 329–338.

Tang, Z.C., Zhenzhou, L., Zhiwen, L., Ningcong, X., 2015. Uncertainty analysis and global sensitivity analysis of techno-economic assessments for biodiesel production. Bioresour. Technol. 175, 502–508.

Tanniou, A., Vandanjon, L., Incera, M., Serrano Leon, E., Husa, V., Le Grand, J., Nicolas, J.-L., Poupart, N., Kervarec, N., Engelen, A., Walsh, R., Guerard, F., Bourgougnon, N., Stiger-Pouvreau, V., 2013. Assessment of the spatial variability of phenolic contents and associated bioactivities in the invasive alga Sargassum muticum sampled along its European range from Norway to Portugal. J. Appl. Phycol. 1–16.

Terasaki, M., Hirose, A., Narayan, B., Baba, Y., Kawagoe, C., Yasui, H., Saga, N., Hosokawa, M., Miyashita, K., 2009. Evaluation of recoverable functional lipid components of several brown seaweeds (phaeophyta) from Japan with special reference to fucoxanthin and fucosterol contents1. J. Phycol. 45, 974–980.

Terme, N., Boulho, R., Kucma, J.P., Bourgougnon, N., Bedoux, G., 2018. Radical scavenging activity of lipids from seaweeds isolated by solid-liquid extraction and supercritical fluids. OCL - Oilseeds fats, Crop. Lipids 25.

Thomas, N.V., Kim, S.-K., 2013. Beneficial effects of marine algal compounds in cosmeceuticals. Mar. Drugs 11, 146–64.

Thomassen, G., Van Passel, S., Dewulf, J., 2020. A review on learning effects in prospective technology assessment. Renew. Sustain. Energy Rev. 130, 109937.

Tibbetts, S.M., Milley, J.E., Lall, S.P., 2016. Nutritional quality of some wild and cultivated seaweeds: Nutrient composition, total phenolic content and in vitro digestibility. J. Appl. Phycol. 28, 1–11.

Torres-Acosta, M.A., Mayolo-Deloisa, K., González-Valdez, J., Rito-Palomares, M., 2019. Aqueous Two-Phase Systems at Large Scale: Challenges and Opportunities. Biotechnol. J. 14, 1–12.

Torres, Maria Dolores, Flórez-Fernández, N., Domínguez, H., 2019. Integral utilization of red seaweed for bioactive production. Mar. Drugs 17.

Torres, M. D., Kraan, S., Domínguez, H., Domı, H., 2019. Seaweed biorefinery. Rev. Environ. Sci. Bio/Technology 0123456789, 335–388.

Towler, G., Sinnott, R., 2008. Chemical Engineering Design: Principles, Practice and Economics of Plant and Process Design, First Edit. ed. Elsevier Inc.

Troncoso, N., Saavedra, R., Olivares-Molina, A., Farías, J., San-Martín, S., Urrutia, H., Agurto, C., 2015. Identification of antibacterial compounds obtained from seaweeds present in the Biobío Region, Chile. Rev. Biol. Mar. Oceanogr. 50, 199–204.

Tyskiewicz, K., Tyskiewicz, R., Konkol, M., Rój, E., Jaroszuk-Sciseł, J., Skalicka-Wozniak, K., 2019. Antifungal Properties of Fucus vesiculosus L. Supercritical Fluid

Extract against Fusarium culmorum and Fusarium oxysporum. Molecules 24.

UNEP/SETAC Life Cycle Initiative, 2011. Global Guidance principles for life cycle assessment databases. Science (80-.). 160.

Vásquez, V., Martínez, R., Bernal, C., 2019. Enzyme-assisted extraction of proteins from the seaweeds Macrocystis pyrifera and Chondracanthus chamissoi: characterization of the extracts and their bioactive potential. J. Appl. Phycol. 31, 1999–2010.

Vavilala, S.L., D'Souza, J.S., 2015. Algal Polysaccharides and Their Biological Applications. In: Marine Algae Extracts: Processes, Products and Applications. pp. 411–451.

Venkatesan, J., Anil, S., Kim, S.-K., 2017. Seaweed Polysaccharides: Isolation, Biological and Biomedical Applications.

Vera, J., Castro, J., Gonzalez, A., Moenne, A., 2011. Seaweed polysaccharides and derived oligosaccharides stimulate defense responses and protection against pathogens in plants. Mar. Drugs 9, 2514–25.

Vicente, F.A., Cardoso, I.S., Martins, M., Gonçalves, C.V.M., Dias, A.C.R. V., Domingues, P., Coutinho, J.A.P., Ventura, S.P.M., 2019. R-phycoerythrin extraction and purification from fresh Gracilaria sp. using thermo-responsive systems . Green Chem.

Viera, I., Pérez-Gálvez, A., Roca, M., 2018. Bioaccessibility of Marine Carotenoids. Mar. Drugs 16, 397.

Vilkhu, K., Mawson, R., Simons, L., Bates, D., 2008. Applications and opportunities for ultrasound assisted extraction in the food industry - A review. Innov. Food Sci. Emerg. Technol. 9, 161–169.

Wan-Loy, C., Siew-Moi, P., 2016. Marine Algae as a Potential Source for Anti-Obesity Agents. Mar. Drugs 2016, Vol. 14, Page 222 14, 222.

Wang, L., Weller, C.L., 2006. Recent advances in extraction of nutraceuticals from plants. Trends Food Sci. Technol. 17, 300–312.

Wang, Xueliang, Wang, Xin, Jiang, H., Cai, C., Li, G., Hao, J., Yu, G., 2018. Marine polysaccharides attenuate metabolic syndrome by fermentation products and altering gut microbiota: An overview. Carbohydr. Polym. 195, 601–612.

Ward, O.P., Singh, A., 2005. Omega-3/6 fatty acids: Alternative sources of production. Process Biochem. 40, 3627–3652.

Wellburn, A.R., 1994. The Spectral Determination of Chlorophylls a and b, as well as Total Carotenoids, Using Various Solvents with Spectrophotometers of Different Resolution. J. Plant Physiol. 144, 307–313.

Wenda, S., Illner, S., Mell, A., Kragl, U., 2011. Industrial biotechnology—the future of green chemistry? Green Chem. 13, 3007–3047.

Wernet, G., Bauer, C., Steubing, B., Reinhard, J., Moreno-Ruiz, E., Weidema, B., 2016. The ecoinvent database version 3 (part I): overview and methodology. Int. J. Life Cycle Assess. 21, 1218–1230.

Westermeier, R., Gómez, I., 1996. Biomass, Energy Contents and Major Organic Compounds in the Brown Alga Lessonia nigrescens (Laminariales, Phaeophyceae) from Mehuín, South Chile. Bot. Mar. 39, 553–560.

White, W.L., Wilson, P., 2015. World seaweed utilization. In: Tiwari, B.K., Troy, D.J. (Eds.), Seaweed Sustainability: Food and Non-Food Applications. Elsevier Inc., pp. 7–25.

Widjanarko, S.B., Soehono, L.A., Sugiono, Bambang Widjanarko, S., Adi Soehono, L., Widjanarko, S.B., Soehono, L.A., 2014. Extraction Optimization by Response Surface Methodology and Characterization of Fucoidanfrom Brown Seaweed Sargassum polycystum. Int. J. ChemTech Res. 6, 195–205.

Wiendahl, M., Oelmeier, S.A., Dismer, F., Hubbuch, J., 2012. High-throughput screening-based selection and scale-up of aqueous two-phase systems for pDNA purification. J. Sep. Sci. 35, 3197–3207.

Wijesinghe, W.A.J.P., Jeon, Y.-J., 2012. Enzyme-assistant extraction (EAE) of bioactive components: a useful approach for recovery of industrially important metabolites

from seaweeds: a review. Fitoterapia 83, 6–12.

Wood, D., Capuzzo, E., Kirby, D., Mooney-McAuley, K., Kerrison, P., 2017. UK macroalgae aquaculture: What are the key environmental and licensing considerations? Mar. Policy 83, 29–39.

Wright, S.W., Jeffrey, S.W., Mantoura, R.F.C., Llewellyn, C.A., Bjørnland, T., Repeta, D., Welschmeyer, N., 1991. Improved HPLC method for the analysis of chlorophylls and carotenoids from marine phytoplankton. Mar. E 77, 183–196.

Xavier, L., Freire, M.S., Vidal-Tato, I., González-Álvarez, J., 2014. Aqueous two-phase systems for the extraction of phenolic compounds from eucalyptus (*Eucalyptus globulus*) wood industrial wastes. J. Chem. Technol. Biotechnol. 89, 1772–1778.

Xavier, L., Freire, M.S., Vidal-Tato, I., González-Álvarez, J., 2015. Application of aqueous two phase systems based on polyethylene glycol and sodium citrate for the recovery of phenolic compounds from Eucalyptus wood. Maderas. Cienc. y Tecnol. 17, 0–0.

Xavier, L., Freire, M.S., Vidal-Tato, I., González-Álvarez, J., 2017. Recovery of Phenolic Compounds from Eucalyptus globulus Wood Wastes using PEG/phosphate Aqueous Two-Phase Systems. Waste and Biomass Valorization 8, 443–452.

Yuan, Y., Macquarrie, D., 2015a. Microwave assisted extraction of sulfated polysaccharides (fucoidan) from Ascophyllum nodosum and its antioxidant activity. Carbohydr. Polym. 129, 101–107.

Yuan, Y., Macquarrie, D.J., 2015b. Microwave assisted step-by-step process for the production of fucoidan, alginate sodium, sugars and biochar from Ascophyllum nodosum through a biorefinery concept. Bioresour. Technol. 198, 819–827.

Yuan, Y., Zhang, J., Fan, J., Clark, J., Shen, P., Li, Y., Zhang, C., 2018. Microwave assisted extraction of phenolic compounds from four economic brown macroalgae species and evaluation of their antioxidant activities and inhibitory effects on α-amylase, α-glucosidase, pancreatic lipase and tyrosinase. Food Res. Int. 113, 288–297.

Yunpu, W., Leilei, D., Liangliang, F., Shaoqi, S., Yuhuan, L., Roger, R., 2016. Review of microwave-assisted lignin conversion for renewable fuels and chemicals. J. Anal. Appl. Pyrolysis 119, 104–113.

Zhang, R., Yuen, A.K.L., Magnusson, M., Wright, J.T., de Nys, R., Masters, A.F., Maschmeyer, T., 2018. A comparative assessment of the activity and structure of phlorotannins from the brown seaweed Carpophyllum flexuosum. Algal Res. 29, 130–141.

Zhang, X., Thomsen, M., 2021. Techno-economic and environmental assessment of novel biorefinery designs for sequential extraction of high-value biomolecules from brown macroalgae Laminaria digitata, Fucus vesiculosus, and Saccharina latissima. Algal Res. 60, 102499.

Zhao, Y., Zheng, Y., Wang, J., Ma, S., Yu, Y., White, W., Yang, S., Yang, F., Lu, J., 2018. Fucoidan Extracted from Undaria pinnatifida: Source for Nutraceuticals/Functional Foods. Mar. Drugs 16, 321.

Zimmermann, A.W., Wunderlich, J., Müller, L., Buchner, G.A., Marxen, A., Michailos, S., Armstrong, K., Naims, H., Mccord, S., Styring, P., Sick, V., Schomäcker, R., 2020. Techno-Economic Assessment Guidelines for CO 2 Utilization. Front. Energy Res. 8, 1–23.

Zimmermann, S., Scheeder, C., Zimmermann, P.K., Bogsnes, A., Hansson, M., Staby, A., Hubbuch, J., 2017. High-throughput downstream process development for cell-based products using aqueous two-phase systems (ATPS) – A case study. Biotechnol. J. 12.

Zubia, M., Payri, C., Deslandes, E., 2008. Alginate, mannitol, phenolic compounds and biological activities of two range-extending brown algae, Sargassum mangarevense and Turbinaria ornata (Phaeophyta: Fucales), from Tahiti (French Polynesia). J. Appl. Phycol. 20, 1033–1043.

.

Appendix A: List of key assumptions for the techno-economic analysis of all biorefinery scenarios

Table A-1. Key assumptions for the TEA of the scenarios evaluated in this project.

Key analysis inputs				
Flowsheet	*Solvent-based*	*Novel Tech*	*Green Chem v1*	*Green Chem v2*
Biomass/batch	3,425 kg	3,425 kg	3,425 kg	3,425 kg
Duration	49.7 h	33.1 h	41.0 h	23.5 h
Final residue/batch	1,370.2 kg	1,303.4 kg	1,291.2 kg	1,517.8 kg
Fucoxanthin extraction				
Mode	Batch	Batch	Batch	-
Duration	4.61 h	4 h	2 h	-
Yield	0.07% DW	0.08% DW	0.26% DW	-
Volumetric conc.	62.2 %v/v	0.002 % w/v	27:15.25 w/w	-
Fucoxanthin recovered	2.6 kg	2.8 kg	8.9 kg	-
Reference	*Shannon and Abu-Ghannam (2017)*	*Phong et al. (2017)*	*Gómez-Loredo et al. (2014)*	-
Lipid extraction				
Mode	Batch	Batch	-	-
Duration	3 h	4 h	-	-
Yield	1.98% DW	8.15% DW	-	-
Volumetric conc.	10:1	5:1	-	-
Lipid recovered	67.8 kg	279.1 kg	-	-
Reference	*Ashokkumar et al. (2017)*	*Ashokkumar et al. (2017)*	-	-
Protein extraction				
Mode	-	-	Batch	Batch
Duration	-	-	4.5 h	6.0 h
Yield	-	-	18.00% DW	3.78% DW
Volumetric conc.	-	-	20:30 w/w	20:30 w/w
Protein recovered	-	-	603.3 kg	129.5 kg
Reference	-	-	*Phong et al. (2017)*	*This study*
Polyphenol extraction				
Mode	Batch	Batch	Batch	Batch
Duration	6 h	1.1 h	1.5 h	1.5 h
Yield	7.99%DW	13.58% DW	1.89% DW	4.07% DW
Volumetric conc.	70:30 v/v	0.033% w/v	22:10.5 w/w	27:4 w/w
Polyphenol recovered	267.2 kg	465.2 kg	64.6 kg	139.4 kg
Reference	*Koivikko et al. (2005)*	*Magnusson et al. (2017)*	*Xavier et al. (2017)*	*This study*
Fucoidan extraction				
Mode	Batch	Batch	Batch	Batch
Duration	18.1 h	12.3 h	18.1 h	5.0 h
Yield	3.15% DW	14.09% DW	3.15% DW	11.92% DW
Volumetric conc.	7.5% w/v	7.5% w/v	7.5% w/v	7.5% w/v
Fucoidan recovered	107.9 kg	482.6 kg	107.9 kg	408.2 kg
Reference	*Lorbeer et al. (2015a)*	*Yuan and Macquarrie (2015a)*	*Lorbeer et al. (2015a)*	*This study*
Alginate extraction				
Mode	Batch	Batch	Batch	Batch
Duration	18 h	12.17 h	18 h	10 h
Yield	39.00% DW	18.24% DW	39.00% DW	35.91% DW
Volumetric conc.	7.5% w/v	7.5% w/v	7.5% w/v	7.5% w/v
Alginate recovered	1,335.8 kg	624.7 kg	1,335.8 kg	1,229.8 kg
Reference	*Lorbeer et al. (2015a)*	*Yuan and Macquarrie (2015a)*	*Lorbeer et al. (2015a)*	*This study*

Unit costs				
Acetone	£1.99/kg	£1.99/kg	-	-
HCl	£0.17/kg	£0.17/kg	£0.17/kg	-
Ethanol	£0.87/L	£0.87/L	£0.87/L	£0.87/L
Na_2CO_3	£0.14/kg	£0.14/kg	£0.14/kg	£0.14/kg
Cyclohexane	£1.04/kg	£1.04/kg	-	-
Methanol		£0.69/L	£0.69	£0.69
PEG 2000	-	-	£1.04/kg	£1.04/kg
KH_2PO_4	-	-	-	£0.80/kg
K_2HPO_4	-	-	£0.91/kg	£0.91/kg
K_3PO_4	-	-	£1.04/kg	£1.04/kg
$CaCl_2$	-	£0.66/kg	-	-
Citric acid	-	-	-	£0.04/kg
Water	£0.001/L	£0.001/L	£0.001/L	£0.001/L
Electricity	£0.13/kWh	£0.13/kWh	£0.13/kWh	£0.13/kWh
Key analysis outputs				
Number of batches	292	292	292	292
Campaign time	300 d	300 d	300 d	300 d

Table A-2. Labour costs assumed for the operation of the biorefinery scenarios.

Labour	**Annual salary**	**Operators per section**	**Process sections**	**Shifts**	**Total**
Production operator	£40,000	2	5	3	£1,200,000
Production supervisor	£60,000	1	5	3	£900,000
QC	£40,000	2	1	3	£240,000
QA	£40,000	2	1	3	£240,000

Table A-3. Capital costs assumptions for the biorefinery scenarios in this project.

Capital investment (CAPEX)	**Value**	**Unit**
Contingency	10	%
Lang factor	3.0	-
Total equipment purchases cost (TEPC)	Σ(£equipment)	£
Fixed capital investment (FCI)	TEPC*Lang factor	£
Working capital (WC)	FCI*0.05	£
Total capital investment	FCI+WC	£
Indirect costs (IC)	**Value**	**Unit**
Maintenance	FCI*0.1	£/y
Local taxes	FCI*0.02	£/y
Insurance	FCI*0.01	£/y
Depreciation	FCI*0.1	£/y
Direct costs (DC)		
Raw materials	Σ[£(materials)*vol. conc.]	£/y
Utilities	Σ[£(utilities)*total consumption]	£/y
Labour	Σ[£(labour)*no. operators]	£/y
Process cost		
Cost of goods (CoG)	IC+DC	£/y
CoG per processed biomass	CoG/annual input	£/kg
Production costs	DC/annual input	£/kg

Appendix B: Process flowsheet calculations

Extraction operation

The extraction operation started calculating the amount of extractant needed for the operation to be performed; hence the amount V_{solv} of extractant was calculated using the equation below:

$$V_{Solv} = \frac{B_i}{\left(\frac{S}{L}\right)}$$

Where, B_i = initial biomass

S/L = solid:liquid ratio

To calculate the amount of a given high-value compound recovered from an extraction stage the following equation was used:

$$Ext = B_i \times Rec\%$$

Where, Ext = recovered extract

B_i = biomass at the start of the operation

Rec% = recovery yield

Centrifugation operation

Centrifugation is performed using a continuous disc-stack centrifuge. Based on the volume to be processed and the target concentration factor to achieve in the given timeframe, given between 2 – 4 hours, the total required flow rate is calculated.

$$F = \frac{V}{t \times CF \times R}$$

Where: F = total flow rate

t = time of operation

CF = clarification factor

R = removal efficiency

Heating processes

When heating was required the specific heat relation was applied, whereas heat was needed for the extraction process i.e., fucoidan in *Solvent-based* scenario, polyphenols in *Novel Tech* scenario, or to recover solvents in the lipids extraction stages, using the formula below:

$$Q = mc_p\Delta T$$

Where, Q = heat energy needed

m = mass of extraction mix (assumed with a density of 1 g/mL)

c_p = specific heat

ΔT = change in temperature

Table B-1. Equipment list for purchase in a biorefinery scenario based in the use of solvents.

	Equipment	Capacity	Unit	Actual cost	Actual consumption (kWh/m^3)	No. of units	Total cost	Total consumption (kWh/m^3)
Fucoxanthin	Pump	10,714	L/h	£9,160	0.05	8	£73,280	0.4
	Agitation tank	49,978	L	£315,227	197.47	2	£630,454	394.93
	Centrifuge	10,465	L/h	£1,017,266	20	2	£2,034,533	502.33
	Washing tank	49,978	L	£315,227	7.41	2	£630,454	14.82
	Filter	5,000	L	10,294	0	2	£20,587	0
	Storage tank	342,843	L	£745,619	0	1	£745,619	0
Lipids	Pump	3893	L/h	£9,160	0.05	6	54,960	0.3
	Agitation tank	93,433	L	£464,435	4.94	2	£928,871	9.87
	Centrifuge	39,929	L/h	£2,271,718	20	2	£4,543,436	718.71
	Re-agitation tank	93,433	L	£464,435	4.94	2	£928,871	9.87
Polyphenol	Pump	28041	L/h	£9,160	0.05	5	£45,800	0.25
	Agitation tank	806,759	L	£1,693,059	19.75	2	£3,386,117	39.49
	Centrifuge	172,384	L/h	£5,463,653	20	2	£10,927,306	12,411.68
	Storage tank	560,825	L	£993,415	0	1	£993,415	0
Fucoidan	Pump	5,728	L/h	£9,160	0.05	7	£64,120	0.35
	Agitation tank	80,184	L	£423,720	9.87	2	£847,440	19.75
	Centrifuge	160,368	L	£1,367,382	20	2	£2,734,764	1,233.6
	Precipitation tank	17,133	L	£472,641	0	2	£945,282	0
Alginate	Pump	8,712	L/h	£9,160	0.05	9	£82,440	0.45
	Agitation tank	78,404	L	£418,050	9.87	2	£836,100	19.75
	Dilution tank	313,615	L	£706,804	49.37	2	£1,413,608	98.73
	Centrifuge 1	16,753	L/h	£3,099,382	20	2	£6,198,765	1,206.2
	Precipitation tank	313,615	L	£706,804	0	1	£706,804	0
	Centrifuge 2	16,753	L/h	3,099,382	20	2	6,198,765	4,824.85

Table B-2. Equipment list for purchase in a biorefinery scenario using novel technologies

	Equipment	Capacity	Unit	Actual cost	Actual consumption (kWh/m^3)	No. of units	Total cost	Total consumption (kWh/m^3)
Fucoxanthin	Pump		L/h	£9,160	0.05	6	£54,960	0.3
	Agitation tank UAE	48,978	L	£315,227	197.47	2	£630,454	394.93
	Centrifuge	10,465	L/h	£1,651,911	20	2	£3,303,822	26.84
	Dilution tank	393,077	L	£792,883	0	2	£1,585,766	0
Lipid	Pump	7,058	L/h	£9,160	0.05	2	£18,320	0.1
	Ultrasound extractor	56,467	L	£1,385,220	3.75	1	£1,385,220	211,752
	Distiller	56,467	L	£2,502	4	1	£2,520	225,869
Polyphenol	Pump		L/h	£9,160	0.05	2	£18,320	0.1
	Microwave extractor	115,901	L	£17,412,803	3.75	1	£17,412,803	434,630
	Filter housing	5,000	L	£7,254	0.05	1	£7,254	1.08
	Filter	5,000	L	£10,294	0	2	£20,587	0
Fucoidan	Pump		L/h	£9,160	0.05	7	£64,120	0.35
	Microwave extractor	59,782	L	£11,704,688	3.75	1	£11,704,688	224,184
	Centrifuge 1	12,774	L/h	£1,861,800	20	2	£3,723,599	129
	Washing tank	153,291	L	£450,643	0	2	£901,286	0
	Centrifuge 2	32,755	L/h	£3,275,664	20	2	£6,551,327	129
Alginate	Pump		L/h	£9,160	0.05	7	£64,120	0.35
	Microwave extractor	55,868	L	£11,238,637	3.75	1	£11,238,637	209,505
	Centrifuge	11,938	L/h	£1,787,667	20	2	£3,575,335	129.47
	Precipitation tank	80,977	L	£426,229	0	2	£852,459	0
	Centrifuge	22,494	L/h	£2,614,403	20	2	£5,228,806	129.47

Table B-3. Equipment list for purchase in a biorefinery scenario using green chemistry principles

	Equipment	Capacity	Unit	Actual cost	Actual consumption (kWh/m^3)	No. of units	Total cost	Total consumption (kWh/m^3)
Fucoxanthin	Pump		L/h	£9,160	0.05	4	£36,640	0.2
	Extraction tank	13,358	L	£106,389	197.47	1	£106,389	14.7
	Settling tank	13,358	L	£106,389	20	1	£106,389	0
	Centrifuge	2,854	L/h	£466,522	7.41	2	£933,043	205.5
Protein	Pump		L/h	£9,160	0.05	2	£18,320	0.1
	Extraction tank	1,679,033	L	£2,628,216	197.47	1	£2,628,216	197.47
	Centrifuge	104,940	L/h	£37,783	20	1	£37,783	839.5
Polyphenol	Pump		L/h	£9,160	0.05	2	£18,320	0.1
	Extraction tank	93,259	L	£1,316,344	4.94	1	£1,316,344	4.94
	Filter housing	1,427	L/h	£7,254	0.05	1	£7,254	1.08
	Filter			£10,294	0	2	£20,587	0
Fucoidan	Pump	5,728	L/h	£9,160	0.05	7	£64,120	0.35
	Agitation tank	80,184	L	£423,720	9.87	2	£847,440	19.75
	Centrifuge	160,368	L	£1,367,382	20	2	£2,734,764	1,233.6
	Precipitation tank	17,133	L	£472,641	0	2	£945,282	0
Alginate	Pump	8,712	L/h	£9,160	0.05	9	£82,440	0.45
	Agitation tank	78,404	L	£418,050	9.87	2	£836,100	19.75
	Dilution tank	313,615	L	£706,804	49.37	2	£1,413,608	98.73
	Centrifuge 1	16,753	L/h	£3,099,382	20	2	£6,198,765	1,206.2
	Precipitation tank	313,615	L	£706,804	0	1	£706,804	0
	Centrifuge 2	16,753	L/h	3,099,382	20	2	6,198,765	4,824.85

Table B-4. Equipment purchase list for the updated green chemistry biorefinery.

	Equipment	Capacity	Unit	Actual cost	Actual consumption (kWh/m^3)	No. of units	Total cost	Total consumption (kWh/m^3)
Fucoidan	Pump		L/h	£9,160	0.05	6	£54,960	0.3
	Agitation tank	93,493	L	£464,615	9.87	2	£929,231	19.75
	Centrifuge	19,977	L/h	£1,499,355	20	2	£2,998,711	958.90
	Precipitation tank	280,479	L	£660,999	0	2	£1,321,999	0
Alginate	Pump		L/h	£9,160	0.05	6	£54,960	0.3
	Agitation tank	118,829	L	£394,834	9.87	2	£789,668	19.75
	Centrifuge	25,391	L/h	£1,731,374	20	2	£3,462,749	958.9
	Precipitation tank	356,488	L	£763,286	0	2	£1,526,573	0
Polyphenol	Pump	14,517	L/h	£9,160	0.05	2	£18,320	0.1
	Extraction tank	116,132	L	£1,501,497	4.94	1	£1,501,497	4.94
	Filter housing	29,033	L/h	£7,254	0.05	1	£7,254	1.08
	Filter	-		£10,294	0	2	£20,587	0
Protein	Pump	103,160	L/h	£9,160	0.05	2	£18,320	0.1
	Extraction tank	825,277	L	£1,716,270	197.47	1	£1,716,270	197.47
	Filter housing	206,319	L/h	£7,254	0.05	1	£7,254	1.08
	Filter	-		£10,294	0	2	£20,587	0

Appendix C: Cumulative cash flow of all biorefinery scenarios

Table C-1. Total cash flow of a solvent-based biorefinery scenario after 10 years of operation.

Year	***-2***	***-1***	***0***	***1***	***2***	***3***	***4***	***5***	***6***	***7***	***8***	***9***	***10***
Fixed Capital Investment	£84,574,255	£42,287,128	£42,287,128										
Working Capital Investment			£8,457,426										
Annual kg input				1,000	1,000	1,000	1,000	1,000	1,000	1,000	1,000	1,000	1,000
Sales revenue													
Fucoxanthin sales				£165,310	£165,310	£165,310	£165,310	£165,310	£165,310	£165,310	£165,310	£165,310	£165,310
Lipid sales				£13,050	£13,050	£13,050	£13,050	£13,050	£13,050	£13,050	£13,050	£13,050	£13,050
Polyphenol sales				£17,729,254	£17,729,254	£17,729,254	£17,729,254	£17,729,254	£17,729,254	£17,729,254	£17,729,254	£17,729,254	£17,729,254
Fucoidan sales				£6,989,631	£6,989,631	£6,989,631	£6,989,631	£6,989,631	£6,989,631	£6,989,631	£6,989,631	£6,989,631	£6,989,631
Alginate sales				£942,496	£942,496	£942,496	£942,496	£942,496	£942,496	£942,496	£942,496	£942,496	£942,496
Total sales	£-	£-	£-	£25,839,741	£25,839,741	£25,839,741	£25,839,741	£25,839,741	£25,839,741	£25,839,741	£25,839,741	£25,839,741	£25,839,741
CoG (incl. depr'n)				£303,114	£303,114	£303,114	£303,114	£303,114	£303,114	£303,114	£303,114	£303,114	£303,114
Selling, General & Administrative Expenses				£15,156	£15,156	£15,156	£15,156	£15,156	£15,156	£15,156	£15,156	£15,156	£15,156
Profit before Tax	-£84,574,255	-£42,287,128	-£42,287,128	£25,521,471	£25,521,471	£25,521,471	£25,521,471	£25,521,471	£25,521,471	£25,521,471	£25,521,471	£25,521,471	£25,521,471
Tax				£3,382,970	£3,382,970	£3,382,970	£3,382,970	£3,382,970	£3,382,970	£3,382,970	£3,382,970	£3,382,970	£3,382,970
Profit after Tax	-£84,574,255	-£42,287,128	-£42,287,128	£22,138,501	£22,138,501	£22,138,501	£22,138,501	£22,138,501	£22,138,501	£22,138,501	£22,138,501	£22,138,501	£22,138,501

Depreciation	£16,914,851	£16,914,851	£16,914,851	£16,914,851	£16,914,851	£16,914,851	£16,914,851	£16,914,851	£16,914,851	£16,914,851	£16,914,851	£16,914,851	£16,914,851
Cash flow	-£67,659,404	-£25,372,277	-£25,372,277	£39,053,352	£39,053,352	£39,053,352	£39,053,352	£39,053,352	£39,053,352	£39,053,352	£39,053,352	£39,053,352	£39,053,352
Discount factor (10%)		1.210	1.100	1.000	0.9091	0.8264	0.7513	0.6830	0.6209	0.5645	0.5132	0.4665	0.4241
Discounted cash flow = PV	-£67,659,404	-£30,700,455	-£27,909,504	£39,053,352	£35,503,047	£32,275,498	£29,341,361	£26,673,965	£24,249,059	£22,044,599	£20,040,545	£18,218,677	£16,562,434
Discounted cumulative cash flow = NPV	**-£67,659,404**	**-£98,359,859**	**-£126,269,363**	**-£87,216,011**	**-£51,712,963**	**-£19,437,466**	**£9,903,896**	**£36,577,861**	**£60,826,920**	**£82,871,519**	**£102,912,063**	**£121,130,740**	**£137,693,174**

Total cash flow	**£137,693,174**
NPV	**£3,905,335**
IRR, %	**21.5%**

Table C-2. Total cash flow of a biorefinery scenario based in the use of novel technologies after 10 years of operation.

Year	***-2***	***-1***	***0***	***1***	***2***	***3***	***4***	***5***	***6***	***7***	***8***	***9***	***10***
Fixed Capital Investment	£58,133,056	£116,266,112	£58,133,056										
Working Capital Investment			£11,626,611										
Annual MT input				1,000	1,000	1,000	1,000	1,000	1,000	1,000	1,000	1,000	1,000
Sales revenue													
Fucoxanthin sales				£267,652	£267,652	£267,652	£267,652	£267,652	£267,652	£267,652	£267,652	£267,652	£267,652
Lipid sales				£80,727	£80,727	£80,727	£80,727	£80,727	£80,727	£80,727	£80,727	£80,727	£80,727
Polyphenol sales				£45,295,705	£45,295,705	£45,295,705	£45,295,705	£45,295,705	£45,295,705	£45,295,705	£45,295,705	£45,295,705	£45,295,705
Fucoidan sales				£46,986,416	£46,986,416	£46,986,416	£46,986,416	£46,986,416	£46,986,416	£46,986,416	£46,986,416	£46,986,416	£46,986,416
Alginate sales				£662,457	£662,457	£662,457	£662,457	£662,457	£662,457	£662,457	£662,457	£662,457	£662,457
Total sales	£-	£-	£-	£93,292,957	£93,292,957	£93,292,957	£93,292,957	£93,292,957	£93,292,957	£93,292,957	£93,292,957	£93,292,957	£93,292,957
CoG (incl. depr'n)				£445,700	£445,700	£445,700	£445,700	£445,700	£445,700	£445,700	£445,700	£445,700	£445,700
Selling, General & Administrative Expenses				£22,285	£22,285	£22,285	£22,285	£22,285	£22,285	£22,285	£22,285	£22,285	£22,285
Profit before Tax	-£58,133,056	-£116,266,112	-£69,759,667	£92,824,973	£92,824,973	£92,824,973	£92,824,973	£92,824,973	£92,824,973	£92,824,973	£92,824,973	£92,824,973	£92,824,973
Tax				£4,650,644	£4,650,644	£4,650,644	£4,650,644	£4,650,644	£4,650,644	£4,650,644	£4,650,644	£4,650,644	£4,650,644
Profit after Tax	-£58,133,056	-£116,266,112	-£69,759,667	£88,174,328	£88,174,328	£88,174,328	£88,174,328	£88,174,328	£88,174,328	£88,174,328	£88,174,328	£88,174,328	£88,174,328
Depreciation				£16,914,851	£16,914,851	£16,914,851	£16,914,851	£16,914,851	£16,914,851	£16,914,851	£16,914,851	£16,914,851	£16,914,851
Cash flow	-£58,133,056	-£116,266,112	-£69,759,667	£105,089,179	£105,089,179	£105,089,179	£105,089,179	£105,089,179	£105,089,179	£105,089,179	£105,089,179	£105,089,179	£105,089,179
Discount factor (10%)		1.210	1.100	1.000	0.9091	0.8264	0.7513	0.6830	0.6209	0.5645	0.5132	0.4665	0.4241

Discounted cash flow = PV	-£58,133,056	-£116,266,112	-£69,759,667	£105,089,179	£95,535,618	£86,850,561	£78,955,056	£71,777,324	£65,252,112	£59,320,102	£53,927,366	£49,024,878	£44,568,071
Discounted cumulative cash flow	**-£58,133,056**	**-£174,399,169**	**-£244,158,836**	**-£139,069,657**	**-£43,534,039**	**£43,316,522**	**£122,271,578**	**£194,048,902**	**£259,301,014**	**£318,621,116**	**£372,548,482**	**£421,573,360**	**£466,141,430**

Total cash flow, £	**443,232,802**
NPV, £	**10,467,353**
IRR, %	**28.2%**

Table C-3. Total cash flow of a green chemistry-compliant biorefinery scenario after 10 years of operation.

Year	***-2***	***-1***	***0***	***1***	***2***	***3***	***4***	***5***	***6***	***7***	***8***	***9***	***10***
Fixed Capital Investment	£7,098,348	£14,196,696	£7,098,348										
Working Capital Investment			£1,419,670										
Annual MT input				1,000	1,000	1,000	1,000	1,000	1,000	1,000	1,000	1,000	1,000
Sales revenue													
Fucoxanthin sales				£706,374	£706,374	£706,374	£706,374	£706,374	£706,374	£706,374	£706,374	£706,374	£706,374
Protein Sales				£23,925,705	£23,925,705	£23,925,705	£23,925,705	£23,925,705	£23,925,705	£23,925,705	£23,925,705	£23,925,705	£23,925,705
Polyphenol sales				£5,121,446	£5,121,446	£5,121,446	£5,121,446	£5,121,446	£5,121,446	£5,121,446	£5,121,446	£5,121,446	£5,121,446
Fucoidan sales				£8,557,994	£8,557,994	£8,557,994	£8,557,994	£8,557,994	£8,557,994	£8,557,994	£8,557,994	£8,557,994	£8,557,994
Alginate sales				£1,153,977	£1,153,977	£1,153,977	£1,153,977	£1,153,977	£1,153,977	£1,153,977	£1,153,977	£1,153,977	£1,153,977
Total sales	£-	£-	£-	£39,465,496	£39,465,496	£39,465,496	£39,465,496	£39,465,496	£39,465,496	£39,465,496	£39,465,496	£39,465,496	£39,465,496
CoG (incl. depr'n)				£79,300	£79,300	£79,300	£79,300	£79,300	£79,300	£79,300	£79,300	£79,300	£79,300
Selling, General & Administrative Expenses				£3,965	£3,965	£3,965	£3,965	£3,965	£3,965	£3,965	£3,965	£3,965	£3,965
Profit before Tax	-£7,098,348	-£14,196,696	-£8,518,018	£39,382,231	£39,382,231	£39,382,231	£39,382,231	£39,382,231	£39,382,231	£39,382,231	£39,382,231	£39,382,231	£39,382,231
Tax				£567,868	£567,868	£567,868	£567,868	£567,868	£567,868	£567,868	£567,868	£567,868	£567,868
Profit after Tax	-£7,098,348	-£14,196,696	-£8,518,018	£38,814,363	£38,814,363	£38,814,363	£38,814,363	£38,814,363	£38,814,363	£38,814,363	£38,814,363	£38,814,363	£38,814,363
Depreciation				£2,839,339	£2,839,339	£2,839,339	£2,839,339	£2,839,339	£2,839,339	£2,839,339	£2,839,339	£2,839,339	£2,839,339
Cash flow	-£7,098,348	-£14,196,696	-£8,518,018	£41,653,702	£41,653,702	£41,653,702	£41,653,702	£41,653,702	£41,653,702	£41,653,702	£41,653,702	£41,653,702	£41,653,702

Discount factor (10%)		1.210	1.100	1.000	0.9091	0.8264	0.7513	0.6830	0.6209	0.5645	0.5132	0.4665	0.4241
Discounted cash flow = PV	-£7,098,348	-£14,196,696	-£8,518,018	£41,653,702	£37,867,002	£34,424,547	£31,295,043	£28,450,039	£25,863,672	£23,512,429	£21,374,935	£19,431,760	£17,665,236
Discounted cumulative cash flow	**-£7,098,348**	**-£21,295,044**	**-£29,813,062**	**£11,840,641**	**£49,707,643**	**£84,132,190**	**£115,427,233**	**£143,877,272**	**£169,740,944**	**£193,253,373**	**£214,628,309**	**£234,060,068**	**£251,725,304**

Total cash flow, £	**251,725,304**
NPV, £	**4,165,370**
IRR, %	**75.2%**

Table C-4. Total cash flow of the re-iterated green chemistry-compliant biorefinery scenario after 10 years of operation

Year	***-2***	***-1***	***0***	***1***	***2***	***3***	***4***	***5***	***6***	***7***	***8***	***9***	***10***
Fixed Capital Investment	£12,460,224	£24,920,448	£12,460,224										
Working Capital Investment			£2,373,376										
Annual MT input				1,000	1,000	1,000	1,000	1,000	1,000	1,000	1,000	1,000	1,000
Sales revenue													
Fucoidan sales				£59,758,211	£59,758,211	£59,758,211	£59,758,211	£59,758,211	£59,758,211	£59,758,211	£59,758,211	£59,758,211	£59,758,211
Alginate sales				£1,960,686	£1,960,686	£1,960,686	£1,960,686	£1,960,686	£1,960,686	£1,960,686	£1,960,686	£1,960,686	£1,960,686
Polyphenol sales				£20,404,020	£20,404,020	£20,404,020	£20,404,020	£20,404,020	£20,404,020	£20,404,020	£20,404,020	£20,404,020	£20,404,020
Protein Sales				£9,475,085	£9,475,085	£9,475,085	£9,475,085	£9,475,085	£9,475,085	£9,475,085	£9,475,085	£9,475,085	£9,475,085
Total sales	£-	£-	£-	£91,598,002	£91,598,002	£91,598,002	£91,598,002	£91,598,002	£91,598,002	£91,598,002	£91,598,002	£91,598,002	£91,598,002
CoG (incl. depr'n)				£45,785	£45,785	£45,785	£45,785	£45,785	£45,785	£45,785	£45,785	£45,785	£45,785
Selling, General & Administrative Expenses				£2,289	£2,289	£2,289	£2,289	£2,289	£2,289	£2,289	£2,289	£2,289	£2,289
Profit before Tax	-£12,460,224	-£24,920,448	-£14,833,600	£91,549,928	£91,549,928	£91,549,928	£91,549,928	£91,549,928	£91,549,928	£91,549,928	£91,549,928	£91,549,928	£91,549,928
Tax				£949,350	£949,350	£949,350	£949,350	£949,350	£949,350	£949,350	£949,350	£949,350	£949,350
Profit after Tax	-£12,460,224	-£24,920,448	-£14,833,600	£90,600,578	£90,600,578	£90,600,578	£90,600,578	£90,600,578	£90,600,578	£90,600,578	£90,600,578	£90,600,578	£90,600,578
Depreciation				£2,839,339	£2,839,339	£2,839,339	£2,839,339	£2,839,339	£2,839,339	£2,839,339	£2,839,339	£2,839,339	£2,839,339
Cash flow	-£12,460,224	-£24,920,448	-14,833,600	£93,439,917	£93,439,917	£93,439,917	£93,439,917	£93,439,917	£93,439,917	£93,439,917	£93,439,917	£93,439,917	£93,439,917
Discount factor (10%)		1.210	1.100	1.000	0.9091	0.8264	0.7513	0.6830	0.6209	0.5645	0.5132	0.4665	0.4241

Discounted cash flow = PV	-£12,460,224	-£24,920,448	-£14,833,600	£93,439,917	£84,945,379	£77,223,072	£70,202,793	£63,820,721	£58,018,837	£52,744,397	£47,949,452	£43,590,411	£39,627,646
Discounted cumulative cash flow	**-£12,460,224**	**-£37,380,672**	**-£52,214,272**	**£41,225,64**	**£126,171,024**	**£203,394,096**	**£273,596,889**	**£337,417,609**	**£395,436,446**	**£448,180,843**	**£496,130,295**	**£539,720,706**	**£579,348,353**

Total cash flow, £	**579,348,353**
NPV, £	**9,343,992**
IRR, %	**82.1%**

Appendix D: Life cycle process parameters

Table D-1. Climate change process parameters of all scenarios evaluated in this project

Process	Unit	Green Chem v2	Green Chem v1	Novel tech	Solvent-based
Total of all processes	kg CO_2-eq.	16.30	18.93	299.69	38.21
Remaining processes	kg CO_2-eq.	0.69	0	0	7.11E-15
Acetone, liquid {GLO}| market for | Cut-off, S	kg CO_2-eq.	0	0	11.82	12.38
Calcium chloride {GLO}| market for | Cut-off, S	kg CO_2-eq.	0	0.063	0	0
Citric acid {GLO}| market for | Cut-off, S	kg CO_2-eq.	1.51	0	0	0
Electricity, medium voltage {GB}| market for | Cut-off, S	kg CO_2-eq.	0.70	0.15	241.40	5.02
Ethanol, without water, in 99.7% solution state, from ethylene {GLO}| market for | Cut-off, S	kg CO_2-eq.	52.57392	0	0	-0.22
Ethanol, without water, in 99.7% solution state, from ethylene {RoW}| ethylene hydration | Cut-off, S	kg CO_2-eq.	-51.13	0	0	0
Ethylene oxide {RoW}| production | Cut-off, U	kg CO_2-eq.	0.07	0	0	0
Ethylene, average {RER}| production | Cut-off, U	kg CO_2-eq.	0.19	0	0	0
Ethylene, average {RoW}| production | Cut-off, U	kg CO_2-eq.	0.38	0	0	0
Hard coal {CN}| hard coal mine operation and hard coal preparation | Cut-off, U	kg CO_2-eq.	0.059	0	0	0
Heat, from steam, in chemical industry {RoW}| market for heat, from steam, in chemical industry | Cut-off, S	kg CO_2-eq.	0	0	29.48	0
Hydrochloric acid, without water, in 30%	kg CO_2-eq.	0	0.021	0.33	0.45

solution state {RER}| market for | Cut-off, S					
Municipal solid waste {GB}| treatment of, incineration | Cut-off, S	kg CO_2-eq.	1.70	3.16	2.84	3.20
Municipal solid waste {RoW}| treatment of, sanitary landfill | Cut-off, S	kg CO_2-eq.	8.20	15.20	13.64	15.37
Neutralising agent, sodium hydroxide-equivalent {GLO}| soda ash, dense, to generic market for neutralising agent | Cut-off, S	kg CO_2-eq.	0.95	0	0	0
Phosphoric acid, industrial grade, without water, in 85% solution state {GLO}| market for | Cut-off, S	kg CO_2-eq.	0.053	0	0	0
Potassium hydroxide {GLO}| market for | Cut-off, S	kg CO_2-eq.	0.15	0	0	0
Soda ash, dense {GLO}| market for | Cut-off, S	kg CO_2-eq.	0	0	0.14	0
Sodium hydroxide, without water, in 50% solution state {GLO}| market for | Cut-off, S	kg CO_2-eq.	0	0	0.61	2.72
Wastewater - untreated, organic contaminated EU-27 S	kg CO_2-eq.	-0.36	-1.28	-1.51	-2.21
Wastewater - untreated, slightly organic and anorganic contaminated EU-27 S	kg CO_2-eq.	-1.64	-0.36	-1.51	-2.67
Water, ultrapure {GLO}| market for | Cut-off, S	kg CO_2-eq.	2.18	1.98	2.42	4.15

Table D-2. Ozone depletion process parameters of all scenarios evaluated in this project

Process	Unit	Green Chem v2	Green Chem v1	Novel tech	Solvent-based
Total of all processes	kg CFC-11 eq	1.19E-6	4.41E-07	1.20E-05	2.88E-06
Remaining processes	kg CFC-11 eq	8.17E-9	0	-1.69E-21	-8.47E-22
Acetone, liquid {GLO}| market for | Cut-off, S	kg CFC-11 eq	0	0	1.74E-07	1.82E-07
Calcium chloride {GLO}| market for | Cut-off, S	kg CFC-11 eq	0	2.79E-9	0	0
Citric acid {GLO}| market for | Cut-off, S	kg CFC-11 eq	1.73E-7	0	0	0
Electricity, medium voltage {GB}| market for | Cut-off, S	kg CFC-11 eq	2.39E-8	4.98E-9	8.23E-6	1.71E-7
Ethanol, without water, in 99.7% solution state, from ethylene {GLO}| market for | Cut-off, S	kg CFC-11 eq	1.28E-6	0	0	-5.41E-9
Ethanol, without water, in 99.7% solution state, from ethylene {RoW}| ethylene hydration | Cut-off, S	kg CFC-11 eq	-8.18E-7	0	0	0
Heat, from steam, in chemical industry {RoW}| market for heat, from steam, in chemical industry | Cut-off, S	kg CFC-11 eq	0	0	2.52E-06	0
Hydrochloric acid, without water, in 30% solution state {RER}| market for | Cut-off, S	kg CFC-11 eq	0	1.41E-8	2.19E-07	2.97E-7
Municipal solid waste {GB}| treatment of, incineration | Cut-off, S	kg CFC-11 eq	1.24E-8	2.31E-8	2.07E-08	2.33E-8
Municipal solid waste {RoW}| treatment of, sanitary landfill | Cut-off, S	kg CFC-11 eq	4.92E-8	9.11E-8	8.17E-08	9.21E-8
Natural gas, high pressure {RoW}| petroleum and gas production, onshore | Cut-off, U	kg CFC-11 eq	1.68E-9	0	0	0
Natural gas, high pressure {US}| petroleum and gas production, onshore | Cut-off, U	kg CFC-11 eq	1.78E-9	0	0	0
Neutralising agent, sodium hydroxide-	kg CFC-11 eq	8.66E-8	0	0	0

equivalent {GLO}| soda ash, dense, to generic market for neutralising agent | Cut-off, S					
Petroleum {RME}| production, onshore | Cut-off, U	kg CFC-11 eq	5.95E-9	0	0	0
Petroleum {RoW}| petroleum and gas production, onshore | Cut-off, U	kg CFC-11 eq	6.34E-9	0	0	0
Petroleum {RU}| production, onshore | Cut-off, U	kg CFC-11 eq	2.54E-9	0	0	0
Phosphoric acid, industrial grade, without water, in 85% solution state {GLO}| market for | Cut-off, S	kg CFC-11 eq	6.69E-9	0	0	0
Potassium hydroxide {GLO}| market for | Cut-off, S	kg CFC-11 eq	8.96E-9	0	0	0
Soda ash, dense {GLO}| market for | Cut-off, S	kg CFC-11 eq	0	0	1.30E-8	0
Sodium hydroxide, without water, in 50% solution state {GLO}| market for | Cut-off, S	kg CFC-11 eq	0	0	3.34E-7	1.49E-6
Transport, pipeline, long distance, natural gas {RU}| processing | Cut-off, U	kg CFC-11 eq	3.19E-9	0	0	0
Uranium, enriched 3.8%, per separative work unit {US}| uranium production, diffusion, enriched 3.8% | Cut-off, U	kg CFC-11 eq	5.05E-9	0	0	0
Uranium, enriched 4.2%, per separative work unit {US}| uranium production, diffusion, enriched 4.2% | Cut-off, U	kg CFC-11 eq	5.84E-9	0	0	0
Wastewater - untreated, organic contaminated EU-27 S	kg CFC-11 eq	-2.05E-9	-7.16E-09	-8.43E-9	-1.23E-8
Wastewater - untreated, slightly organic and anorganic contaminated EU-27 S	kg CFC-11 eq	-9.85E-9	-2.21E-9	-9.06E-9	-1.60E-8
Water, ultrapure {GLO}| market for | Cut-off, S	kg CFC-11 eq	3.45E-7	3.14E-07	3.84E-7	6.58E-7

Table D-3. Terrestrial acidification process parameters of all scenarios evaluated in this project

Process	Unit	Green Chem v2	Green Chem v1	Novel tech	Solvent-based
Total of all processes	kg SO_2-eq.	0.041	0.013	1.18	0.10
Remaining processes	kg SO_2 -eq.	0.0030	1.73E-18	2.22E-16	0
Acetone, liquid {GLO}| market for | Cut-off, S	kg SO_2-eq.	0	0	0.048	0.051
Calcium chloride {GLO}| market for | Cut-off, S	kg SO_2-eq.	0	0.00062	0	0
Citric acid {GLO}| market for | Cut-off, S	kg SO_2-eq.	0.0096	0	0	0
Electricity, medium voltage {GB}| market for | Cut-off, S	kg SO_2-eq.	0.0029	0.00062	1.02	0.021
Ethanol, without water, in 99.7% solution state, from ethylene {GLO}| market for | Cut-off, S	kg SO_2-eq.	0.17	0	0	-0.00074
Ethanol, without water, in 99.7% solution state, from ethylene {RoW}| ethylene hydration | Cut-off, S	kg SO_2-eq.	-0.16	0	0	0
Ethylene, average {RER}| production | Cut-off, U	kg SO_2-eq.	0.00047	0	0	0
Ethylene, average {RoW}| production | Cut-off, U	kg SO_2-eq.	0.00097	0	0	0
Hard coal {CN}| hard coal mine operation and hard coal preparation | Cut-off, U	kg SO_2-eq.	0.00023	0	0	0
Heat, from steam, in chemical industry {RoW}| market for heat, from steam, in chemical industry | Cut-off, S	kg SO_2-eq.	0	0	0.090	0
Hydrochloric acid, without water, in 30% solution state {RER}| market for | Cut-off, S	kg SO_2-eq.	0	0.00013	0.0021	0.0029
Municipal solid waste {GB}| treatment of, incineration | Cut-off, S	kg SO_2-eq.	0.00077	0.0014	0.0012	0.0014

Municipal solid waste {RoW}| treatment of, sanitary landfill | Cut-off, S	kg SO_2-eq.	0.0023	0.0042	0.0038	0.0043
Neutralising agent, sodium hydroxide-equivalent {GLO}| soda ash, dense, to generic market for neutralising agent | Cut-off, S	kg SO_2-eq.	0.0044	0	0	0
Phosphoric acid, industrial grade, without water, in 85% solution state {GLO}| market for | Cut-off, S	kg SO_2-eq.	0.00065	0	0	0
Potassium hydroxide {GLO}| market for | Cut-off, S	kg SO_2-eq.	0.00069	0	0	0
Soda ash, dense {GLO}| market for | Cut-off, S	kg SO_2-eq.	0	0	0.00066	0
Sodium hydroxide, without water, in 50% solution state {GLO}| market for | Cut-off, S	kg SO_2-eq.	0	0	0.0027	0.012
Transport, freight, sea, transoceanic ship {GLO}| processing | Cut-off, U	kg SO_2-eq.	0.000174	0	0	0
Wastewater - untreated, organic contaminated EU-27 S	kg SO_2-eq.	-0.00077	-0.0026	-0.0031	-0.0046
Wastewater - untreated, slightly organic and anorganic contaminated EU-27 S	kg SO_2-eq.	-0.00343	-0.00077	-0.0031	-0.0055
Water, ultrapure {GLO}| market for | Cut-off, S	kg SO_2-eq.	0.011	0.010	0.012	0.021

Table D-4. Freshwater eutrophication process parameters of all scenarios evaluated in this project

Process	Unit	Green Chem v2	Green Chem v1	Novel tech	Solvent-based
Total of all processes	kg P eq	0.003909	0.002478	0.078428	0.009024
Remaining processes	kg P eq	9.95E-06	-1.16E-06	-2.13E-06	-3.44E-06
Acetone, liquid {GLO}| market for | Cut-off, S	kg P eq	0	0	0.001553	0.001626
Calcium chloride {GLO}| market for | Cut-off, S	kg P eq	0	3.48E-05	0	0
Citric acid {GLO}| market for | Cut-off, S	kg P eq	0.000531	0	0	0
Electricity, medium voltage {GB}| market for | Cut-off, S	kg P eq	0.000203	4.22E-05	0.069831	0.001451
Ethanol, without water, in 99.7% solution state, from ethylene {GLO}| market for | Cut-off, S	kg P eq	0.022336	0	0	-9.48E-05
Ethanol, without water, in 99.7% solution state, from ethylene {RoW}| ethylene hydration | Cut-off, S	kg P eq	-0.02233	0	0	0
Heat, from steam, in chemical industry {RoW}| market for heat, from steam, in chemical industry | Cut-off, S	kg P eq	0	0	0.003711	0
Hydrochloric acid, without water, in 30% solution state {RER}| market for | Cut-off, S	kg P eq	0	1.77E-05	0.000274	0.000372
Municipal solid waste {GB}| treatment of, incineration | Cut-off, S	kg P eq	0.000127	0.000235	0.00021	0.000237
Municipal solid waste {RoW}| treatment of, sanitary landfill | Cut-off, S	kg P eq	0.000273	0.000507	0.000455	0.000512
Neutralising agent, sodium hydroxide-equivalent {GLO}| soda ash, dense, to generic market	kg P eq	0.000367	0	0	0

for neutralising agent | Cut-off, S					
Phosphoric acid, industrial grade, without water, in 85% solution state {GLO}| market for | Cut-off, S	kg P eq	7.30E-05	0	0	0
Potassium hydroxide {GLO}| market for | Cut-off, S	kg P eq	7.35E-05	0	0	0
Soda ash, dense {GLO}| market for | Cut-off, S	kg P eq	0	0	5.51E-05	0
Sodium hydroxide, without water, in 50% solution state {GLO}| market for | Cut-off, S	kg P eq	0	0	0.000331	0.001478
Spoil from hard coal mining {GLO}| treatment of, in surface landfill | Cut-off, U	kg P eq	0.000122	0	0	0
Spoil from lignite mining {GLO}| treatment of, in surface landfill | Cut-off, U	kg P eq	0.000209	0	0	0
Sulfidic tailing, off-site {GLO}| treatment of | Cut-off, U	kg P eq	0.000104	0	0	0
Water, ultrapure {GLO}| market for | Cut-off, S	kg P eq	0.001806	0.001643	0.00201	0.003445

Table D-5. Marine eutrophication process parameters of all scenarios evaluated in this project

Process	Unit	Green Chem v2	Green Chem v1	Novel Tech	Solvent-based
Total of all processes	kg N-eq.	0.051345	0.084326	0.112484	0.088238
Remaining processes	kg N-eq.	0.000211	2.24E-05	0	0
Acetone, liquid {GLO}| market for | Cut-off, S	kg N eq	0	0	0.001207	0.001265
Citric acid {GLO}| market for | Cut-off, S	kg N eq	0.001893	0	0	0
Electricity, medium voltage {GB}| market for | Cut-off, S	kg N eq	9.53E-05	1.98E-05	0.032815	0.000682
Ethanol, without water, in 99.7% solution state, from ethylene {GLO}| market for | Cut-off, S	kg N eq	0.005583	0	0	-2.37E-05
Ethanol, without water, in 99.7% solution state, from ethylene {RoW}| ethylene hydration | Cut-off, S	kg N eq	-0.00507	0	0	0
Heat, from steam, in chemical industry {RoW}| market for heat, from steam, in chemical industry | Cut-off, S	kg N eq	0	0	0.002274	0
Hydrochloric acid, without water, in 30% solution state {RER}| market for | Cut-off, S	kg N eq	0	7.93E-06	0.000123	0.000167
Municipal solid waste {GB}| treatment of, incineration | Cut-off, S	kg N eq	0.000162	0.000301	0.00027	0.000304
Municipal solid waste {RoW}| treatment of, sanitary landfill | Cut-off, S	kg N eq	0.04501	0.083419	0.074829	0.084333
Neutralising agent, sodium hydroxide-equivalent {GLO}| soda ash, dense, to generic market for neutralising agent | Cut-off, S	kg N eq	0.002775	0	0	0
Soda ash, dense {GLO}| market for | Cut-off, S	kg N eq	0	0	0.000418	0
Sodium hydroxide, without water, in 50% solution state {GLO}| market for | Cut-off, S	kg N eq	0	0	0.000163	0.000729
Spoil from lignite mining {GLO}| treatment of, in surface landfill | Cut-off, U	kg N eq	4.37E-05	0	0	0
Wastewater - untreated, organic contaminated EU-27 S	kg N eq	-0.00014	-0.0005	-0.00059	-0.00086
Wastewater - untreated, slightly organic and anorganic contaminated EU-27 S	kg N eq	-0.0005	-0.00011	-0.00046	-0.00081
Water, ultrapure {GLO}| market for | Cut-off, S	kg N eq	0.001283	0.001167	0.001427	0.002446

Table D-6. Water depletion process parameters of all scenarios evaluated in this project

Process	Unit	Green Chem v2	Green Chem v1	Novel tech	Solvent-based
Total of all processes	m^3-eq.	0.249962	0.089768	0.86405	0.47196
Remaining processes	m^3-eq.	0.002164	0	-1.11E-16	-5.55E-17
Acetone, liquid {GLO}| market for | Cut-off, S	m^3-eq.	0	0	0.15674	0.164143
Calcium chloride {GLO}| market for | Cut-off, S	m^3-eq.	0	0.00213	0	0
Citric acid {GLO}| market for | Cut-off, S	m^3-eq.	0.081633	0	0	0
Electricity, high voltage {BR}| electricity production, hydro, reservoir, tropical region | Cut-off, U	m^3-eq.	0.000397	0	0	0
Electricity, high voltage {NO}| electricity production, hydro, reservoir, alpine region | Cut-off, U	m^3-eq.	0.000299	0	0	0
Electricity, high voltage {PL}| heat and power co-generation, hard coal | Cut-off, U	m^3-eq.	0.000242	0	0	0
Electricity, high voltage {RU}| heat and power co-generation, hard coal | Cut-off, U	m^3-eq.	0.000219	0	0	0
Electricity, medium voltage {GB}| market for | Cut-off, S	m^3-eq.	0.001513	0.000315	0.520987	0.010828
Ethanol, without water, in 99.7% solution state, from ethylene {GLO}| market for | Cut-off, S	m^3-eq.	0.446491	0	0	-0.00189
Ethanol, without water, in 99.7% solution state, from ethylene {RoW}| ethylene hydration | Cut-off, S	m^3-eq.	-0.43172	0	0	0
Ethylene glycol {RER}| production | Cut-off, U	m^3-eq.	0.000482	0	0	0
Ethylene glycol {RoW}| production | Cut-off, U	m^3-eq.	0.003897	0	0	0
Ethylene, average {RER}| production | Cut-off, U	m^3-eq.	0.00157	0	0	0

		5			
Ethylene, average {RoW}| production | Cut-off, U	m^3-eq.	0.00318 9	0	0	0
Heat, from steam, in chemical industry {RoW}| market for heat, from steam, in chemical industry | Cut-off, S	m^3-eq.	0	0	0.02930 2	0
Hydrochloric acid, without water, in 30% solution state {RER}| market for | Cut-off, S	m^3-eq.	0	0.00072 4	0.01124	0.01523
Municipal solid waste {GB}| treatment of, incineration | Cut-off, S	m^3-eq.	0.00373 1	0.00691 5	0.00620 3	0.00699 1
Municipal solid waste {RoW}| treatment of, sanitary landfill | Cut-off, S	m^3-eq.	0.00523 8	0.00970 7	0.00870 8	0.00981 4
Neutralising agent, sodium hydroxide-equivalent {GLO}| soda ash, dense, to generic market for neutralising agent | Cut-off, S	m^3-eq.	0.01988 4	0	0	0
Oxygen, liquid {RER}| air separation, cryogenic | Cut-off, U	m^3-eq.	0.00160 1	0	0	0
Oxygen, liquid {RoW}| air separation, cryogenic | Cut-off, U	m^3-eq.	0.00323 2	0	0	0
Phosphoric acid, industrial grade, without water, in 85% solution state {GLO}| market for | Cut-off, S	m^3-eq.	0.00532 2	0	0	0
Potassium hydroxide {GLO}| market for | Cut-off, S	m^3-eq.	0.00114 6	0	0	0
Soda ash, dense {GLO}| market for | Cut-off, S	m^3-eq.	0	0	0.00299 2	0
Sodium hydroxide, without water, in 50% solution state {GLO}| market for | Cut-off, S	m^3-eq.	0	0	0.01770 2	0.07901 6
Wastewater - untreated, organic contaminated EU-27 S	m^3-eq.	0.00293 7	0.01026 1	0.01206 8	0.01763 7
Wastewater - untreated, slightly organic and anorganic contaminated EU-27 S	m^3-eq.	0.03885 1	0.00871 8	0.03573 3	0.06325 8
Water, decarbonised, at user {RER}| water production and supply, decarbonised | Cut-off, U	m^3-eq.	0.00044 7	0	0	0

Water, decarbonised, at user {RoW}| water production and supply, decarbonised | Cut-off, U	m^3-eq.	0.001124	0	0	0
Water, ultrapure {GLO}| market for | Cut-off, S	m^3-eq.	0.05607	0.050998	0.062376	0.106938

Table D-7. Fossil depletion process parameters of all scenarios evaluated in this project

Process	Unit	Green Chem v2	Green Chem v1	Novel Tech	Solvent-based
Total of all processes	kg oil eq	3.196025	0.907374	82.92805	11.1205
Remaining processes	kg oil eq	0.104208	-1.11E-16	-1.42E-14	0
Acetone, liquid {GLO}| market for | Cut-off, S	kg oil eq	0	0	7.375728	7.7241
Calcium chloride {GLO}| market for | Cut-off, S	kg oil eq	0	0.01425	0	0
Citric acid {GLO}| market for | Cut-off, S	kg oil eq	0.351148	0	0	0
Electricity, medium voltage {GB}| market for | Cut-off, S	kg oil eq	0.190622	0.039685	65.64909	1.364438
Ethanol, without water, in 99.7% solution state, from ethylene {GLO}| market for | Cut-off, S	kg oil eq	42.0048	0	0	-0.17826
Ethanol, without water, in 99.7% solution state, from ethylene {RoW}| ethylene hydration | Cut-off, S	kg oil eq	-41.2472	0	0	0
Ethylene, average {RER}| production | Cut-off, U	kg oil eq	0.198141	0	0	0
Ethylene, average {RoW}| production | Cut-off, U	kg oil eq	0.40121	0	0	0
Hard coal {CN}| hard coal mine operation and hard coal preparation | Cut-off, U	kg oil eq	0.04226	0	0	0
Hard coal {RoW}| hard coal mine operation and hard coal preparation | Cut-off, U	kg oil eq	0.02374	0	0	0
Heat, from steam, in chemical industry {RoW}| market for heat, from steam, in chemical industry | Cut-off, S	kg oil eq	0	0	8.716866	0
Hydrochloric acid, without water, in 30% solution state {RER}| market for | Cut-off, S	kg oil eq	0	0.006914	0.107306	0.145403
Lignite {RoW}| mine operation | Cut-off, U	kg oil eq	0.01289	0	0	0

		7			
Municipal solid waste {GB}| treatment of, incineration | Cut-off, S	kg oil eq	0.02638	0.04889 2	0.04385 7	0.04942 8
Municipal solid waste {RoW}| treatment of, sanitary landfill | Cut-off, S	kg oil eq	0.12829 7	0.23777 7	0.21329 3	0.24038 4
Neutralising agent, sodium hydroxide-equivalent {GLO}| soda ash, dense, to generic market for neutralising agent | Cut-off, S	kg oil eq	0.29222 8	0	0	0
Phosphoric acid, industrial grade, without water, in 85% solution state {GLO}| market for | Cut-off, S	kg oil eq	0.02132 3	0	0	0
Potassium hydroxide {GLO}| market for | Cut-off, S	kg oil eq	0.04232 6	0	0	0
Soda ash, dense {GLO}| market for | Cut-off, S	kg oil eq	0	0	0.04396 4	0
Sodium hydroxide, without water, in 50% solution state {GLO}| market for | Cut-off, S	kg oil eq	0	0	0.15396	0.68721 4
Wastewater - untreated, organic contaminated EU-27 S	kg oil eq	-0.02228	-0.07784	-0.09154	-0.13379
Wastewater - untreated, slightly organic and anorganic contaminated EU-27 S	kg oil eq	-0.09986	-0.02241	-0.09184	-0.16259
Water, ultrapure {GLO}| market for | Cut-off, S	kg oil eq	0.72575 3	0.66010 1	0.80737 8	1.38416 8

Appendix E: Monosaccharide profiles of fucoidan extracts

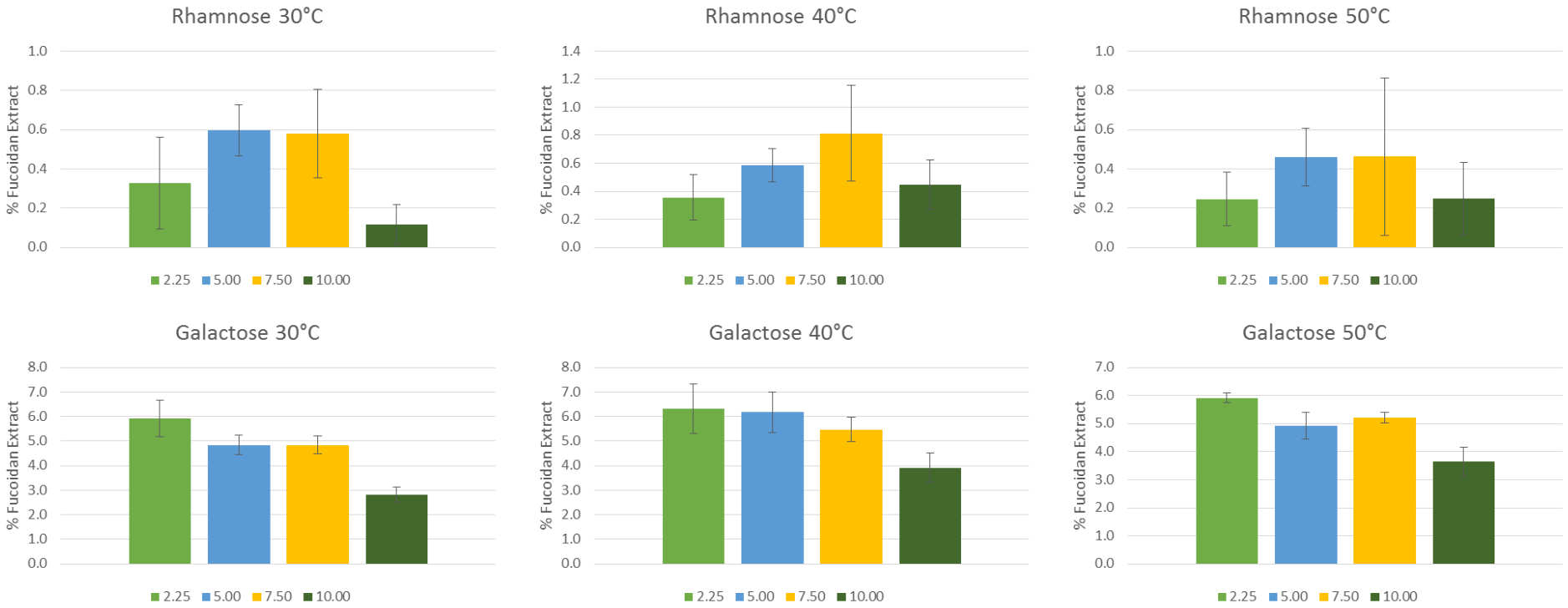

Fig E-1. Comparison of the rhamnose and galactose content in the different conditions analysed for fucoidan extracts using citric acid pH 5.5.

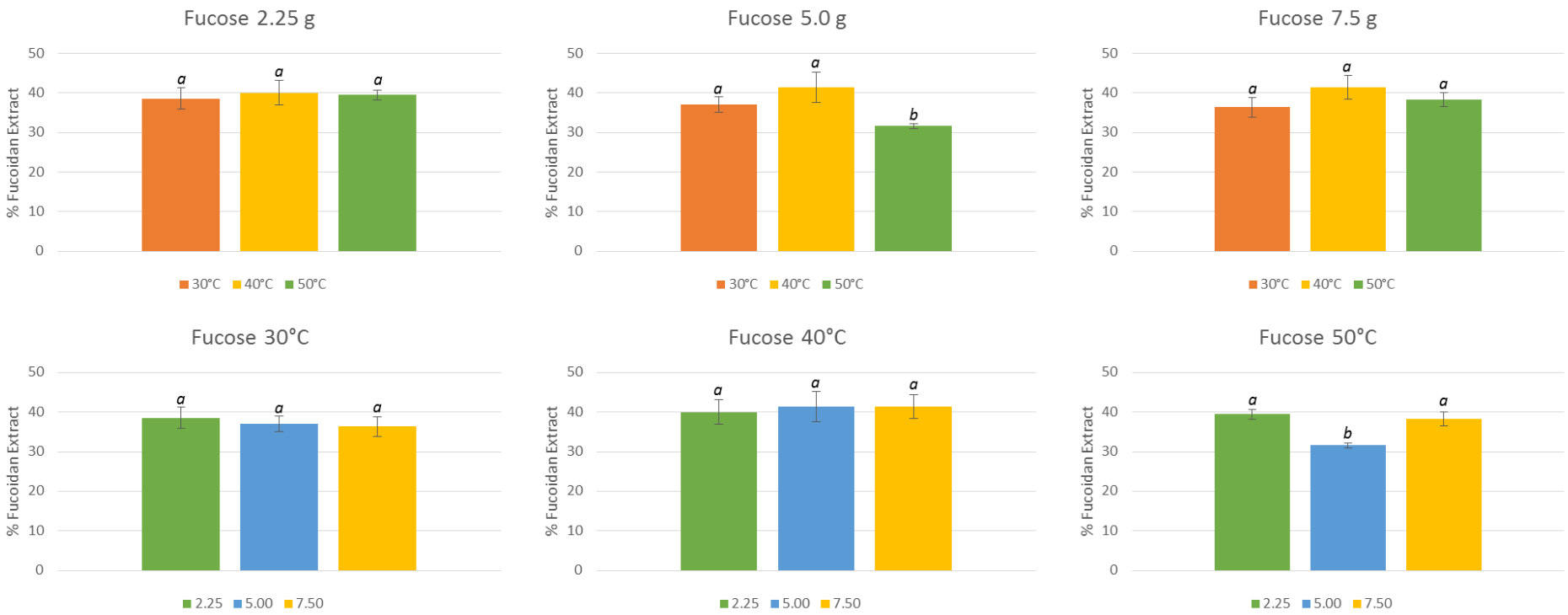

Fig E-2. Comparison of the fucose in the different conditions analysed for fucoidan extracts using citric acid pH 5.5.

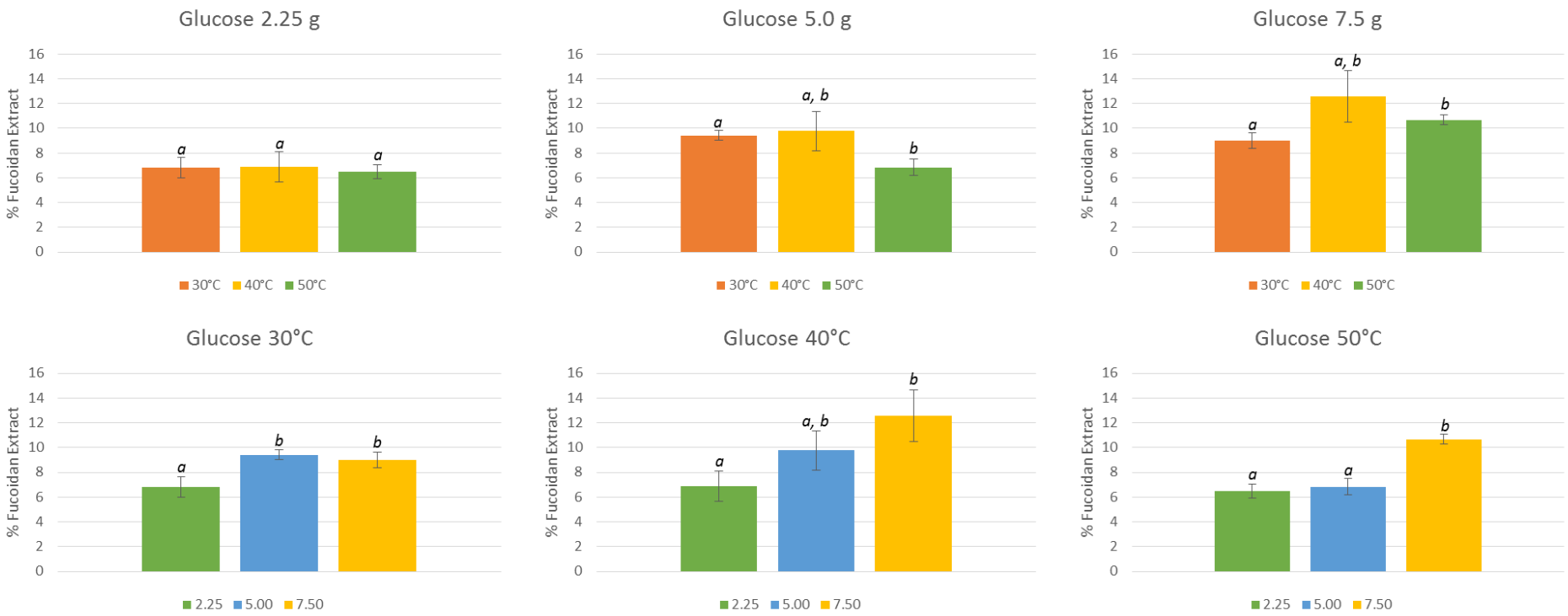

Fig E-3. Comparison of the glucose content in the different conditions analysed for fucoidan extracts using citric acid pH 5.5.

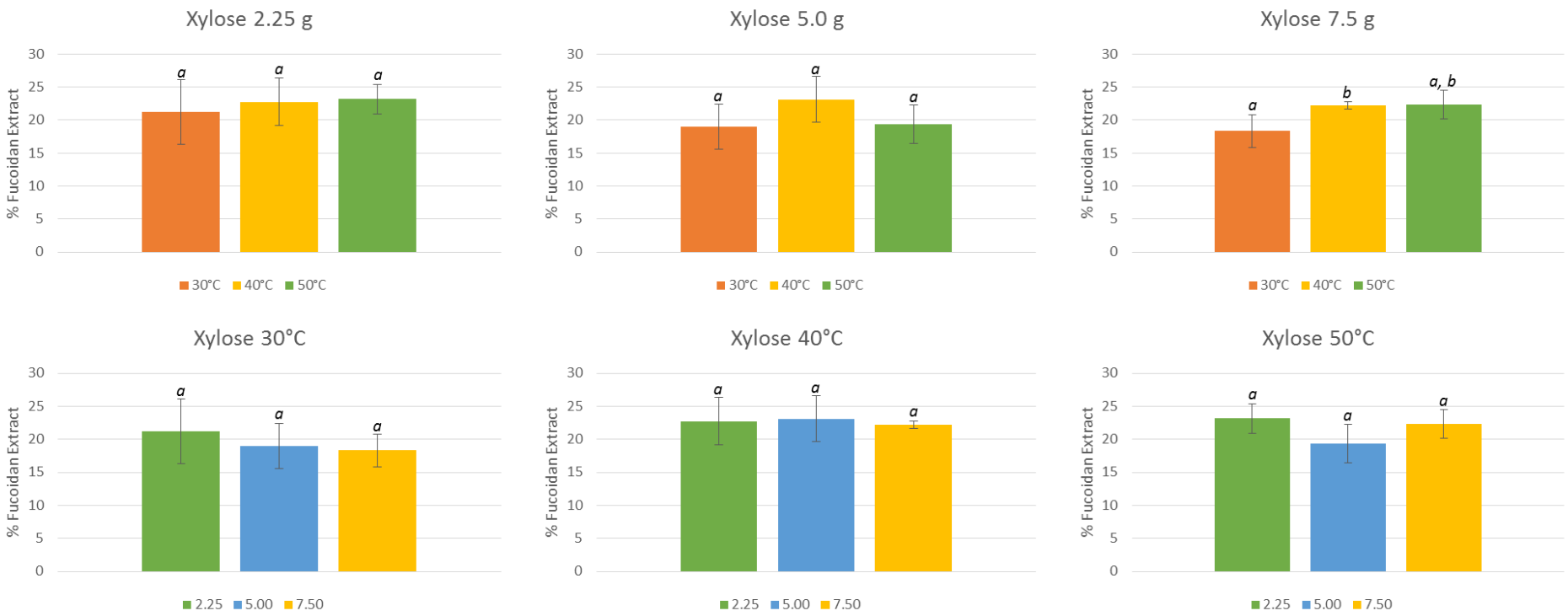

Fig E-4. Comparison of the xylose content in the different conditions analysed for fucoidan extracts using citric acid pH 5.5.

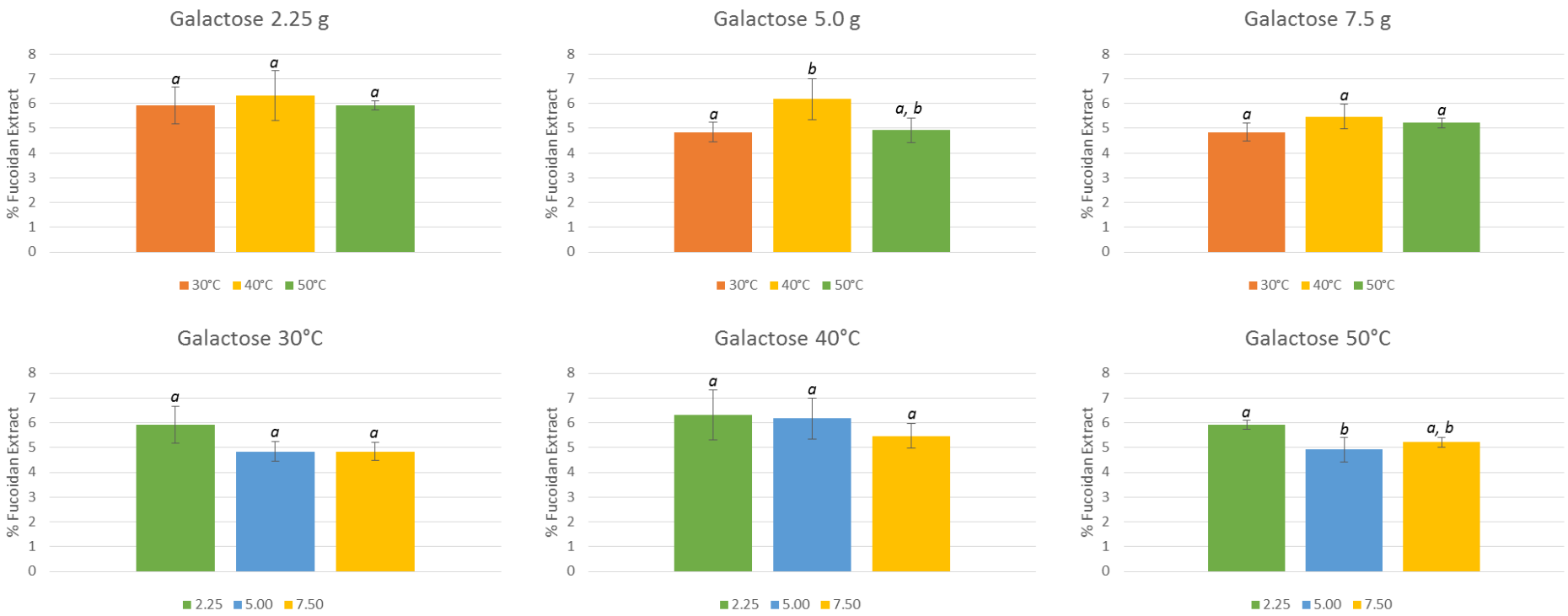

Fig E-5. Comparison of the galactose content in the different conditions analysed for fucoidan extracts using citric acid pH 5.5.

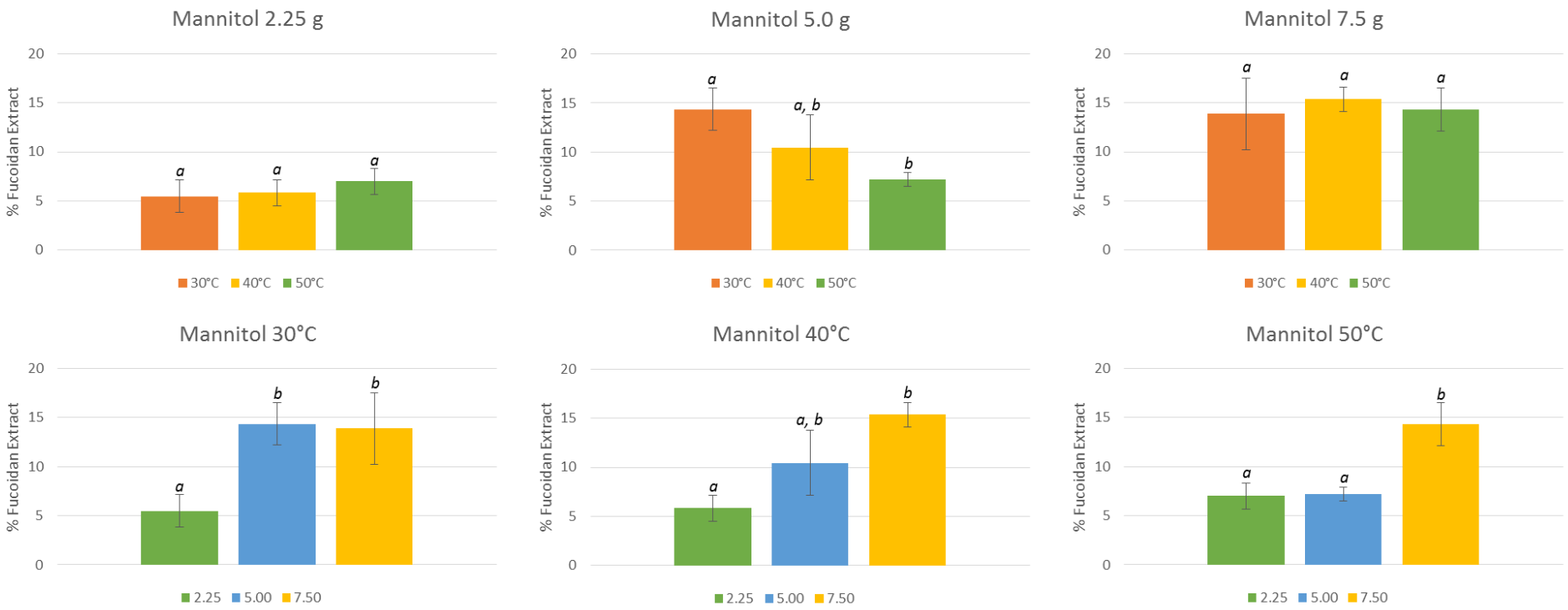

Fig E-6. Comparison of the mannitol content in the different conditions analysed for fucoidan extracts using citric acid pH 5.5.

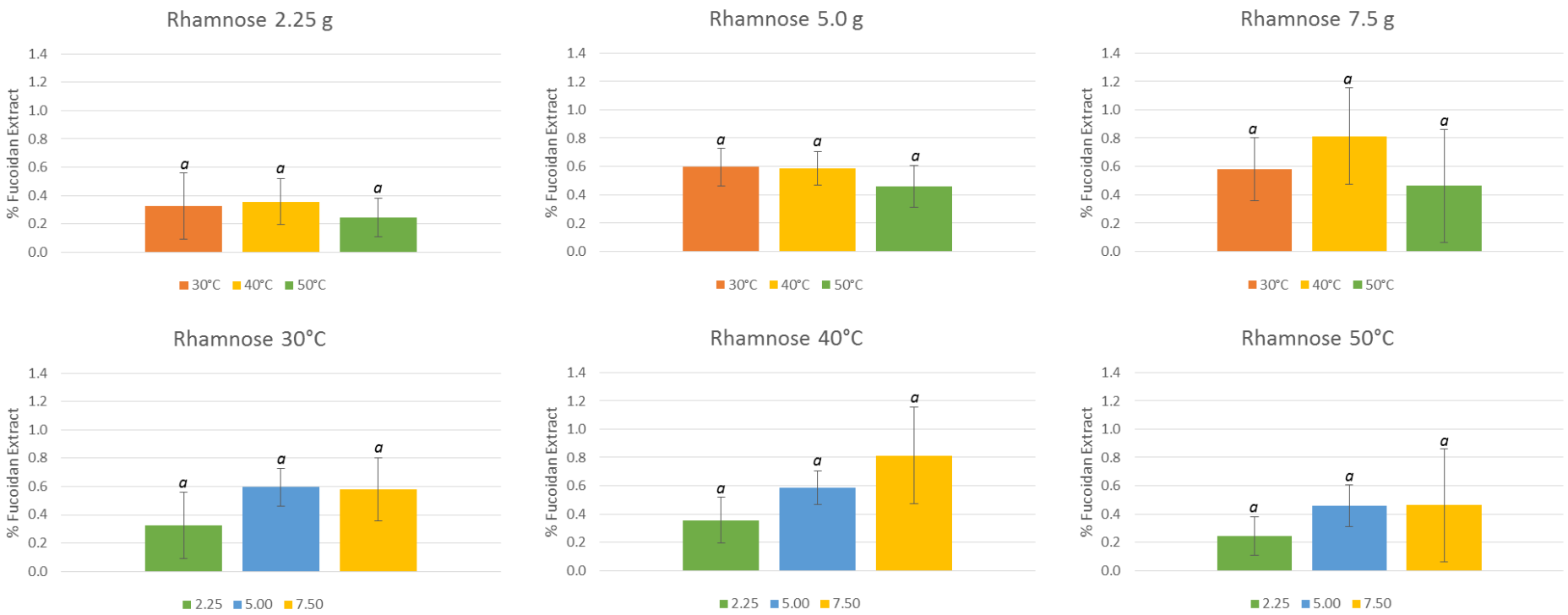

Fig E-7. Comparison of the rhamnose content in the different conditions analysed for fucoidan extracts using citric acid pH 5.5.

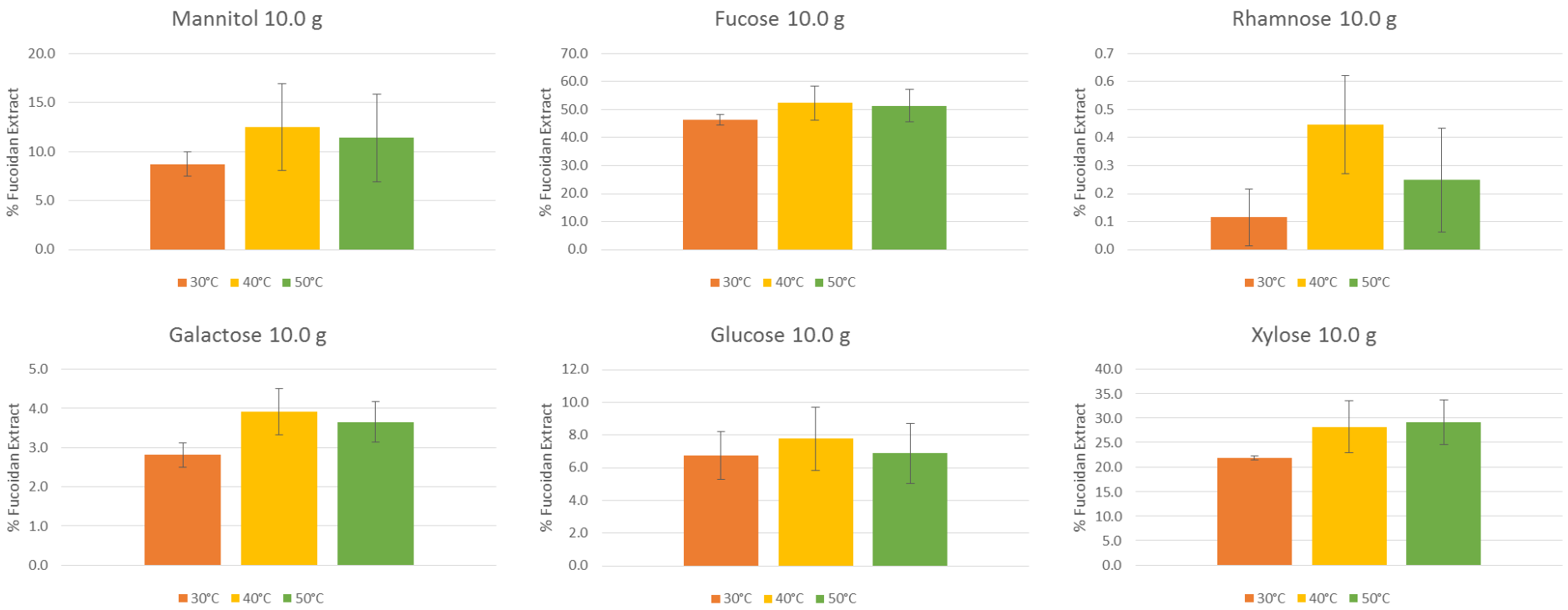

Fig E-8. Comparison of the monosaccharide content in the different conditions analysed for fucoidan extracts using citric acid pH 5.5 using an initial biomass of 10.0 g.